



POLITECNICO DI TORINO

Collegio di Ingegneria Civile
Master of Science program Civil Engineering

Master's degree thesis
CO₂ as a cement based mortar additive

Thesis supervisor
Prof. Alessandro Pasquale Fantilli

Candidate
Paolo Popolizio

Anno Accademico 2019-2020

INDEX

- ABSTRACT 5

- 1. INTRODUCTION 7
 - 1.1 Sustainability and Environmental Impact 9
 - 1.2 Three different approaches 9
 - 1.2.1 Solidia Cement 9
 - 1.2.2 Pre-carbonation 10
 - 1.2.3 CarbonCure 10
 - 1.3 Solidia Cement 11
 - 1.3.1 Features 11
 - 1.3.2 Absorption of CO₂ 11
 - 1.3.3 Compression strength 12
 - 1.3.4 Property comparison 14
 - 1.3.5 Other properties 14
 - 1.3.5.1 Reinforced concrete 14
 - 1.3.5.2 Thermogravimetric tests 14
 - 1.3.5.3 Elastic properties 15
 - 1.3.5.4 Interfacial transition zone 16
 - 1.4 Pre-carbonation 17
 - 1.4.1 The method 17
 - 1.4.2 Hydration of cement 18
 - 1.4.3 Compressive strength 19
 - 1.4.4 Flexural strength 20
 - 1.5 CarbonCure 20
 - 1.5.1 CO₂ capture and storage 20
 - 1.5.2 Cement saving 22
 - 1.5.3 Compressive strength 23

2. TESTS AND INVESTIGATIONS	27
2.1 Purpose and principles	29
2.2 Test #1 e #2	30
2.2.1 Materials used.....	30
2.2.2 Preparation of specimens.....	35
2.2.3 Test setup	37
2.2.3.1 Bending test	37
2.2.3.2 Compression test	39
2.2.3.3 Carbonation test	41
2.2.3.4 pH test	45
2.2.4 Test results.....	47
2.2.5 Interpretation of results	54
2.3 Test #3	57
2.3.1 Materials used.....	57
2.3.2 Preparation of specimens.....	60
2.3.3 Test setup	62
2.3.3.1 Compression test	62
2.3.3.2 Carbonation test	62
2.3.4 Test results.....	62
2.3.5 Interpretation of results	64
2.4 Test #4	66
2.4.1 Materials used.....	66
2.4.2 Preparation of specimens.....	66
2.4.3 Interpretation of results	70
3. CONCLUSION	73
4. BIBLIOGRAPHY.....	75
5. FIGURES AND TABLES LIST.....	77
6. ANNEX.....	81
ACKNOWLEDGEMENT.....	211

ABSTRACT

The increase of the global concentration of CO₂ in the atmosphere is largely attributable to the increasing use of fossil fuels for the production of energy. The construction sector is one of the largest producers of CO₂. Hence the need to find a solution to reduce emissions or to reuse the carbon dioxide produced in a circular economy system.

There are currently three different approaches to the use of CO₂ in cementitious compounds. A first approach in which CO₂ is inserted as an additive in the cement mix, a second that uses low-limestone aggregates and a third more commonly used that includes the possibility of inserting CO₂ into the fresh concrete cast.

This thesis aims to analyze the sustainability of concrete structures and to suggest a solution in the field of Civil Engineering to increase the reuse of CO₂. Tests were carried out on the mechanical properties to verify the mechanical and chemical performance due to the use of carbon dioxide in the concrete mix.

1. INTRODUCTION

1.1 SUSTAINABILITY AND ENVIRONMENTAL IMPACT

Population development and the ever-increasing demand for fossil fuel energy production have increased the level of carbon dioxide from an annual increase of 1.5 ppm between 1989 and 1990¹ to an increase of 2.5 ppm between 2018 and 2019². Coal, oil and natural gas are fossil fuels which, when burned, release large amounts of carbon dioxide into the atmosphere, faster than plants can accumulate through photosynthesis. Consequently, the excess of carbon dioxide and other greenhouse gases in the atmosphere gives rise to current climate changes in the form of global warming.

According to the World Green Building Council (World GBC) report buildings and the construction sector are responsible for 39% of all CO₂ emissions in the world, with operating emissions (from the energy used to heat, cool and light buildings) which account for 28%. The remaining 11% comes from embedded, or 'initial', CO₂ emissions associated with construction materials and processes throughout the building's entire life cycle³. Cement production alone, on the other hand, is responsible for around 5% of global CO₂ emissions⁴. In fact, cement is a material widely used in the construction sector for its easy production and for its reuse at the end of its life cycle. The latter is crushed and reused in other structures such as roads or bridges where it constitutes the filling material. Thanks to its good mechanical characteristics, it is the most used building material and an average consumption is estimated, for Italy, of two cubic meters per year per capita and globally of about one cubic meter per year per capita⁵.

However, such a vast use worldwide has a great environmental impact and this requires a decisive intervention through policies aimed at reducing emissions and making concrete a more sustainable material.

1.2 THREE DIFFERENT APPROACHES

Currently, the use of CO₂ in cement compounds has been implemented through three approaches:

- ⊗ Solidia;
- ⊗ Pre-Carbonation;
- ⊗ CarbonCure.

1.2.1 Solidia Cement

This approach consists in using carbon dioxide (CO₂) to harden the concrete. In this way, the new cement, called **Solidia Cement**, represents a challenge. It constitute an alternative cementitious binder with a lower CO₂ footprint than ordinary Portland cement, OPC. The

1 <https://www.oliveoiltimes.com/it/world/carbon-dioxide-levels-in-atmosphere-rise-for-seventh-consecutive-year/68451>

2 <https://ancler.com/noaa-rapporto-sullo-stato-del-clima-2019/>

3 <https://gbcitalia.org/web/guest/-/nuovo-report-del-world-gbc-il-settore-delle-costruzioni-puo-azzerare-le-emissioni-entro-il-2050>

4 G. Habert e N. Roussel, Study of two concrete mix-design strategies to reach carbon mitigation objectives, *Cement & Concrete Composites* (n°31 (2009) pp. 397–402).

5 www.cobeton.com

cement is based on **calcium silicate (CSC, calcium silicate cement)** and therefore forms a non-hydraulic binder that hardens with the carbonation reaction. The main components of CSC are low-limestone calcium silicates, including rankinite, wollastonite and pseudo-wollastonite. During carbonation, the CSC binder forms modified silica gel with calcium and CaCO_3 .

Thanks to a microscopic analysis of the CSC mixture, it was found that the silica gel phase indicates a substantially higher degree of polymerization than that of hydrated calcium silicates, C-S-H. Furthermore, the elastic modulus and hardness of this gel phase were found to be close to those of the high density C-S-H phase [1].

1.2.2 Pre-carbonation

The system consists in using CO_2 as an additive in the mixture of ordinary Portland concrete, OPC, in order to improve its performance through a new technique called “pre-carbonation method”. CO_2 is added to the concrete through a carbonation process of fresh or hardened concrete. The chemical carbonation process of concrete requires a high concentration of CO_2 . Through traditional methods it is not possible to administer CO_2 to the concrete during the casting in situ, therefore these methods allow to create only prefabricated structures. The pre-carbonation method allows you to bypass this limit by adding CO_2 in gaseous form directly into the fresh concrete mix.

The method initially involves absorbing the CO_2 in a mixture of cementitious material rich in calcium, and subsequently combining the mixture obtained with the aggregates to obtain concrete. This method has as its final product CaCO_3 particles which favor the hydration of the OPC cement. In particular, ettringite is formed which through the increase in volume generates a denser structure in favor of greater compressive strength [4].

1.2.3 CarbonCure

CarbonCure is a new technology with the aim of recycling CO_2 and reducing the carbon footprint of the concrete industry, without compromising its performance. CarbonCure integrates existing concrete plants with a system that introduces CO_2 gas into the concrete mix during production. When introduced, CO_2 undergoes a chemical reaction that chemically converts it into a solid mineral and makes the concrete more resistant.

According to the principle of circular economy, carbon dioxide comes from the chimneys of industrial emitters. The gas is purified and delivered in pressurized containers to the concrete production plant. Here the CO_2 is precisely injected into the concrete mix and reacts to form calcium carbonate, which is permanently embedded in the concrete. Furthermore, when the structure is demolished and pulverized, the gas will not be able to escape, because it no longer exists [6].

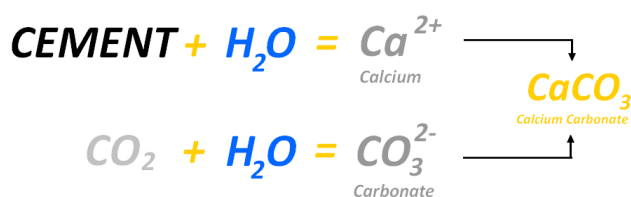


Figura 1.1 Reactions within the plant

Figure 1 shows the reactions that take place inside the plant. In addition to increasing the compressive strength of the concrete, the system does not affect its properties. Neither the properties of fresh concrete such as setting time, workability and air content, nor the properties of hardened concrete such as pH, density and the freezing-thawing effect are changed. CarbonCure is a technology that optimizes product mixing as it includes the reduction of the cement content and accelerated hydration by introducing economic and climatic advantages. On average a structure can be built with a reduction of the cement content of 4-8%. An observation should be made on the corrosion of the armor. Carbonation due to atmospheric agents occurs in concrete when calcium hydroxide compounds react with CO₂ contained in the atmosphere and form solid calcium carbonate. Depletion of calcium hydroxide causes the pH of the porous concrete solution to drop below 13, which can cause corrosion of the reinforcement. When CO₂ is injected into wet concrete using CarbonCure technology, CO₂ immediately reacts with the cement to form a solid calcium carbonate mineral, therefore, calcium carbonate does not affect reinforcement corrosion [7].

1.3 SOLIDIA CEMENT

1.3.1 Features

Solidia Cement was patented in 2015. It is a binder composed mostly of non-hydraulic calcium silicate minerals with low calcium content, such as wollastonite (CaO · SiO₂) and rankinite (3CaO · 2SiO₂). Calcium silicates with a low limestone content have the advantage of significantly reducing the carbon footprint compared to Ordinary Portland Cement OPC, as the production temperature of the clinker and the amount of limestone required are lower. The CSC requires a temperature of about 1200° C, which is about 250° C lower than that of the OPC.

Low-limestone calcium silicates have been observed to exhibit greater reactivity in the presence of CO₂. In fact, if subjected to carbonation, CSC paste can accumulate up to 17% (by mass) of CO₂ in the form of stable carbonates. Taking into account its CO₂ storage capacity, the low production temperature and the reduced need for limestone, CCSC calcium silicate concrete generates an overall CO₂ footprint of approximately 70% lower than that of OPC concrete. However, Solidia cement has one limitation, it can only be used for precast concrete products.

1.3.2 Absorption of CO₂

In figure 2 it is evident that as the polymerization time increases, the absorption of CO₂ also increases. It shows the mass curve of the low calcium content clinker samples, following the 48h CO₂ polymerization. The absorption of CO₂ increases rapidly in the first 6 hours, during which 60% of carbonation is already reached. It is observed that the maximum absorbed CO₂ value corresponds to 25.9% since the carbonation polymerization produces a layer of calcium carbonate on the surface of the samples which prevents further carbonation reaction [2].

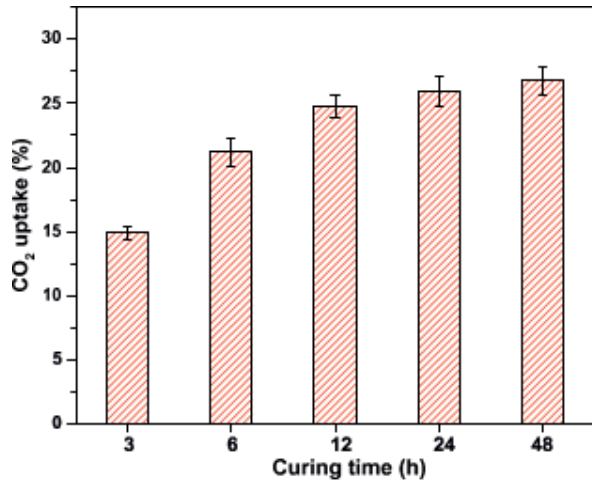


Figura 1.2 CO₂ absorption from low calcium clinker (Lu, B., Shi, C., & Hou, G, 2018)

1.3.3 Compression strength

Figure 3 shows the compressive strength of low calcium clinker samples depending on the hardening times of the carbonation.

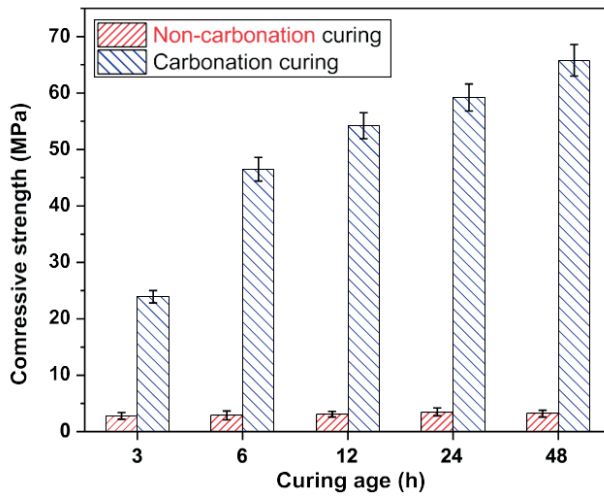


Figura 1.3 Compressive strength curve of low calcium clinker (Lu, B., Shi, C., & Hou, G, 2018)

It is clear that the resistance of samples subjected to accelerated polymerization with carbonation is far greater than that of samples not subject to carbonation. As in the CO₂ absorption process, here too it is noted that the compressive strength shows a rapid increase in the first hours of carbonation, until the value stabilizes at about 65 Mpa.

The increase in compressive strength is attributed to a much denser structure due to the formation of calcium carbonate and silica gel during polymerization with carbonation. In reality, it is the same calcium carbonate that slows down the increase in compressive strength in the following hours. On the other hand, the samples polymerized without carbonation show a constant and lower resistance since less calcium carbonate is formed which would have the task of welding the aggregates together.

To confirm this, it is observed that porosity is significantly reduced due to the carbonation polymerization. The comparison of the pore volume and the pore size distribution before and after the carbonation polymerization shows that both decrease. The diameter of the pores goes from 0.08 microns to 0.04 microns after 24h of polymerization with carbonation. This is attributable to the formation of CaCO₃ and silica gel which fill the pores and densify the microstructure, resulting in improved mechanical properties (Figure 4).

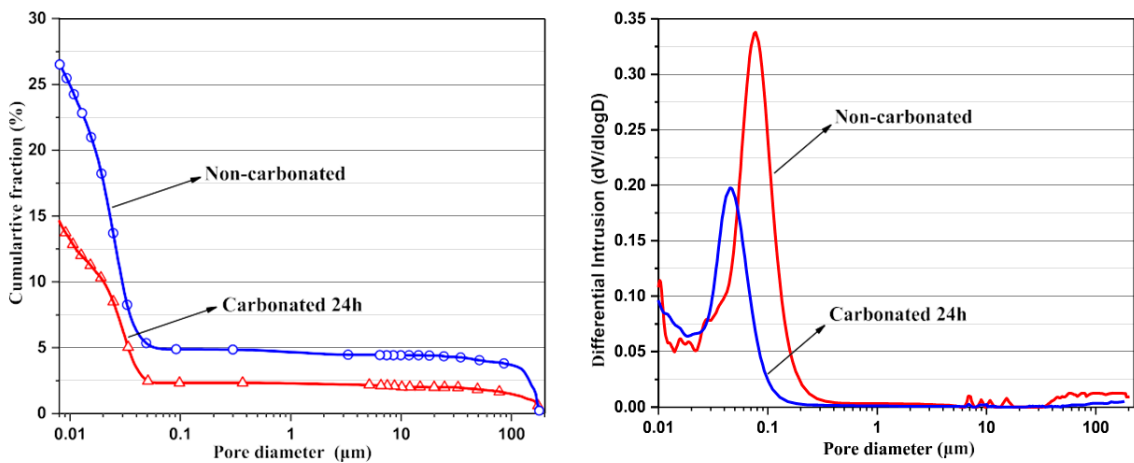


Figure 1.4 Differential curves of the pore size distribution of low calcium clinker pastes (Lu, B., Shi, C., & Hou, G, 2018)

1.3.4 Property comparison

It is interesting to compare the compressive strength with the degree of polymerization (percentage of CO₂ absorbed). It can be deduced that the resistance increases proportionally to the polymerization time, and in both cases the growth rate is regulated by the presence of calcium carbonate (Figure 5).

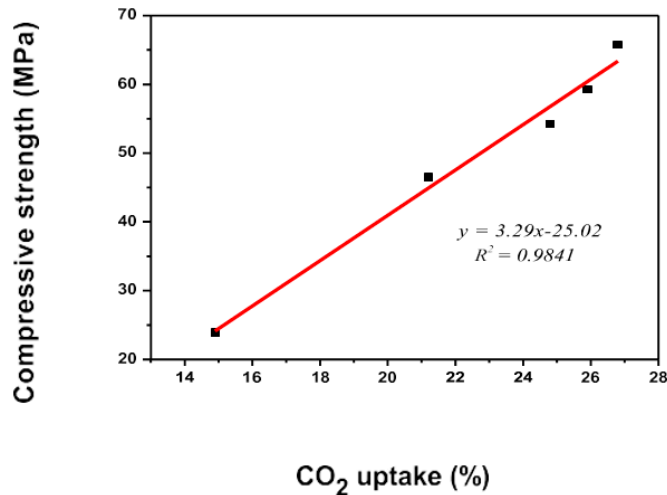


Figura 1.5 Relationship between the degree of CO₂ absorption and the compressive strength (Lu, B., Shi, C., & Hou, G, 2018)

1.3.5 Other properties

1.3.5.1 Reinforced concrete

A necessary consideration concerns the steel bars in the case of reinforced concrete. These are protected from corrosion by a thin layer of oxide which, due to the alkaline environment, forms on their surface. The carbonation reaction generates a gradual conversion of calcium hydroxide, Ca (OH) ₂, into CaCO₃, reducing the alkalinity of the concrete. Therefore, in the case of OPC concrete the reinforcing oxide layer will be more vulnerable to corrosion than CSC concrete. The accelerated polymerization of carbonation reacts with only 30% of the clinker minerals (ie producing less CaCO₃) without causing corrosion problems [2].

1.3.5.2 Thermogravimetric tests

The Thermal Decomposition Curve (Figure 6) demonstrates the non-hydraulic nature of the carbonated calcium silicate cement (CCSC) system as no substantial mass loss associated with the decomposition of Ca (OH)₂ is observed. The greatest mass loss, observed between 500 ° C and 900 ° C, is attributed to the decomposition of CaCO₃ and indicates the loss of water present both physically and chemically in the gel phases.

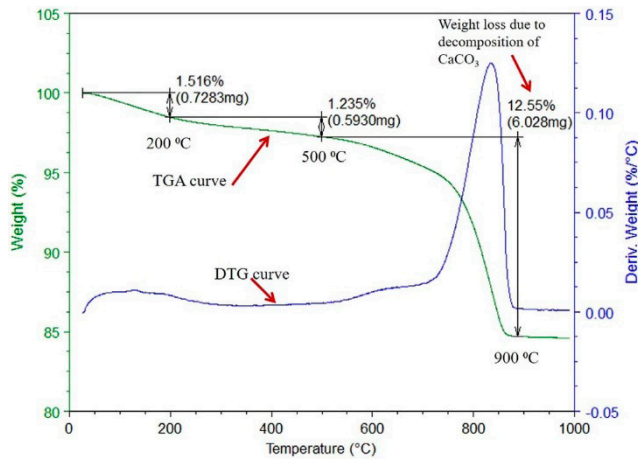


Figure 1.6 Thermogravimetric analysis chart for the CCSC paste sample (Ashraf, W., Olek, J., & Jain, J, 2017)

A thermogravimetric test was performed which consists in the continuous measurement over time of the mass variation of a sample of material as a function of time itself (isotherm) or temperature (heating / cooling ramp), in conditions of controlled atmosphere, inert, reducing or oxidant.

The result of this test, referred to as a Thermogram or Thermal Decomposition Curve, is represented by a graph where the Y axis reports the weight variation, in absolute or percentage value, and the X axis reports the time or temperature.

1.3.5.3 Elastic properties

Nanoindentation consists of a variety of indentation hardness tests (hardness of a material to deformation) applied to small volumes. It is the most common method for testing the mechanical properties of materials. It can also be used to determine the elastic properties of the microstructural phases present in the OPC system. The method determines the frequency distributions of the elastic properties (i.e. elastic modulus and hardness).

Figure 7 shows an example of analysis to determine the average elastic modulus of each microstructural phase present in the CCSC system, for a cementitious paste.

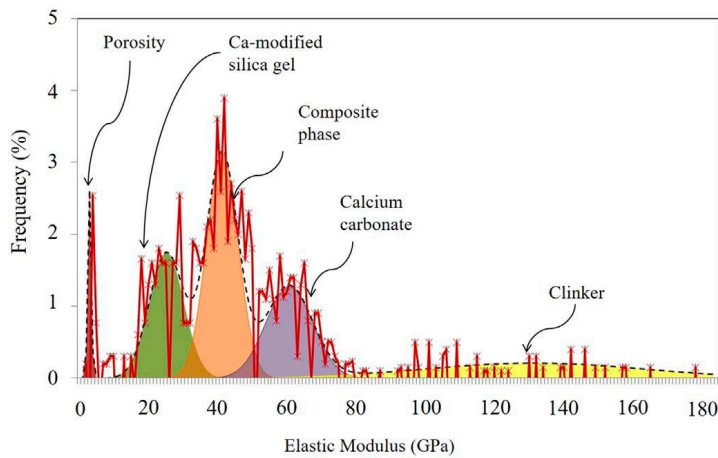


Figure 1.7 Elastic modulus frequency distribution graph for CCSC paste samples (Ashraf, W., Olek, J., & Jain, J, 2017)

Observing the figure it can be seen that for the CCSC system the remains of unreacted cement granules produce the highest values of elastic modulus while the highly porous region produces the lowest ones. Similar results are reported for hydrated OPC systems in which cement granules and porous regions are also associated with the highest and lowest elastic modulus values, respectively.

Five phases can be seen in the figure (porosity, calcium-modified silica gel, composite phase, calcium carbonate phase and unreacted cement grains). The distribution diagram was created through 5 modal Gaussian distribution functions to minimize the error between theoretical and experimental cumulative distribution functions.

1.3.5.4 Interfacial transition zone

The interfacial transition zone, ITZ, between the aggregate particles and the paste matrix determines the mechanical aspects and durability of the OPC concrete. The ITZ is considered the weakest area of the matrix as it has a high porosity (with respect to the mass volume) and the propensity to deposit Portlandite. If the size of the aggregate is greater, by an order of magnitude, compared to the concrete particles, there is no impact on the properties of the ITZ. In concrete, the surface of the grains of sand is much greater than the surface of the coarse aggregates, therefore the ITZ is associated with grains of sand. In the case of the CCSC paste, how does the properties of the ITZ that forms at the border between the grains of sand and the matrix change?

From the chemical composition point of view it should be noted that OPC samples usually have portlandite deposits around the aggregated particles. These deposits can constitute a “weak zone” for the microstructure of OPC mortar samples, due to the tendency to dissolve in the presence of water. In the CCSC mortar, on the other hand, there are no deposits of a particular microscopic phase around the aggregate, and this denotes greater resistance of the interfacial transition zone compared to concrete.

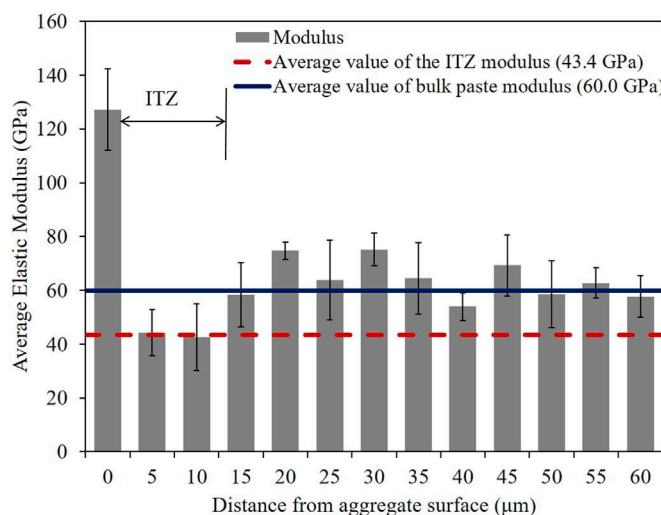


Figura 1.8 Variation of the elastic modulus along the IZ of CSCC samples (Ashraf, W., Olek, J., & Jain, J, 2017)

Also from the point of view of elastic properties, some studies have reported a comparison between OPC and CCSC. By carrying out the nanoindentation tests at the center of the surface of the grain of sand, the average elastic modulus was determined, equal to about 120 GPa. The average values of the elastic modulus calculated on the paste near the surface of the aggregate, are evaluated with respect to the perpendicular distance to the aggregate surface. They have an average value of the bulk pasta sample of 60 GPA, and an average value with respect to the surface of the aggregate, of 43.4 GPa which represents the average module of the ITZ for the CCSC system. And which corresponds to 72% of that of the bulk pasta region (dotted line). This attitude to have lower elastic modulus values close to the aggregate is also observed in hydrated OPCs. The lower values around a more rigid element are attributable to the “wall effect”, ie the alteration of the structure of the pores in that region. (Figure 8).

1.4 PRE-CARBONATION

1.4.1 The method

The pre-carbonation method, respect to Solidia cement, does not involve polymerization with carbonation. The polymerization requires a closed chamber, and this condition limits Solidia cement to the application of prefabricated concretes only. In addition, excessive polymerization with carbonation could destroy the hydrated calcium silicates and therefore reduce resistance. Therefore this method lends itself as an advantageous alternative not only to reduce the carbon footprint but to significantly improve its performance (strength and durability). To optimize CO₂ absorption, it is proposed to add CO₂ directly into the concrete mix. Considering that CO₂ is present in a gaseous state, absorbents are used to capture the CO₂, which are finally added to the mixture. Just to name a few, the materials for the absorption of CO₂ are calcium ash, slag from blast furnaces, dust from cement kilns and slaked lime, these being rich in calcium react with CO₂ to form calcium carbonate. The approach consists of two steps, the first involves making a mixture of cementitious material rich in calcium and water to form a mixture. The carbon dioxide is then bubbled into this suspension and reacting with the calcium ions forms a calcium carbonate mixture. The second step instead involves inserting the other ingredients into the mixture such as OPC concrete and aggregates that together form the final concrete. (Figure 9).

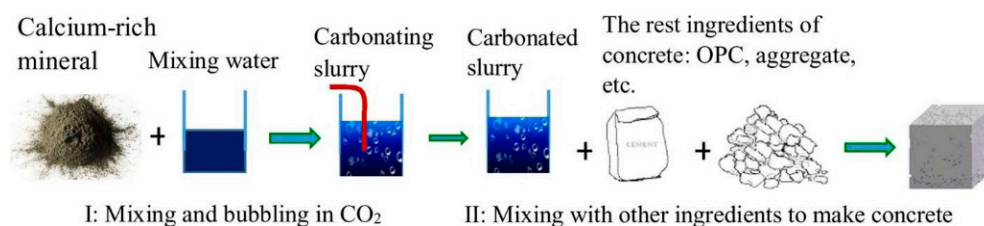


Figura 1.9 Production of concrete with the pre-carbonation method (Qian, X., Wang, J., Fang, Y., & Wang, L, 2018)

Carbonation occurs before the concrete casting, which is why the method is called pre-carbonation. In this way, the slow diffusion process of CO₂ in the concrete matrix is avoided. The polymerization process is no longer applied and therefore the closed polymerization chamber is no longer necessary, this guarantees the possibility of applying the method also in situ.

Among the different absorbents that can be used for CO₂, reference will be made to slaked lime since its carbonation reaction is easier to analyze, but any other absorbent can be used equally in the realization of concrete.

One study compared a control sample, without carbonation, and two different carbonate samples at 1% and 3% respectively. The latter two were obtained through a carbonation lasting 5 and 15 min respectively.

Through a scanning electron microscope it is possible to notice the difference between the two mixtures, it is observed that the 3% mixture has particles of precipitate larger than those produced by the 1% mixture. This is because in the case of 3% more time was required for the filtration of the precipitated particles, which consequently aggregated to form larger particles. These precipitate particles are formed of CaCO₃ calcite [5].

1.4.2 Hydration of cement

From figure 10 it can be seen that the cement paste produced from slaked lime with 1% carbonation reacts in a slightly longer time than the control sample. This is due to the reaction between the bicarbonate ions obtained from the carbonation mixture and the calcium ions released from the cement particles to produce CaCO₃. On the other hand, in the case of 3% carbonated slaked lime it is observed that the reaction occurs much earlier, it means, it can be anticipated. This is attributable to the formation of larger CaCO₃ particles which can accelerate the hydration of cementitious pastes. It can also be observed that neither limestone (limestone) nor slaked lime affect the hydration of the cement paste, so the carbonation in the case of slaked lime promotes the early hydration of the cement paste.

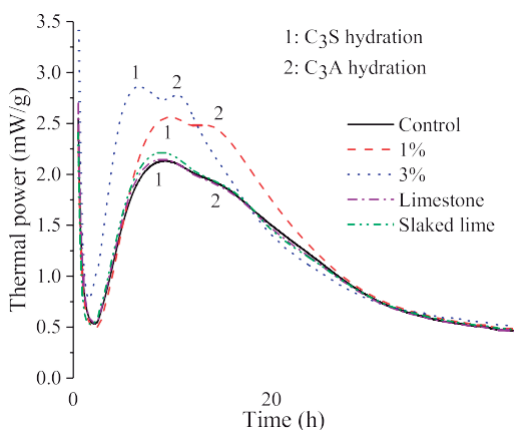


Figure 1.10 Effect of pre-carbonation on the hydration of the cement paste (Qian, X., Wang, J., Fang, Y., & Wang, L. 2018)

It has been observed that the addition of CO₂ in concrete changes the mineralogy of hydrated cement. In particular, more ettringite originates and stabilizes, more monocarbonate is generated and monosulfate is reduced or eliminated. The three variations favor the strength and durability of the concrete starting from the formation of ettringite which, increasing in volume, solidifies the concrete and reduces its porosity with a consequent increase in strength. The production of monocarbonate also increases the strength and stiffness of the concrete as its mass modulus is considerably higher than other hydration products. Finally, the reduction or elimination of the monosulfate increases the durability of the concrete because if the monosulfate is present it could transform into ettringite causing cracks in the matrix.

1.4.3 Compressive strength

From the analysis of the mechanical properties of compression and bending tests, the characteristics of cement mortars subject to 1% and 3% carbonation are highlighted by comparing them with the non-carbonate control sample. From the comparison it emerges that the pre-carbonation method greatly improves the compressive strength. (Figure 11).

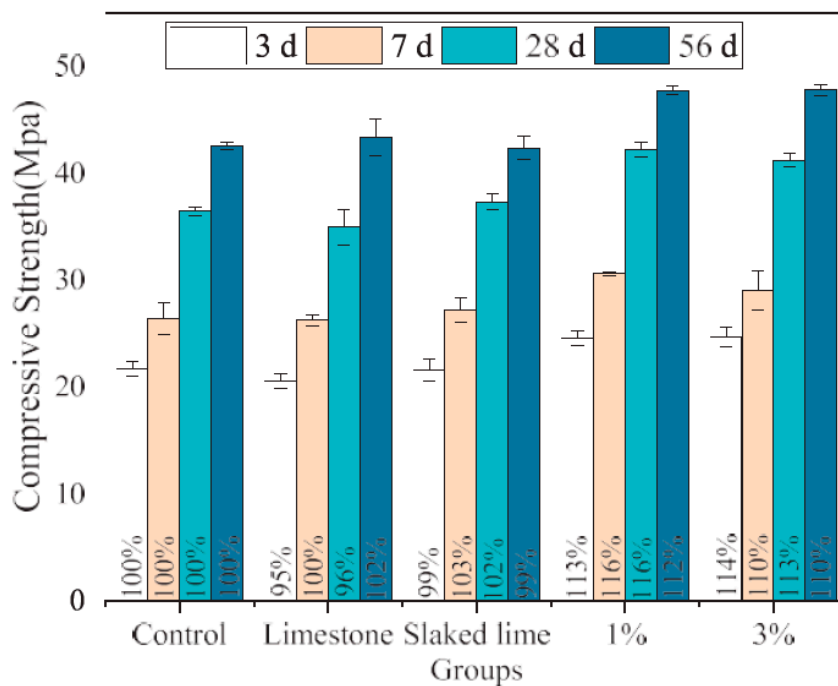


Figura 1.11 Compressive strength of cement mortars produced with different methods (Qian, X., Wang, J., Fang, Y., & Wang, L, 2018)

The compressive strength of the 1% group is higher than that of the control specimen both after a life of 3 days and after 7, 28 and 56 days. Conversely, without pre-carbonation, quicklime shows similar compressive strength to the control sample. Even if limestone is used instead of OPC, the compressive strength is similar or slightly reduced.

The increase in resistance is also present in the 3% group, slightly lower than in the 1% group, but this is attributed to the difference in the surface of the precipitate particles discussed above [5].

1.4.4 Flexural strength

Figure 12 shows the comparison between the flexural strength of the mortar of the control sample and the two mortars produced by pre-carbonation of the slaked lime mixture at 1% and 3%. It is found that in the case of the 1% and 3% groups also the flexural strength increases compared to the control sample.

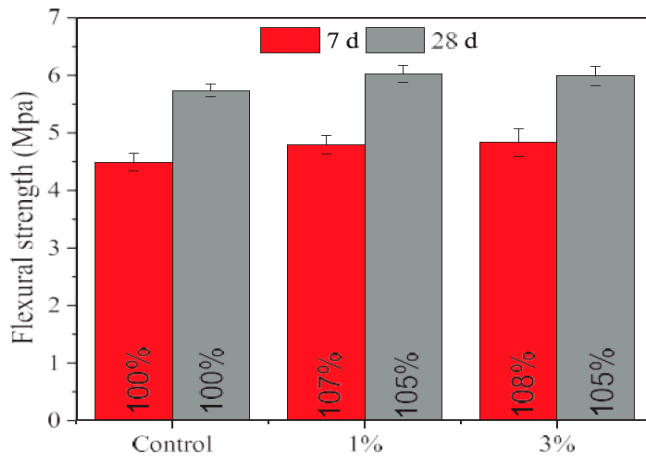


Figura 1.12 Flexural strengths of cement mortar samples produced with and without the precarbonation method (Qian, X., Wang, J., Fang, Y., & Wang, L, 2018)

It is interesting to note that the pH values are very similar between the 1% group and the control sample, this implies that the pre-carbonation does not affect the corrosion of the steel.

Finally, we can say that the precarbonation method improves the compressive and flexural strength of OPC-based mortar samples as it induces better hydration and produces a larger volume of the cement's hydration products. One of these products is ettringite which by filling the pores increases resistance.

1.5 CARBONCURE

1.5.1 CO₂ capture and storage

The cement and concrete industry has set itself the goal of optimizing production processes by following four methodologies:

1. Reduction of CO₂ emissions for the production of Portland cements through a greater use of alternative fuels and / or alternative raw materials (potentially 24% of the required reduction)
2. Improvement of the energy efficiency of cement kilns (10%)
3. Increase of clinker replacement through increased use of supplementary low carbon cementitious materials (SCM) (10%)
4. Carbon Capture and Storage (CCS) of carbon dioxide emissions released by cement factories (56%)

The first three methods have practical limits both with respect to the supply of cementitious material and with respect to the real possibility of reducing the energy required during production. As a result, most of the expected carbon reduction depends on the implementation of sequestration, storage and subsequent reuse technologies in concrete. At first, we tried to maximize the amount of CO₂ that can be sequestered and stored inside construction products and to contain the CO₂ gas supplied during the reaction, closed cells were used for hardening, this implies the construction of only prefabricated concrete. Later, given the limited amount of CO₂ that Portland cement can absorb, construction products based on binders that react with CO₂ were developed. This allows for greater absorption as this system can be integrated as a modernization in the typical production of concrete.

The guidelines for a sustainable concrete plant have outlined goals for improving its sustainability. The main goal is to reduce the carbon footprint, that is the amount of CO₂ emitted. For this purpose, it is necessary to take into account the production of concrete, the extraction of raw materials, the transport linked to the delivery to construction sites and any disposal or reuse.

The impact to improve the sustainability characteristics is evaluated in terms of one m³ of concrete. Greenhouse gas emissions associated with the transport of materials, the use of electricity and fossil fuels are also considered. In addition, the CO₂ produced to store and liquefy other CO₂, for transport, and that necessary to operate the CO₂ injection equipment must now be considered.

Once the CO₂ has been recovered, it must be liquefied for off-site transport or on-site storage. Carbon dioxide is commonly transported in tanks where it is compressed and liquefied at 2 MPa and -31.8 °C.

The treatment of industrial gases from which liquid CO₂ is obtained requires about 200 kWh / tonne of CO₂. This means that about 102 kg of carbon dioxide are emitted into the atmosphere to produce a ton of liquid CO₂. If we want to refer to m³, we can say that to produce a quantity of CO₂ of 482g / m³ of concrete, CO₂ emissions are estimated to be 49.4 g / m³.

The transport between the industrial source of CO₂ to the concrete producer involves an emissions rate of approximately 0.063 Kg CO₂ / tonne / Km. If we consider an average round trip distance of about 300 km, the emissions are calculated as 6.1 g of CO₂ / m³.

The gas injection equipment is made up of steel, brass and plastic. Considering the quantities used and the CO₂ emission factors associated with the production of these materials, an estimated CO₂ emission of 80.7 kg is obtained. The transport emissions associated with the delivery of a gas injection system amount to 12.3 kg of CO₂. However, it must be considered that the production of equipment and transport emissions are amortized over an operational life of 20 years and an annual production of 50,000 m³ of concrete, therefore the associated emissions are 0.09 g of CO₂ / m³ of concrete (of which 0.08 g from production and 0.01 from transport). The electricity required for the use of the equipment provides for the emission of 9.2 g of CO₂ / m³. Therefore the overall emission is estimated at 9.3 gCO₂ / m³.

Following the capture and storage of CO₂ it is possible to quantify how much CO₂ is actually absorbed. The carbon dioxide used in concrete is about 50% solid and 50% gas. If the

solid fraction, while adhering directly to the wet concrete, is incorporated into the concrete with a high efficiency (about 90%) that in the form of gas, which is heavier than air but remains above the concrete mix, it is incorporated at low efficiency (about 30%) then the overall combined absorption efficiency can be estimated at 60%.

However, excessive absorption of CO₂ can decrease the strength of the concrete. The optimal dose of carbon dioxide distributes over the nuclei of CaCO₃ homogeneously in the system while an excessive dose can compromise subsequent hydration. The reaction would initially occur in the pores, but after the continued addition of carbon dioxide there are more CO₂ ions in solution and the Ca²⁺ may not be replenished as fast as it is consumed. The carbon dioxide which reacts later can combine with Ca²⁺ preferentially located near or above the active dissolution sites rather than at a distance and in solution.

An alternative solution, which would seem to save energy and costs associated with the CO₂ separation and recovery process, involves the direct use of combustion gases. However, the reaction efficiency is lower since there is only a fraction of carbon dioxide available for the reaction at a given pressure and also the transport of the combustion gases would be unfavorable as they contain CO₂ in dilute form [8].

1.5.2 Cement saving

The addition of carbon dioxide allows a reduction of the cement load in the concrete. The concrete in turn has a carbon impact which is directly avoided both through the reduction of the material and the relative transport which is not required. The 5% reduction in cement means that 16.9 kg of cement are removed per m³ of concrete. Additionally, the fine aggregate (sand) load in the mix design can be increased to compensate for the volume of cement removed. The sand would have increased by 14.0 kg. It was calculated that the modified design mix would result in a net reduction in transport emissions of 124 g CO₂ / m³. The environmental impacts of 1 m³ of concrete are summarized in Figure 13.

Summary of the Environmental Impact on 1 cubic meter of concrete.

Factor	g CO ₂ / m ³ concrete
Emissions e CO ₂ from gas processing	49.4
Emissions e CO ₂ from gas transport	6.1
Emissions e CO ₂ from equipment production	0.1
Emissions e CO ₂ from equipment transport	0.0
Emissions e CO ₂ from equipment operation	9.2
Emissions e Avoided CO ₂ from materials transport	—123.6
CO ₂ AB: CO ₂ absorbed	—289.1
CO ₂ AV: Avoided CO ₂ emissions from cement	—17584.8
Total CO ₂ avoided and absorbed	—17997.4
CO ₂ EM: Total CO ₂ produced	64.7
Net CO ₂ reduction	—17932.7

Figura 1.13 Summary of the environmental impact of 1 m³ of concrete (Monkman, S., & MacDonald, M, 2017)

The environmental benefit associated with using less cement is an order of magnitude greater than the calculated direct CO₂ absorption. A generic cement in the United States has an emission intensity of 1040 kg CO₂ / ton of finished cement (Portland Cement Association, 2016). Cement reduction has a net environmental impact on the process given the avoided carbon dioxide emissions associated with cement production. There are 17.6 kg of CO₂ associated with the 16.9 kg of cement removed from each cubic meter of concrete. Cement emissions avoided would be responsible for 97.7% of the net environmental impact.

A generic case suggests that a 4.6% reduction in the carbon footprint is feasible. The energy and materials needed to implement the approach (construction of the equipment, capture of carbon dioxide, transport of the equipment and carbon dioxide) result in a small CO₂ emission which is less than the amount of CO₂ absorbed or in any case rapidly overcome by the environmental impact associated with the optimization of the mix design. Cement producers would then be able to use their CO₂ waste for beneficial use in concrete production, thereby recycling a portion of their primary waste product and using the resources in a way consistent with circular economy principles [13].

1.5.3 Compressive strength

The use of CO₂ as an additive in concrete was studied through a durability analysis on five different batches of fresh and hardened concrete. The first batch was used as a reference, the second contains a conventional accelerator mixture (without chlorides) and the other three are composed of increasing doses of CO₂. In the latter three, CO₂ was supplied for periods of 60, 90, and 120 s respectively.

The analysis found that the addition of CO₂ reduces the initial setting time by 40% and increases the compressive strength by 14% after one day and by 10% after three days compared to traditional concrete. On the contrary, the addition of the accelerator, despite the reduction in setting time, resulted in a lower initial resistance. As for durability, this has not been compromised by the addition of CO₂, so it can be concluded that CO₂ is a valid additive for improving the performance of concrete.

In the case of fresh concrete, it can be deduced that the use of CO₂ has not produced any change in the plastic properties (slump, air contents, temperatures and unit weights). On the hardening times, on the other hand, it can be observed that the conventional accelerating mixture reduced the initial setting time by 173 min (a reduction of 40%) and the final setting time by 162 min (a reduction of 33%). Doses of carbon dioxide reduced the initial hardening time between 95 and 118 min (22-28% reduction) and the final setting time by 104-126 min (21% and 25% reduction). The average CO₂ dose provided the greatest acceleration benefit among the carbon dioxide treated batches.

A reflection on the calorimetric results shows that (Figure 14) hydration, following the induction period, occurs earlier in all batches treated with CO₂ than the reference sample. In addition, the rate of hydration is comparable to that accelerated after the end of induction. Finally, it can be noted that the increase in the CO₂ dose corresponds to a lower release of thermal energy, a lower value in the graph, whereas the higher value corresponds to the mixture with accelerator. The integration of the power curves provides the cumulative heat of hydration.

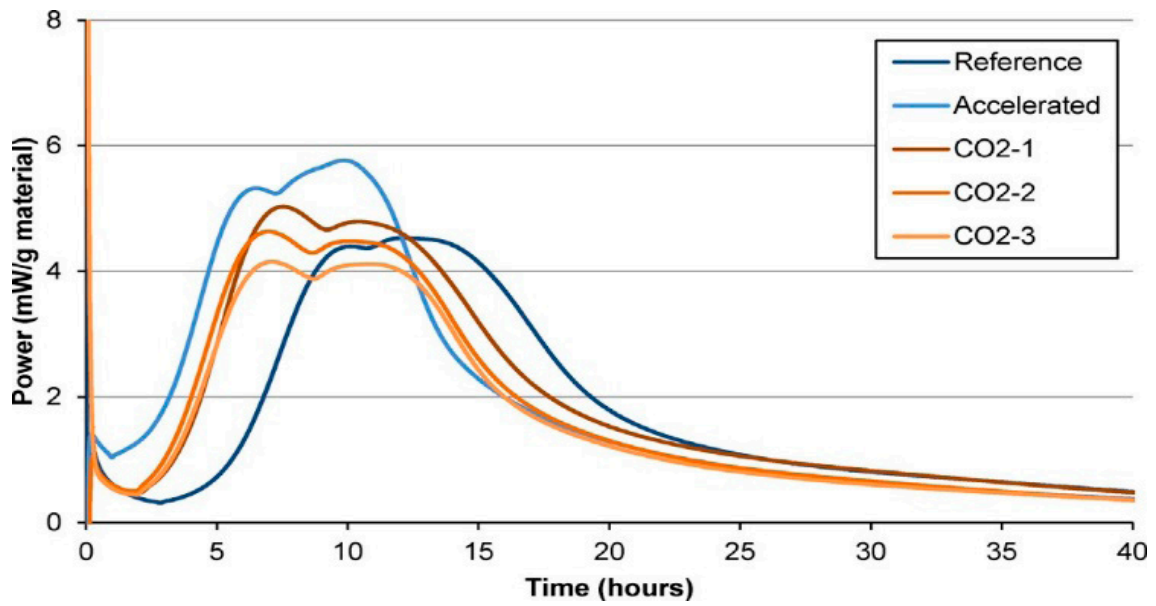


Figura 1.14 Conduction calorimetry (power curves) of sieved mortar samples (Monkman, S., MacDonald, M., Hooton, R. D., & Sandberg, P. 2016)

In the case of hardened concrete, compressive strength tests are carried out on the five batches, each of which represents the average of three samples. See figures 15 and 16.

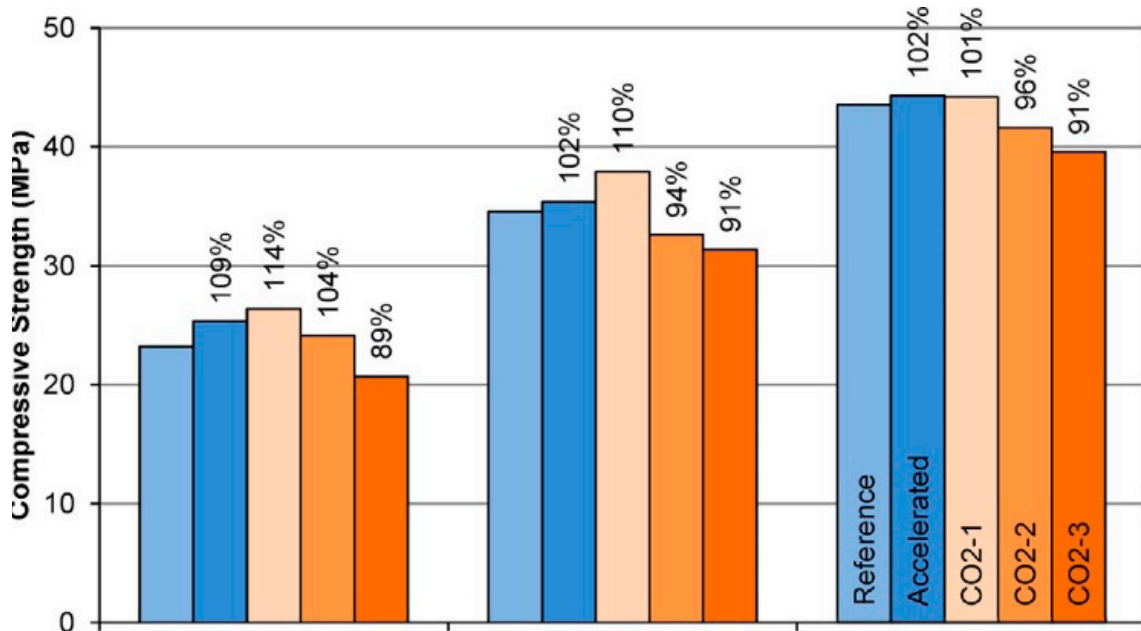


Figura 1.15 Compressive strength in the first age at 1, 3 and 7 days (Monkman, S., MacDonald, M., Hooton, R. D., & Sandberg, P. 2016)

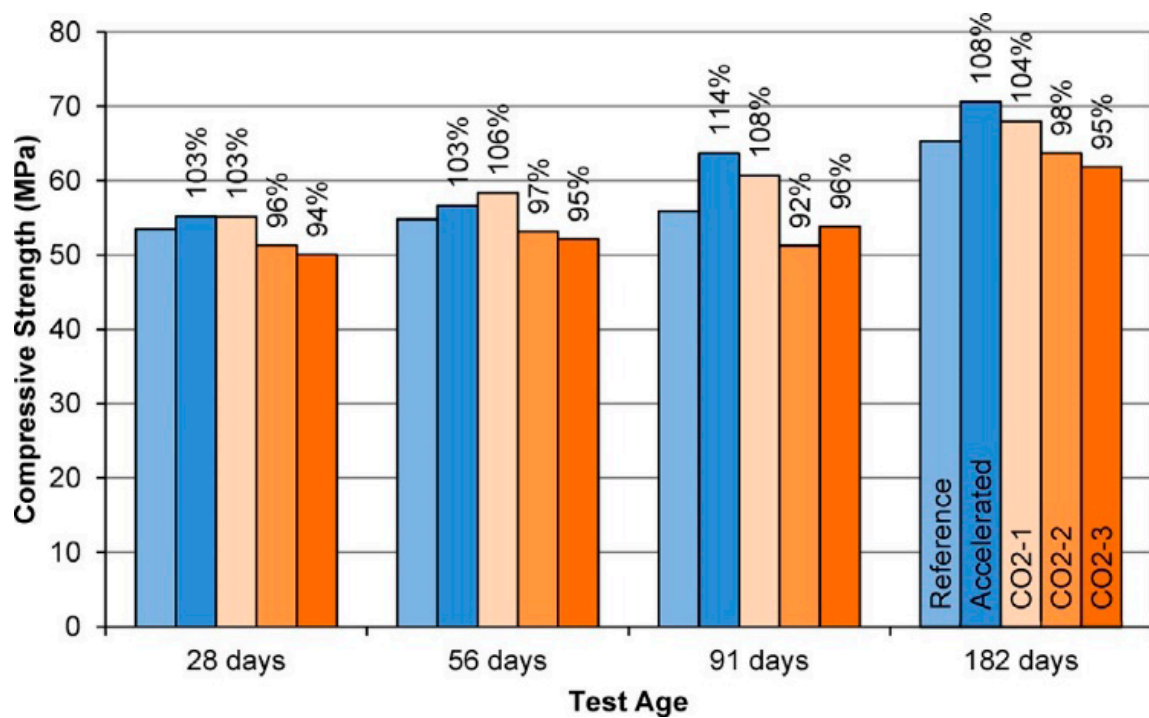


Figura 1.16 Compressive strength in old age at 28, 56, 91 and 182 days (Monkman, S., MacDonald, M., Hooton, R. D., & Sandberg, P, 2016)

Compressive strength measurements of CO₂-injected concrete batches revealed that the best results came from the lowest dose, which provided a 14% improvement in compressive strength for the cylinders tested at 1 day and 10% at 3 days.

The differences in the strengths of the concrete produced with the different doses of CO₂ reflect the potential level of sensitivity of the interaction between carbon dioxide and the binder system.

Concrete with the lowest CO₂ dose has been shown to have higher strength than concrete produced with the conventional accelerator at 1 and 3 days. Thereafter there was little difference between the two batches until the latter showed a benefit of 14% at 91 days and 8% at 182 days.

Finally, we can conclude that the cost of using a carbon dioxide injection as a stock accelerator is favorable compared to using a chloride-free accelerator, however, the accelerating effect of the CO₂ injection does not appear to be particularly high [9].

2.TESTS AND INVESTIGATIONS

2.1 PURPOSE AND PRINCIPLES

The goal of the work is to determine the compressive and flexural strength of specimens made with a cement mortar obtained by adding CO₂ in the form of dry ice.

In tests # 1 and # 2, compression and flexural strength tests were carried out and it was verified that the results comply with the EN 196-1 standard. Finally, for test # 1 the pH of the mortar was also analyzed through chemical tests.

The samples made are prismatic samples of 40 mm x 40 mm x 160 mm. The mortar preparation procedure involves mechanical mixing and pressing into a mold using a reference shaker apparatus. The samples are stored in the mold in a humid atmosphere for 24 hours and, after demoulding, the samples are stored under water until the resistance test. The difference between tests # 1 and # 2 consists in the different type of cement used (CEM I 42.5 and CEM I 52.5) and in the different amount of CO₂ added.

After 28 days, the specimens are removed from their wet storage, flexed to failure, determining flexural strength where required, and each half tested to determine compressive strength.

In test # 3, cubic formworks with dimensions of 70 mm x 70 mm x 70 mm were made. Also in this case the cement mortar was made through mechanical mixing and pressed into a mold through a vibrating device.

The samples during preparation were stored in the humidity-controlled laboratory for 24 hours and were subsequently removed and stored in a water tank for 28 days. Once hardened, they underwent compression tests and chemical tests.

In test # 4, samples of cement mortar with dimensions of 40 mm x 40 mm x 100 mm are made. The procedure used is similar to that of tests # 1 and # 2. Three different series were studied and compared, one used as a reference and consisting of cement only, another with the addition of CO₂ and the last one with the addition of carbon fibers.

2.2 TEST #1 E #2

2.2.1 Materials used

The cement mortar used in tests # 1 and # 2 was made through the composition of sand, cement, water and CO₂.

The sand used is a natural silica sand created from rounded particles and has a silica content of at least 98%. The quantity used was 1350 g per bag. (Figure 2.1).

According to the regulatory limits, its particle size distribution must respect the values indicated in table 1.

Tabella 1. CEN particle size distribution: Reference sand

SQUARE MESH SIZE [MM]	2.00	1.60	1.00	0.50	0.16	0.08
CUMULATIVE SIEVE RESIDUE [%]	0	7 ±5	33±5	67±5	87±5	99±1

The two tests are different in the type of cement used: in the first case the CEM I 42.5 cement is used and in the second case the CEM I 52.5 cement, both have the same composition but the second has a reduced particle size. (Table 2). All the cement was supplied by BuzziUnicem. (Figure 2.2).



Figura 2.2 Cement during weighing

Tabella 2 Cement composition [BuzziUnicem]

%	CEM I 42.5 R	CEM I 52.5 R
SiO ₂	20.2	19.9
Al ₂ O ₃	4.5	5.1
Fe ₂ O ₃	3.56	1.8
TiO ₂	0.2	0.2
MnO	0.07	0.06
P ₂ O ₅	0.06	0.04
CaO	63	62.9
SrO	0.03	0.04
MgO	1.44	1.6
K ₂ O	1.13	0.8
SO ₃	2.54	3.2
ppc	3.6	4.1
<hr/>		
Trattenuto a 24µm	38.7	21.1
Blaine (cm ² /g)	3600	4600



Figura 2.1 Sand used

Distilled water was used for packaging the samples. (Figura 2.3).



Figura 2.3 Water measurement



Figura 2.4 CO₂ in the package



Figura 2.5 CO₂ measurement

Carbon dioxide was supplied by SIAD in the form of dry ice. (Figures 2.4 and 2.5).

To have the right ratio between the components, the legislation requires to have: one mass portion of cement, three portions of standard CEN sand and one half by mass of water (water / cement ratio 0.50).

Each batch of three samples should consist of (450 ± 2) g of cement, (1350 ± 5) g of sand and (225 ± 1) g of water.

All samples created have the same mass ratios. The only parameter that differs is the amount of CO₂ introduced into the mortar for the different samples.

The following table shows the components of the mortar:

Tabella 3 Mortar components 29_01

SAMPLE	TYPE OF CEMENT	CEMENT (G)	WATER (G)	SAND (G)	CO ₂ (G)	% CO ₂ /CEM
29_01_00	N	450	225	1350	0	0
29_01_04	N	450	225	1350	1.8	0.4
29_01_08	N	450	225	1350	3.6	0.8
29_01_12	N	450	225	1350	5.4	1.2
29_01_16	N	450	225	1350	7.2	1.6
29_01_32	N	450	225	1350	14.4	3.2

Tabella 4 Mortar components - 31_05

SAMPLE	TYPE OF CEMENT	CEMENT (G)	WATER (G)	SAND (G)	CO ₂ (G)	% CO ₂ /CEM
31_05_00	N	450	225	1350	0	0
31_05_08	N	450	225	1350	3.60	0.8
31_05_16	N	450	225	1350	7.20	1.6
31_05_24	N	450	225	1350	10.8	2.4
31_05_32	N	450	225	1350	14.4	3.2
31_05_40	N	450	225	1350	18.0	4.0

After weighing all the components with the scale and checking the correct weight measurement, the mixing procedure was carried out according to the EN 196-1 standard (Figure 2.6). It includes the following steps:

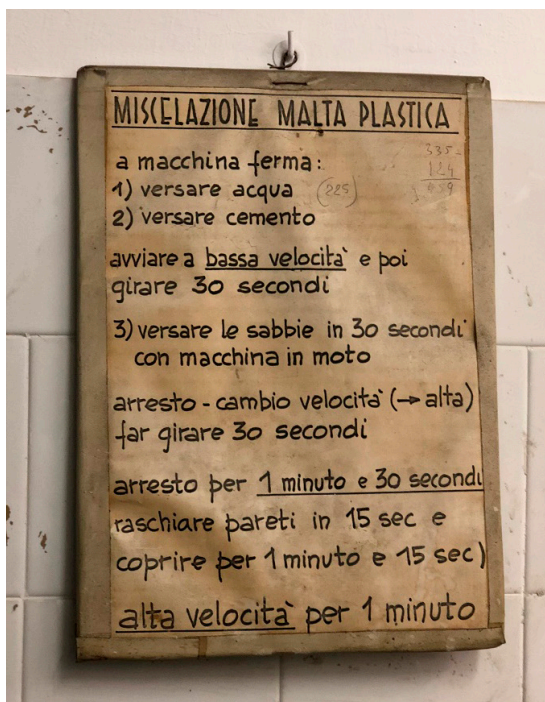


Figura 2.6 Rules for mixing in the laboratory of the Polvtechnic of Turin

1. Water and cement are placed in the bowl, taking care to avoid leaks.
2. Meanwhile, CO₂ is added
3. The mixer is then started at low speed and run for 30 seconds.
4. Sand is added over the next 30 seconds.
5. The system stops, the speed is changed to the highest speed, and is run again for 30 seconds.
6. The system shuts down for 90 seconds. During the first 30 seconds, the mortar attached to the wall and the bottom of the bowl is removed with a rubber or plastic spatula and placed in the center of the bowl; in the remaining minute the bowl is covered.
7. Continue mixing again for 60 seconds, before stopping the process.

To make the cement mortar, a stainless steel container with a capacity of up to 5 liters and standard shapes indicated in figure 2.7 is used. This is fixed to the mixer frame and the height of the blade is adjusted. The blade rotates around its own axis and can vary the speed thanks to an electric motor (Figures 2.8 and 2.9).

The speeds are defined by table 5:

Tabella 5. Speed of the mixer blade

	ROTATION MIN ⁻¹	PLANETARY MOVEMENT MIN ⁻¹
Low speed	140±5	62±5
high speed	285±10	125±10

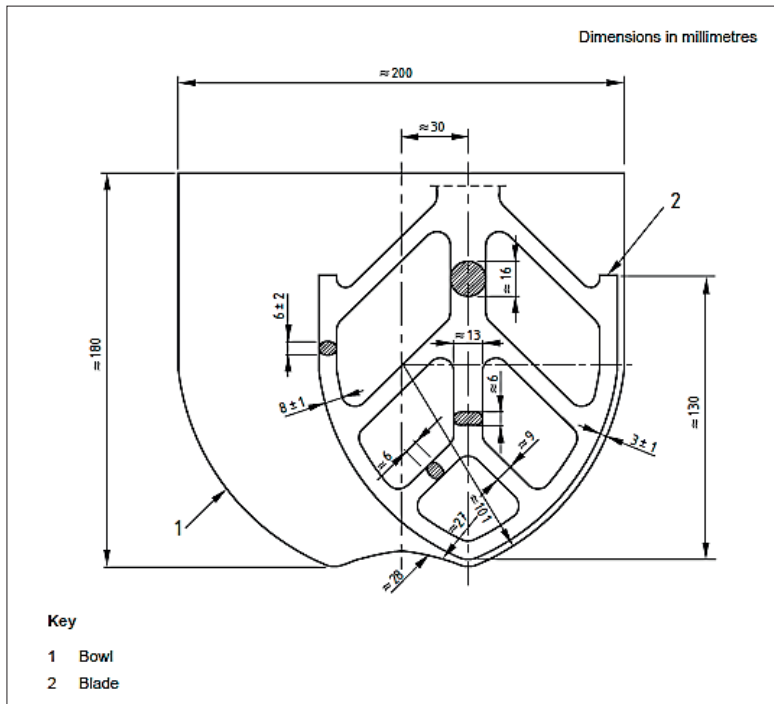


Figura 2.7 Bowl and blade



Figura 2.8 Mixer and blade in the laboratory



Figura 2.9 Mixing

2.2.2 Preparation of specimens

Once created, the mortar is introduced into the molds directly from the jug. The mold that was used is composed of three horizontal compartments so that three prismatic specimens with a section of 40 mm × 40 mm and length of 160 mm can be prepared simultaneously. The material of the mold is steel and the walls are about 10 mm thick. The mold design allows for easy and safe removal of samples. (Figure 2.10).

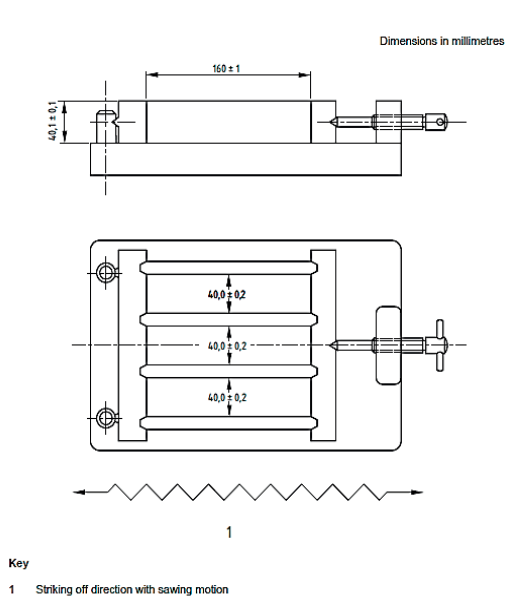


Figure 2.10 Specific mold

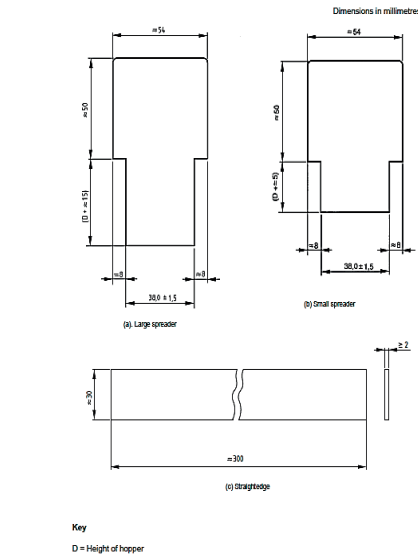


Figure 2.11 Specific metal spreader

According to regulations, the mold and its internal compartments have the following dimensions:

1. length: (160 ± 1) mm;
2. width: (40.0 ± 0.2) mm;
3. depth: (40.1 ± 0.1) mm.

To facilitate the filling of the mold it is necessary to provide a metal hopper well adhering to the vertical walls from 20 mm to 40 mm in height. When viewed on a flat surface, the walls of the hopper overlap the inner walls of the mold by no more than 1mm. The external walls of the hopper were equipped with positioning means to ensure correct positioning on the mold. A metal spreader must be used to spread and remove the excess mortar. (Figure 2.11).

Once assembled, the mold was then locked and fixed to a plate that belongs to an apparatus used for compaction. The contact between the plate and the mold must be adequate so as not to cause secondary vibrations. (Figure 2.12). The mold is filled in two stages, after the first layer has been laid and at the end of the second layer the samples are subjected to 60 pulses.

The shaking apparatus (Figure 2.13) consists of a rectangular plate rigidly connected by two light arms to a pin nominally 800 mm from the center of the plate. When the plate is initially placed it must be horizontal.

The operation consists in lifting the plate from a steel cam and letting it fall freely from a height of (15.0 ± 0.3) mm. The electric motor supplies about 250W of energy with a rotation

speed of one revolution per second. To count the beats there is a control mechanism and a counter which ensures that a period of (60 ± 3) s contains exactly 60 beats. The whole apparatus is mounted on a concrete block of about 600 kg.



Figura 2.13 The apparatus with regulatory measures

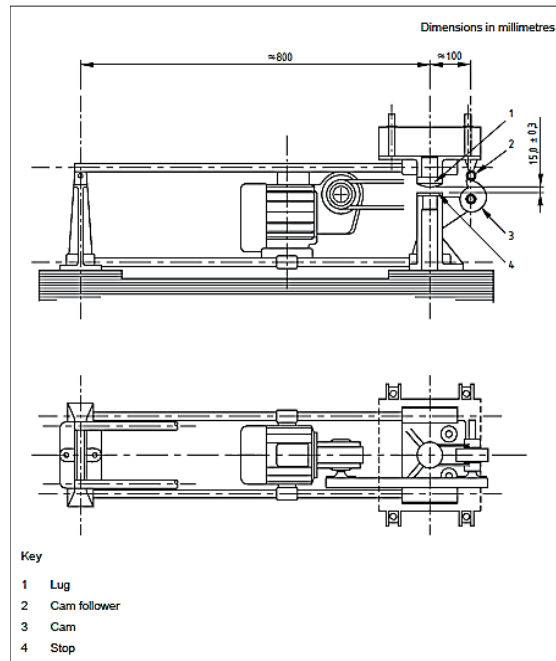


Figura 2.12 Shaking apparatus

During the preparation of the samples in the laboratory, a temperature of (20 ± 2) ° C and a relative humidity of not less than 50% was maintained. Instead, the storage of the samples in the mold took place in a humid chamber placed at a temperature of (20.0 ± 1.0) ° C and a relative humidity of not less than 90%.

Finally, hardening takes place in water maintained at (20.0 ± 1.0) ° C and the samples are placed on grids made with material that does not react with concrete and made so that the sample is completely surrounded by water. (Figure 2.14).

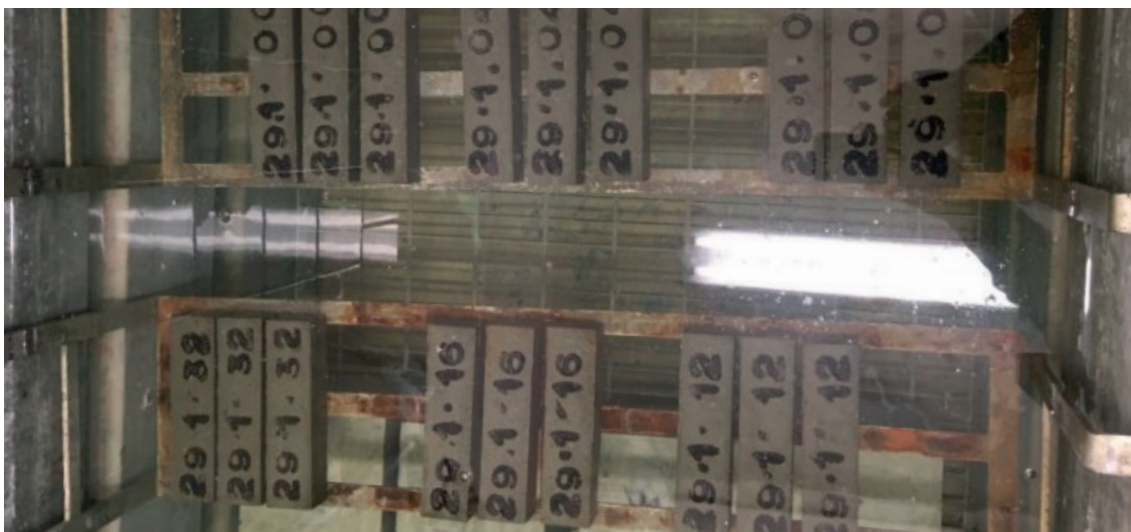


Figura 2.14 Samples in water

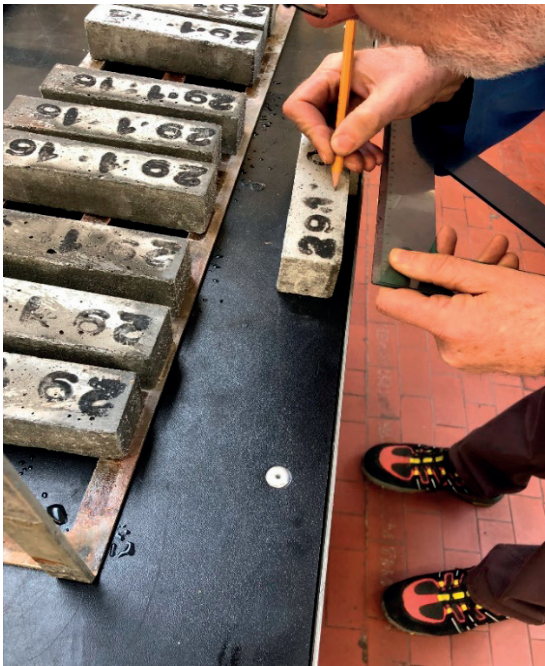


Figura 2.15 Samples after maturation

After 28 days, the samples were removed from the water and prepared for mechanical testing. (Figure 2.15).

2.2.3 Test setup

2.2.3.1 Bending test

In applied mechanics, bending characterizes the behavior of a slender structural element subjected to an external load, applied perpendicular to the longitudinal axis of the element.

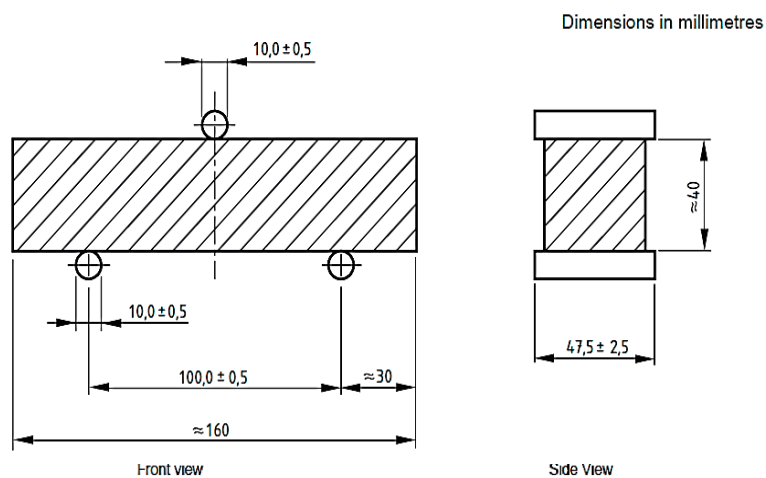


Figura 2.16 Arrangement of the load for the determination of the flexural strength

Flexural strength can be measured using a flexural strength testing machine which must meet certain requirements. It must be capable of applying loads up to 10 kN with an accuracy of $\pm 1.0\%$ of the registered load, at load speeds of $(50 \pm 10) \text{ N / s}$. It must also be equipped with a bending machine that incorporates two steel support rollers with a diameter $(10.0 \pm 0.5) \text{ mm}$ spaced apart $(100.0 \pm 0.5) \text{ mm}$ and a third steel load roller of the same diameter placed centrally between the other two. The length of these rollers must be between 45mm and 50mm. The loading arrangement is shown in Figure 2.16.

The three vertical planes passing through the axes of the three rollers must be parallel and remain parallel, equidistant and normal with respect to the direction of the specimen under examination. One of the support rollers and the loading roll must be slightly inclined to allow for even distribution of the load across the width of the sample without subjecting it to torsional stress. (Figure 2.17).



Figura 2.18 Sample in the bending machine



Figura 2.17 Flexural strength apparatus



Figura 2.19 Sample in the bending machine

The specimen is positioned in the equipment with a side face on the support rollers and with its longitudinal axis normal to the supports. The load is applied vertically through the loading roller on the opposite side face of the prism and gradually increased at the rate of $(50 \pm 10) \text{ N / s}$ until failure. (Figures 2.18 and 2.19).

2.2.3.2 Compression test

Compressive strength is the ability of a material or structure to withstand loads tending to reduce size, as opposed to tensile strength, which tends to stretch the specimen. Compressive strength is one of the most important engineering properties of concrete. It is standard industry practice for concrete to be classified based on compressive strength.

The testing machine for determining the compressive strength is shown in Figure 2.20 and provides a rate of load increase of $(2400 \pm 200) \text{ N / s}$. The vertical axis of the piston will coincide with the vertical axis of the machine and during loading the direction of movement of the piston will be along the vertical axis of the machine. Furthermore, the resulting force will pass through the center of the sample.

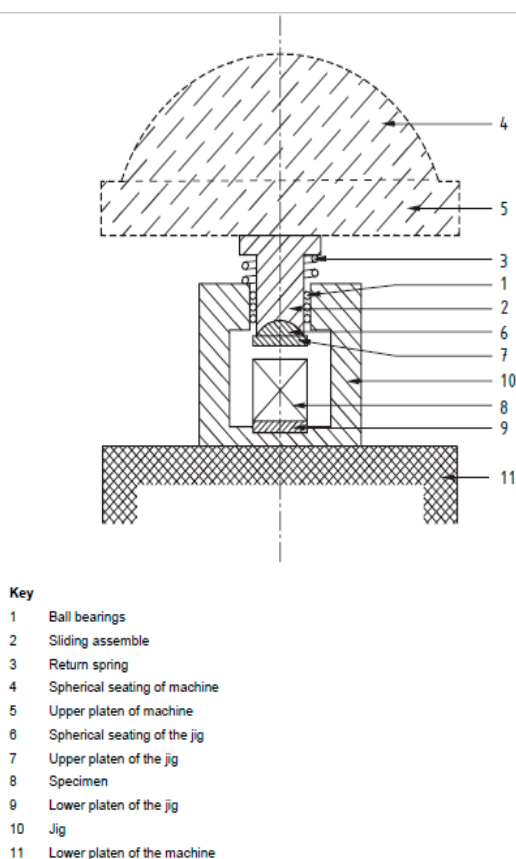


Figure 6 — Typical jig for compressive strength testing

Figura 2.20. Typical structure for compressive strength testing

The test is performed by taking the two halves of the sample broken in the bending test.

The load is placed on each half of the prism. The center of the prism is centered to the sides of the machine plates within ± 0.5 mm and longitudinally so that the front surface of the prism protrudes approximately 10 mm over the plates or auxiliary plates. (Figures 2.21 and 2.22).

The load is increased uniformly at the rate of (2400 ± 200) N / s for the entire load application until failure. (Figures 2.23 and 2.24).



Figura 2.21 Compressive strength machine



Figura 2.22 Compressive Strength Machine Sample



Figura 2.23 Fractured specimen



Figura 2.24 Compressive Strength Machine Sample

2.2.3.3 Carbonation test

The test was conducted at the DISAT department of the Politecnico di Torino. The aim is to obtain the quantity of calcium carbonate (CaCO_3) present in a mixture of calcium carbonate and silica, by measuring the volume of gas developed by the following reaction:



The carbon dioxide formed accumulates in the upper part of the calcimeter, the percentage of calcium carbonate in the sample can be calculated by measuring the quantity of carbon dioxide, expressed in moles. In fact, as can be seen from the reaction, one mole of CO_2 is formed per mole of CaCO_3 reacted.



Figura 2.25 Sample after mechanical tests

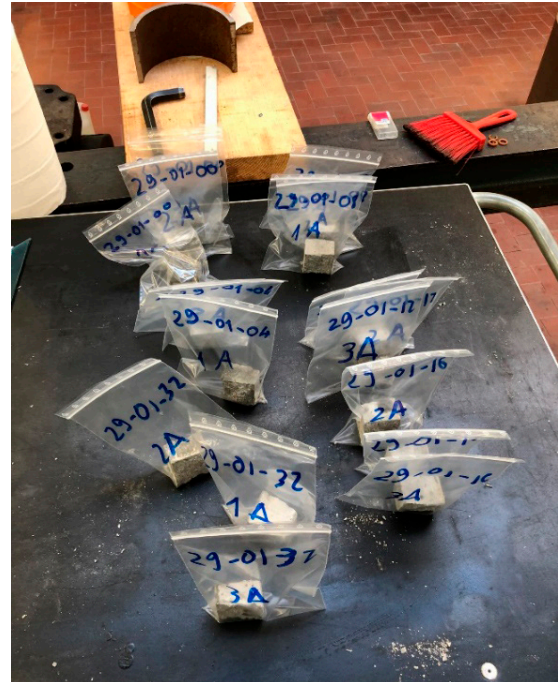


Figura 2.26 All sample before chemical tests

The test was performed using the calcimeter. This instrument is composed of two parallel metal rods that act as support, a test tube for storing the reagent, a graduated glass cylinder from 0 to 200 ml, a leveling tank, a coil that connects the two vessels. It uses the principle of communicating vessels and the ability of a gas to move volumes of water, allowing the direct reading of calcium carbonate expressed as a percentage. (Figure 2.27).



Figura 2.27 Calcimeter



Figura 2.28 Liquid level in the calcimeter



Figura 2.29 Measurement of HCl

The procedure used is the following:

1. The calcimeter is zeroed by moving the smaller non-graduated cylinder so that the liquid level is equal to zero on the graduated cylinder. This is possible thanks to the opening of the valve which allows to have the same pressure in the two cylinders. (Figure 2.28).
2. 0.5 g of the $\text{CaCO}_3 + \text{SiO}_2$ mixture is introduced into the bottle, after being pulverized. (Figures 2.25 and 2.26).
3. 5 ml of diluted hydrochloric acid (HCl) is measured and placed in a test tube. (Figure 2.29).
4. The test tube is inserted into the glass bottle taking care not to overturn it
5. The glass jar is then closed with a hermetic rubber stopper, taking care not to let the HCl content escape from the inside of the tube
6. The valve is closed in the upper part of the graduated cylinder
7. The mixture is then stirred causing the HCl to react and developing carbon dioxide.
8. The volume of CO_2 developed causes the water level to drop in the graduated cylinder. To restore balance and eliminate the depression that has been generated, the opposite cylinder is operated, lowering it until the two levels coincide. After a few minutes, thanks to the principle of communicating vessels, the levels will stabilize and it will be possible to read the value that represents the quantity of CO_2 developed.
9. Thanks to the state law of ideal gases it is possible to obtain the quantity of molar calcium carbonate present, this is then converted into grams and finally into a percentage by weight:

$$PV = nRT$$

Where is it:

1. P is the gas pressure,
2. V is the volume of the gas,
3. n is the amount of substance in the gas (also known as the number of moles),
4. R is the ideal, or universal gas constant, equal to the product of Boltzmann's constant and Avogadro's constant,
5. T is the absolute temperature of the gas.

From the moles it is possible to trace the grams and therefore the percentage of CaCO_3 . (Tables 6 and 7).

Tabella 6 % CaCO₃ in sample 29_01

SAMPLE	%CO2	%CACO3
	0	5.90
29_01_00	0	4.70
	0	3.50
	0.40	5.40
29_01_04	0.40	5.50
	0.40	6.00
	0.80	6.10
29_01_08	0.80	4.60
	0.80	5.30
	1.20	7.00
29_01_12	1.20	6.20
	1.20	7.00
	1.60	7.40
29_01_16	1.60	8.10
	1.60	6.80
	3.20	6.60
29_01_32	3.20	6.70
	3.20	7.30

Tabella 7 % CaCO₃ in sample 31_05

SAMPLE	%CO2	%CACO3
	0	6.10
31_05_00	0	5.31
	0	5.60
	0.80	5.69
31_05_08	0.80	5.54
	0.80	6.23
	1.60	7.20
31_05_16	1.60	6.57
	1.60	5.78
	2.40	5.85
31_05_24	2.40	5.76
	2.40	6.70
	3.20	6.73
31_05_32	3.20	6.00
	3.20	4.76
	4.00	5.85
31_05_40	4.00	6.53
	4.00	7.23

2.2.3.4 pH test

The pH measurement was performed only for samples 29_01 and using an automatic digital water meter. The method consists in adding 10 g of the crushed mixture into a polypropylene cylinder containing 100 g of distilled water. (Figures 2.30, 2.31 and 2.32).



Figura 2.30 Samples ready for testing

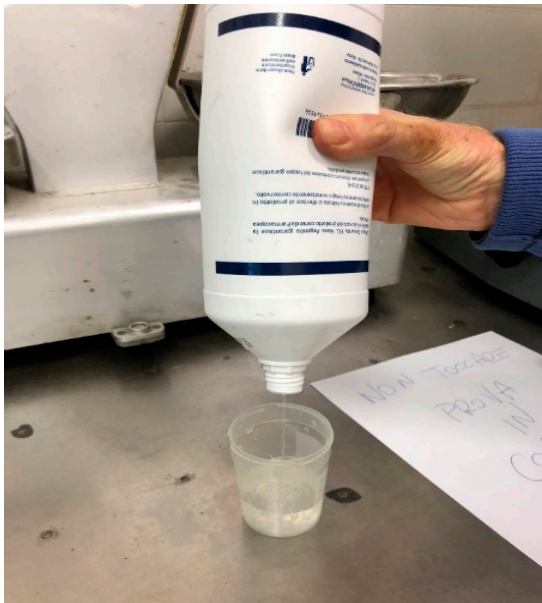


Figura 2.31 Distilled water



Figura 2.32 pH test instrument

The pH tests were performed on three different days. The laboratory temperature was also recorded. (Table 8 and Figure 2.33).

Tabella 8 Results of the pH test

SAMPLE	%CO ₂	13-MAG	15-MAG	20-MAG		
29_01_00	1A	0	12.15	12.29	12.38	12.27
	2A	0	12.15	12.31	12.37	12.28
	3A	0	12.15	12.29	12.31	12.25
29_01_04	1A	0.4	12.19	12.32	12.29	12.27
	2A	0.4	12.16	12.28	12.28	12.24
	3A	0.4	12.13	12.30	12.26	12.23
29_01_08	1A	0.8	12.18	12.31	12.28	12.26
	2A	0.8	12.16	12.32	12.31	12.26
	3A	0.8	12.16	12.31	12.31	12.26
29_01_12	1A	1.2	12.15	12.30	12.26	12.24
	2A	1.2	12.16	12.29	12.23	12.23
	3A	1.2	12.18	12.31	12.29	12.26
29_01_16	1A	1.6	12.19	12.30	12.27	12.25
	2A	1.6	12.16	12.31	12.25	12.24
	3A	1.6	12.18	12.29	12.24	12.24
29_01_32	1A	3.2	12.05	12.29	12.24	12.19
	2A	3.2	12.10	12.29	12.25	12.21
	3A	3.2	12.18	12.30	12.26	12.25
Temperature			21.5 °C	21.8°C	21.7°C	

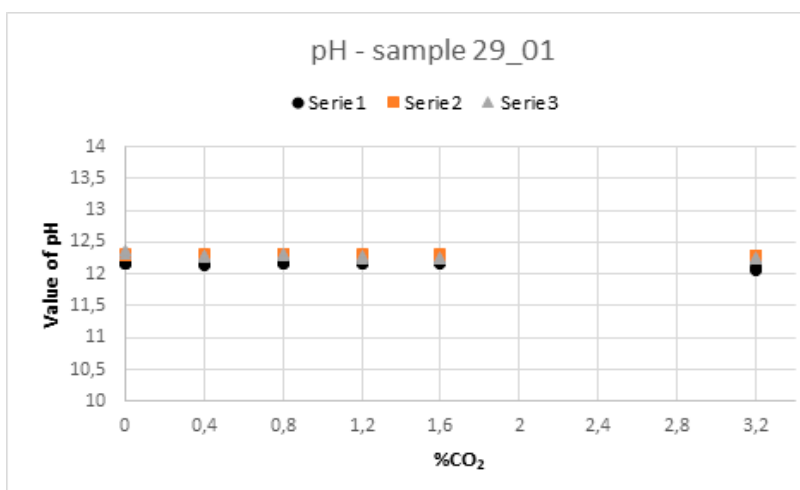


Figura 2.33 pH in sample 29_01 in 3 different days

2.2.4 Test results

Flexural strength

The results of the flexural strength are shown in Tables 9 and 10 and in Figures 2.34 and 2.35. With the classic formula it is possible to evaluate the flexural strength:

$$\sigma = \frac{M}{W} = \frac{PL6}{4BH^2}$$

Where:

1. M = maximum bending moment
2. W = section
3. P = applied load
4. L, B, H = specimens size

All results for each individual sample are in Appendix 7.1.

Tabella 9.

Results of bending strength 29_01

FLEXURAL STRENGTH		
SAMPLE	% CO ₂ /CEM	Σ _{FLEX} [MPA]
		7.51
29_01_00	0	6.94
		6.27
		0.00
29_01_04	0.4	6.84
		6.51
		6.04
29_01_08	0.8	6.02
		7.05
		6.53
29_01_12	1.2	6.88
		6.61
		6.22
29_01_16	1.6	6.72
		6.86
		6.61
29_01_32	3.2	6.70
		6.42

Tabella 10.

Flexural strength 31_05

FLEXURAL STRENGTH		
SAMPLE	% CO ₂ /CEM	Σ _{FLEX} [MPA]
		7.10
31_05_00	0	7.92
		7.47
		7.54
31_05_08	0.8	7.66
		7.94
		7.42
31_05_16	1.6	7.29
		-
		6.64
31_05_24	2.4	7.47
		6.81
		7.08
31_05_32	3.2	7.08
		6.69
		7.28
31_05_40	4	6.45
		6.54

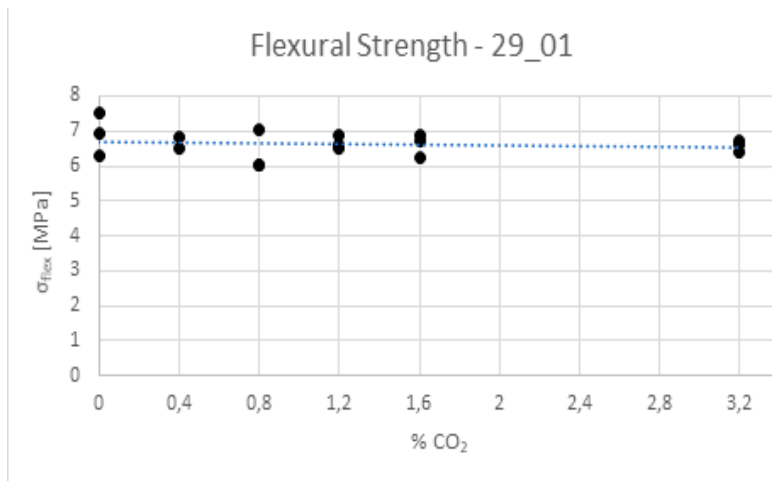


Figura 2.34 Flexural strength 29_01

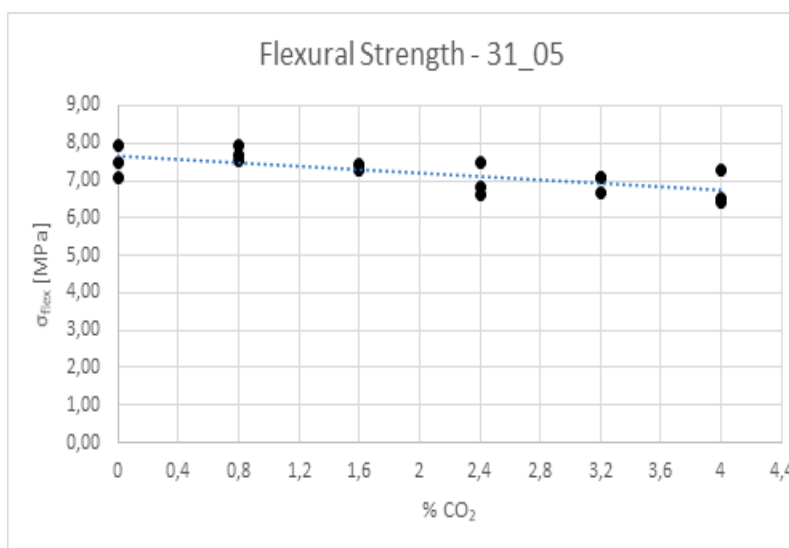


Figura 2.35 Flexural strength 31_05

Compressive strength

The results of the compressive strength are shown in Tables 11 and 12 and in Figures 2.36 and 2.37. The machine measures the force F with which the specimen breaks, which divided by the area A of the specimen, leads to the measurement of the compressive strength:

$$\sigma = \frac{F}{A}$$

All results for each individual sample are in Appendix 6.

Tabella 11. Compression test - 29_01

COMPRESSIVE STRENGTH			
SAMPLE	% CO2/CEM	$\Sigma 1$ [MPa]	$\Sigma 2$ [MPa]
29_01_00	0	54.64	46.58
		44.77	42.11
		43.15	41.71
29_01_04	0.4	34.48	41.55
		44.38	45.33
		43.51	46.72
29_01_08	0.8	38.84	44.46
		41.26	40.48
		41.10	44.19
29_01_12	1.2	42.82	41.47
		43.35	45.39
		44.45	42.93
29_01_16	1.6	43.41	44.63
		42.74	44.72
		41.68	42.63
29_01_32	3.2	41.75	41.44
		44.02	42.47
		40.60	41.35

Tabella 12. Compression test - 31_05

COMPRESSIVE STRENGTH			
SAMPLE	% CO2/CEM	$\Sigma 1$ [MPa]	$\Sigma 2$ [MPa]
31_05_00	0	58.90	59.32
		59.18	62.19
		60.31	58.55
31_05_08	0.8	57.97	58.57
		59.40	58.90
		60.72	61.53
31_05_16	1.6	56.57	57.30
		56.71	58.30
		57.23	57.35
31_05_24	2.4	59.12	57.70
		61.12	59.65
		62.10	58.79
31_05_32	3.2	58.33	59.99
		58.96	56.45
		58.36	55.79
31_05_40	4	56.58	54.43
		59.51	59.59
		58.92	60.05

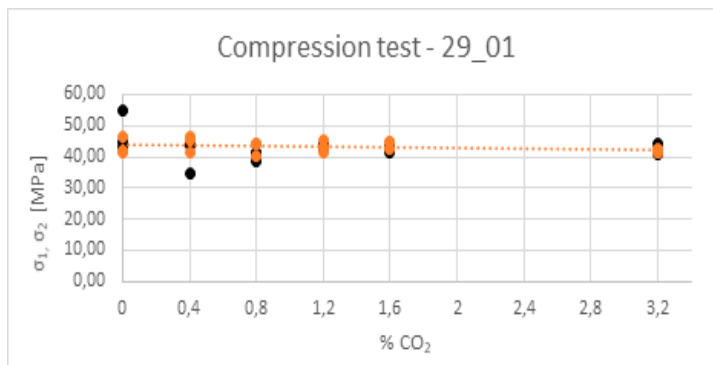


Figura 2.36 Compression test - 29_01

W

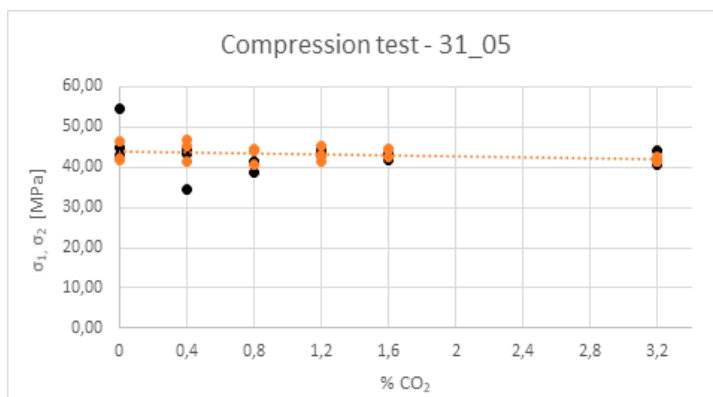


Figura 2.37 Compression test - 31_05

Carbonation test

The results of the calcimetry tests are shown in figures 2.38 and 2.39:

Specimen 29_01:

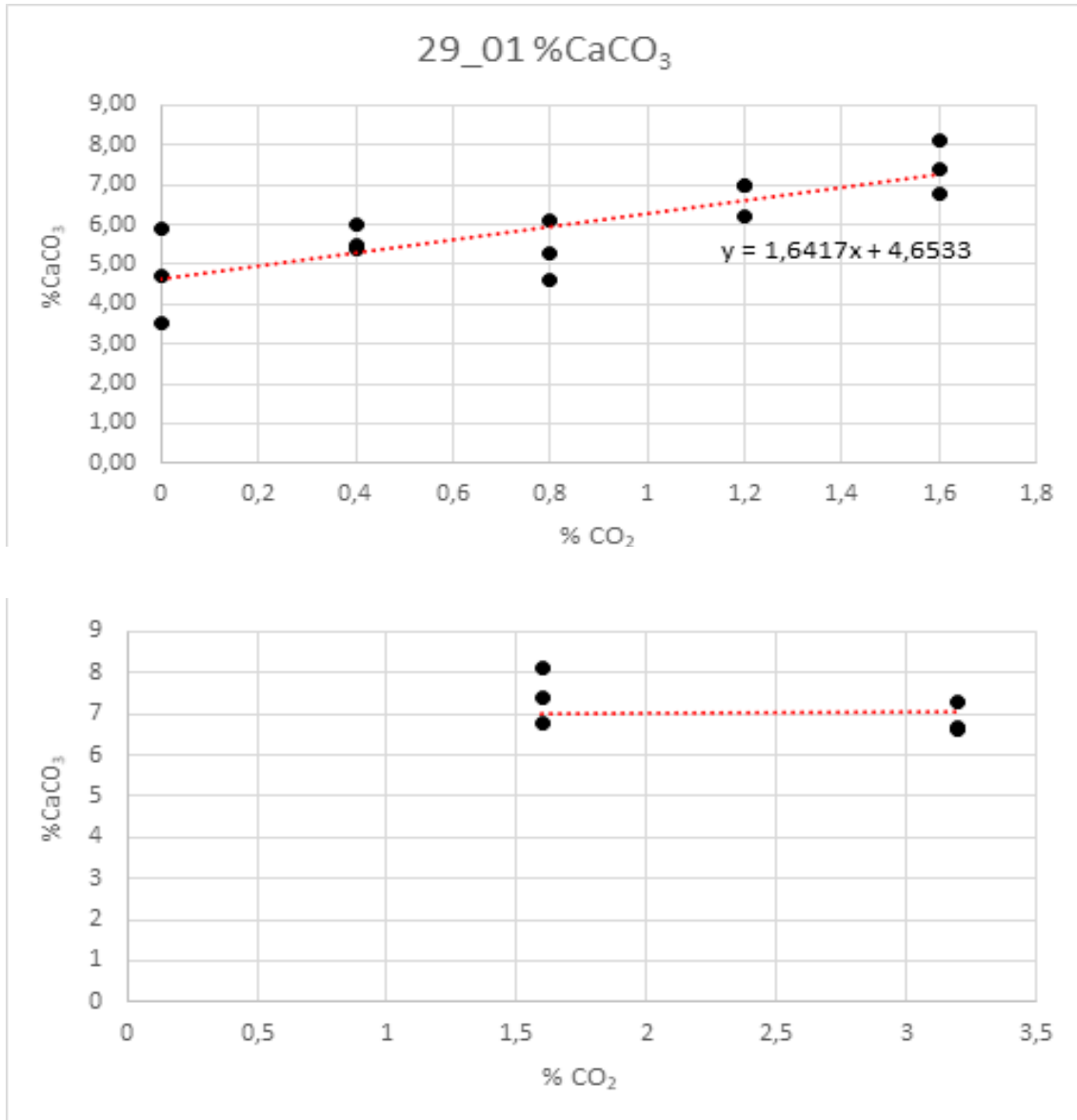


Figura 2.38 %CaCO₃ - 29_01

Specimen 31_05:

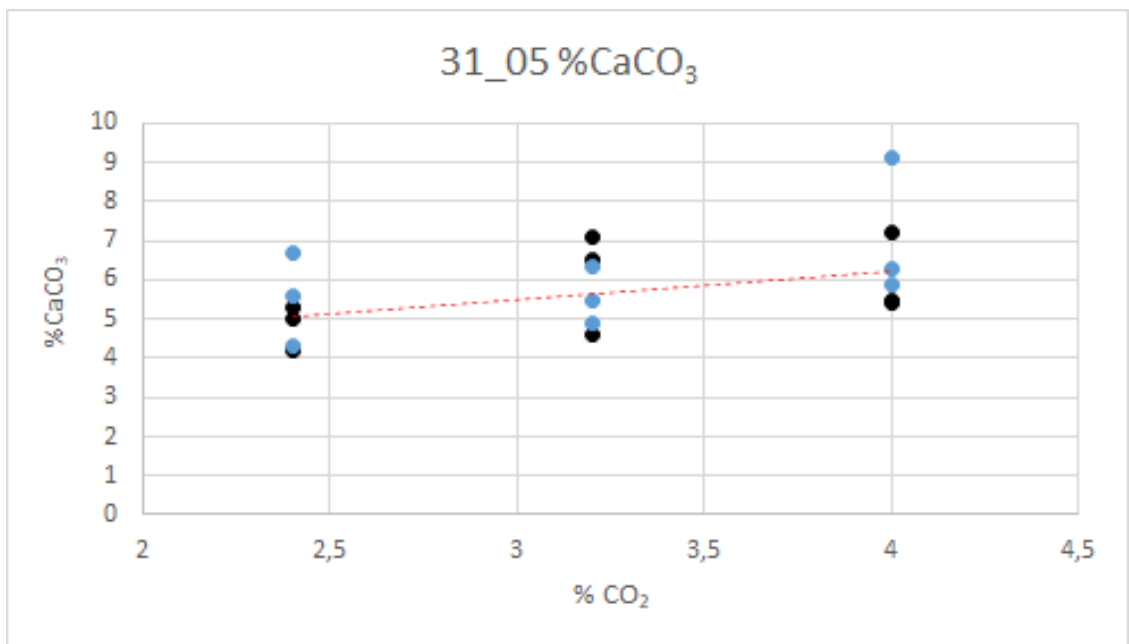
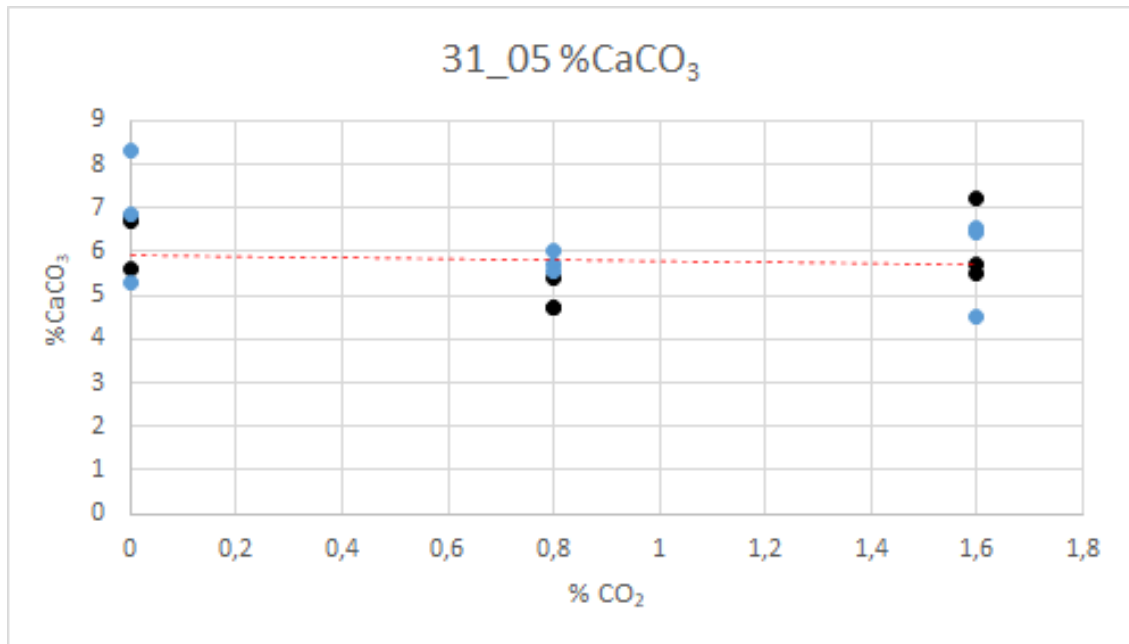


Figura 2.39 %CaCO₃ - 31_05

Amount of carbon dioxide absorbed

The amount of carbon dioxide absorbed, or the efficiency, for samples 29_01 and 31_05 is reported in Tables 13 and 14. From the reaction $\text{Ca(OH)}_2 + \text{CO}_2 \rightarrow \text{CaCO}_3 + \text{H}_2\text{O}$, it is possible to obtain the amount of CO_2 absorbed by the mortar. So, we can calculate the efficiency of carbon dioxide absorption:

$$\text{Efficienza} = \frac{\text{CO}_2 \text{ assorbita}}{\text{CO}_2 \text{ aggiunta}}$$

Tabella 13 Calculation of efficiency 29_01

SAMPLE	%CO2	% AVEREGE CAC03	CAC03 [g]	CO2 ABSORBED [g]	ΔCO2 ABSORBED [g]	CO2 GIVEN[G]	EFFICIENCY
29_01_00	0	5.90	26.55	11.68	0.0	0	-
		4.70	21.15	9.310	0.0	0	-
		3.50	15.75	6.930	0.0	0	-
29_01_04	0.4	5.40	24.30	10.69	1.4	1.80	0.8
		5.50	24.75	10.89	1.6	1.80	0.9
		6.00	27.00	11.88	2.6	1.80	1.4
29_01_08	0.8	6.10	27.45	12.08	2.8	3.60	0.8
		4.60	20.70	9.110	-0.2	3.60	-0.1
		5.30	23.85	10.49	1.2	3.60	0.3
29_01_12	1.2	7.00	31.50	13.86	4.6	5.40	0.8
		6.20	27.90	12.28	3.0	5.40	0.6
		7.00	31.50	13.86	4.6	5.40	0.8
29_01_16	1.6	7.40	33.30	14.65	5.3	7.20	0.7
		8.10	36.45	16.04	6.7	7.20	0.9
		6.80	30.60	13.46	4.2	7.20	0.6
29_01_32	3.2	6.60	29.70	13.07	3.8	14.4	0.3
		6.70	30.15	13.27	4.0	14.4	0.3
		7.30	32.85	14.45	5.1	14.4	0.4

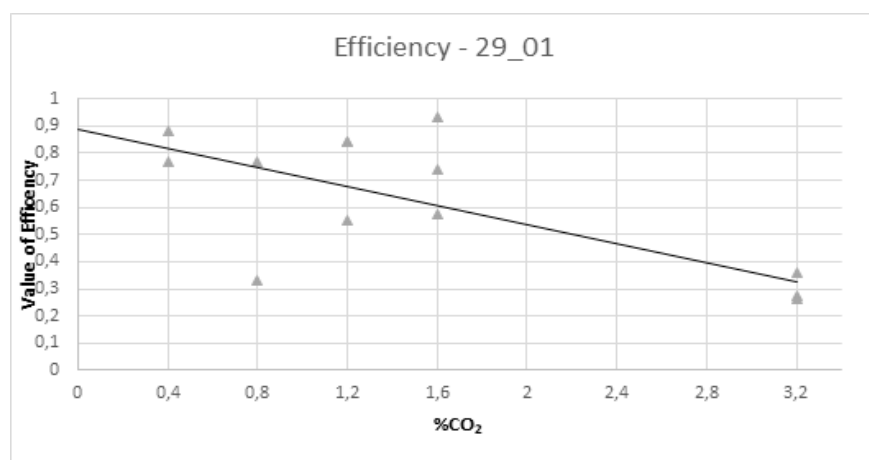


Figura 2.40 Calculation of efficiency 29_01

Tabella 14 Calculation of efficiency 31_05

SAMPLE	%CO2	%CACO3	AVERAGE %CACO3	CACO3 [G]	CO2 ABSORBED [G]	ΔCO2 ABSORBED [G]	CO2 GIVEN[G]	EFFICIENCY
31_05_00	0	6.8	5.67	27.45	12.08	0.00	0.0	-
	0	6.7		23.90	10.51	0.00	0.0	-
	0	5.6		25.20	11.09	0.00	0.0	-
31_05_08	0.8	4.7	5.82	25.61	11.27	0.04	3.6	0.01
	0.8	5.4		24.93	10.97	-0.26	3.6	-0.07
	0.8	4.7		28.04	12.34	1.11	3.6	0.31
31_05_16	1.6	7.2	6.52	32.40	14.26	3.03	7.2	0.42
	1.6	5.7		29.57	13.01	1.78	7.2	0.25
	1.6	5.5		26.01	11.44	0.22	7.2	0.03
31_05_24	2.4	4.2	6.10	26.33	11.58	0.36	10.8	0.03
	2.4	5.3		25.92	11.40	0.18	10.8	0.02
	2.4	5		30.15	13.27	2.04	10.8	0.19
31_05_32	3.2	7.1	5.83	30.29	13.33	2.10	14.4	0.15
	3.2	6.5		27.00	11.88	0.65	14.4	0.05
	3.2	4.6		21.42	9.42	-1.80	14.4	-0.13
31_05_40	4.0	5.5	6.54	26.33	11.58	0.36	18.0	0.02
	4.0	7.2		29.39	12.93	1.70	18.0	0.09
	4.0	5.4		32.51	14.31	3.08	18.0	0.17

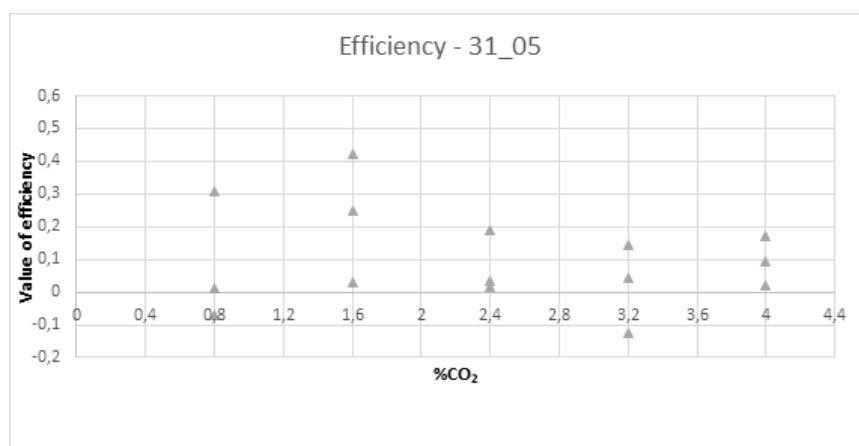


Figura 2.41 Calculation of efficiency 31_05

2.2.5 Interpretation of results

Following the results, the following conclusions can be drawn:

1. CO₂ can be easily added (via dry ice pellets) to cementitious mortars. The procedure can be easily applied by construction workers.
2. Mortars can absorb the CO₂ introduced as an additive during the casting phase. Calcimetry tests revealed the increase in calcite with the amount of CO₂ introduced. So the CO₂ carbonated the Portlandite
3. Mechanical properties are not affected by the addition of CO₂
4. Even the pH of the mortar does not change (we can use steel reinforcements, but not wool)
5. Mortar cannot absorb more than 1.5% of CO₂ compared to cement (this according to the data we found in the literature)
6. If larger amounts of CO₂ are added, they will not carbonize the Portlandite and be released into the atmosphere. The efficiency of the procedure is also reduced (the maximum efficiency is 80% according to previous tests we found in the literature).

We naturally ask ourselves, can we increase the amount of CO₂ absorbed by reducing the grain size of the cement?

In test # 2 the CEM I 52.5 with reduced particle size is used. From the comparison of the series of samples 31_05 compared to the series of samples 29_01 it emerges that the series 31_05 shows an increase in resistance both to bending and to compression. This is due to the increased strength of the cement type CEM I 52.5.

From here one would also expect an increase in calcite (i.e. an increase in absorbed CO₂) but this does not happen. Why?

The answer depends on the formation of Ca(OH)₂ which serves to make the CO₂ react. The presence of Ca(OH)₂ is mainly produced by C₃S (and to a small extent by C₂S). (Figure 2.44).

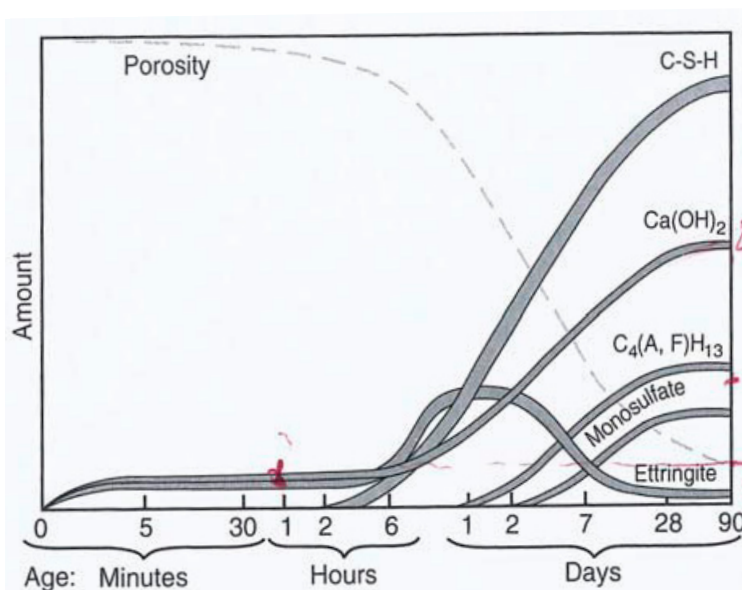


Figure 2.42 Product formation times

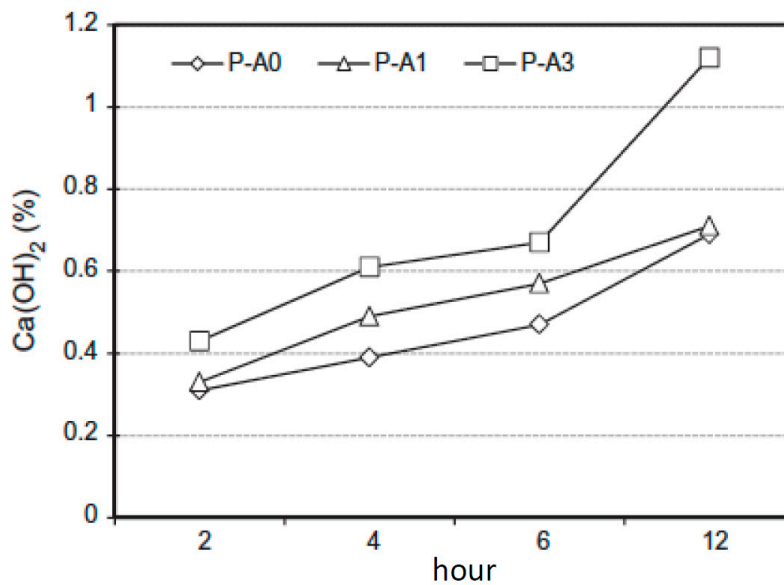


Figura 2.43 In P - A3 the accelerant / cement ratio = 3%

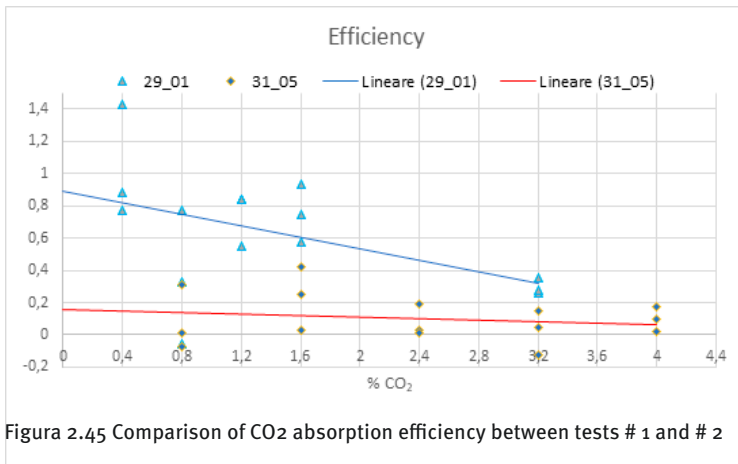
In the presence of water, only Ca^{++} and OH^- are formed from the presence of C_3S (there is a process of dissolution and precipitation), the amount of which is independent of the diameter of the cement. In fact, the presence of $\text{Ca}(\text{OH})_2$ in the initial phase is very low. (Figure 2.42).

To increase the presence of $\text{Ca}(\text{OH})_2$ in the first minutes of casting, it is necessary to accelerate the chemical processes involving C_3S . This is possible by adding a calcium-based hardening accelerator. (Figure 2.43).

The main idea would be to make sure to absorb more carbon dioxide in the concrete. Approximately 20-25% of $\text{Ca}(\text{OH})_2$ is present in the cement and water paste with regulatory measures (450g and 250g). By varying the pressure P or the temperature T it would be possible to increase the % of CaCO_3 . This method is certainly feasible but expensive and incompatible in the vision of finding an easily usable method in situ. The hypothesis would be to modify the fineness of the cement and therefore to halve the diameter of the $\text{Ca}(\text{OH})_2$, reduce the volume of the single particle, increase the available surface. For this reason the second test was carried out with CEM I 52.5 cement. However, laboratory results have shown that the size of Portlandite remains basically constant. What varies is the thickness of the calcium carbonate that forms. It decreases according to the diameter of the aggregate, so tests show that to absorb a greater amount of carbon dioxide I have to use a larger cement. The efficiency varies with the fineness of the cement used. (Figure 2.45).

2 ($3\text{CaO} \cdot \text{SiO}_2$) Tricalcium silicate	+ 11 H_2O Water	= $3\text{CaO} \cdot 2\text{SiO}_2 \cdot 8\text{H}_2\text{O}$ Calcium silicate hydrate (C-S-H)	+ 3 ($\text{CaO} \cdot \text{H}_2\text{O}$) Calcium hydroxide
2 ($2\text{CaO} \cdot \text{SiO}_2$) Dicalcium silicate	+ 9 H_2O Water	= $3\text{CaO} \cdot 2\text{SiO}_2 \cdot 8\text{H}_2\text{O}$ Calcium silicate hydrate (C-S-H)	+ $\text{CaO} \cdot \text{H}_2\text{O}$ Calcium hydroxide

Figura 2.44 Chemical reactions



Surely the most interesting data is that relating to the maximum absorption of carbon dioxide. In fact, a peak of 1.6% by weight is recorded. (Figure 2.46). Above this threshold the absorption does not change or in some cases decreases. These data have also been found in the literature. [19]

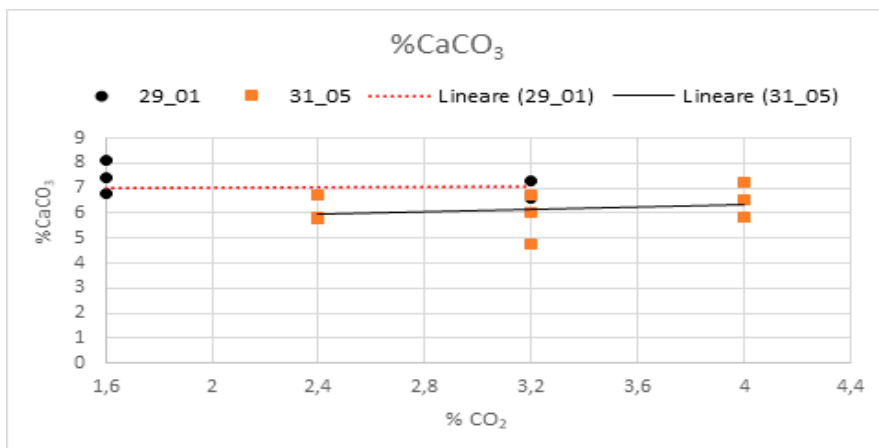
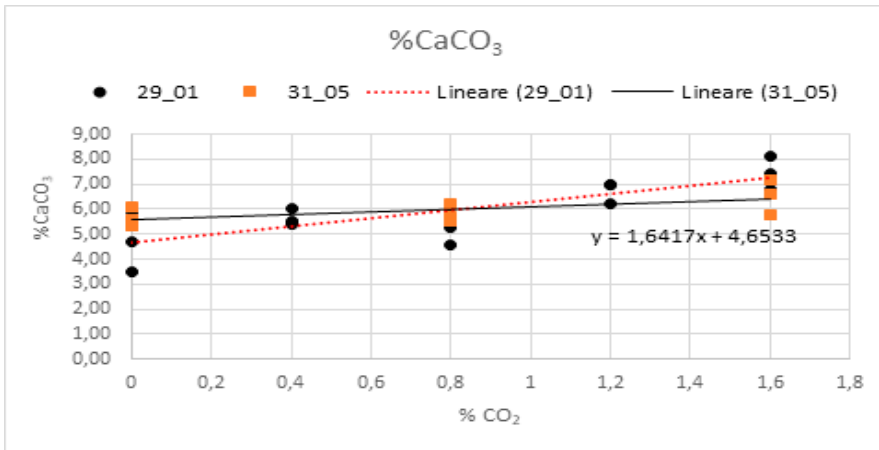


Figure 2.46 Comparison of the % by weight of CO₂ absorbed with respect to concrete

2.3 TEST #3

2.3.1 Materials used

The cement mortar used in test # 3 was made through the composition of cement, water, CO₂ and two types of additive.

In compliance with UNI EN 197-1, the specimens are made of CEM I 42.5 N portland cement, i.e. with a percentage of at least 95% clinker. Drinking water was used.

Compared to the first two specimens, in this case two different types of additives were used:

- ⊕ The Basf MasterSet AC 50 CF, a hardening additive (Figure 2.47)
- ⊕ The Basf Master Life SRA 150, a viscosifying additive (Figure 2.48)



Figura 2.47 Hardener additive MasterSet AC 50CF (BASF)



Figura 2.48 Viscous additive Master Life SRA 150 (BASF)

Also in this case the carbon dioxide was added in the form of dry ice pellets.

The composition of the mortar was obtained through a water / cement ratio of 0.5. (450 ± 2) g of cement and (225 ± 1) g of water were used for all specimens, this time no sand was added compared to tests # 1 and # 2. The only parameters that vary during the test are the amount of CO₂ introduced into the specimens and the presence or absence of the additive. The table below shows the component quantities of the two specimen series:

Tabella 15 Constituents of mortar - series # 1

PROVINO	TIPO DI CEMENTO	CEMENTO (G)	ACQUA (G)	CO ₂ (G)	% CO ₂ /CEM	AC 50 CF (G)
#1_1	N	450	225	0	0	13.5
#1_2	N	450	225	3.60	0.8	13.5
#1_3	N	450	225	5.40	1.2	13.5
#1_4	N	450	225	7.20	1.6	13.5
#1_5	N	450	225	14.4	3.2	13.5
#1_6	N	450	225	18.0	4.0	13.5
#1_7	N	450	225	21.6	4.8	13.5

Tabella 16 Constituents of mortar - series # 2

PROVINO	TIPO DI CEMENTO	CEMENTO (G)	ACQUA (G)	CO ₂ (G)	% CO ₂ /CEM	SRA 150 (G)
#2_1	N	450	225	0	0	31.5
#2_2	N	450	225	3.60	0.8	31.5
#2_3	N	450	225	5.40	1.2	31.5
#2_4	N	450	225	7.20	1.6	31.5
#2_5	N	450	225	14.4	3.2	31.5
#2_6	N	450	225	18.0	4.0	31.5
#2_7	N	450	225	21.6	4.8	31.5

In addition to the previous specimens, 3 specimens defined as series # 0 were prepared, which served as comparison specimens since they do not require the addition of additives.

Tabella 17 Constituents of mortar - series # 0

PROVINO	TIPO DI CEMENTO	CEMENTO (G)	ACQUA (G)	CO ₂ (G)	% CO ₂ /CEM
#0_1	N	450	225	0	0
#0_4	N	450	225	7.20	1.6
#0_5	N	450	225	14.4	3.2

The mixing process involves a succession of steps listed below:

- The cement, water and additive were mixed for 3 minutes
- The mixture obtained was left to rest for 2 minutes
- CO₂ was added and the mixer was started for 2 minutes



Figura 2.49 Cement added to the mixer



Figura 2.50 Water added to the mixer



Figura 2.51 Mixing cement, water and additive



Figura 2.52 CO₂ addition and mixing

2.3.2 Preparation of specimens

The molds, made of steel, were built through the assembly of two molds with dimensions of 75 mm x 70 mm x 10 mm and 2 molds of 70 mm x 70 mm x 10 mm effectively interlocked together in order to create cubes of 70 mm x 70 mm x 70 mm. Finally, they were welded with silicone to a wooden board, to avoid water leaks during the casting phase.

Once the mortar with its plastic consistency has been obtained, it is introduced into the mold, pouring the mixture and making sure that there are no segregations or leaks (Figure 2.53, 2.54 and 2.55).



Figura 2.53 Specimen filling - serie #0



Figura 2.54 Specimen filling - serie #1



Figura 2.55 Specimen filling - serie #2

The excavation took place the day after the laying of the mortar and the cubic specimens were named and placed in a water tank for hardening at $(20.0 \pm 1.0)^\circ \text{C}$. (Figures 2.56, 2.57 and 2.58).

Following a period of 28 days, the specimens were removed from the water and prepared for the compression test. (Figure 2.61).



Figura 2.56 Specimen removal from the mold



Figura 2.57 Specimen removal from the mold



Figura 2.58 Immersion of the specimens through a grid in

2.3.3 Test setup

2.3.3.1 Compression test

An instrument equipped with a circular metal support capable of transmitting the load of the test machine to the specimen in a uniform way was used to carry out the compression test. The test was performed under load control and in particular to avoid a too fast failure of the specimen and consequently an unwelcome result was carried out at a stress speed of 1000 N / s.

The specimen is placed in the center of the instrument, the load increases by (1000 ± 100) N / s until failure (Figures 2.59 and 2.60).

2.3.3.2 Carbonation test

The test as previously described has the purpose of obtaining the quantity of calcium carbonate (CaCO₃) present in a mixture of calcium carbonate and silica. Subsequently the tables with the percentages by weight of CO₂ and CaCO₃ are shown.

2.3.4 Test results

Compressive strength

The compressive strength results are shown in the following tables and graph. The machine measures the force F with which the specimen breaks, which divided by the area A of the specimen, leads to the measurement of the compressive strength:

$$\sigma = \frac{F}{A}$$

Tabella 18 Compressive strength - serie #0

PROVINO	% CO ₂ /CEM	Σ (MPA)
#0_1	0	47.4
#0_4	1.6	36.24
#0_5	3.2	37.65

Tabella 19 Compressive strength - serie #1

PROVINO	% CO ₂ /CEM	Σ (MPA)
#1_1	0	37.80
#1_2	0.8	40.53
#1_3	1.2	43.72
#1_4	1.6	42.99
#1_5	3.2	42.77
#1_6	4.0	39.95
#1_7	4.8	39.44

Tabella 20 Compressive strength- serie #2

PROVINO	% CO ₂ /CEM	Σ (MPA)
#2_1	0	-*
#2_2	0.8	39.88
#2_3	1.2	35.00
#2_4	1.6	33.51
#2_5	3.2	38.25
#2_6	4.0	36.51
#2_7	4.8	40.35

* specimen 2_1 returned an incorrect result, so it was discarded.

Carbonation test

From the calcimetric test the following results are obtained:

Tabella 21 Calcimetry serie #0

PROVINO	% CaCO ₃	Δ CaCO ₃
#0_1	10.1	0
#0_4	14.3	4.2
#0_5	11.7	1.6

Tabella 22 Calcimetry serie #1

PROVINO	% CaCO ₃	Δ CaCO ₃
#1_1	10.8	0
#1_2	13.2	2.4
#1_3	11.0	0.2
#1_4	14.1	3.3
#1_5	8.30	-2.5
#1_6	9.50	-1.3
#1_7	6.20	-4.6

Tabella 23 Calcimetry serie #2

PROVINO	% CaCO_3	ΔCaCO_3
#2_1	11.7	0
#2_2	12.5	0.8
#2_3	15	3.3
#2_4	10.2	-1.5
#2_5	10.5	-1.2
#2_6	8.3	-3.4
#2_7	7	-4.7

* ΔCaCO_3 is the difference in calcium carbonate content with respect to the first specimen (without CO_2 addition) of each series.

2.3.5 Interpretation of results

Compressive strength

The results show that the values obtained with the compression test are similar to those of the characteristic resistance of the type of cement used (42.5 Mpa). Therefore, the increase in CO_2 does not significantly affect the resistance, on the contrary, in combination with the hardening additive AC 50 CF it has higher resistance values (Figure 2.59).

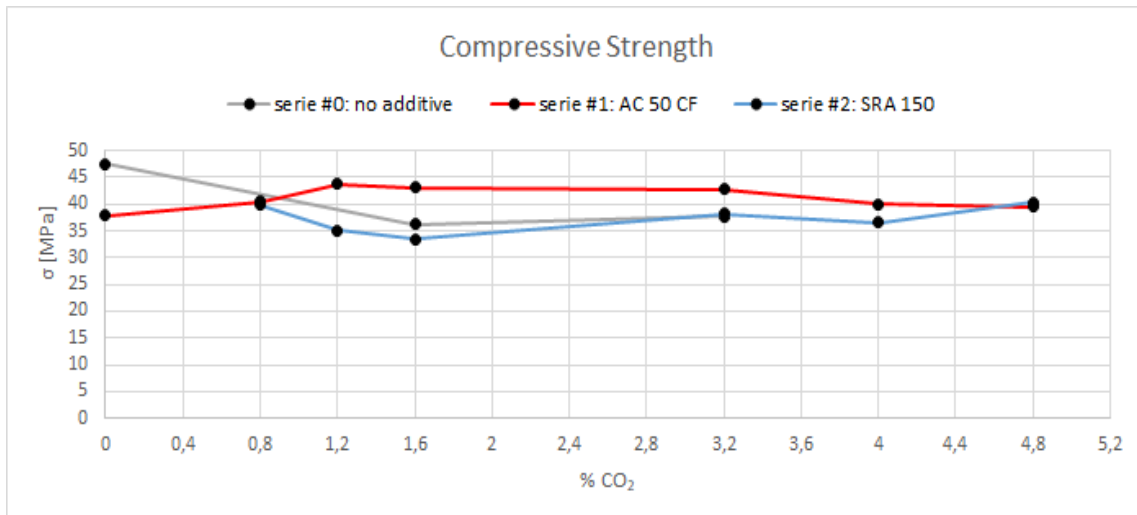


Figura 2.59 Compression test results and comparison

Carbonation test

The test shows a CO₂ absorption peak of 1.2% in relation to the cement, in the case of adding the hardener additive AC 50 FC. Instead, the absorption reaches 1.6% of CO₂ in relation to the cement in the case of addition of the SDC 100 viscosifying additive or without additive. The values found reflect the values defined in the literature⁶ and corresponding to a peak of 1.5% of CO₂. It is noted that if the percentage of CO₂ in relation to the cement increases, the absorption value tends to decrease. This is presumably due to the reduction in the temperature of the cement mortar.

Finally, it is observed that the greatest increase in calcium carbonate corresponds to the specimen without the addition of additives (Figures 2.60 and 2.61).

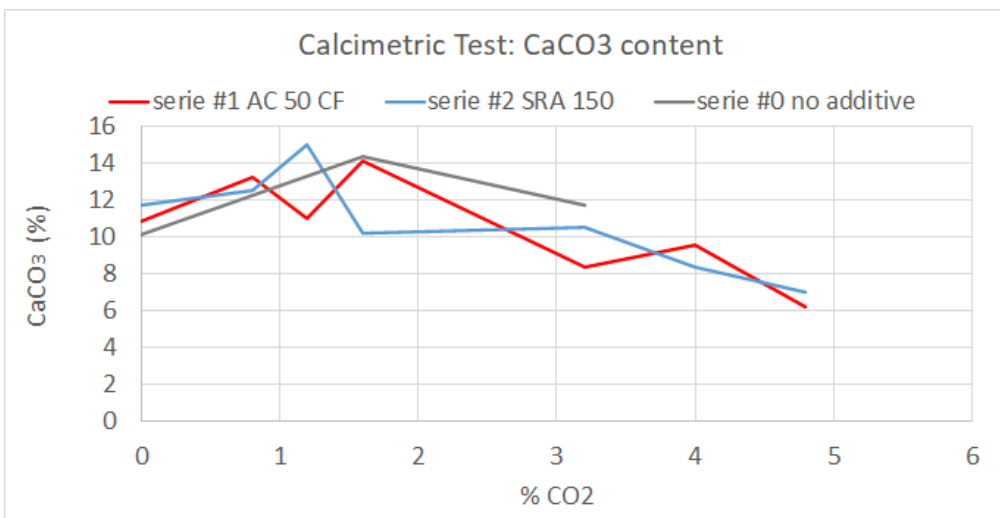


Figura 2.60 Results and comparison of CaCO₃ content. Calcimetric test

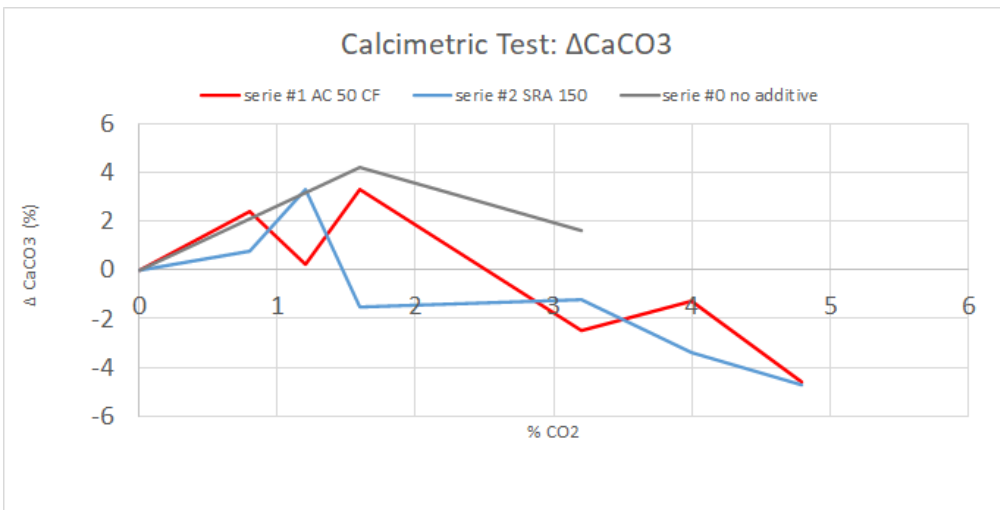


Figura 2.61 Results and comparison of CaCO₃ content. Calcimetric test

⁶ Carbon dioxide as an admixture for better performance of OPC-based concrete (Xin Qian, Jialai Wang, Yi Fang, Liang Wang).

2.4 TEST #4

2.4.1 Materials used

A procedure similar to Tests # 1 and # 2 is used for making the samples. In this case the samples were obtained from a 10 times greater volume of mortar. The cement used is of the CEM 42.5 I type. 3 series of 30 samples each were made, the first, used as a reference, consists only of cement, without CO₂ or steel fibers; the second contains 1.6% of CO₂ compared to cement and the last does not contain CO₂ but 1% by volume of steel fibers (Gramigna gold 0.2 x 13).

The three series have been named for recognition A-Plain, B-Carbon and C-Fiber respectively. No additives were used. (Figure 2.62).

Sample	Type of cement	Cement (g)	Water (g)	Sand (g)	CO ₂ (g)	% CO ₂ /cem	Steel fiber %
A- Plain	N	4500	2250	13500	0	0	0
B-Carbon	N	4500	2250	13500	72	1.6	0
C-Fiber	N	4500	2250	13500	0	0	1

Figura 2.62 Elements and quantities of which the mortar is composed

2.4.2 Preparation of specimens

In this case the samples have the dimensions of 40 mm x 40 mm x 100 mm. They were then subjected to bending and compression tests with the aim of having a statistical distribution of resistance and observing the effect of CO₂ on the distribution.



Figura 2.63 Hardened A-Plain samples

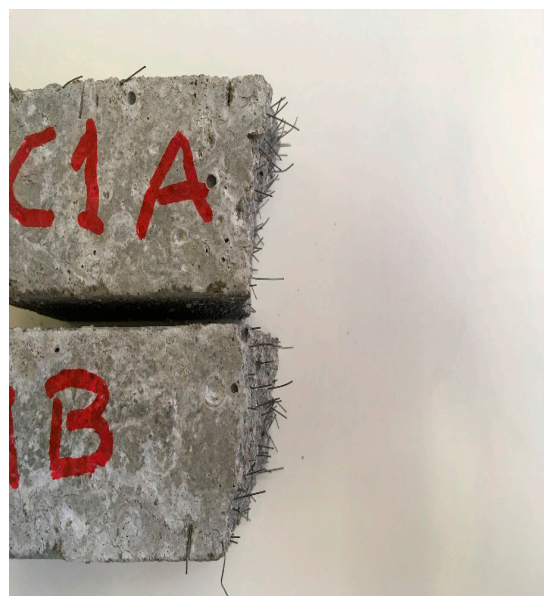


Figura 2.64 Samples with steel fibers



Figura 2.65 Hardened B-Carbon samples



Figura 2.66 Hardened C-Fiber samples

Test results

Bending test

The flexural strength tests were carried out bringing the specimens to break. The 30 tests for each series allowed for a statistical distribution. See figures 2.69, 2.70 and 2.71 which represent the probability density function of samples A, B and C.

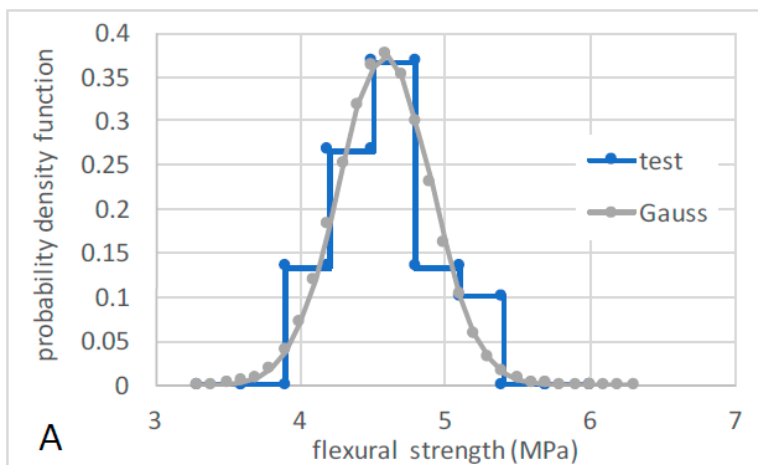


Figura 2.67 Probability density function type A-Plain

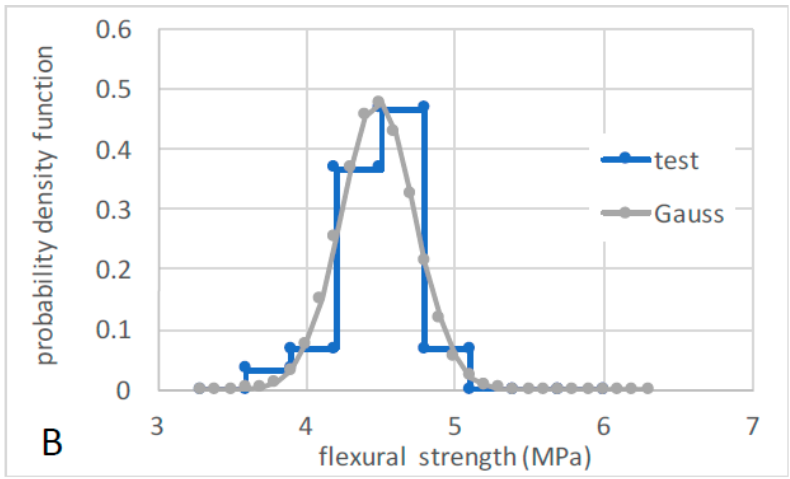


Figure 2.68 Probability density function type B-Carbon

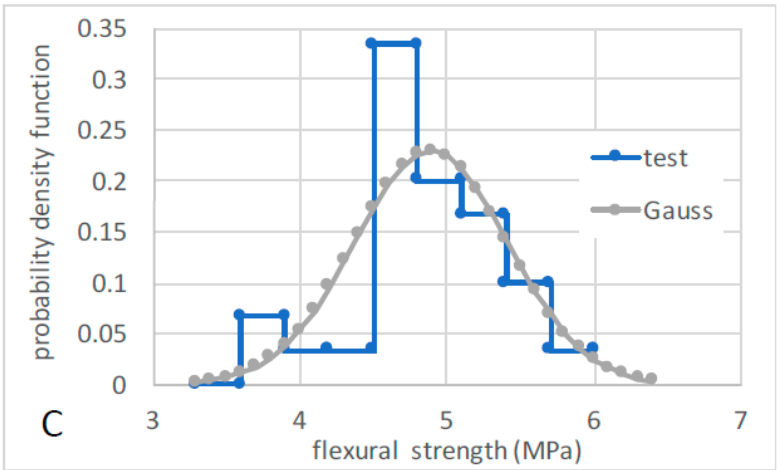


Figure 2.69 Probability density function type C-Fiber

The graphs show that the statistical distribution of the bending strength is similar to the normal distribution (Gaussian).

Compression test

Compression resistance tests were carried out bringing the specimens to break. The 60 tests for each series allowed for a statistical distribution. See figures 2.72, 2.73 and 2.74 which represent the probability density function of samples A, B and C.

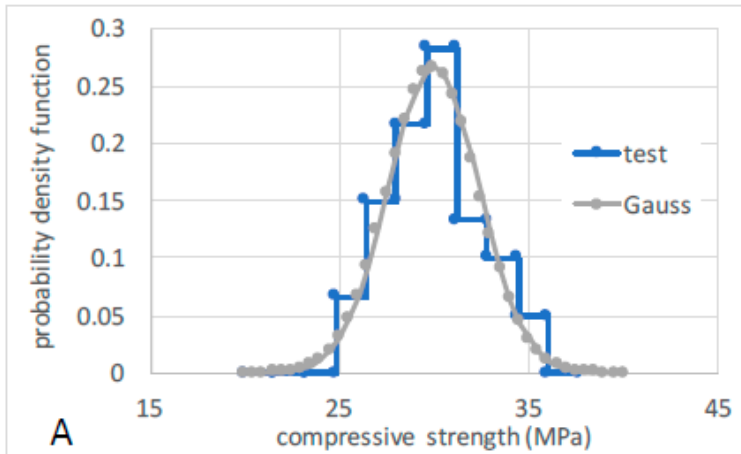


Figure 2.70 Probability density function type A-Plain

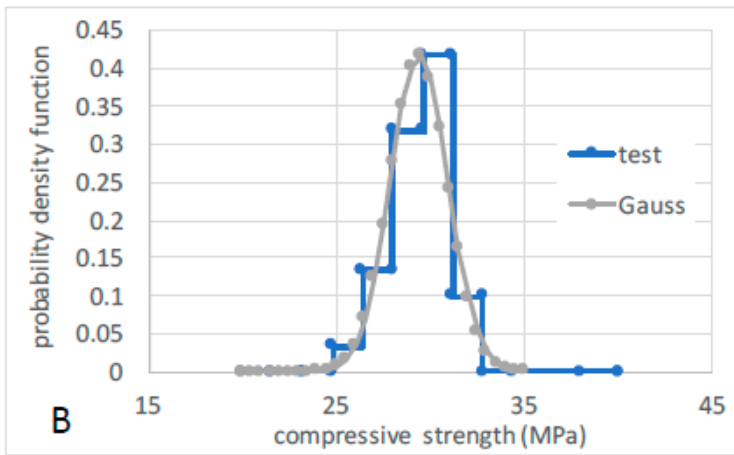


Figure 2.71 Probability density function type B-Carbon

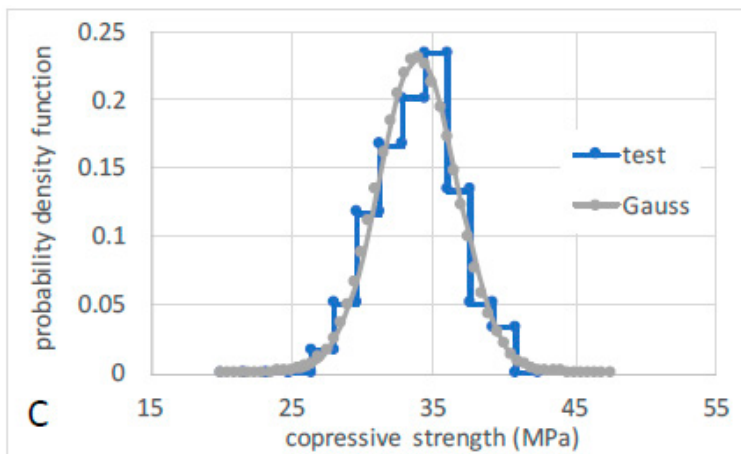


Figure 2.72 Probability density function type C-Fiber

The graphs show that the statistical distribution of compressive strength is similar to the normal distribution (Gaussian).

All results for each individual sample are in Appendix 6.

2.4.3 Interpretation of results

From the statistical distributions of the compressive and bending strength, two important values can be noted. In both distributions the highest value of the probability density is represented by the series B, that is the one containing the CO₂. Furthermore, by calculating the standard deviation of the curve values, it is found that even the smallest standard deviation corresponds to series B, with the addition of CO₂. In addition, by comparing the standard deviation values between the curves, the value of the B series is even half of the value of the C series. average values. On the contrary, with the addition of steel fibers, strength increases but also dispersion increases.

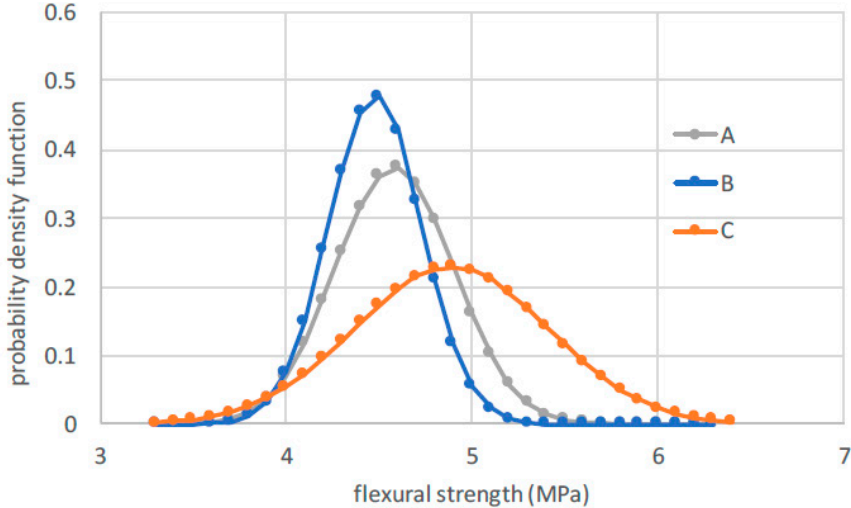


Figura 2.73 Comparison of probability density functions type A, B and C for bending strength

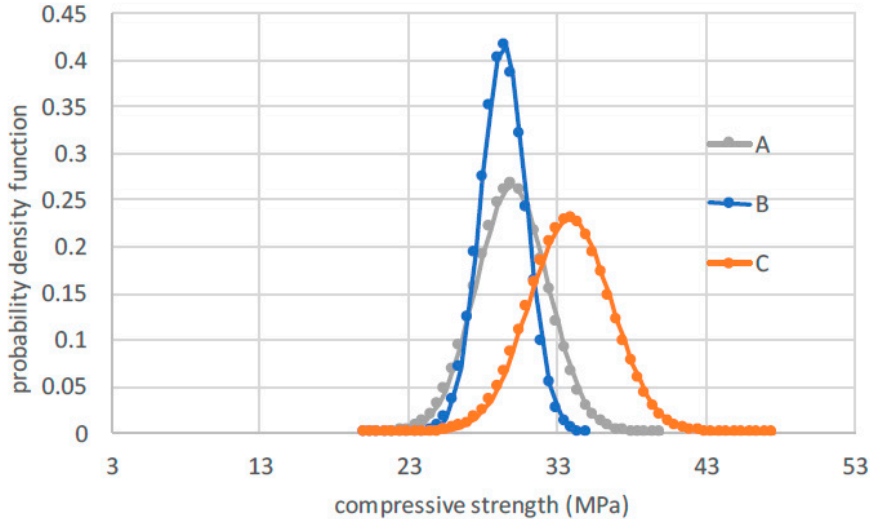


Figura 2.74 Comparison of probability density functions type A, B and C for compressive strength

Tabella 24.
Average resistance and standard deviation

	STANDARD DEVIATION MPA	AVERAGE MPA
A	2.397	29.969
B	1.534	29.395
C	2.775	33.877

Tabella 25.
Average resistance and standard deviation

	STANDARD DEVIATION MPA	AVERAGE MPA
A	0.319	4.585
B	0.250	4.481
C	0.522	4.890

3. CONCLUSION

The construction industry plays an important role in managing greenhouse gas emissions and adopting sustainable policies. The thesis shows that the start of an industrial-scale process of recycling carbon dioxide in ready-mixed concrete does not affect the mechanical performance of the concrete and makes it more sustainable. The main goal was to find a simple method (dry ice pellets) that could be used on site by any operator. It has been observed that the efficiency of the method strictly depends on the type of cement used, but it proves to be an excellent solution for increasing the level of sustainability within the construction sector. As in the literature, mortar cannot absorb more than 1.5% of CO₂ compared to cement, not even by changing the type of cement or by adding traditional accelerating or expansive additives. According to the principles of the circular economy, cement producers could use their own waste products. The idea is simple to apply, but to be competitive, it must be accompanied and evaluated through an economic feasibility analysis.

One of the measures being adopted is to organize the production chain by “optimizing” the transport between the cement kilns and the concrete manufacturing plants. As a rule, CO₂ is transported from the kiln where the cement is produced, ie where it is captured by the exhaust gases emitted into the atmosphere, to the concrete production plant after being liquefied. The integrated link between cement and concrete producer would offer environmental, supply chain and cost synergies. In this way, CO₂ producers would be able to direct their carbon dioxide waste to a profitable downstream use. Finally, future studies can be imagined regarding a more in-depth analysis of the physico-chemical aspects of the carbonation reaction. Other properties of this new mix design can be studied by testing the shrinkage on drying, abrasion, corrosion test in order to determine if there are negative effects deriving from the addition of CO₂ and the reduction of the binder.

4. BIBLIOGRAPHY

1. Lu, B., Shi, C., & Hou, G. (2018). Strength and microstructure of CO₂ cured low-calcium clinker. *Construction and Building Materials*, 188, 417-423.
2. Ashraf, W., Olek, J., & Jain, J. (2017). Microscopic features of non-hydraulic calcium silicate cement paste and mortar. *Cement and Concrete Research*, 100, 361-372.
3. Sahu, S., & Meininger, R. C. (2020). Sustainability and Durability of Solidia Cement Concrete. *Concrete International*, 42(8), 29-34.
4. Li, X., & Ling, T. C. (2020). Instant CO₂ curing for dry-mix pressed cement pastes: Consideration of CO₂ concentrations coupled with further water curing. *Journal of CO₂ Utilization*, 38, 348-354.
5. Qian, X., Wang, J., Fang, Y., & Wang, L. (2018). Carbon dioxide as an admixture for better performance of OPC-based concrete. *Journal of CO₂ Utilization*, 25, 31-38.
6. CARBONCURE SALES BROCHURE 201702
7. CarbonCure-Design-Guide
8. CarbonCure-Spec-Inserts-Ready-Mixed-Concrete3
9. Monkman, S., & Shao, Y. (2010). Integration of carbon sequestration into curing process of precast concrete. *Canadian Journal of Civil Engineering*, 37(2), 302-310.
10. Monkman, S., MacDonald, M., Hooton, R. D., & Sandberg, P. (2016). Properties and durability of concrete produced using CO₂ as an accelerating admixture. *Cement and Concrete Composites*, 74, 218-224.
11. Monkman, S., & MacDonald, M. (2016). Carbon dioxide upcycling into industrially produced concrete blocks. *Construction and Building Materials*, 124, 127-132.
12. Monkman, S., MacDonald, M., & Hooton, D. (2016). Using CO₂ to reduce the carbon footprint of concrete. In *1st International Conference on Grand Challenges in Construction Materials* (pp. 1-8).
13. Monkman, S., & MacDonald, M. (2017). On carbon dioxide utilization as a means to improve the sustainability of ready-mixed concrete. *Journal of Cleaner Production*, 167, 365-375.
14. Monkman, S. (2018). Ready Mixed Concrete Production Using Waste CO₂. ERMCO Congress
15. Monkman, S., Kenward, P. A., Dipple, G., MacDonald, M., & Raudsepp, M. (2018). Activation of cement hydration with carbon dioxide. *Journal of Sustainable Cement-Based Materials*, 7(3), 160-181.
16. Monkman, S. (2018). Sustainable Ready Mixed Concrete Production Using Waste CO₂: A Case Study. Special Publication, 330, 163-174.
17. Monkman, S. (2019). Waste CO₂ upcycling as a means to improve ready mixed concrete sustainability. CarbonCure Technologies, Dartmouth, Canada
18. Monkman, S. (2019). Integrated capture and utilization of cement kiln CO₂ to produce more sustainable concrete. *CarbonCure Technologies, Dartmouth, Canada*
19. Carbon dioxide as an admixture for better performance of OPC-based concrete – Xin Qian, Jialai Wang, Yi Fang, LiangWang

5. FIGURES AND TABLES LIST

Figure

- Figure 1.1 Reactions within the plant
- Figure 1.2 Absorption of CO₂ from low-calcium clinker
- Figure 1.3 Compressive strength curve of low calcium clinker
- Figure 1.4 Differential curves of the pore size distribution of low calcium clinker pastes
- Figure 1.5 Relation between the degree of CO₂ absorption and the compressive strength
- Figure 1.6 Thermogravimetric analysis chart for the CCSC paste sample
- Figure 1.7 Graph of the frequency distribution of the elastic modulus for CCSC paste samples
- Figure 1.8 Variation of the elastic modulus along the IZ of CSCC samples
- Figure 1.9 Production of concrete with the pre-carbonation method
- Figure 1.10 Effect of pre-carbonation on the hydration of the cement paste
- Figure 1.11 Compressive strength of cementitious mortars produced with different methods
- Figure 1.12 Flexural strengths of cement mortar samples produced with and without the precarbonation method
- Figure 1.13 Summary of the environmental impact of 1 m³ of concrete
- Figure 1.14 Conduction calorimetry (power curves) of sieved mortar samples
- Figure 1.15 Compressive strength in the first age at 1, 3 and 7 days
- Figure 1.16 Compressive strength in old age at 28, 56, 91 and 182 days
- Figure 2.1 Sand used
- Figure 2.2 Cement during weighing
- Figure 2.3 Water measurement
- Figure 2.4 CO₂ in the package
- Figure 2.5 CO₂ measurement
- Figure 2.6 Rules for mixing in the laboratory of the Politecnico di Torino
- Figure 2.7 Bowl and blade
- Figure 2.8 Kneader and knife in the laboratory
- Figure 2.9 Mixing
- Figure 2.10 Specific mold
- Figure 2.11 Specific metal spreader
- Figure 2.12 Shaking apparatus
- Figure 2.13 The apparatus with regulatory measures
- Figure 2.14 The samples in water
- Figure 2.15 Samples after ripening
- Figure 2.16 Load arrangement for determining the flexural strength
- Figure 2.17 Bending Strength Apparatus
- Figure 2.18 Sample in the bending machine
- Figure 2.19 Sample in the bending machine

Figure 2.20	Typical structure for compressive strength testing
Figure 2.21	Compressive strength machine in the laboratory
Figure 2.22	Sample in the compressive strength machine
Figure 2.23	Fractured specimen
Figure 2.24	Sample in the compression machine
Figure 2.25	Sample after mechanical tests
Figure 2.26	All sample before chemical tests
Figure 2.27	Calcimeter
Figure 2.28	Liquid level in the calcimeter
Figure 2.29	Measurement of HCl
Figure 2.30	Samples ready for testing
Figure 2.31	Distilled water
Figure 2.32	pH test instrument
Figure 2.33	pH in sample 29_01 in 3 different days
Figure 2.34	Flexural strength 29_01
Figure 2.35	Flexural strength 31_05
Figure 2.36	Compression test - 29_01
Figure 2.37	Compression test - 31_05
Figure 2.38	% CaCO ₃ - 29_01
Figure 2.39	% CaCO ₃ - 31_05
Figure 2.40	Calculation of efficiency 29_01
Figure 2.41	Calculation of efficiency 31_05
Figure 2.42	Product formation times
Figure 2.43	In P - A3 the accelerator / cement ratio = 3%
Figure 2.44	Chemical reactions
Figure 2.45	Comparison of CO ₂ absorption efficiency between tests # 1 and # 2
Figure 2.46	Comparison% by weight of CO ₂ absorbed with respect to concrete
Figure 2.47	MasterSet AC 50CF (BASF) hardener additive
Figure 2.48	MasterMatrix SDC 100 (BASF) viscosifying additive
Figure 2.49	Adding cement to the mixer vessel
Figure 2.50	Adding water to the mixer bowl
Figure 2.51	Mixing cement, water and additive
Figure 2.52	Adding and blending CO ₂
Figure 2.53	Laying of series # 0 specimens
Figure 2.54	Laying of specimens series # 1
Figure 2.55	Laying of specimens series # 2
Figure 2.56	Removing the specimen from the mold
Figure 2.57	Some stripped specimens
Figure 2.58	Immersion of the specimens by means of a grid in the tank for the maturation of 28 days
Figure 2.59	Compression test results and comparison
Figure 2.60	Results and comparison of CaCO ₃ content. Calcimetric test
Figure 2.61	Results and comparison ΔCaCO ₃ . Calcimetric test
Figure 2.62	Elements and quantities of which the mortar is composed

Figure 2.63	A-Plain hardened samples
Figure 2.64	Samples with steel fibers
Figure 2.65	Hardened B-Carbon type samples
Figure 2.66	C-Fiber type hardened samples
Figure 2.67	A-Plain type probability density function
Figure 2.68	B-Carbon type probability density function
Figure 2.69	C-Fiber type probability density function
Figure 2.70	A-Plain type probability density function
Figure 2.71	B-Carbon type probability density function
Figure 2.72	C-Fiber type probability density function
Figure 2.73	Comparison of type A, B and C probability density functions for bending strength
Figure 2.74	Comparison of type A, B and C probability density functions for compressive strength

Tables

Table 1.	CEN particle size distribution: Reference sand
Table 2.	Cement composition [BuzziUnicem]
Table 3.	Mortar components - 29_01
Table 4.	Mortar components - 31_05
Table 5.	Speed of the mixer blade
Table 6.	% CaCO ₃ in sample 29_01
Table 7.	% CaCO ₃ in sample 31_05
Table 8.	Results of the pH test
Table 9.	Results of the flexural strength 29_01
Table 10.	Flexural strength 31_05
Table 11.	Compression test - 29_01
Table 12.	Compression test - 31_05
Table 13.	Calculation of efficiency 29_01
Table 14.	Calculation of efficiency 31_05
Table 15.	Constituents of the mortar - series # 1
Table 16.	Mortar Constituents - Series # 2
Table 17.	Malta constituents - series # 0
Table 18.	Compressive Strength # 0 Series
Table 19.	Compressive strength series # 1
Table 20.	Compressive strength series # 2
Table 21.	Series # 0 calcimetry
Table 22.	Calcimetry series # 1
Table 23.	Calcimetry series # 2
Table 24.	Average resistance and standard deviation
Table 25.	Average resistance and standard deviation

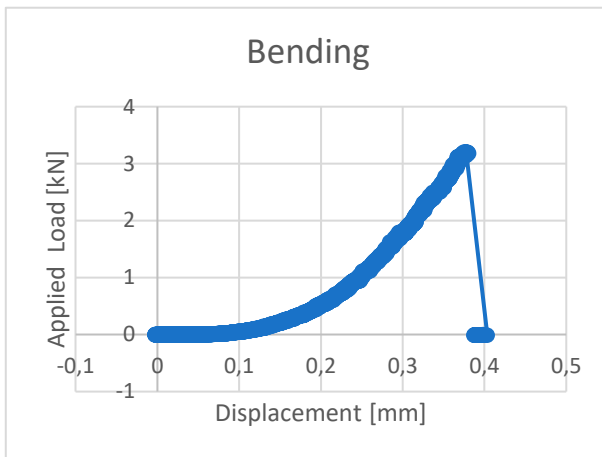
6.ANNEX

Specimen 29_01 CEM I 42,5

In the case of compression tests, 1A, 2A, 3A and 1B, 2B, 3B indicate the two elements of the sample that were broken during the bending test.

29_01_00_1 (0% of CO₂)

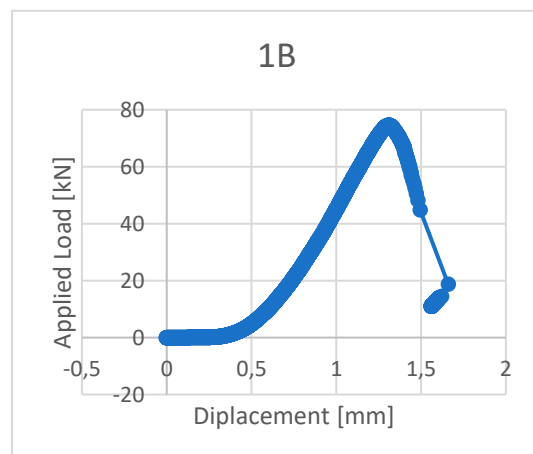
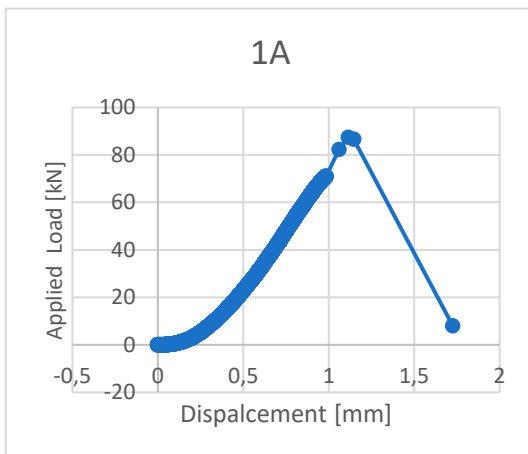
Bending test



Specimen size [mm]		Weight [g]	
160	40.28	41.42	594.9



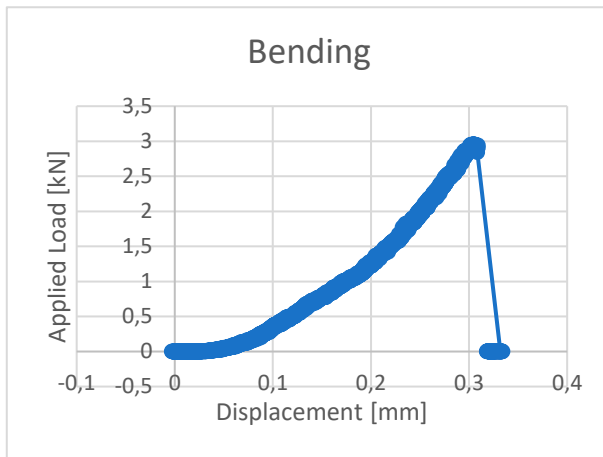
Compression test



P_{max} [kN]	σ_{flex} [MPa]	F_1 [kN]	F_2 [kN]	σ_1 [MPa]	σ_2 [MPa]	% CaCO ₃	pH
3.20	7.51	87.42	74.53	54.64	46.58	5.9	12.27

29_01_00_2 (0% di CO₂)

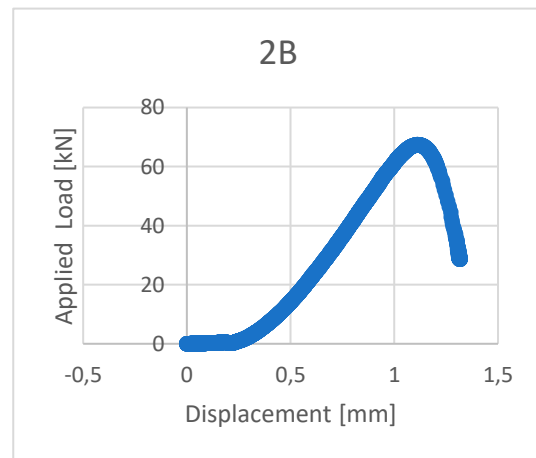
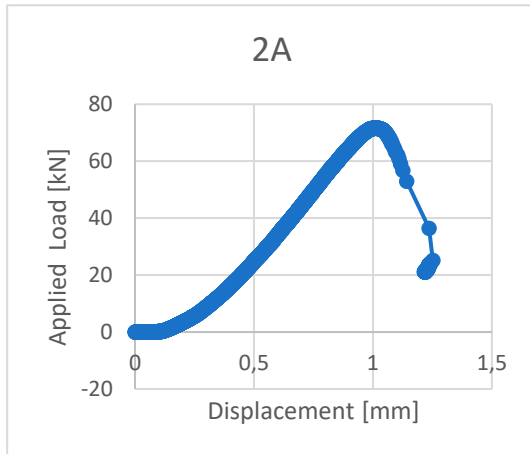
Bending test



Specimen size [mm]		Weight [g]
160	41.03 40.92	606.2



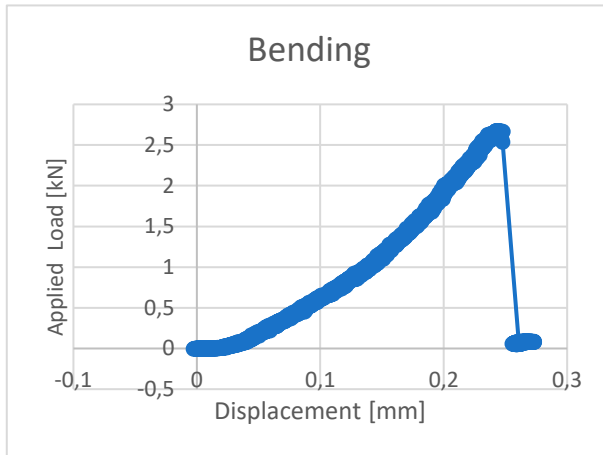
Compression test



P_{max} [kN]	σ_{flex} [MPa]	F_1 [kN]	F_2 [kN]	σ_1 [MPa]	σ_2 [MPa]	% CaCO ₃	pH
2.96	6.94	71.63	67.38	44.77	42.11	4.7	12.28

29_01_00_3 (0% di CO₂)

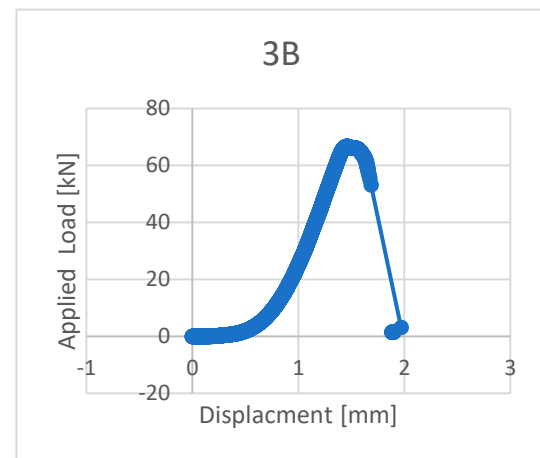
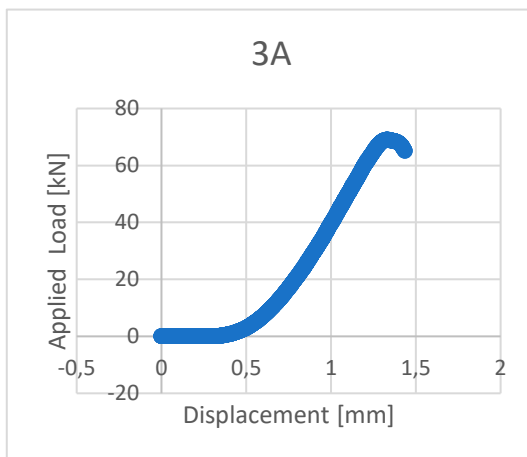
Bending test



Specimen size [mm]		Weight [g]
160	41.25 40.43	583.6



Compression test

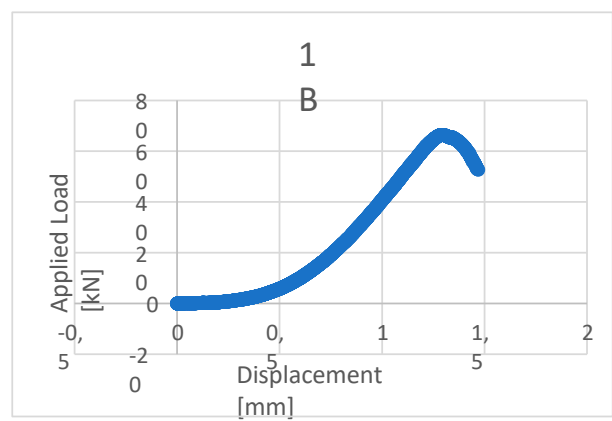
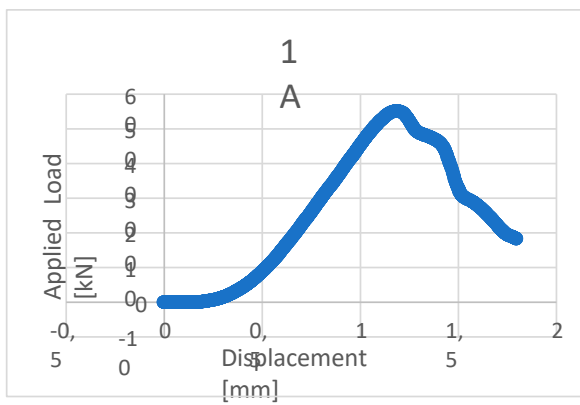


P_{max} [kN]	σ_{flex} [MPa]	F_1 [kN]	F_2 [kN]	σ_1 [MPa]	σ_2 [MPa]	% CaCO ₃	pH
2.68	6.27	69.04	66.73	43.15	41.71	3.5	12.25

29_01_04_1 (0.4% di CO₂)

Compression test

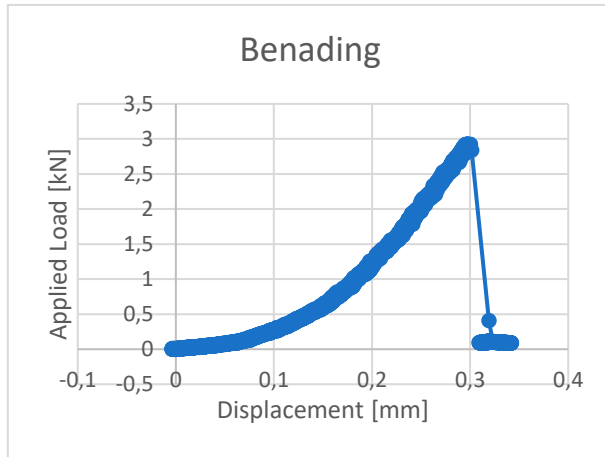
Specimen size [mm]			Weight [g]
160	40.02	40.74	588.2



P_{max} [kN]	σ_{flex} [MPa]	F_1 [kN]	F_2 [kN]	σ_1 [MPa]	σ_2 [MPa]	% CaCO ₃	pH
-	-	55.16	66.47	34.48	41.55	5.4	12.27

29_01_04_2 (0.4% di CO₂)

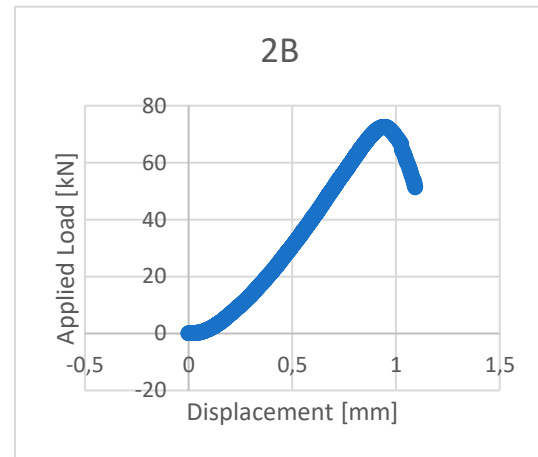
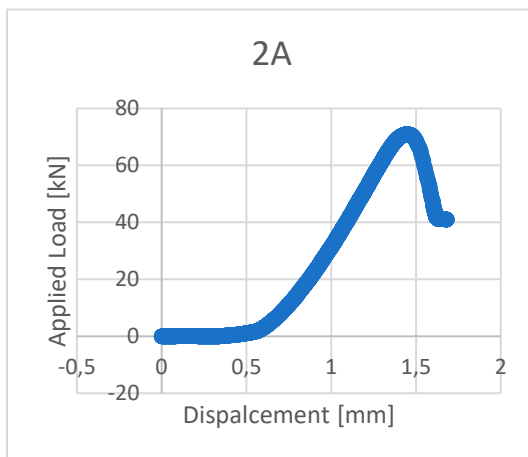
Bending test



Specimen size [mm]			Weight [g]
160	40.35	41.87	601.6



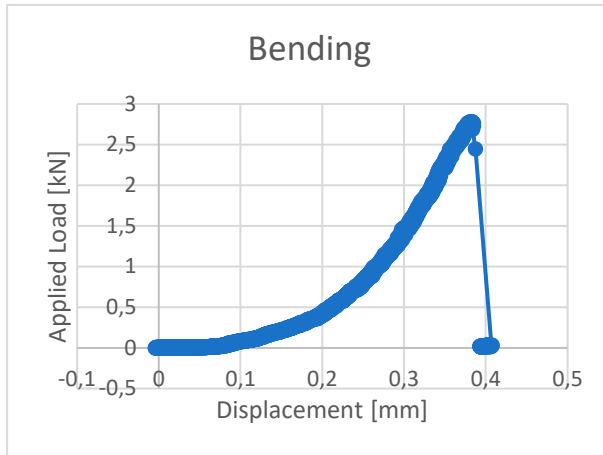
Compression test



P_{max} [kN]	σ_{flex} [MPa]	F_1 [kN]	F_2 [kN]	σ_1 [MPa]	σ_2 [MPa]	% CaCO ₃	pH
2.92	6.84	71.01	72.53	44.38	45.33	5.5	12.24

29_01_04_3 (0.4% di CO₂)

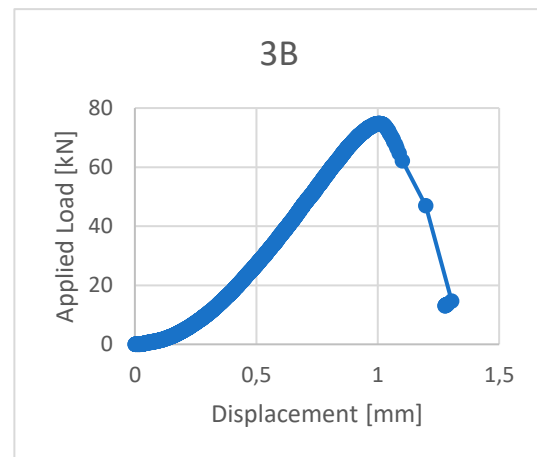
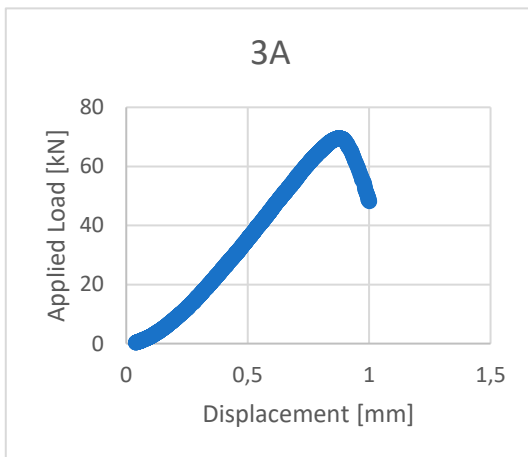
Bending test



Specimen size [mm]			Weight [g]
160	40.04	40.68	587.2



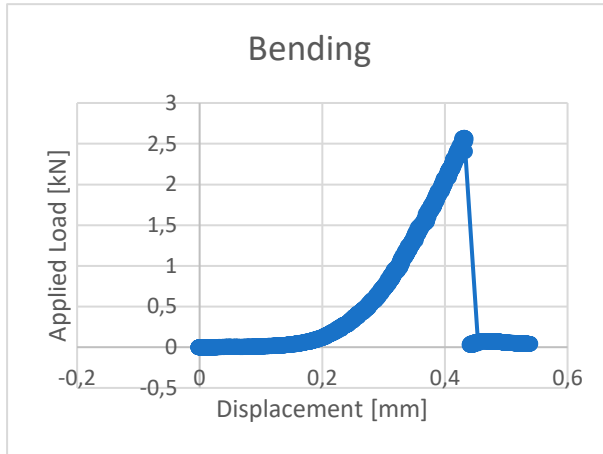
Compression test



P_{max} [kN]	σ_{flex} [MPa]	F_1 [kN]	F_2 [kN]	σ_1 [MPa]	σ_2 [MPa]	% CaCO ₃	pH
2.78	6.51	69.62	74.76	43.51	46.72	6	12.23

29_01_08_1 (0.8% di CO₂)

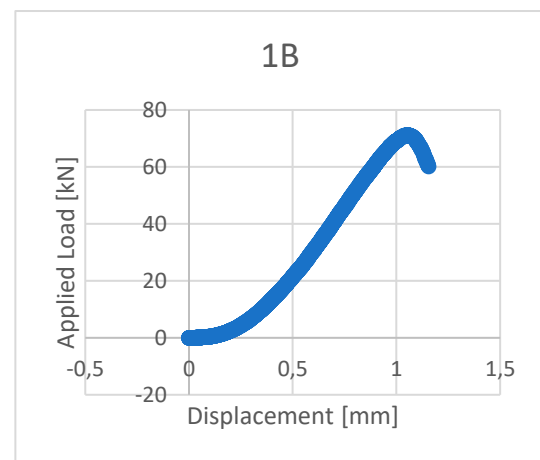
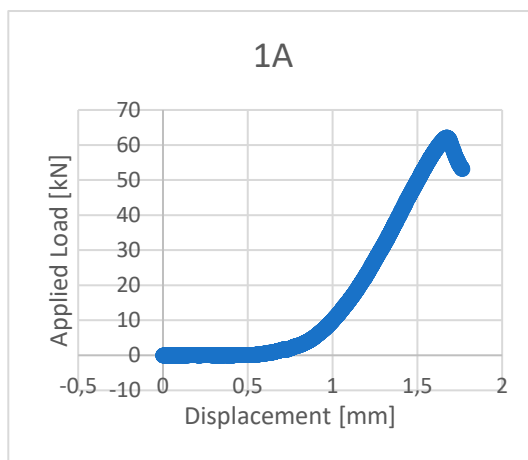
Bending test



Specimen size [mm]		Weight [g]
160	39.96 40.41	584.7



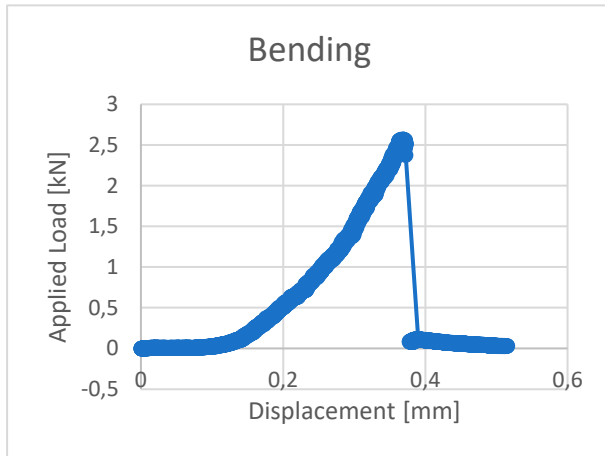
Compression test



P_{max} [kN]	σ_{flex} [MPa]	F_1 [kN]	F_2 [kN]	σ_1 [MPa]	σ_2 [MPa]	% CaCO ₃	pH
2.58	6.04	62.15	71.14	38.84	44.46	6.1	12.26

29_01_08_2 (0.8% di CO₂)

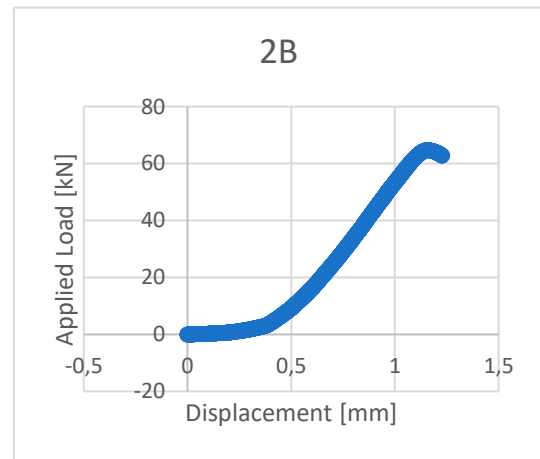
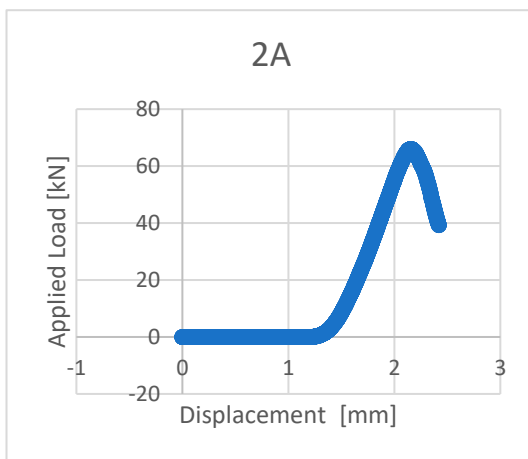
Bending test



Specimen size [mm]			Weight [g]
160	40.06	40.85	582.2



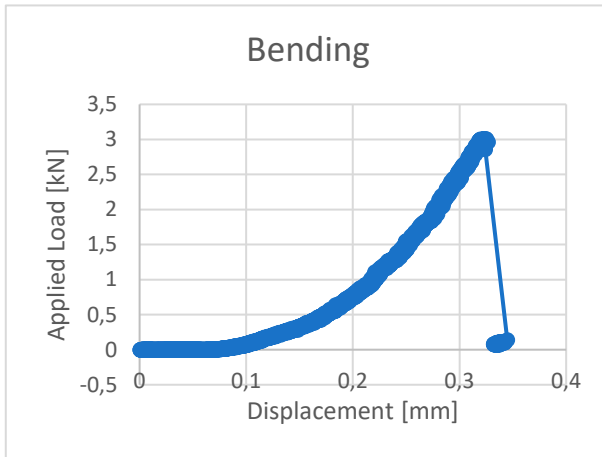
Compression test



P_{max} [kN]	σ_{flex} [MPa]	F_1 [kN]	F_2 [kN]	σ_1 [MPa]	σ_2 [MPa]	% CaCO ₃	pH
2.57	6.02	66.01	64.77	41.26	40.48	4.6	12.26

29_01_08_3 (0.8% di CO₂)

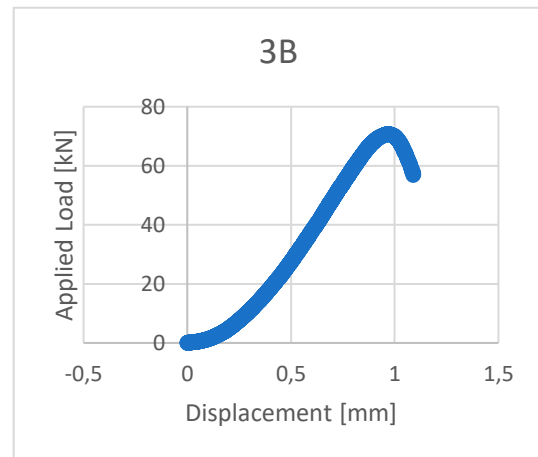
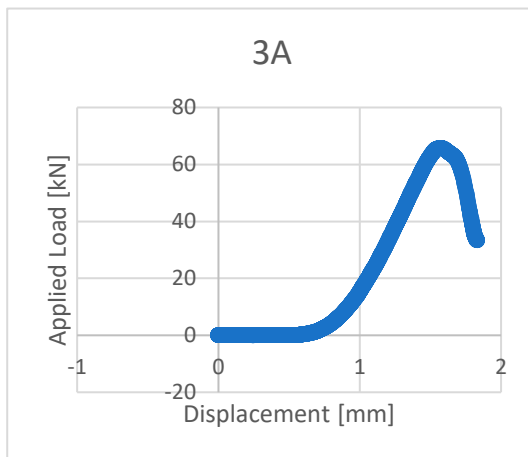
Bending test



Specimen size [mm]		Weight [g]
160	40.26	41.36
		594.4



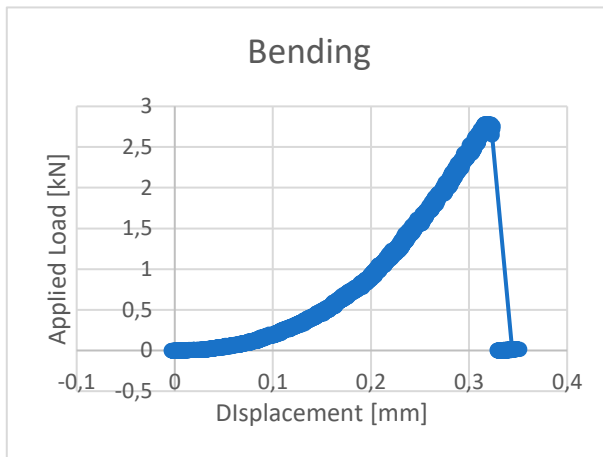
Compression test



P_{max} [kN]	σ_{flex} [MPa]	F_1 [kN]	F_2 [kN]	σ_1 [MPa]	σ_2 [MPa]	% CaCO ₃	pH
3.01	7.05	65.75	70.70	41.10	44.19	5.3	12.26

29_01_12_1 (1.2% di CO₂)

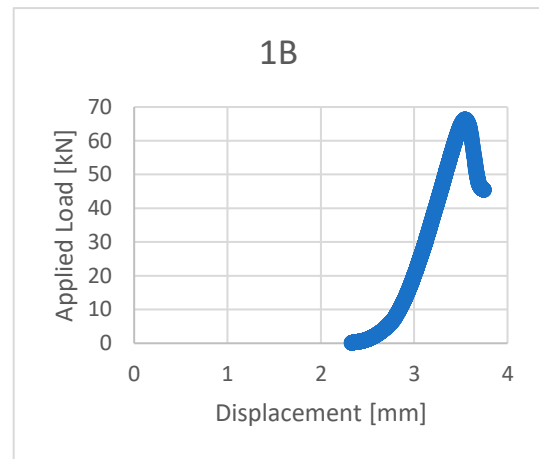
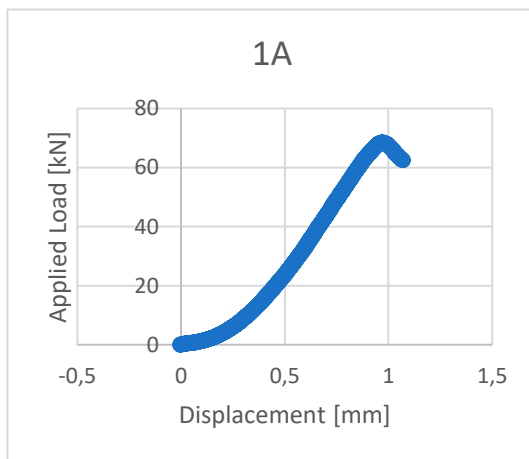
Bending test



Specimen size [mm]			Weight [g]
160	39.98	41.55	591.4



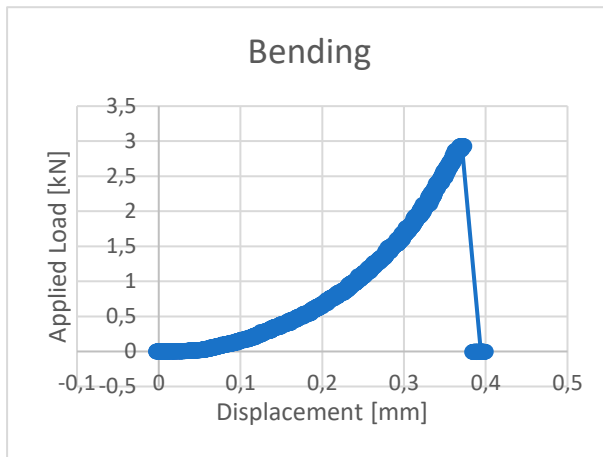
Compression test



P_{max} [kN]	σ_{flex} [MPa]	F_1 [kN]	F_2 [kN]	σ_1 [MPa]	σ_2 [MPa]	% CaCO ₃	pH
2.79	6.53	68.51	66.35	42.82	41.47	7	12.24

29_01_12_2 (1.2% di CO₂)

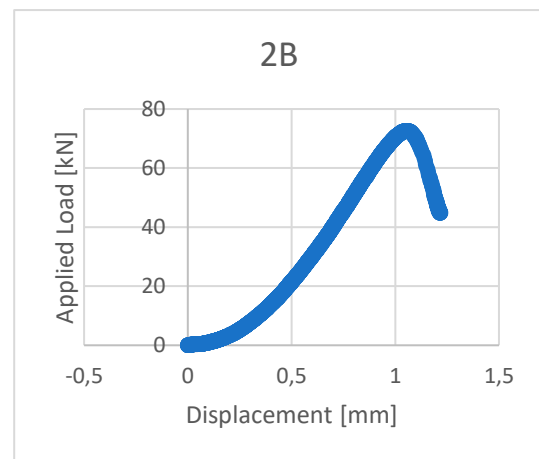
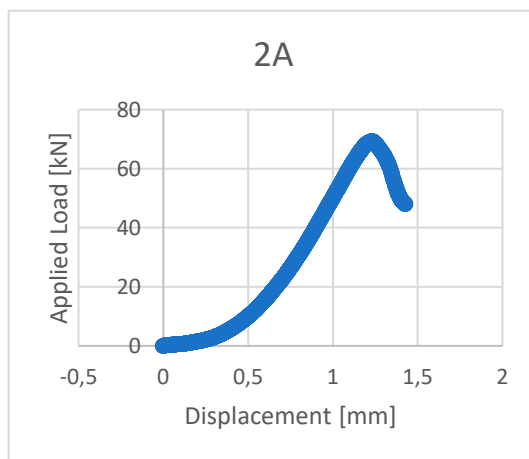
Bending test



Specimen size [mm]			Weight [g]
160	40.04	41.88	597.1



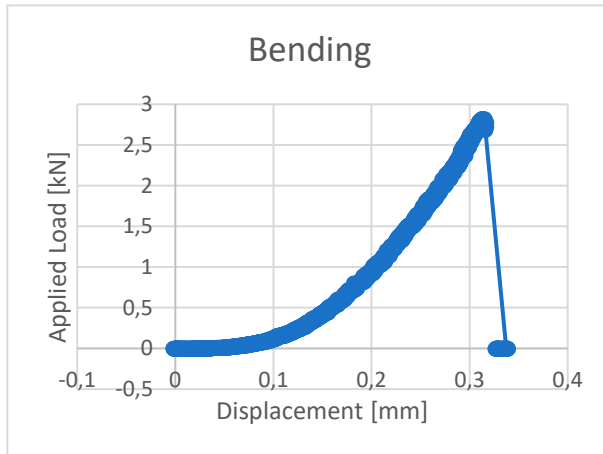
Compression test



P_{max} [kN]	σ_{flex} [MPa]	F_1 [kN]	F_2 [kN]	σ_1 [MPa]	σ_2 [MPa]	% CaCO ₃	pH
2.93	6.88	69.36	72.62	43.35	45.39	6.2	12.23

29_01_12_3 (1.2% di CO₂)

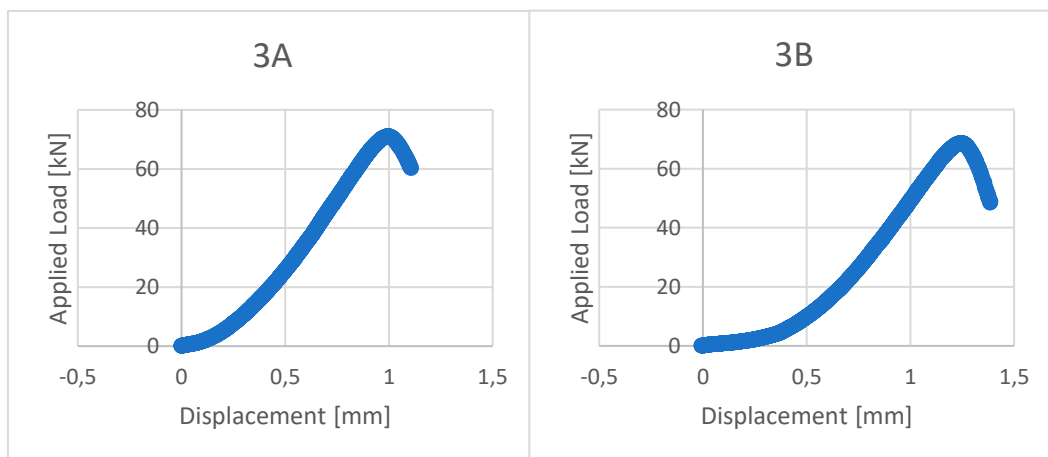
Bending test



Specimen size [mm]			Weight [g]
160	40.17	41.01	590.1



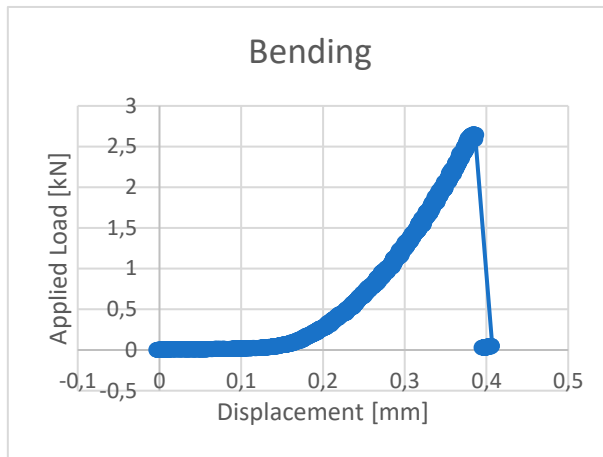
Compression test



P_{max} [kN]	σ_{flex} [MPa]	F_1 [kN]	F_2 [kN]	σ_1 [MPa]	σ_2 [MPa]	% CaCO ₃	pH
2.82	6.61	71.12	68.69	44.45	42.93	7	12.26

29_01_16_1 (1.6% di CO₂)

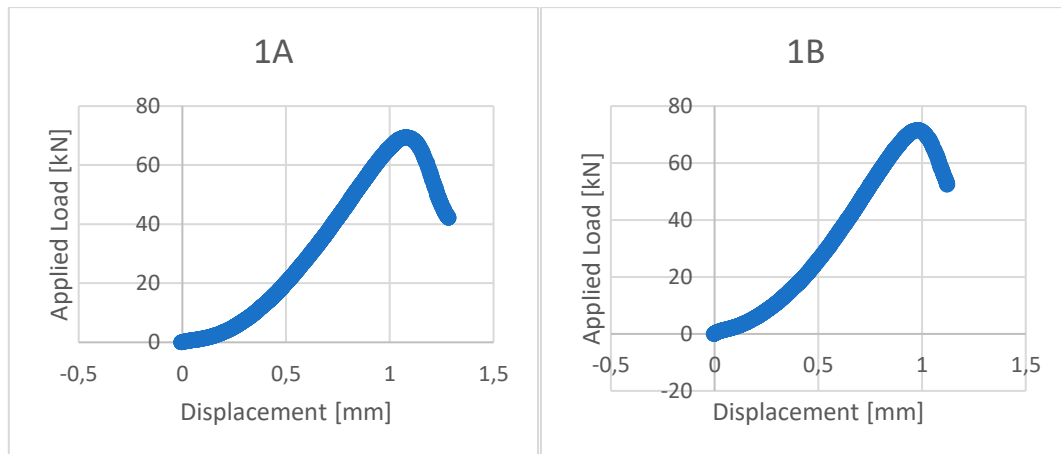
Bending test



Specimen size [mm]			Weight [g]
160	40.32	41.18	594.6



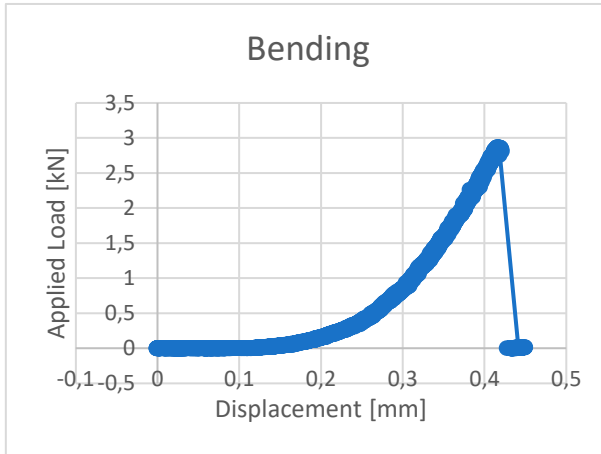
Compression test



P_{max} [kN]	σ_{flex} [MPa]	F_1 [kN]	F_2 [kN]	σ_1 [MPa]	σ_2 [MPa]	% CaCO ₃	pH
2.65	6.22	69.45	71.41	43.41	44.63	7.4	12.25

29_01_16_2 (1.6% di CO₂)

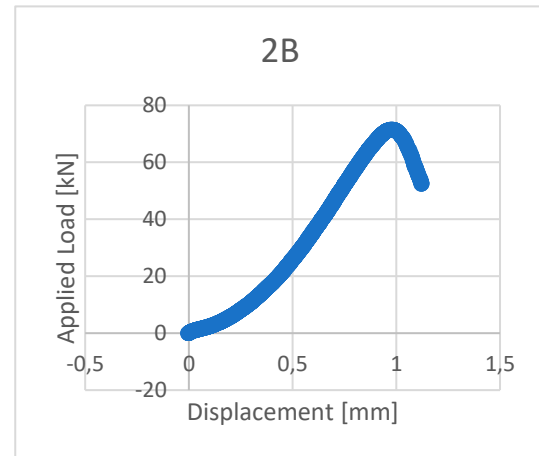
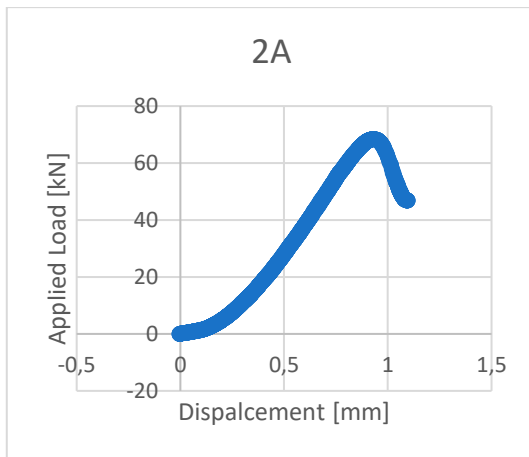
Bending test



Specimen size [mm]			Weight [g]
160	39.96	40.57	587.3



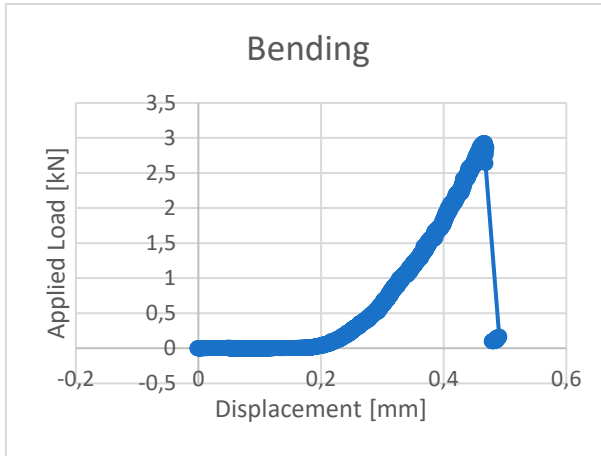
Compression test



P_{max} [kN]	σ_{flex} [MPa]	F_1 [kN]	F_2 [kN]	σ_1 [MPa]	σ_2 [MPa]	% CaCO ₃	pH
2.87	6.72	68.38	71.56	42.74	44.72	8.1	12.24

29_01_16_3 (1.6% di CO₂)

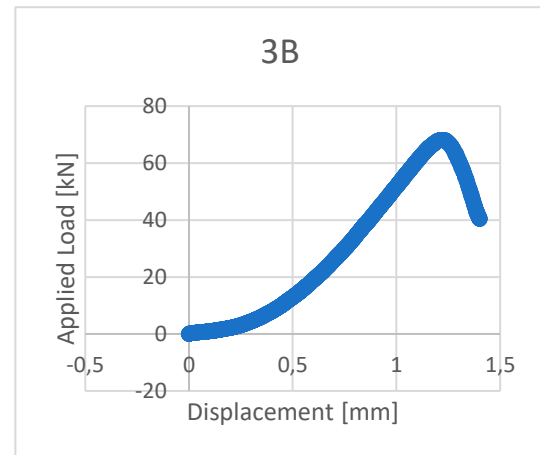
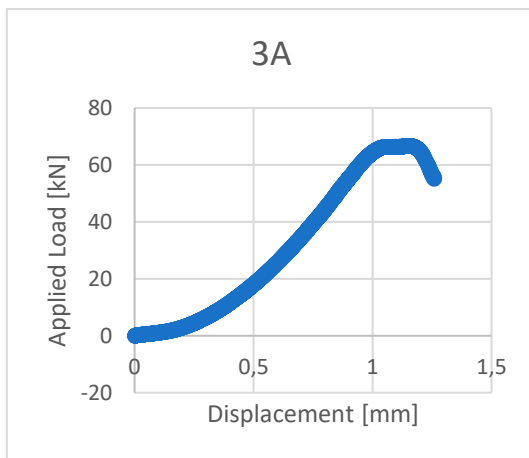
Bending test



Specimen size [mm]			Weight [g]
160	40.12	40.83	596.3



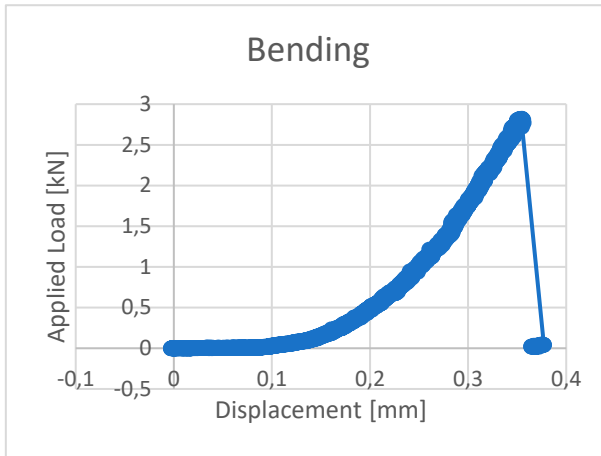
Compression test



P_{max} [kN]	σ_{flex} [MPa]	F_1 [kN]	F_2 [kN]	σ_1 [MPa]	σ_2 [MPa]	% CaCO ₃	pH
2.93	6.86	66.68	68.21	41.68	42.63	6.8	12.24

29_01_32_1 (3.2% di CO₂)

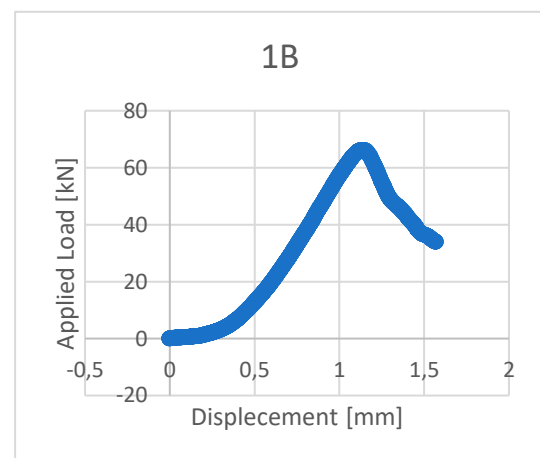
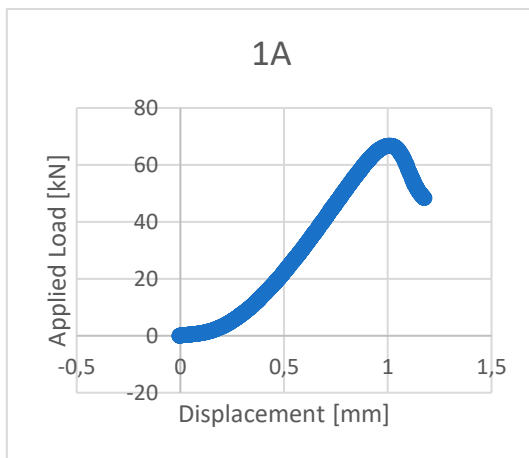
Bending test



Specimen size [mm]			Weight [g]
160	40.28	41.52	588.2



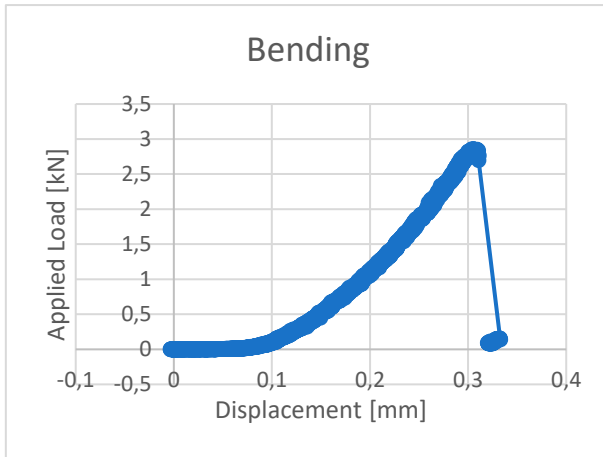
Compression test



P_{max} [kN]	σ_{flex} [MPa]	F_1 [kN]	F_2 [kN]	σ_1 [MPa]	σ_2 [MPa]	% CaCO ₃	pH
2.82	6.61	66.80	66.30	41.75	41.44	6.6	12.19

29_01_32_2 (3.2% di CO₂)

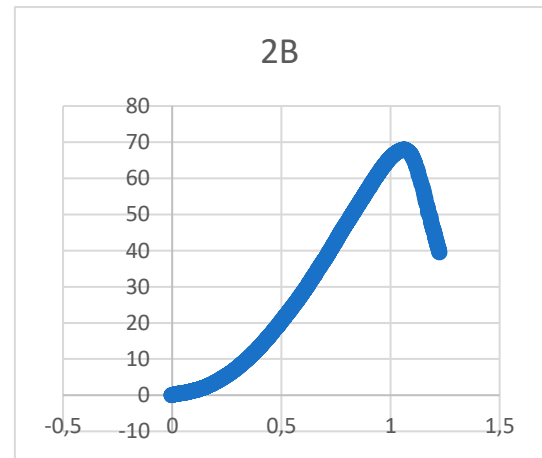
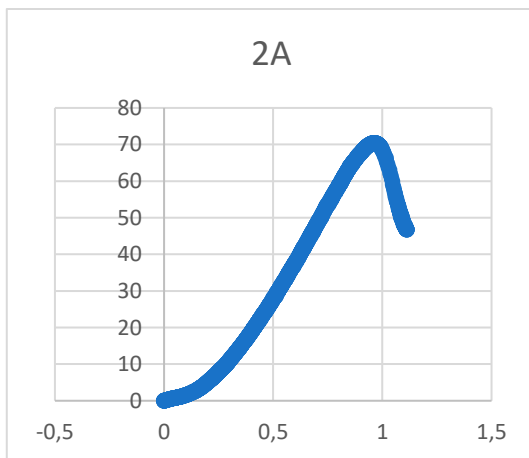
Bending test



Specimen size [mm]			Weight [g]
160	40.05	41.57	589.9



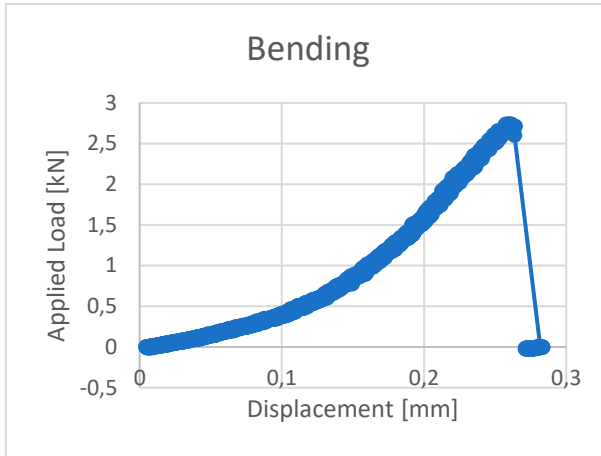
Compression test



P_{max} [kN]	σ_{flex} [MPa]	F_1 [kN]	F_2 [kN]	σ_1 [MPa]	σ_2 [MPa]	% CaCO ₃	pH
2.86	6.70	70.44	67.95	44.02	42.47	6.7	12.21

29_01_32_3 (3.2% di CO₂)

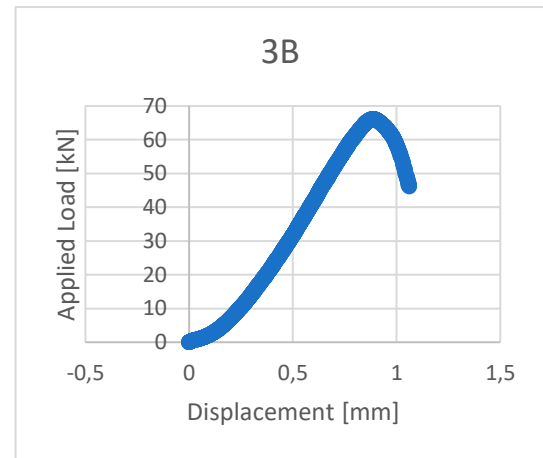
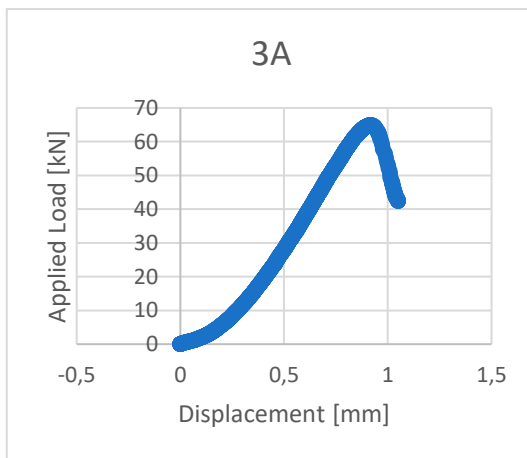
Bending test



Specimen size [mm]			Weight [g]
160	40.10	41.50	588.4



Compression test



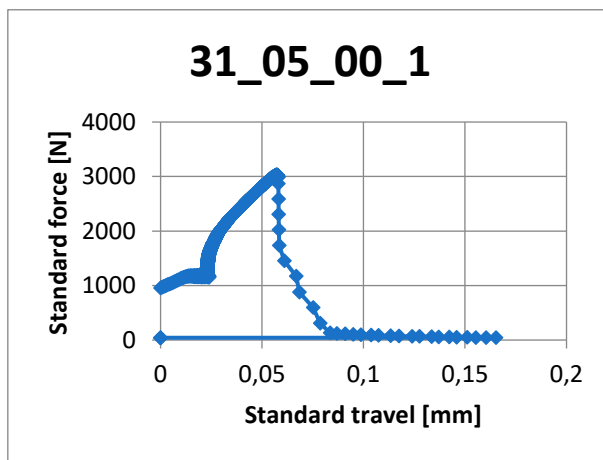
P_{max} [kN]	σ_{flex} [MPa]	F_1 [kN]	F_2 [kN]	σ_1 [MPa]	σ_2 [MPa]	% CaCO ₃	pH
2.74	6.42	64.96	66.16	40.60	41.35	7.3	12.25

Specimen 31_05 CEM I 52,5

In the case of Compression tests, the two elements of the sample that were broken during the Bending test are indicated with 1A, 2A, 3A and 1B, 2B, 3B.

31_05_00_1 (0% di CO₂)

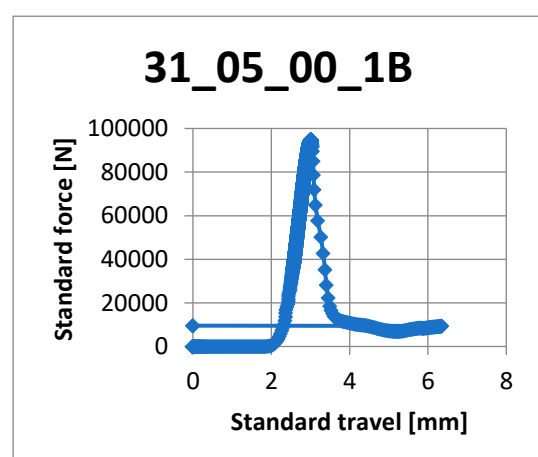
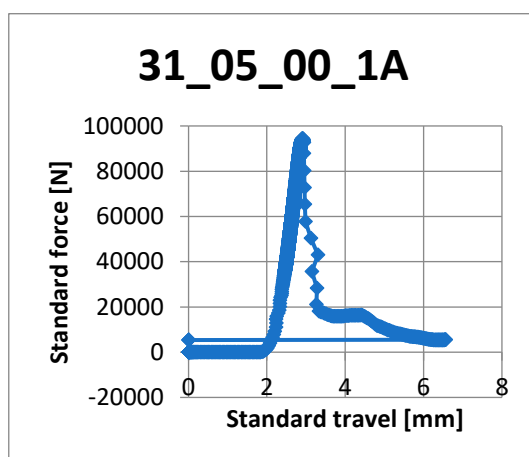
Bending test



Specimen size [mm]		Weight [g]
160	40.28	41.69
		592



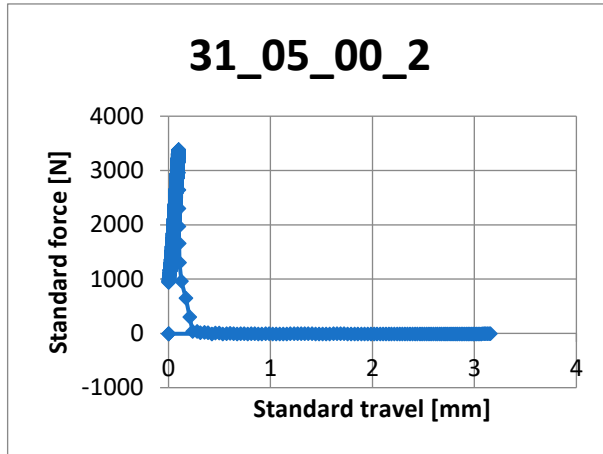
Compression test



P_{max} [kN]	σ_{flex} [MPa]	F_1 [kN]	F_2 [kN]	σ_1 [MPa]	σ_2 [MPa]	% CaCO ₃	pH
3.03	7.10	94.2452	94.9173	58.90	59.32	6.1	-

31_05_00_2 (0% di CO₂)

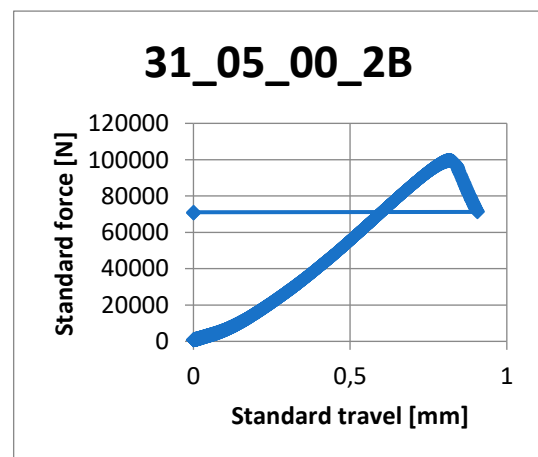
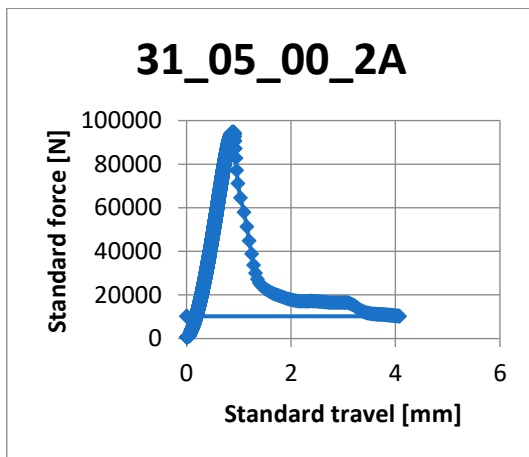
Bending test



Specimen size [mm]			Weight [g]
160	41.03	40.85	588



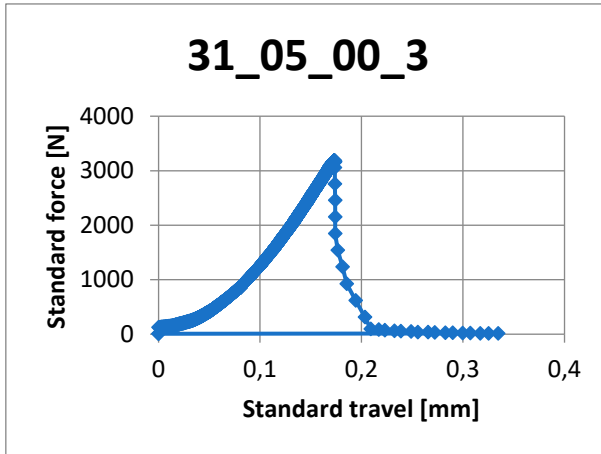
Compression test



P_{max} [kN]	σ_{flex} [MPa]	F_1 [kN]	F_2 [kN]	σ_1 [MPa]	σ_2 [MPa]	% CaCO ₃	pH
3.38	7.92	94.69	99.49	59.18	62.19	5.31	-

31_05_00_3 (0% di CO₂)

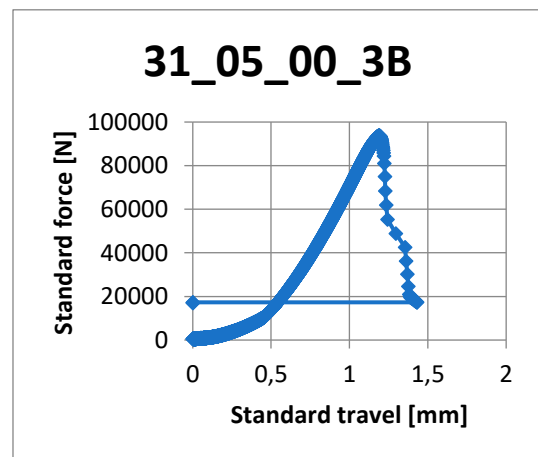
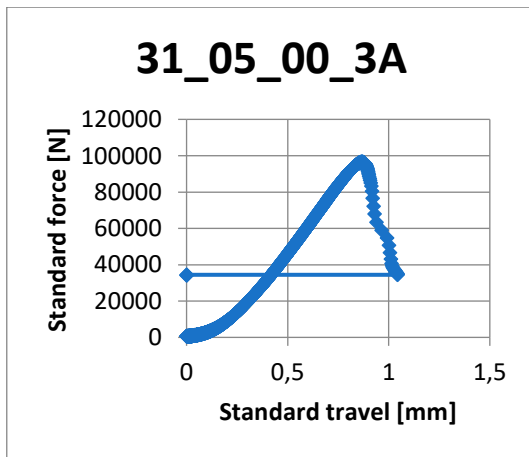
Bending test



Specimen size [mm]			Weight [g]
160	41.25	40.96	586



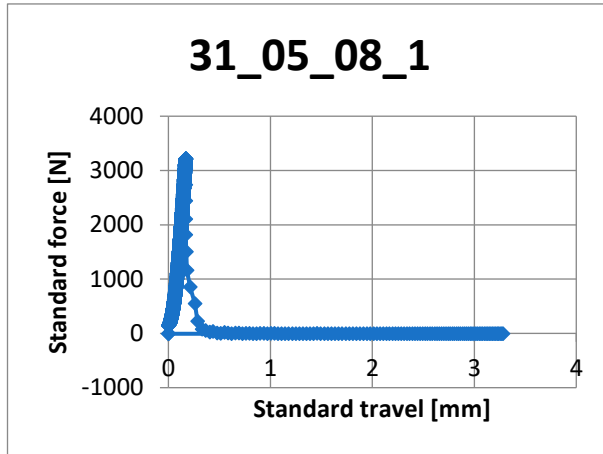
Compression test



P_{max} [kN]	σ_{flex} [MPa]	F_1 [kN]	F_2 [kN]	σ_1 [MPa]	σ_2 [MPa]	% CaCO ₃	pH
3.19	7.47	96.49	93.68	60.31	58.55	5.6	-

31_05_08_1 (0.8% di CO₂)

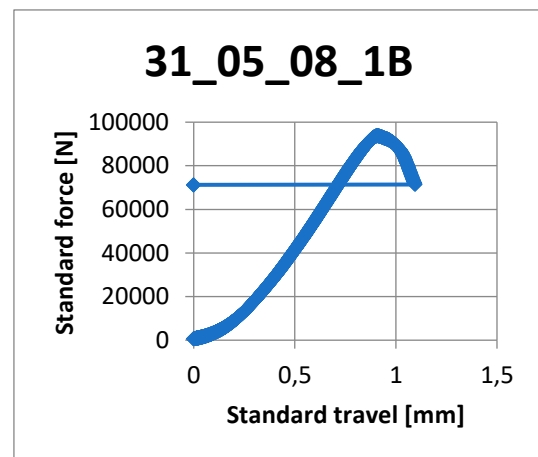
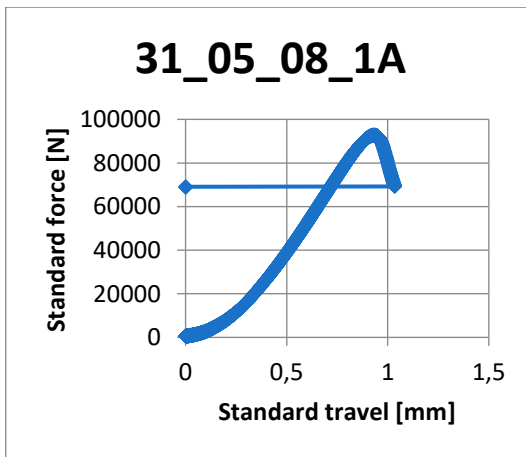
Bending test



Specimen size [mm]		Weight [g]	
160	40.02	40.77	584



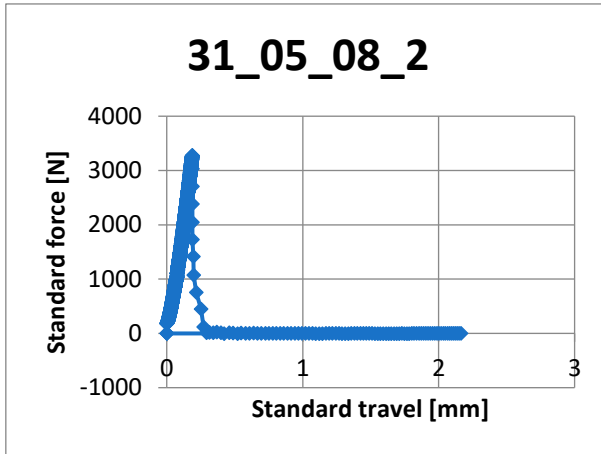
Compression test



P_{max} [kN]	σ_{flex} [MPa]	F_1 [kN]	F_2 [kN]	σ_1 [MPa]	σ_2 [MPa]	% CaCO ₃	pH
3.22	7.54	92.75	93.71	57.97	58.57	5.59	-

31_05_08_2 (0.8% di CO₂)

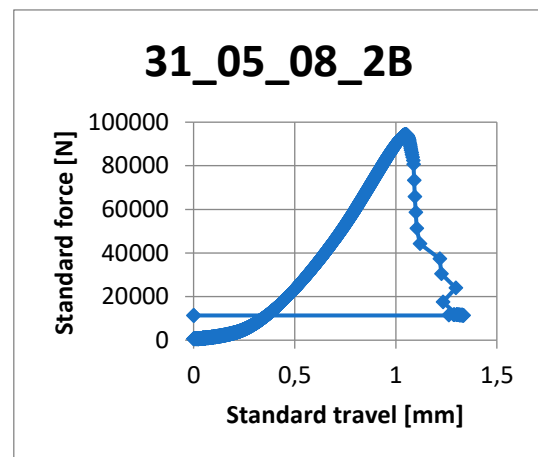
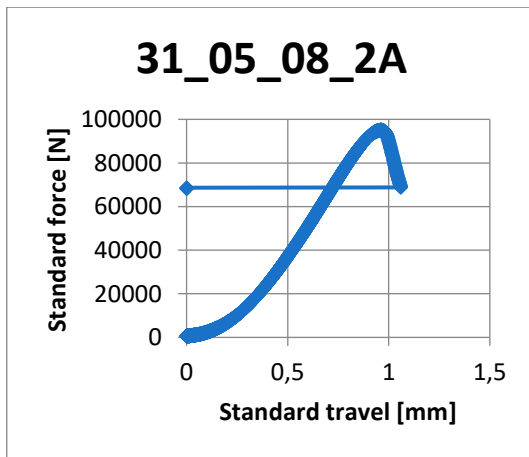
Bending test



Specimen size [mm]		Weight [g]
160	40.35 40.78	585



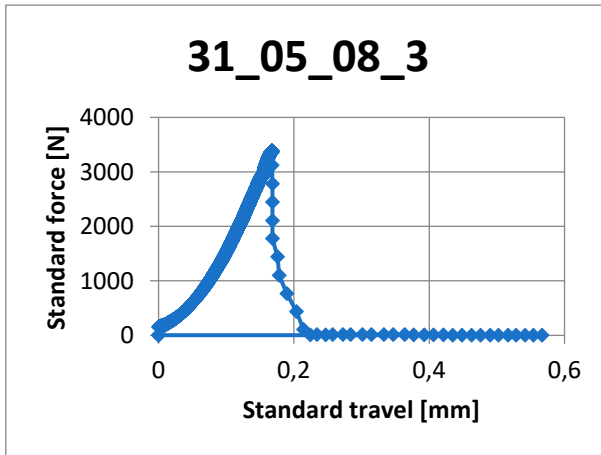
Compression test



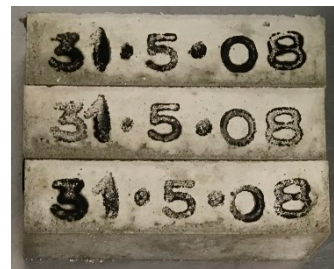
P_{max} [kN]	σ_{flex} [MPa]	F_1 [kN]	F_2 [kN]	σ_1 [MPa]	σ_2 [MPa]	% CaCO ₃	pH
3.27	7.66	95.03	94.24	59.40	58.90	5.54	-

31_05_08_3 (0.8% di CO₂)

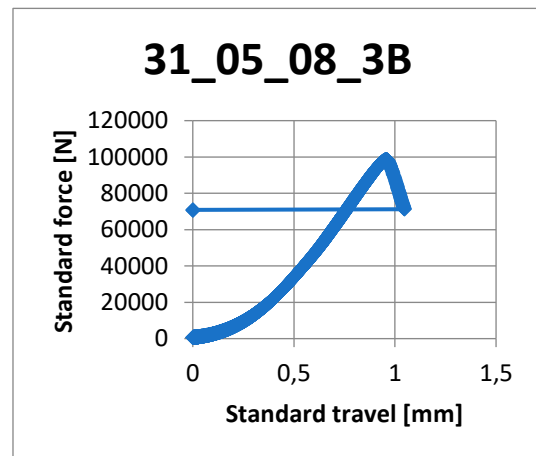
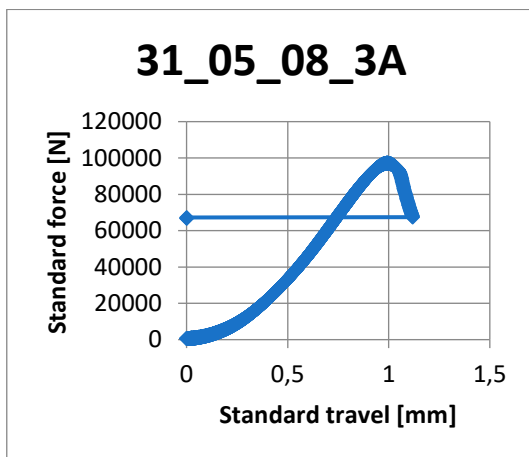
Bending test



Specimen size [mm]		Weight [g]	
160	40.04	41.34	591



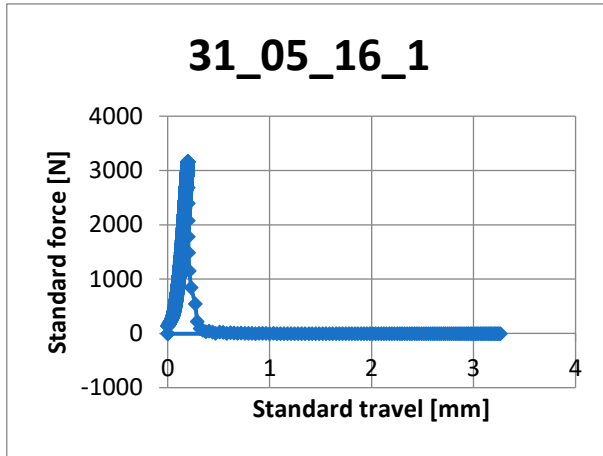
Compression test



P_{max} [kN]	σ_{flex} [MPa]	F_1 [kN]	F_2 [kN]	σ_1 [MPa]	σ_2 [MPa]	% CaCO ₃	pH
3.39	7.94	97.14	98.45	60.72	61.53	6.23	-

31_05_16_1 (1.6% di CO₂)

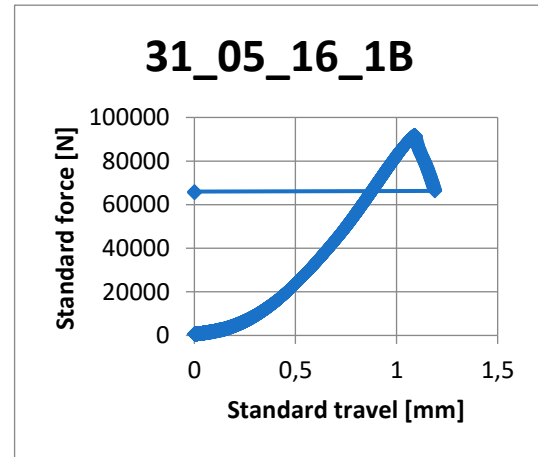
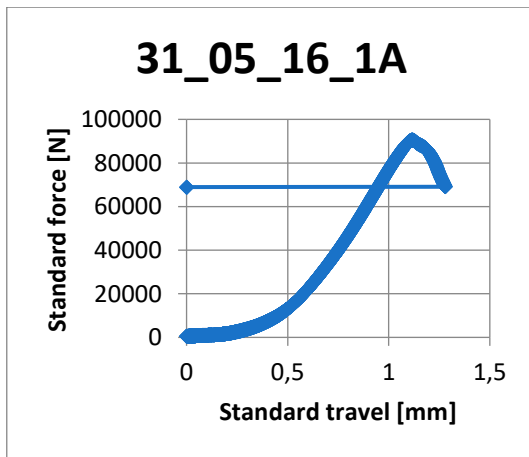
Bending test



Specimen size [mm]		Weight [g]	
160	39.96	41.69	595



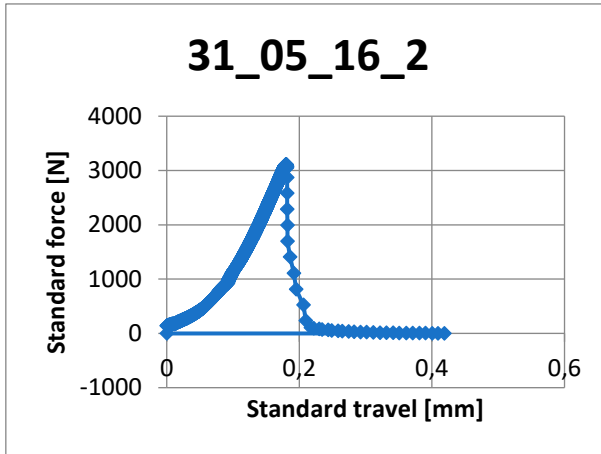
Compression test



P_{max} [kN]	σ_{flex} [MPa]	F_1 [kN]	F_2 [kN]	σ_1 [MPa]	σ_2 [MPa]	% CaCO ₃	pH
3.17	7.42	90.51	91.67	56.57	57.30	7.2	-

31_05_16_2 (1.6% di CO₂)

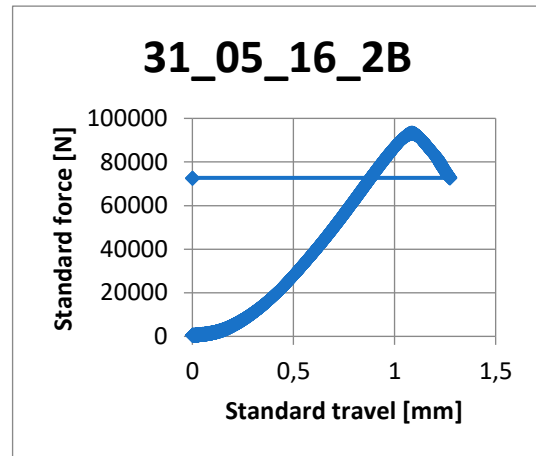
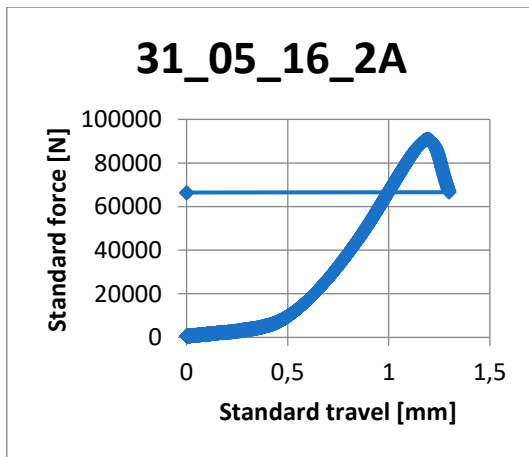
Bending test



Specimen size [mm]		Weight [g]	
160	40.06	41.49	594



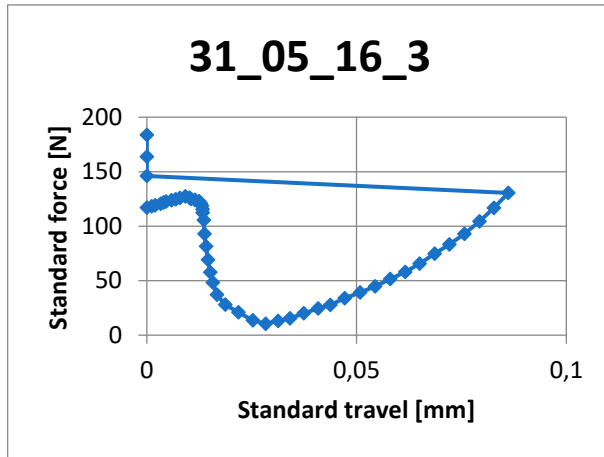
Compression test



P_{max} [kN]	σ_{flex} [MPa]	F_1 [kN]	F_2 [kN]	σ_1 [MPa]	σ_2 [MPa]	% CaCO ₃	pH
3.11	7.29	90.72	93.28	56.71	58.30	6.57	-

31_05_16_3 (1.6% di CO₂)

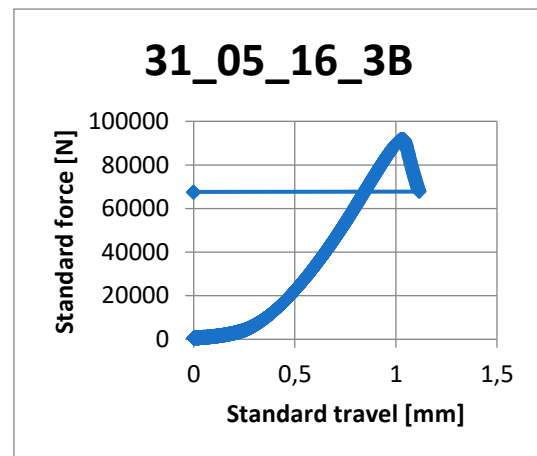
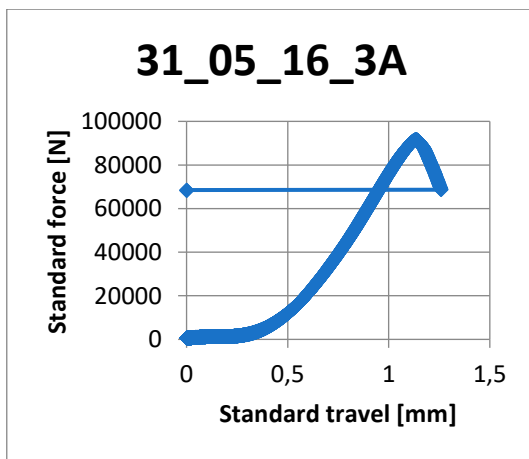
Bending test



Specimen size [mm]		Weight [g]	
160	40.26	41.32	588



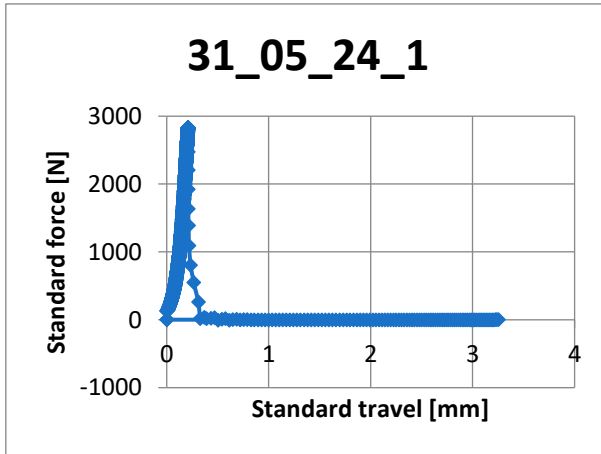
Compression test



P_{max} [kN]	σ_{flex} [MPa]	F_1 [kN]	F_2 [kN]	σ_1 [MPa]	σ_2 [MPa]	% CaCO ₃	pH
-	-	91.56	91.76	57.23	57.35	5.78	-

31_05_24_1 (2.4% di CO₂)

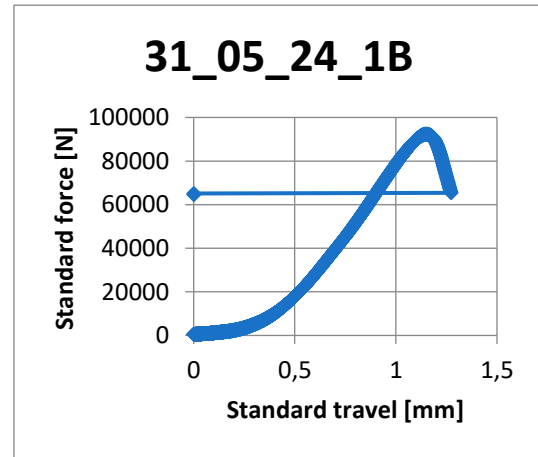
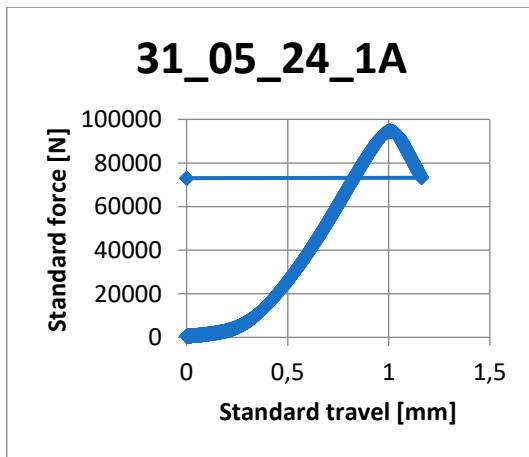
Bending test



Specimen size [mm]		Weight [g]	
160	39.98	40.81	585



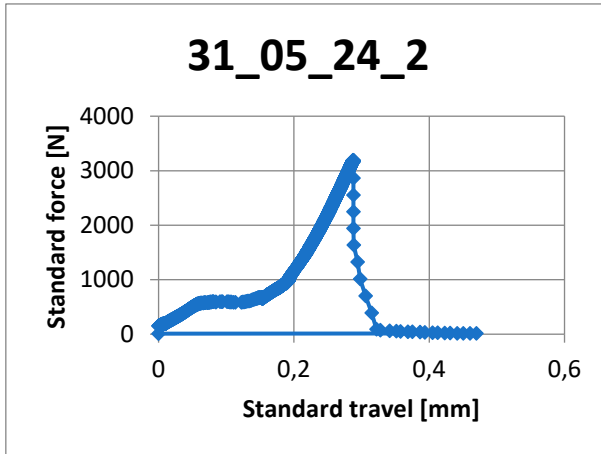
Compression test



P_{max} [kN]	σ_{flex} [MPa]	F_1 [kN]	F_2 [kN]	σ_1 [MPa]	σ_2 [MPa]	% CaCO ₃	pH
2.83	6.64	94.58	92.31	59.12	57.70	5.85	-

31_05_24_2 (2.4% di CO₂)

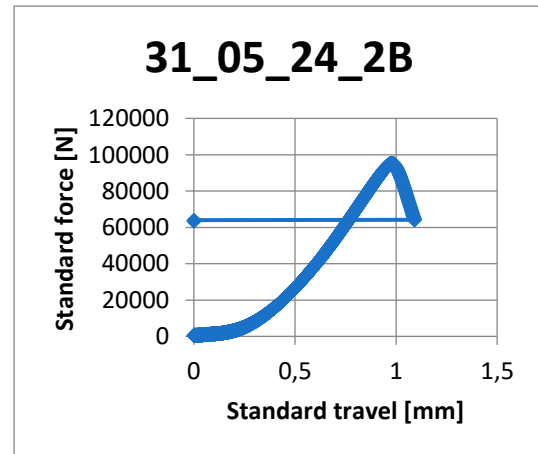
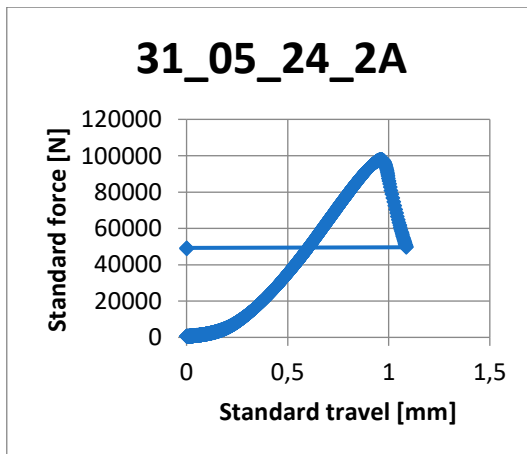
Bending test



Specimen size [mm]		Weight [g]	
160	40.04	41.35	600



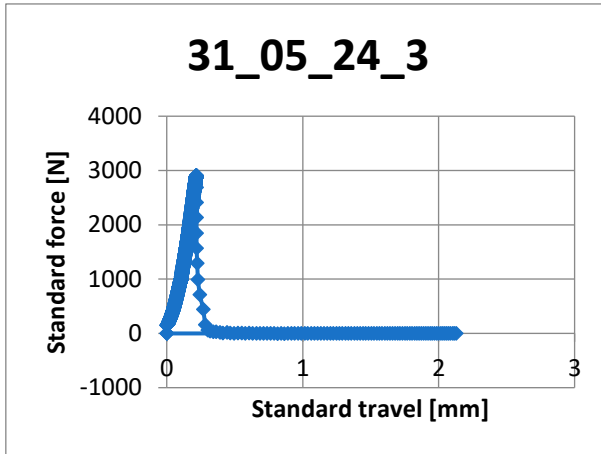
Compression test



P_{max} [kN]	σ_{flex} [MPa]	F_1 [kN]	F_2 [kN]	σ_1 [MPa]	σ_2 [MPa]	% CaCO ₃	pH
3.19	7.47	97.78	95.43	61.12	59.65	5.76	-

31_05_24_3 (2.4% di CO₂)

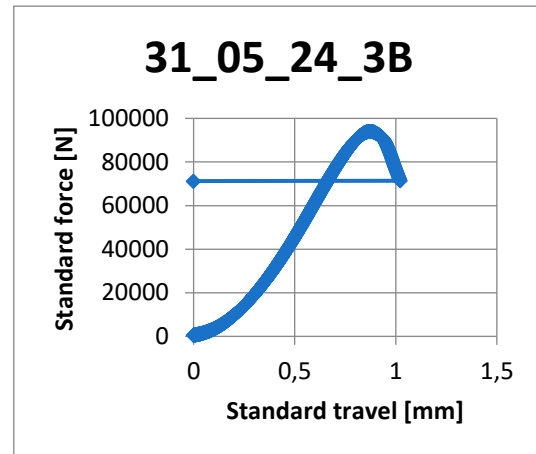
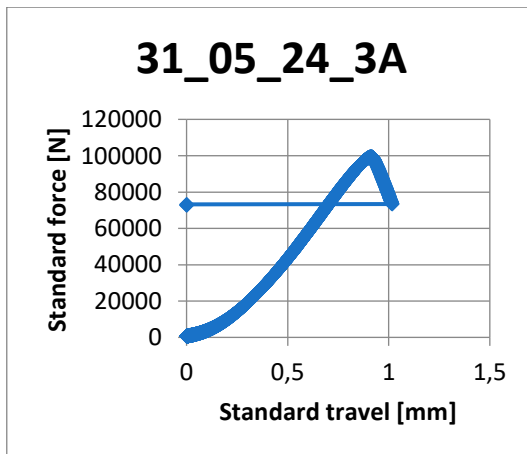
Bending test



Specimen size [mm]		Weight [g]	
160	40.17	41.16	593



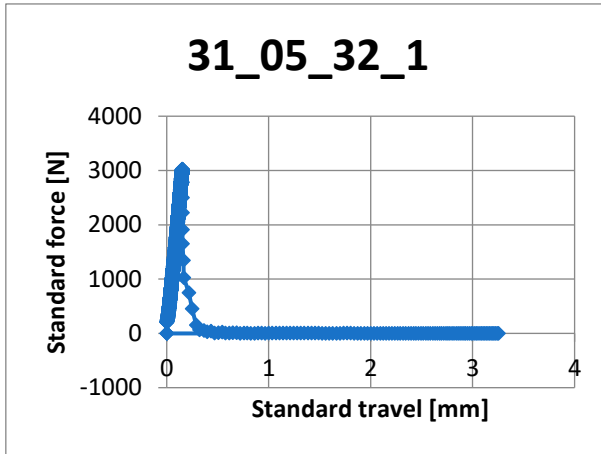
Compression test



P_{max} [kN]	σ_{flex} [MPa]	F_1 [kN]	F_2 [kN]	σ_1 [MPa]	σ_2 [MPa]	% CaCO ₃	pH
2.91	6.81	99.36	94.06	62.10	58.79	6.7	-

31_05_32_1 (3.2% di CO₂)

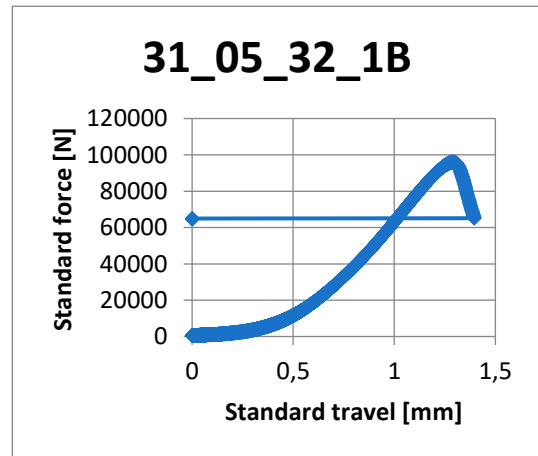
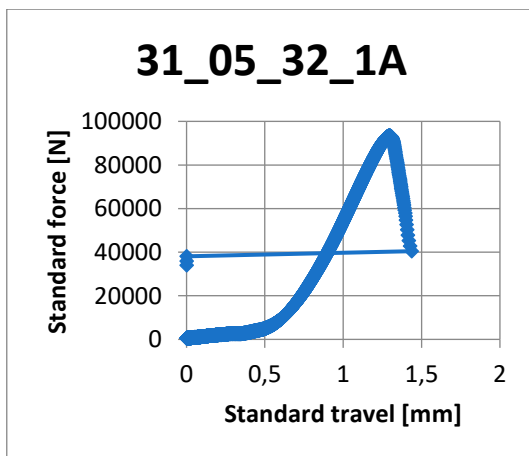
Bending test



Specimen size [mm]		Weight [g]
160	40.32	42.54
		600



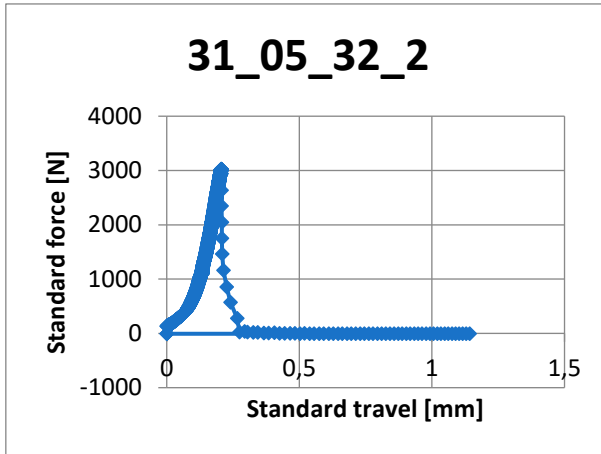
Compression test



P_{max} [kN]	σ_{flex} [MPa]	F_1 [kN]	F_2 [kN]	σ_1 [MPa]	σ_2 [MPa]	% CaCO ₃	pH
3.02	7.08	93.33	95.98	58.33	59.99	6.73	-

31_05_32_2 (3.2% di CO₂)

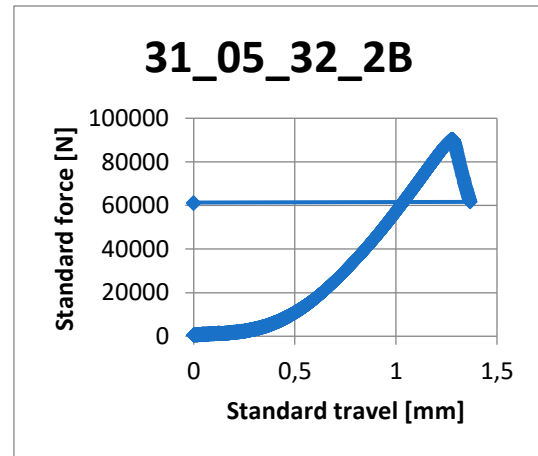
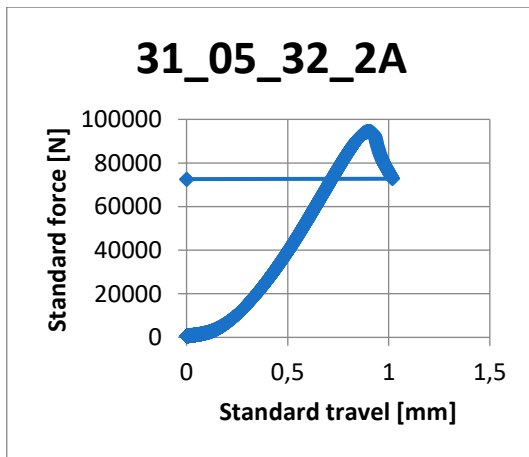
Bending test



Specimen size [mm]		Weight [g]	
160	39.96	41.20	589



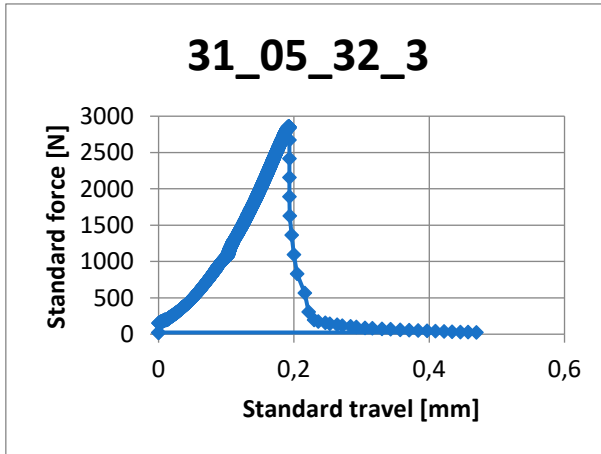
Compression test



P_{max} [kN]	σ_{flex} [MPa]	F_1 [kN]	F_2 [kN]	σ_1 [MPa]	σ_2 [MPa]	% CaCO ₃	pH
3.02	7.08	94.33	90.32	58.96	56.45	6	-

31_05_32_3 (3.2% di CO₂)

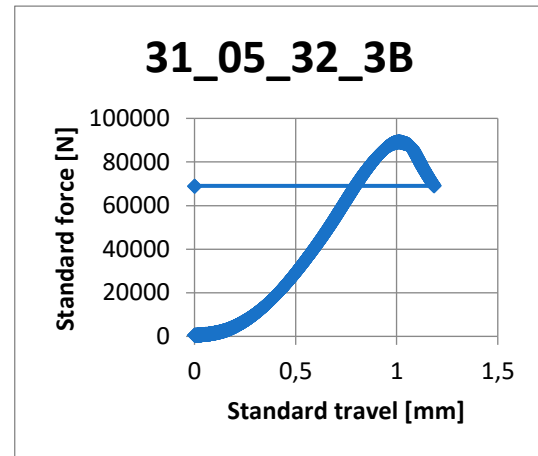
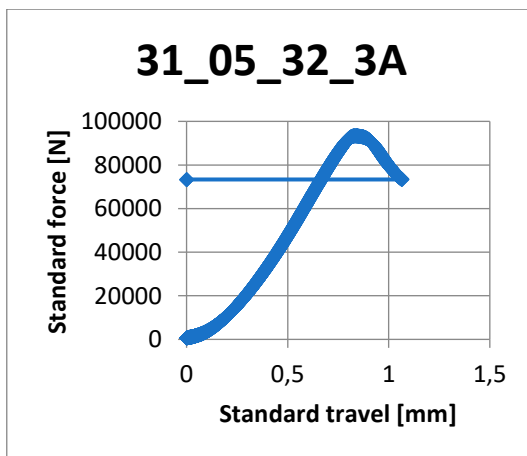
Bending test



Specimen size [mm]		Weight [g]	
160	40.12	40.80	586



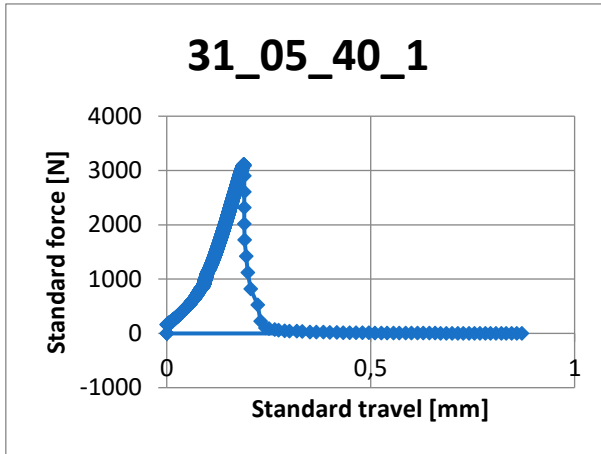
Compression test



P_{max} [kN]	σ_{flex} [MPa]	F_1 [kN]	F_2 [kN]	σ_1 [MPa]	σ_2 [MPa]	% CaCO ₃	pH
2.86	6.69	93.37	89.26	58.36	55.79	4.76	-

31_05_40_1 (4.0% di CO₂)

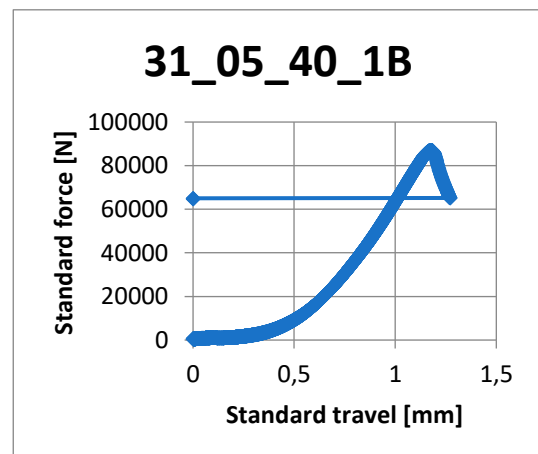
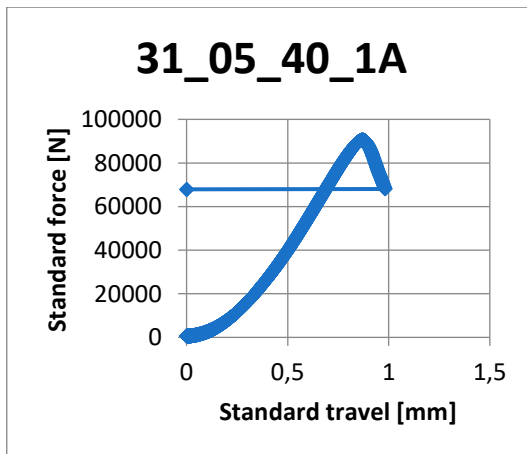
Bending test



Specimen size [mm]		Weight [g]	
160	40.28	41.17	594



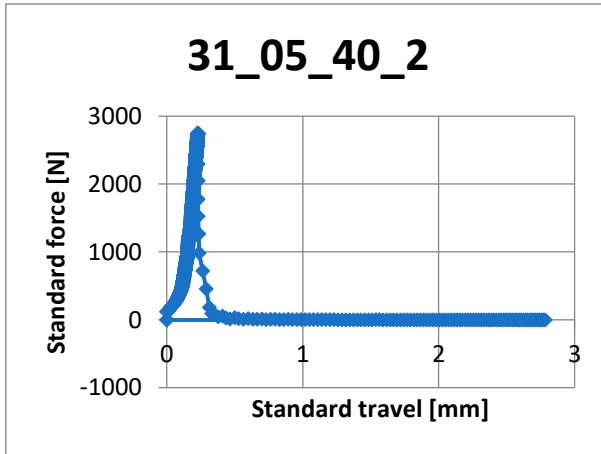
Compression test



P_{max} [kN]	σ_{flex} [MPa]	F_1 [kN]	F_2 [kN]	σ_1 [MPa]	σ_2 [MPa]	% CaCO ₃	pH
3.11	7.28	90.53	87.09	56.58	54.43	5.85	-

31_05_40_2 (4.0% di CO₂)

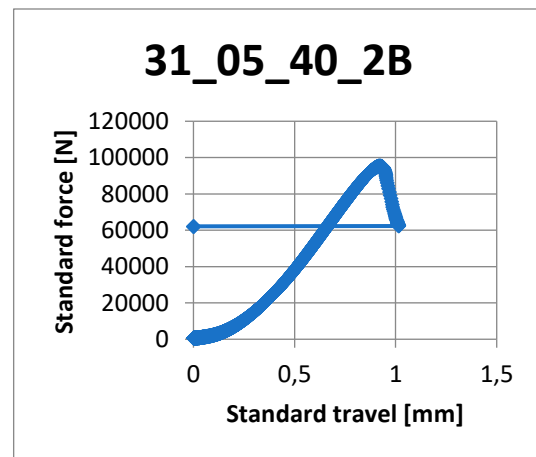
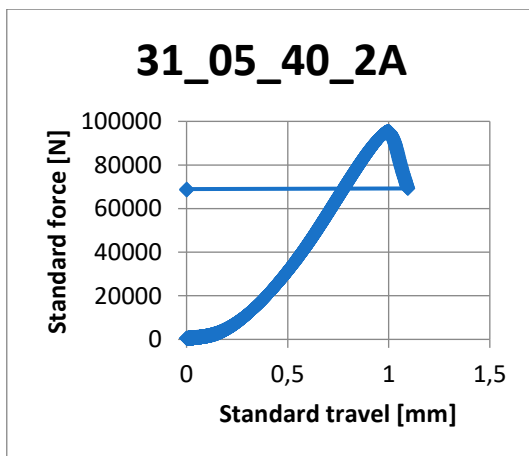
Bending test



Specimen size [mm]		Weight [g]
160	40.05 40.68	584



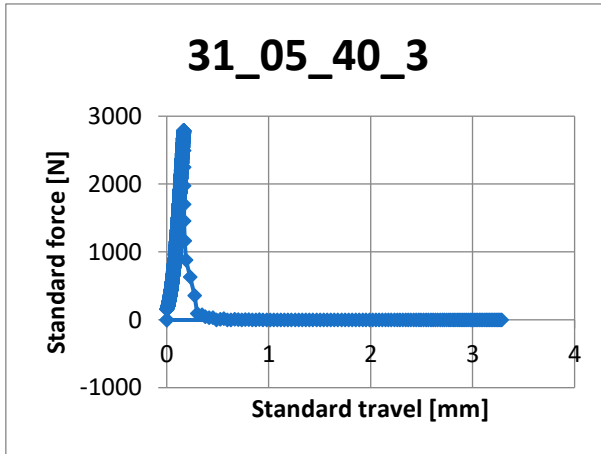
Compression test



P_{max} [kN]	σ_{flex} [MPa]	F_1 [kN]	F_2 [kN]	σ_1 [MPa]	σ_2 [MPa]	% CaCO ₃	pH
2.75	6.45	95.22	95.33	59.51	59.59	6.53	-

31_05_40_3 (4.0% di CO₂)

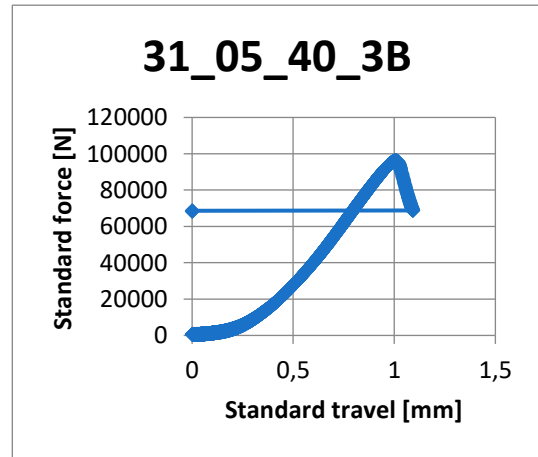
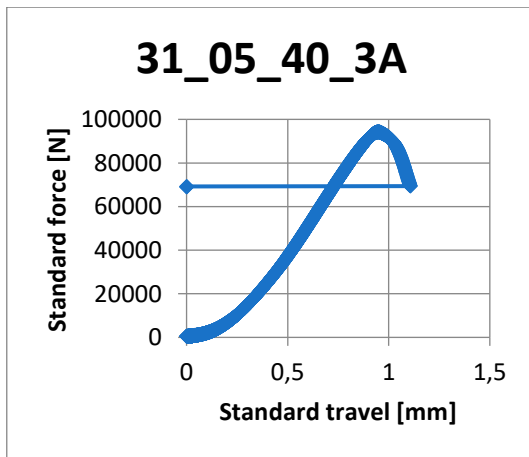
Bending test



Specimen size [mm]		Weight [g]
160	40.10 40.95	587



Compression test



P_{max} [kN]	σ_{flex} [MPa]	F_1 [kN]	F_2 [kN]	σ_1 [MPa]	σ_2 [MPa]	% CaCO ₃	pH
2.79	6.54	94.27	96.07	58.92	60.05	7.25	-

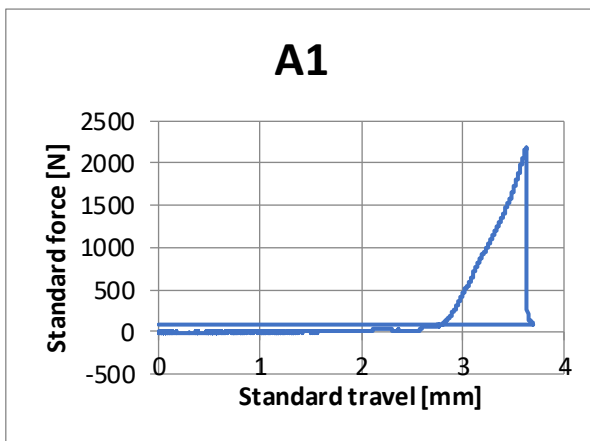
Specimen A- Plain

Here are all the tests done during test # 3.

In some cases there are proofs that have been redone due to technical problems, these are named with the name following the consideration.

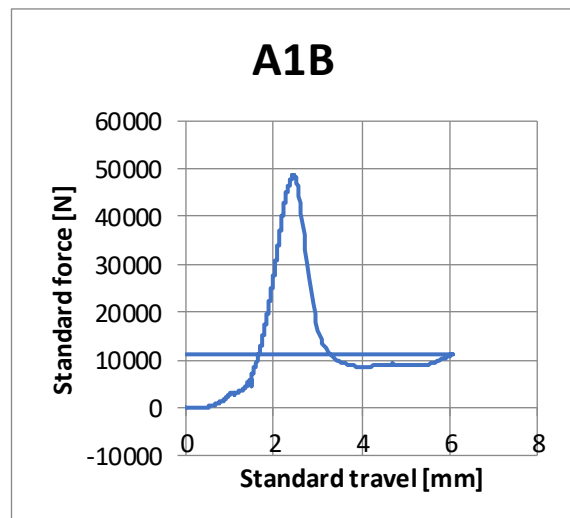
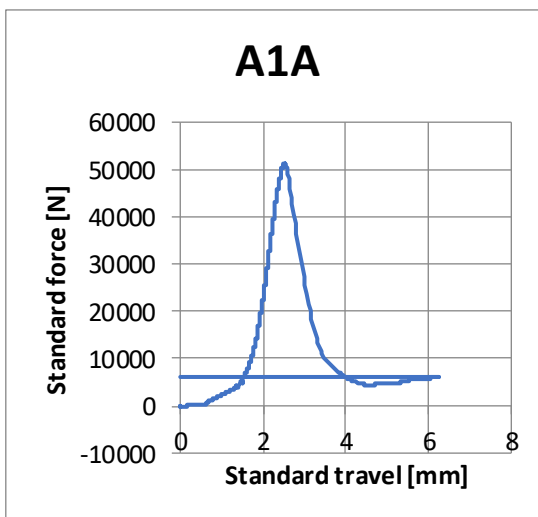
A1

Bending test



Specimen size [mm]		Weight [g]	
160	40,05	40,68	584

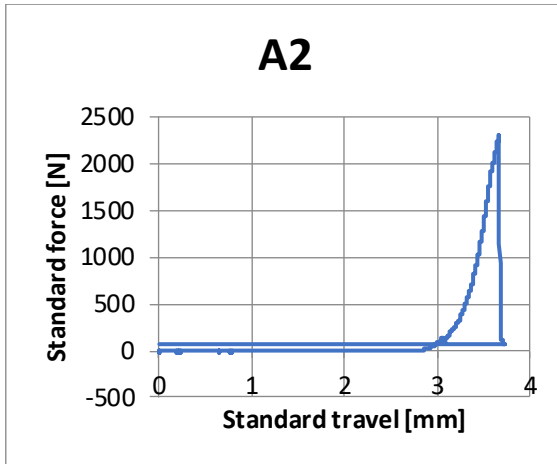
Compression test



Pmax [kN]	σ flex [MPa]	F1 [kN]	F2 [kN]	σ 1 [MPa]	σ 2 [MPa]
2,18	4,82	51,10	48,74	31,94	30,46

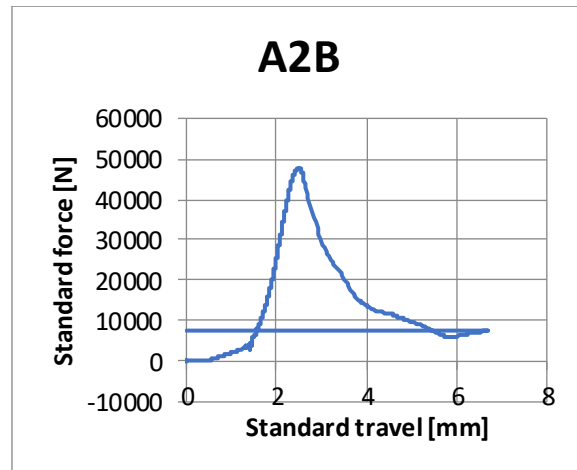
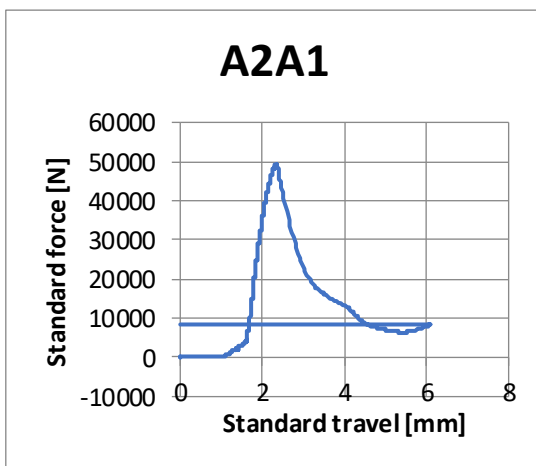
A2

Bending test



Specimen size [mm]		Weight [g]	
160.33	40.64	40.64	543.03

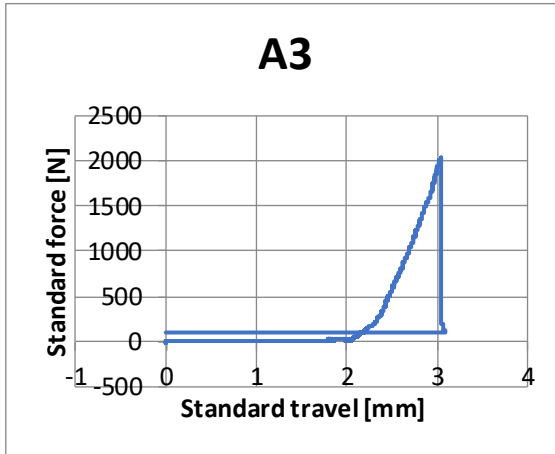
Compression test



Pmax [kN]	σ flex [MPa]	F1 [kN]	F2 [kN]	σ 1 [MPa]	σ 2 [MPa]
2,30	5,13	49,07	47,69	30,67	29,81

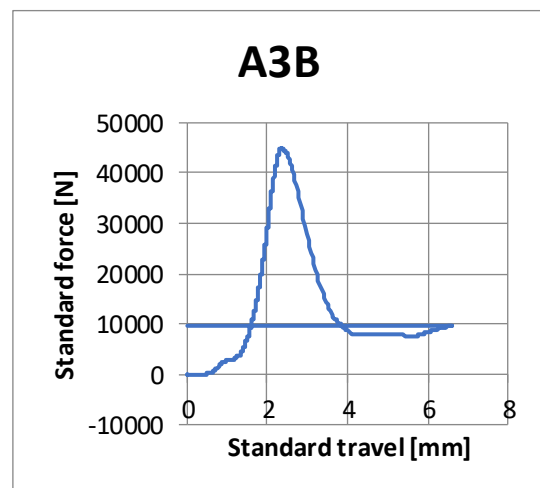
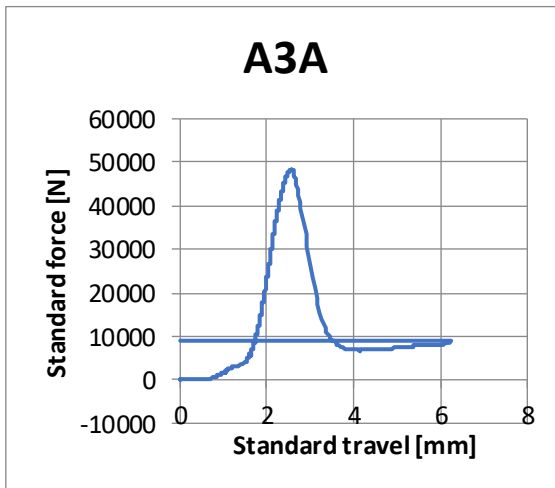
A3

Bending test



Specimen size [mm]		Weight [g]	
160.08	41.24	40.73	555.74

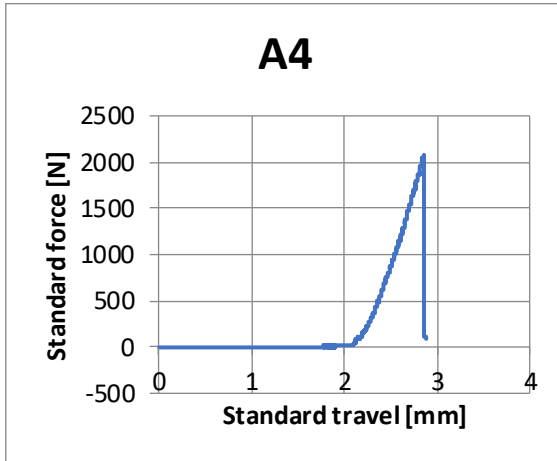
Compression test



Pmax [kN]	σ flex [MPa]	F1 [kN]	F2 [kN]	σ 1 [MPa]	σ 2 [MPa]
2,04	4,48	48,37	44,97	30,23	28,11

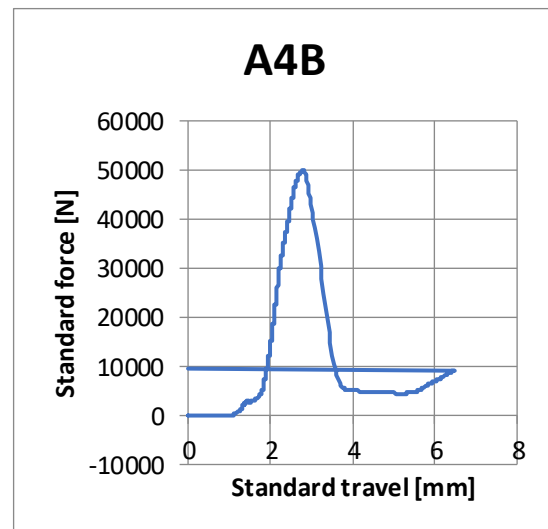
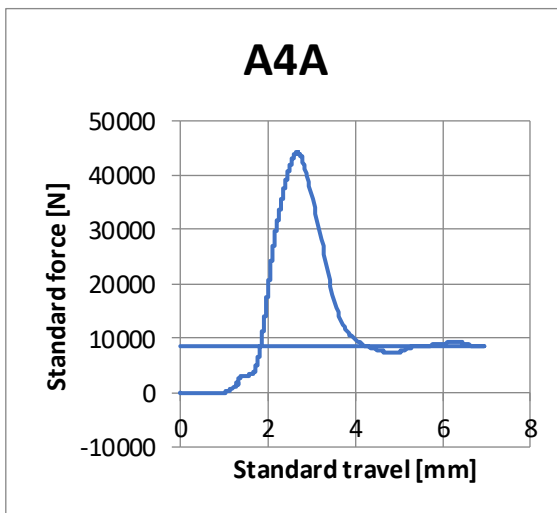
A4

Bending test



Specimen size [mm]		Weight [g]	
160.03	39.38	40.03	535.17

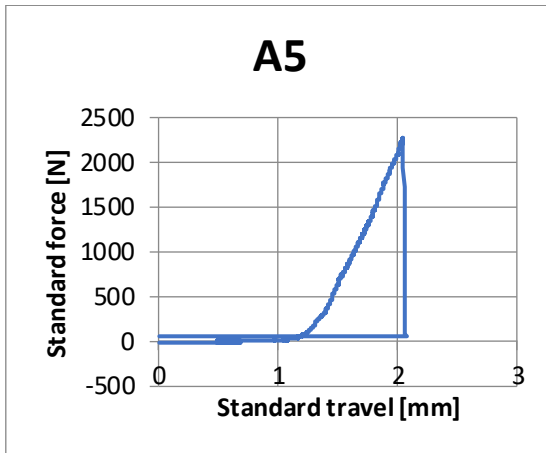
Compression test



Pmax [kN]	σ flex [MPa]	F1 [kN]	F2 [kN]	σ 1 [MPa]	σ 2 [MPa]
2,07	4,85	44,12	49,96	27,58	31,23

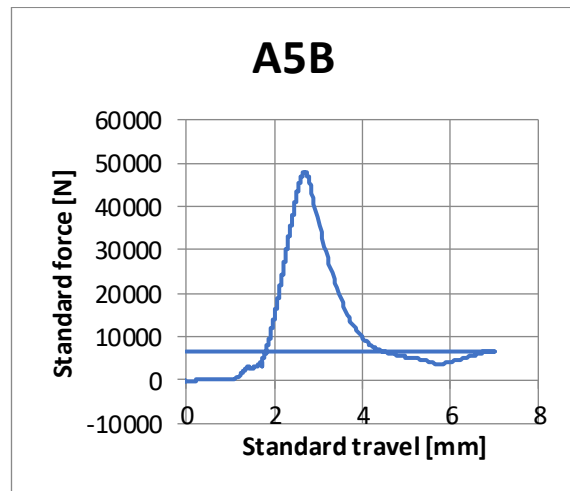
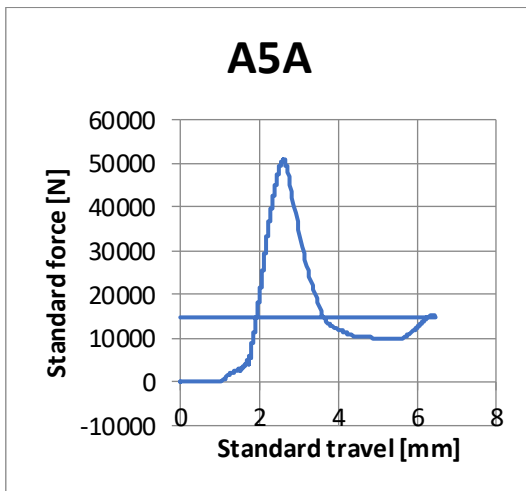
A5

Bending test



Specimen size [mm]		Weight [g]	
160.06	40.38	39.87	540.99

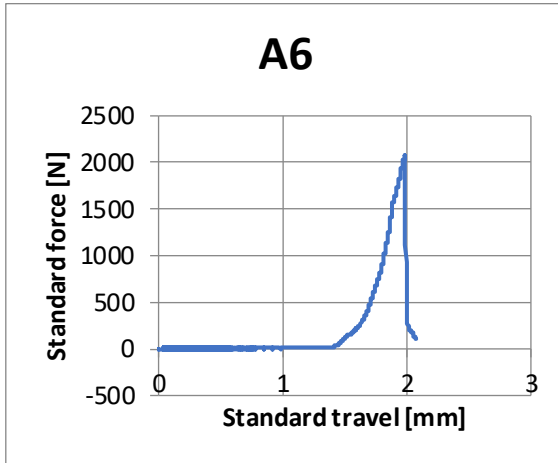
Compression test



Pmax [kN]	σ flex [MPa]	F1 [kN]	F2 [kN]	σ 1 [MPa]	σ 2 [MPa]
2,27	5,30	50,87	47,87	31,79	29,92

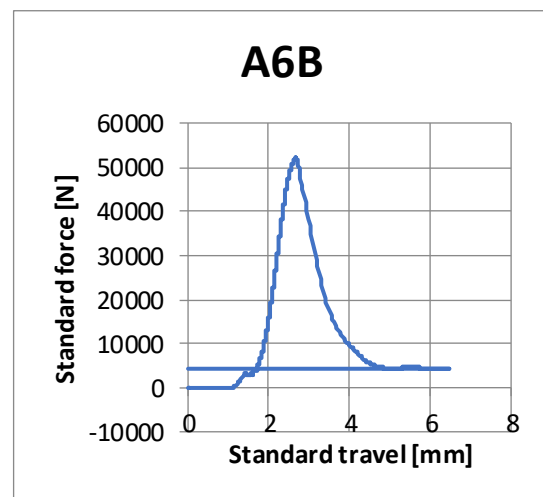
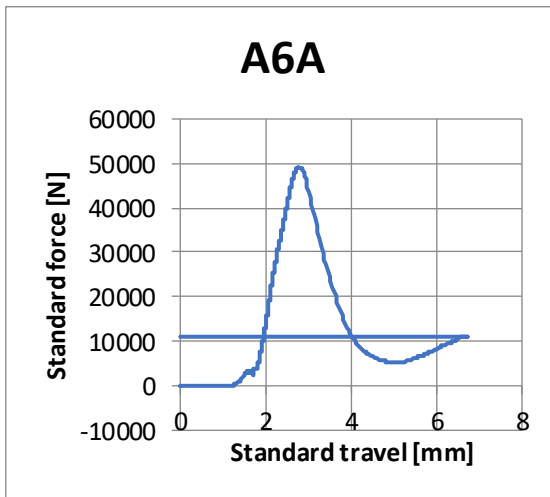
A6

Bending test



Specimen size [mm]		Weight [g]	
159.89	39.5	40.33	535.74

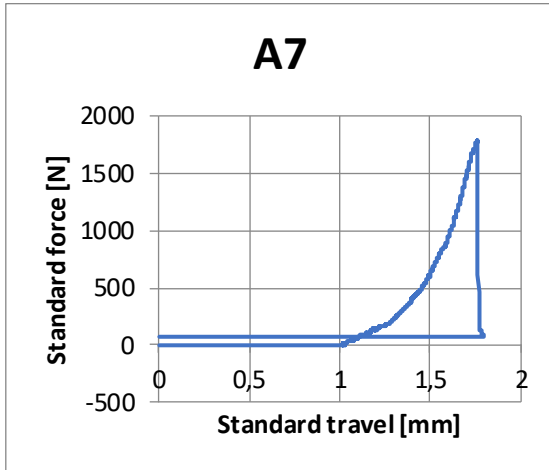
Compression test



Pmax [kN]	σ flex [MPa]	F1 [kN]	F2 [kN]	σ 1 [MPa]	σ 2 [MPa]
2,07	4,83	49,19	51,96	30,74	32,48

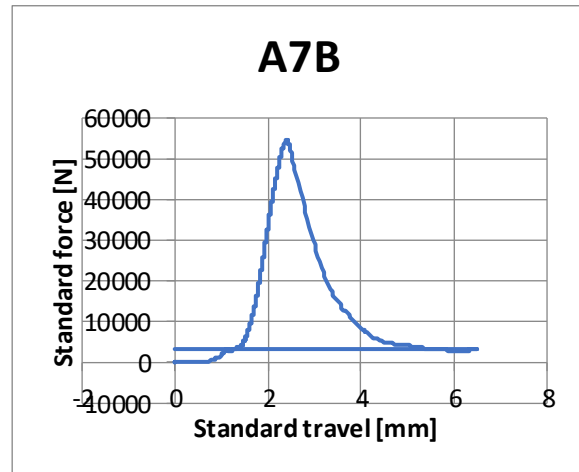
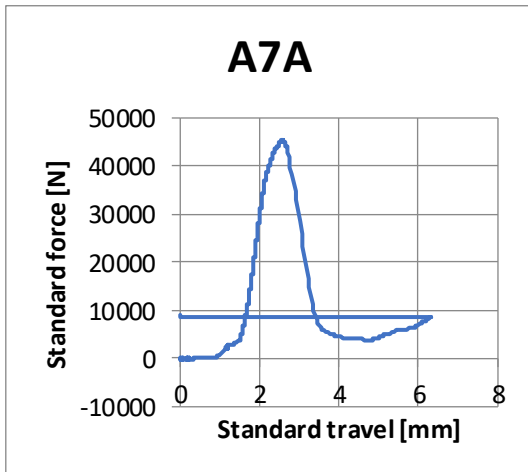
A7

Bending test



Specimen size [mm]		Weight [g]	
160.33	39.58	40.76	536.08

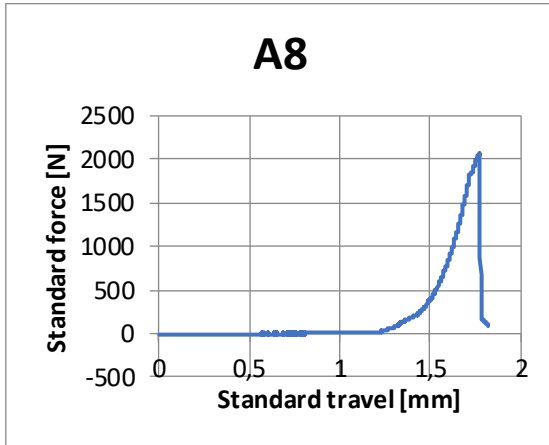
Compression test



Pmax [kN]	σ flex [MPa]	F1 [kN]	F2 [kN]	σ 1 [MPa]	σ 2 [MPa]
1,78	4,06	45,36	54,46	28,35	34,04

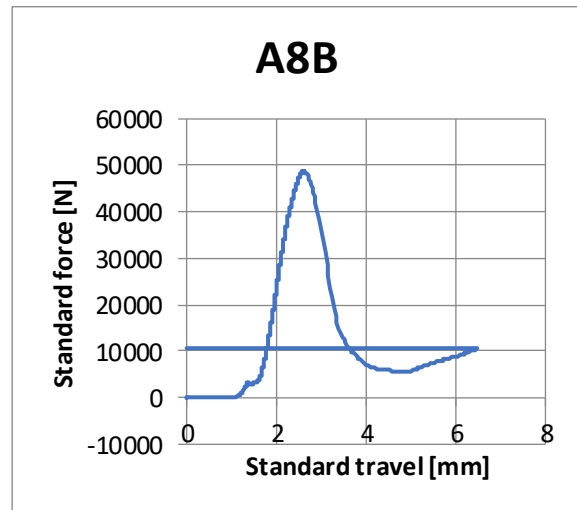
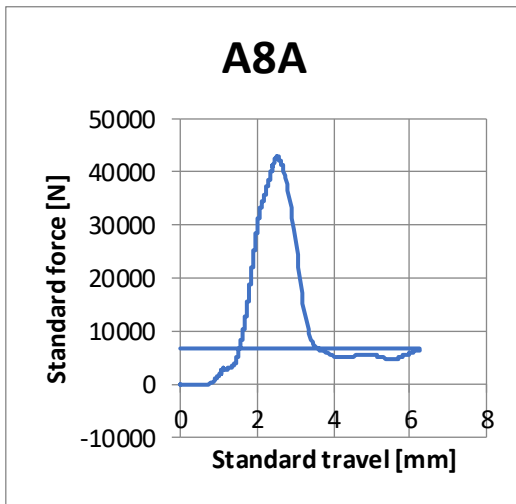
A8

Bending test



Specimen size [mm]		Weight [g]	
160.4	40.25	40.17	541.48

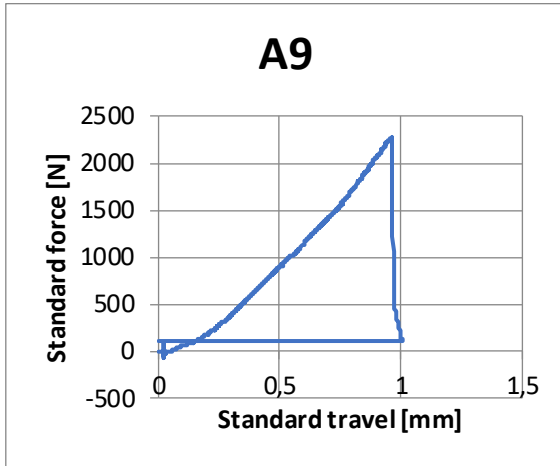
Compression test



Pmax [kN]	σ flex [MPa]	F1 [kN]	F2 [kN]	σ 1 [MPa]	σ 2 [MPa]
2,08	4,80	42,91	48,65	26,82	30,41

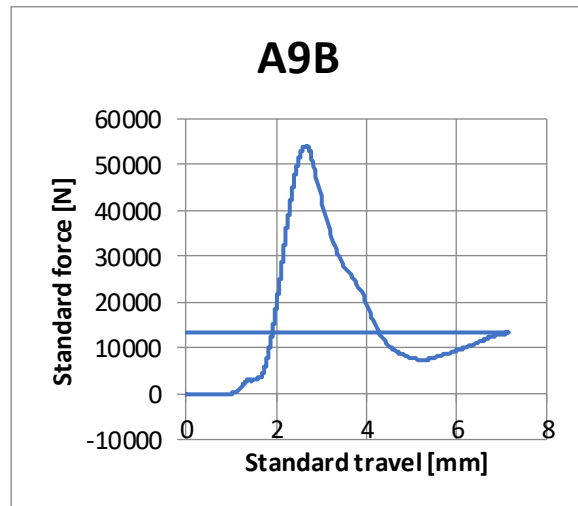
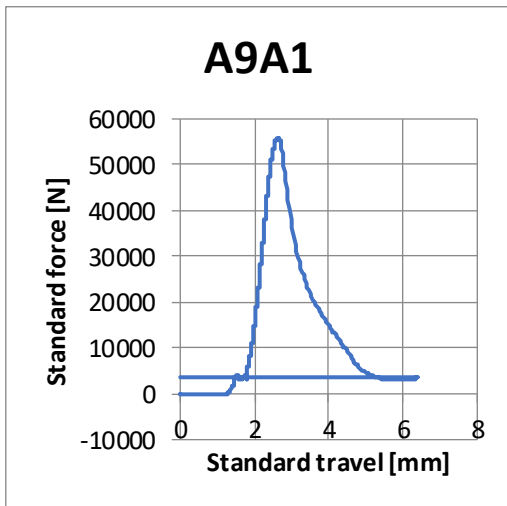
A9

Bending test



Specimen size [mm]		Weight [g]	
160.45	40.65	40.14	548.15

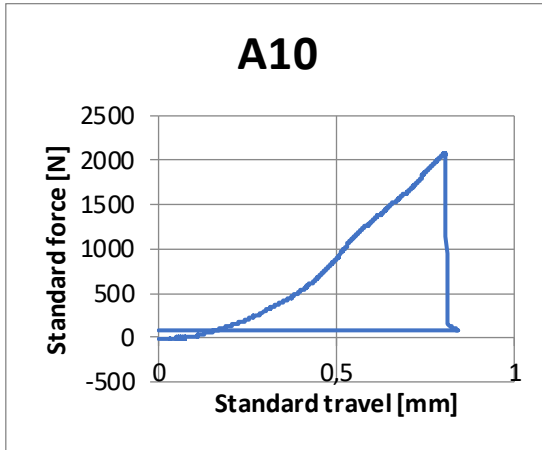
Compression test



Pmax [kN]	σ flex [MPa]	F1 [kN]	F2 [kN]	σ 1 [MPa]	σ 2 [MPa]
2,27	5,21	55,83	54,10	34,89	33,81

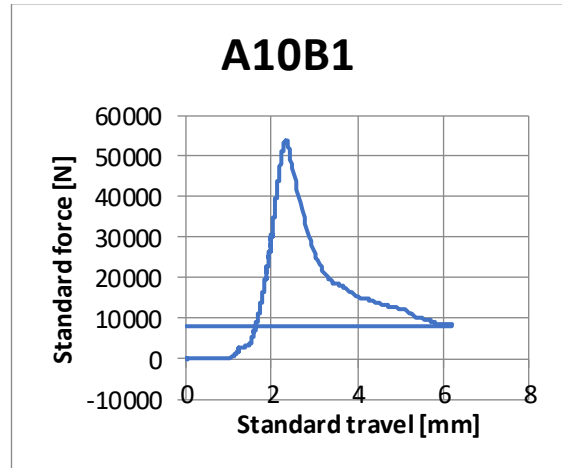
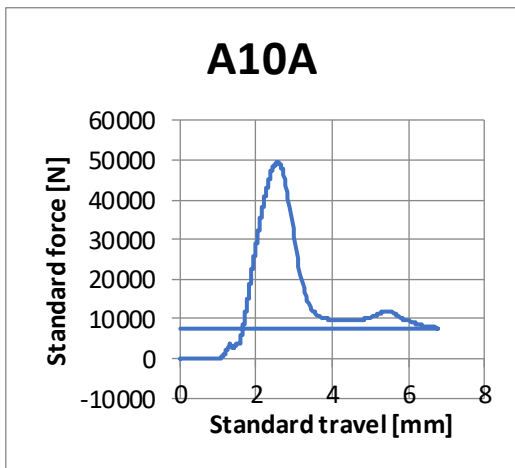
A10

Bending test



Specimen size [mm]		Weight [g]	
159.98	39.97	40.44	545.57

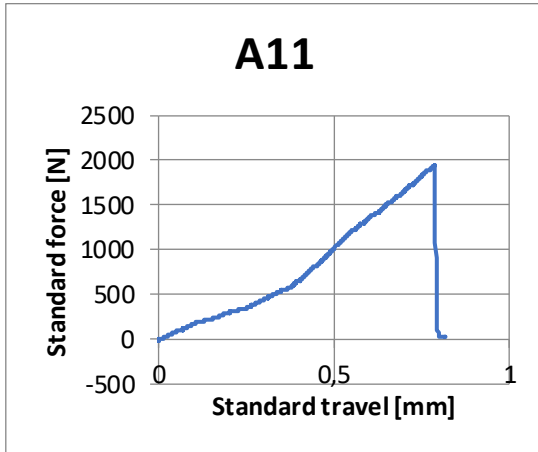
Compression test



Pmax [kN]	σ flex [MPa]	F1 [kN]	F2 [kN]	σ 1 [MPa]	σ 2 [MPa]
2,07	4,75	49,22	53,90	30,76	33,69

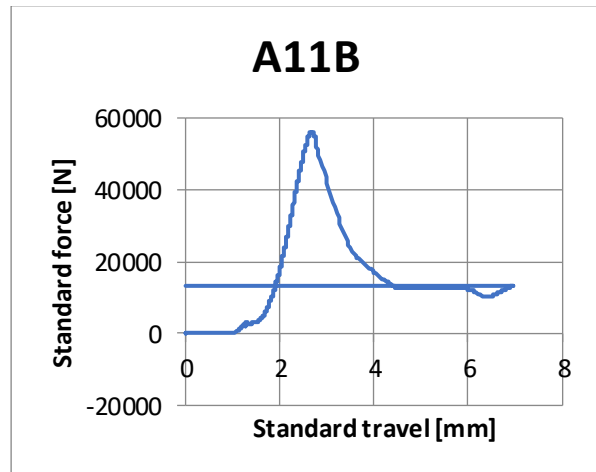
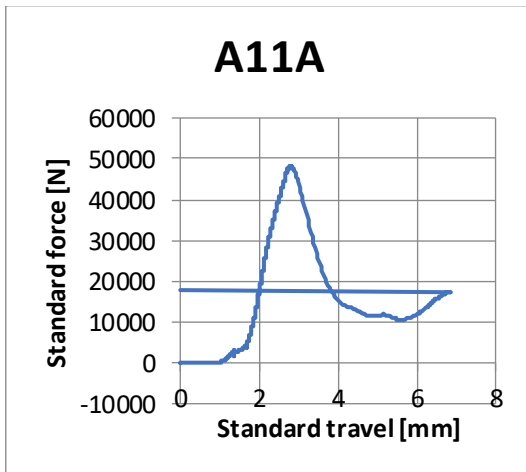
A11

Bending test



Specimen size [mm]		Weight [g]	
160.26	40.2	40.68	545.6

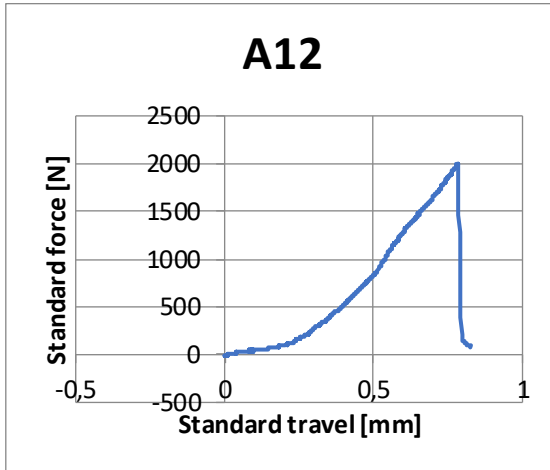
Compression test



Pmax [kN]	σ flex [MPa]	F1 [kN]	F2 [kN]	σ 1 [MPa]	σ 2 [MPa]
1,95	4,40	47,98	55,96	29,98	34,97

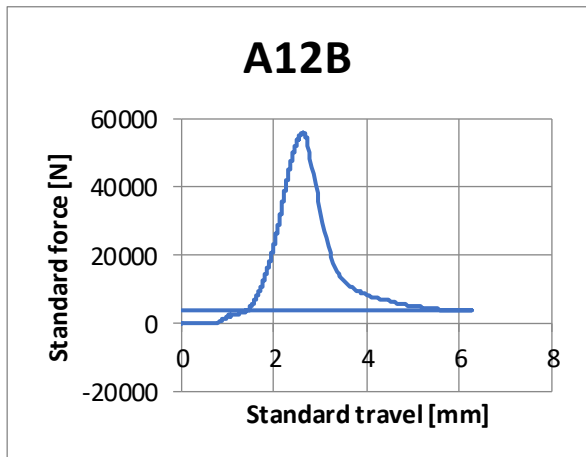
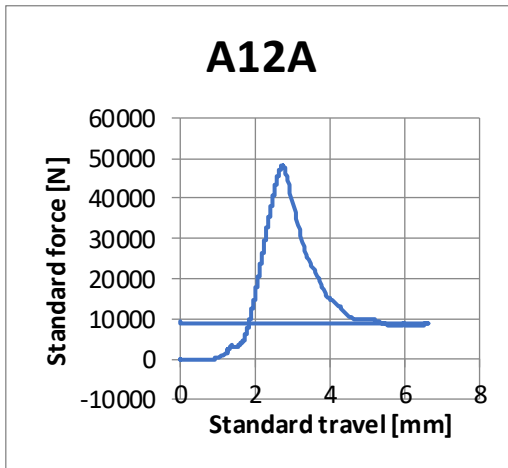
A12

Bending test



Specimen size [mm]		Weight [g]	
160.46	40.55	40.4	547.19

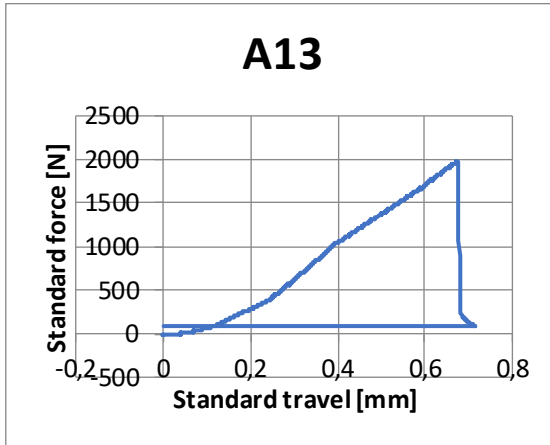
Compression test



Pmax [kN]	σ flex [MPa]	F1 [kN]	F2 [kN]	σ 1 [MPa]	σ 2 [MPa]
2,00	4,53	47,93	56,02	29,95	35,01

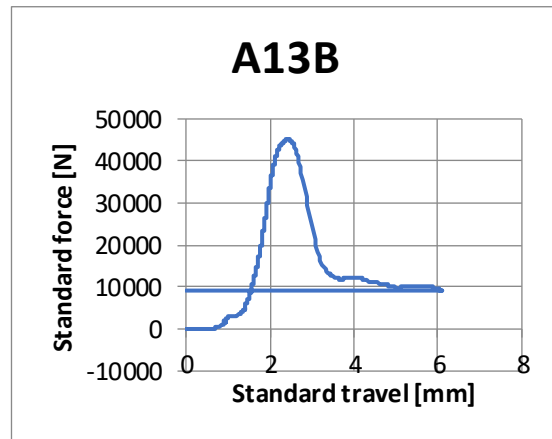
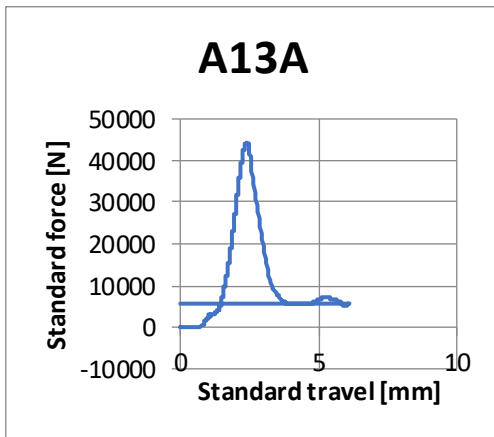
A13

Bending test



Specimen size [mm]		Weight [g]	
160.73	40.73	40.58	539.69

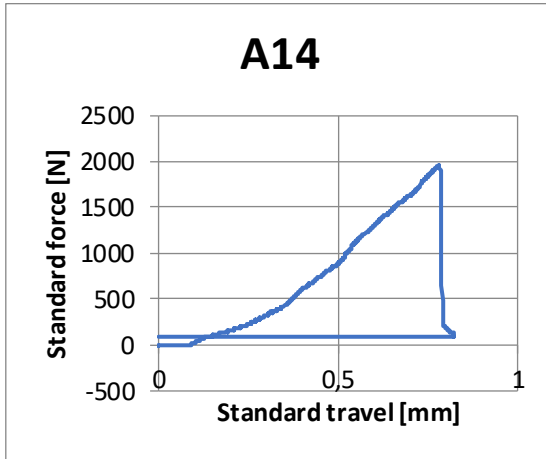
Compression test



Pmax [kN]	σ flex [MPa]	F1 [kN]	F2 [kN]	σ 1 [MPa]	σ 2 [MPa]
1,98	4,43	44,32	45,21	27,70	28,26

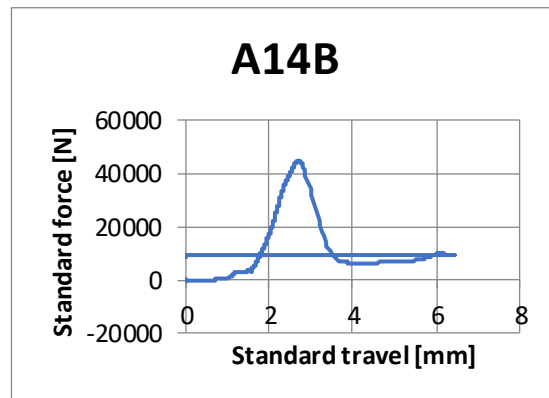
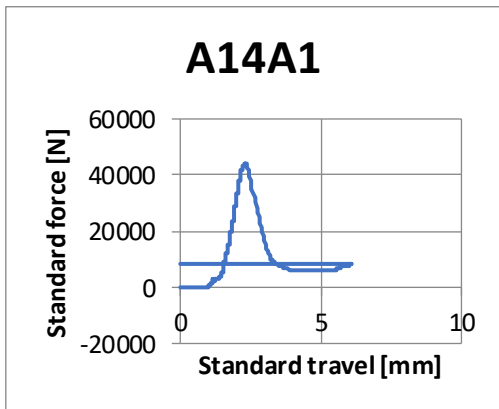
A14

Bending test



Specimen size [mm]		Weight [g]	
160.39	40.57	40.49	539.09

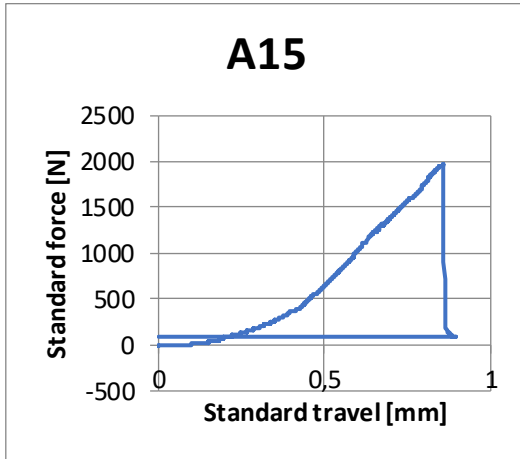
Compression test



Pmax [kN]	σ flex [MPa]	F1 [kN]	F2 [kN]	σ 1 [MPa]	σ 2 [MPa]
1,96	4,43	44,11	44,72	27,57	27,95

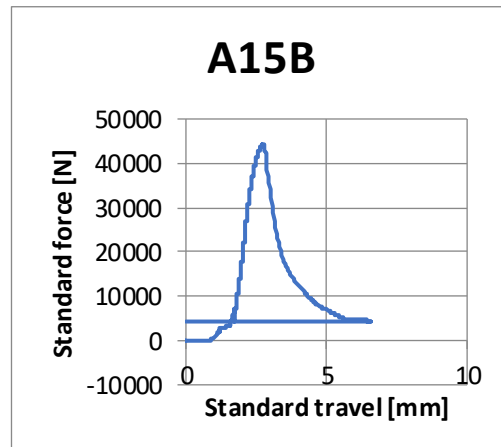
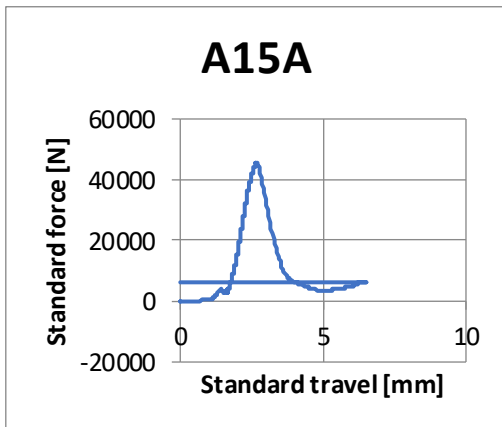
A15

Bending test



Specimen size [mm]		Weight [g]	
160.95	40.24	40.46	534.74

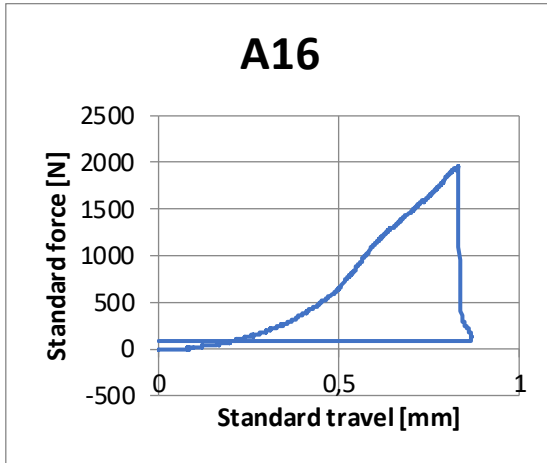
Compression test



Pmax [kN]	σ flex [MPa]	F1 [kN]	F2 [kN]	σ 1 [MPa]	σ 2 [MPa]
1,97	4,48	45,51	44,12	28,44	27,57

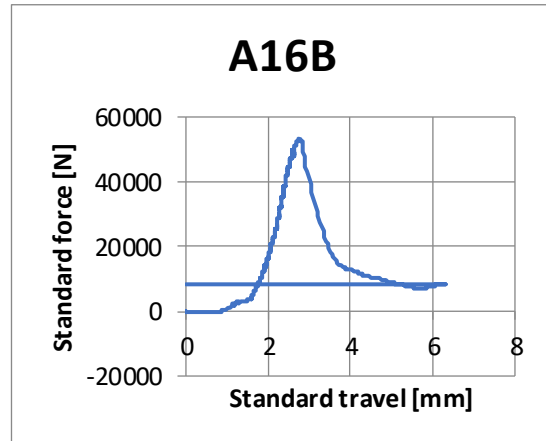
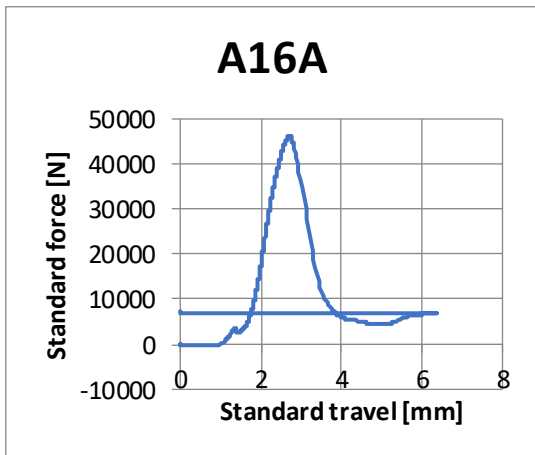
A16

Bending test



Specimen size [mm]		Weight [g]	
160.33	39.77	40.34	538.78

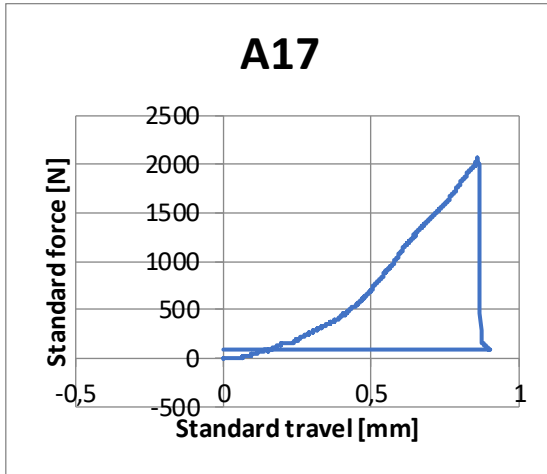
Compression test



Pmax [kN]	σ flex [MPa]	F1 [kN]	F2 [kN]	σ 1 [MPa]	σ 2 [MPa]
1,95	4,53	46,23	53,30	28,90	33,31

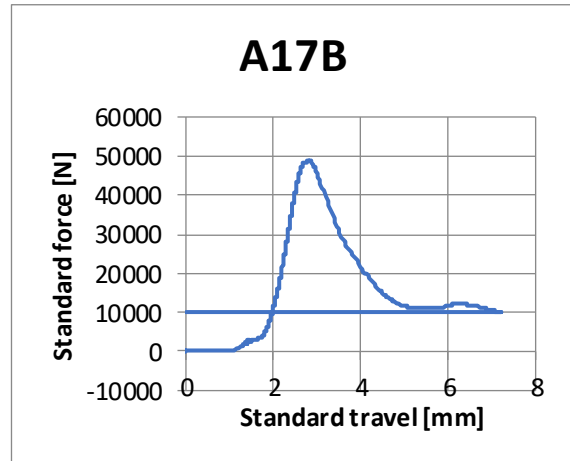
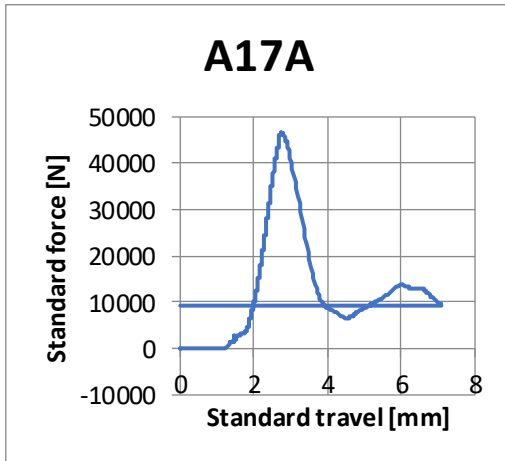
A17

Bending test



Specimen size [mm]		Weight [g]	
160.75	40.67	40.44	542.54

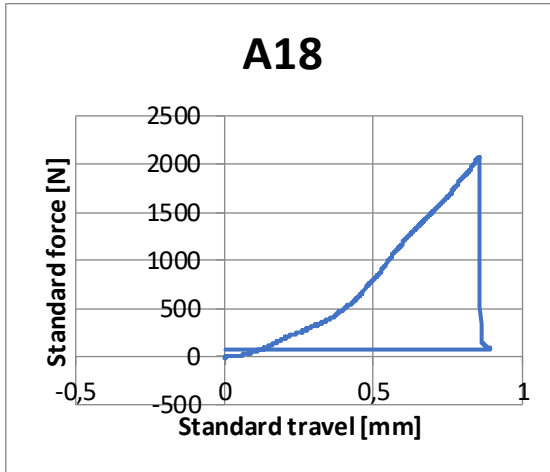
Compression test



Pmax [kN]	σ flex [MPa]	F1 [kN]	F2 [kN]	σ 1 [MPa]	σ 2 [MPa]
2,06	4,65	46,65	48,85	29,16	30,53

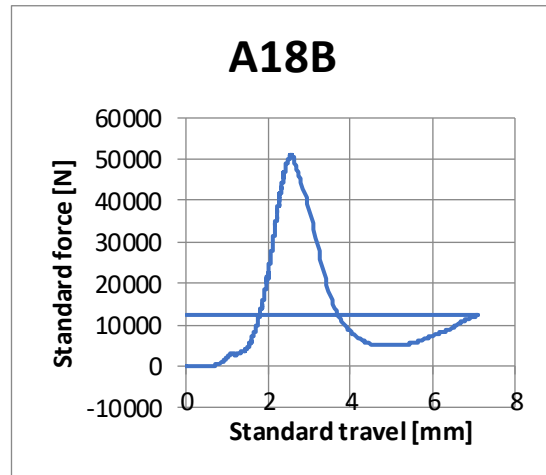
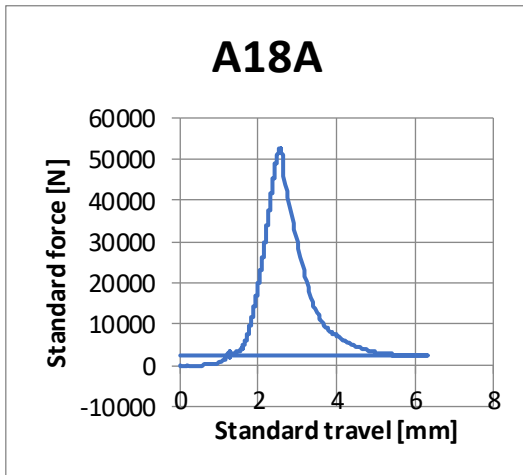
A18

Bending test



Specimen size [mm]		Weight [g]	
159.95	40	40.67	542.4

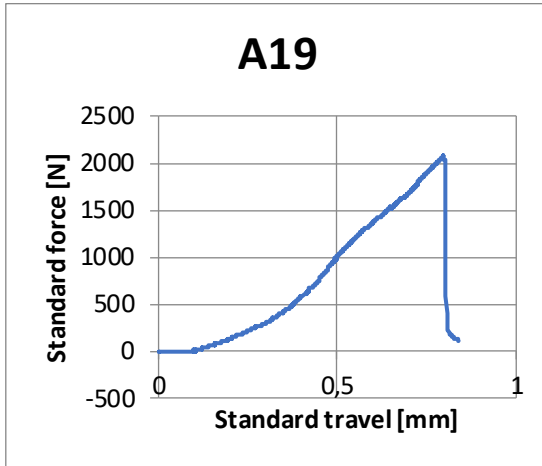
Compression test



Pmax [kN]	σ flex [MPa]	F1 [kN]	F2 [kN]	σ 1 [MPa]	σ 2 [MPa]
2,07	4,70	52,53	51,04	32,83	31,90

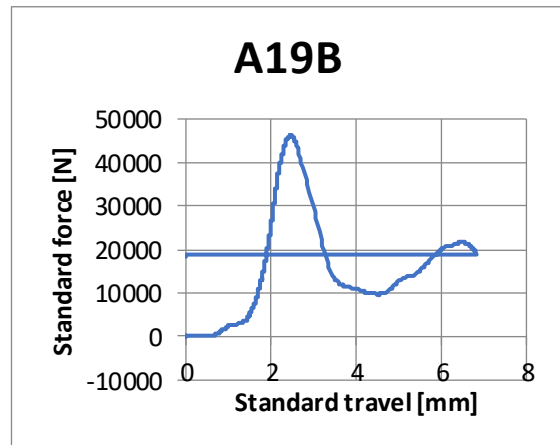
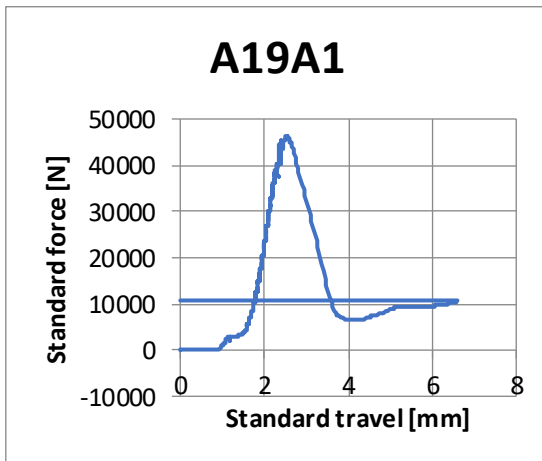
A19

Bending test



Specimen size [mm]		Weight [g]	
160.51	40.22	40.53	544.38

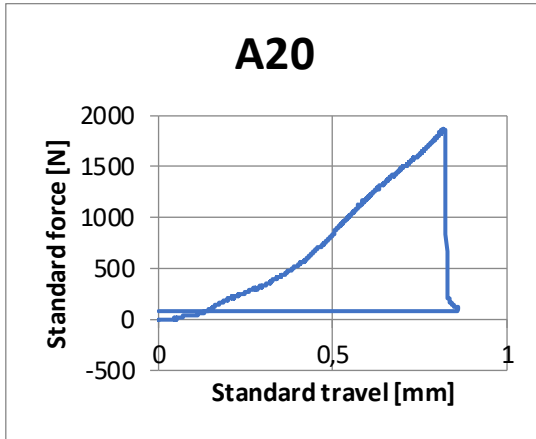
Compression test



Pmax [kN]	σ flex [MPa]	F1 [kN]	F2 [kN]	σ 1 [MPa]	σ 2 [MPa]
2,07	4,70	46,21	46,23	28,88	28,89

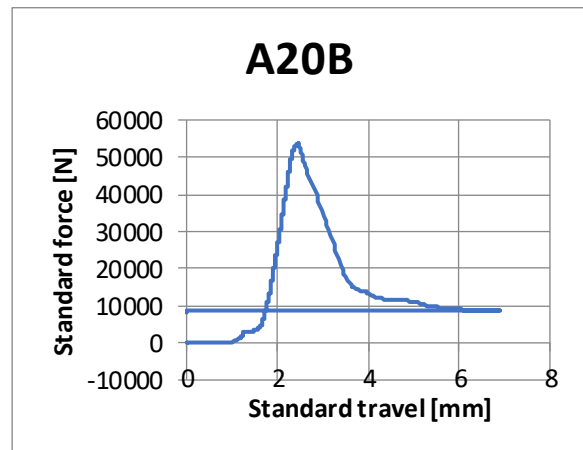
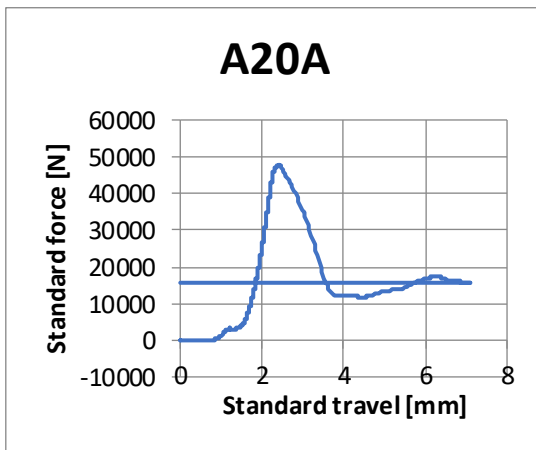
A20

Bending test



Specimen size [mm]		Weight [g]	
159.91	41.16	40.55	550.82

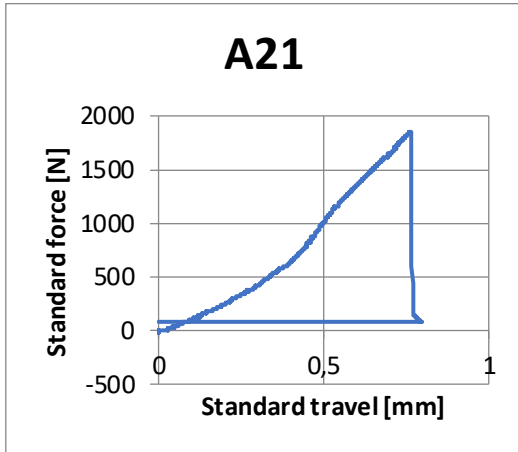
Compression test



Pmax [kN]	σ flex [MPa]	F1 [kN]	F2 [kN]	σ 1 [MPa]	σ 2 [MPa]
1,87	4,15	47,78	53,78	29,86	33,61

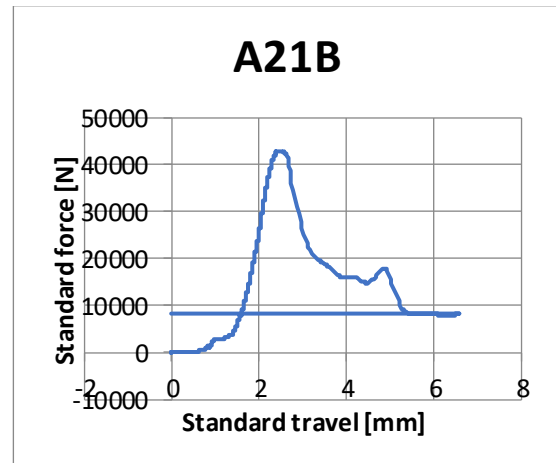
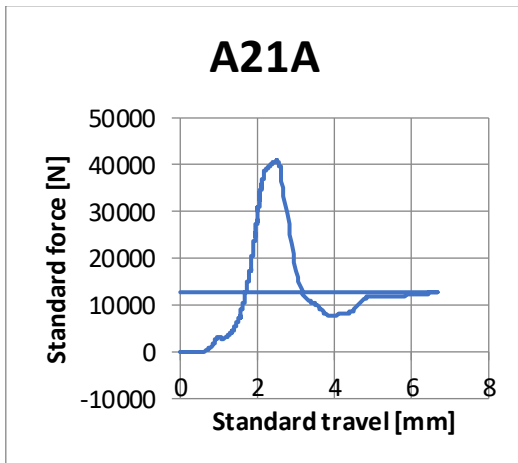
A21

Bending test



Specimen size [mm]		Weight [g]	
159.93	39.39	40.76	530.3

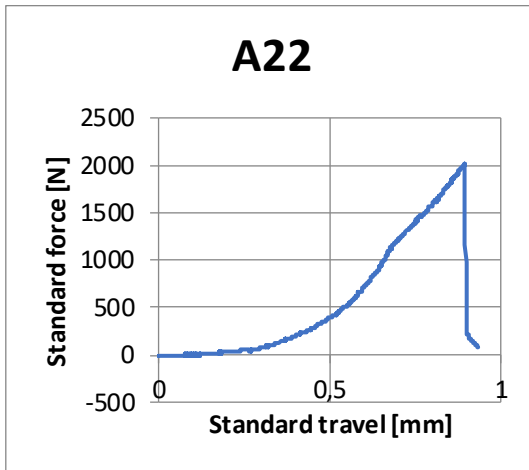
Compression test



Pmax [kN]	σ flex [MPa]	F1 [kN]	F2 [kN]	σ 1 [MPa]	σ 2 [MPa]
1,85	4,23	40,82	42,84	25,51	26,77

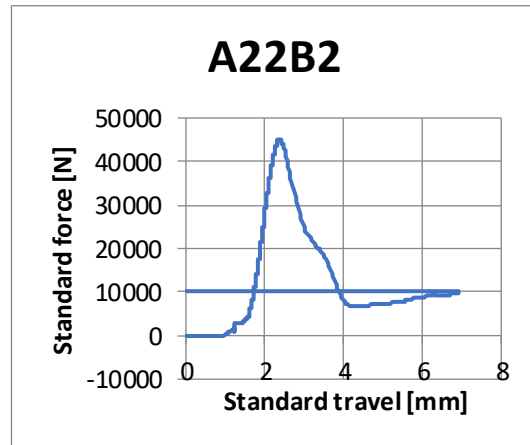
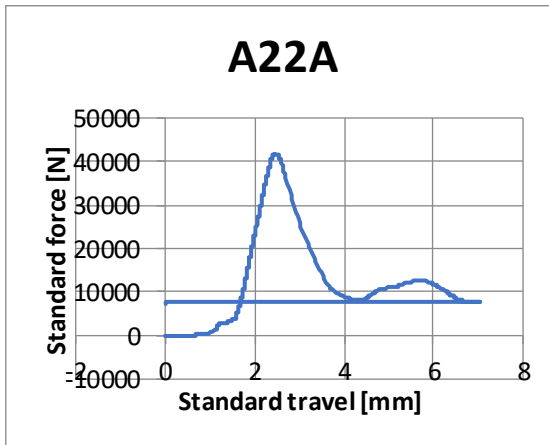
A22

Bending test



Specimen size [mm]		Weight [g]	
160.16	40.63	40.54	536.98

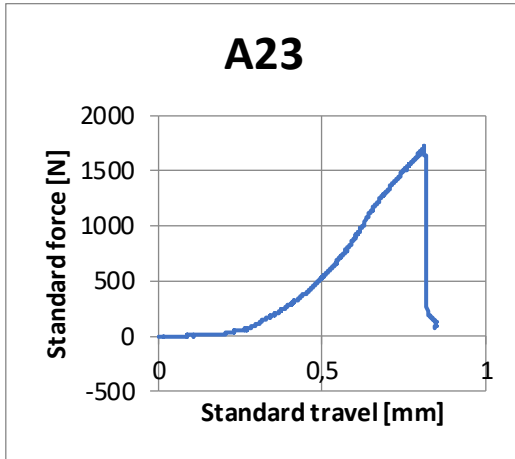
Compression test



Pmax [kN]	σ flex [MPa]	F1 [kN]	F2 [kN]	σ 1 [MPa]	σ 2 [MPa]
2,01	4,52	41,74	45,00	26,09	28,12

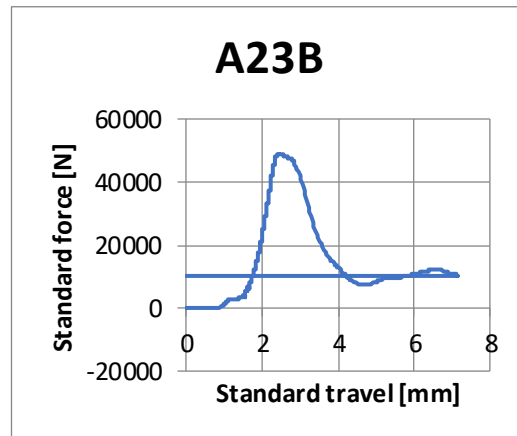
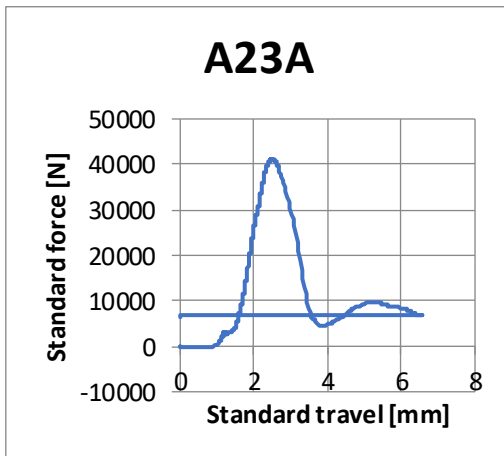
A23

Bending test



Specimen size [mm]		Weight [g]	
160.17	40.64	40.43	544.28

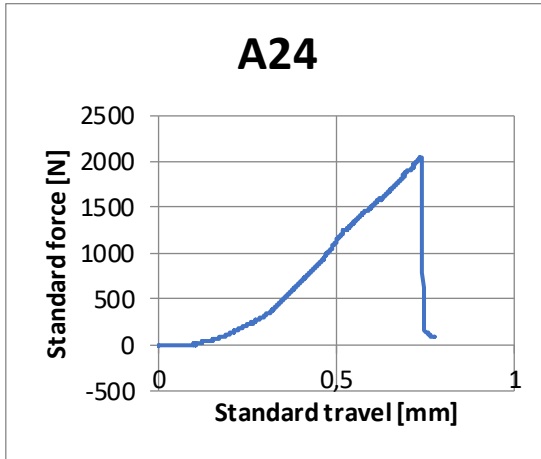
Compression test



Pmax [kN]	σ flex [MPa]	F1 [kN]	F2 [kN]	σ 1 [MPa]	σ 2 [MPa]
1,73	3,90	40,98	48,89	25,61	30,56

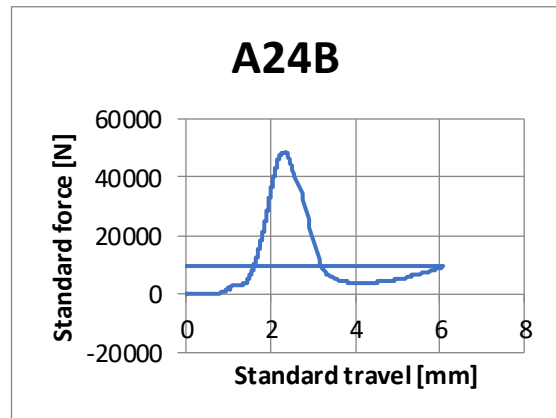
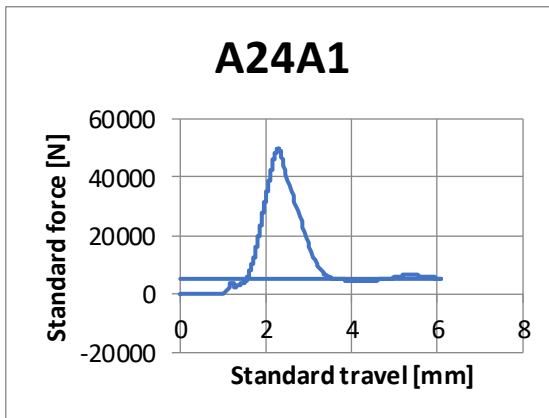
A24

Bending test



Specimen size [mm]		Weight [g]	
160.28	39.58	40.76	533.55

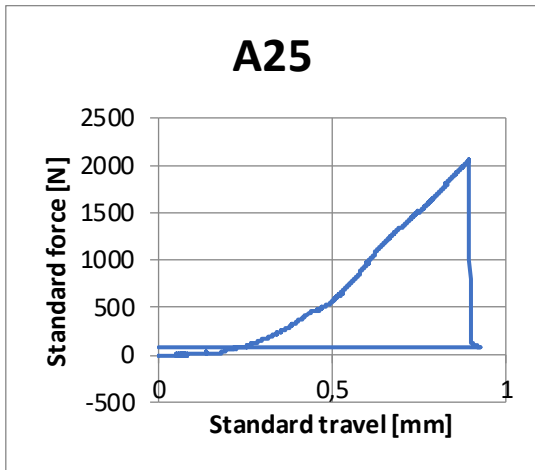
Compression test



Pmax [kN]	σ flex [MPa]	F1 [kN]	F2 [kN]	σ 1 [MPa]	σ 2 [MPa]
2,04	4,66	49,67	48,66	31,04	30,41

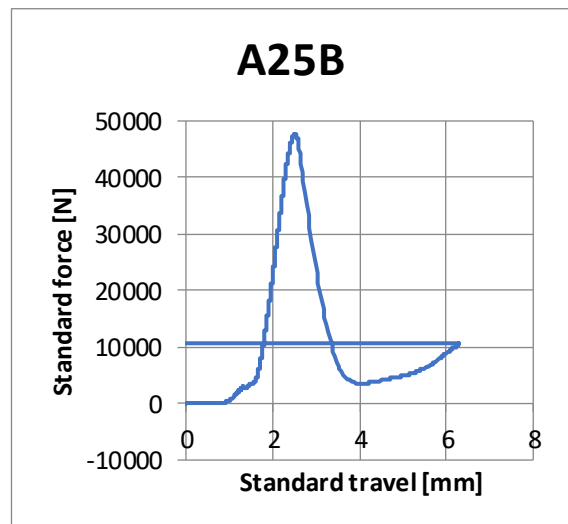
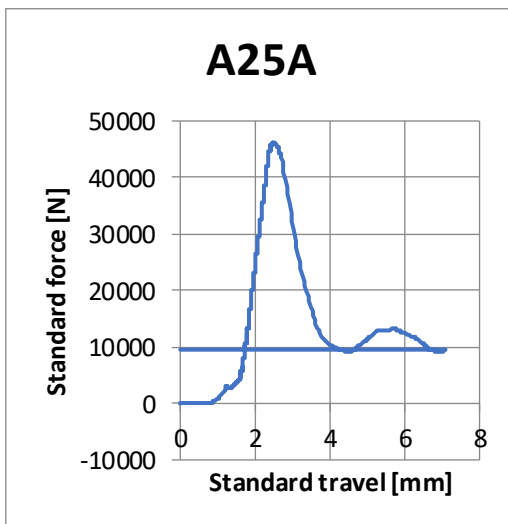
A25

Bending test



Specimen size [mm]		Weight [g]	
160.21	39.83	40.61	533.23

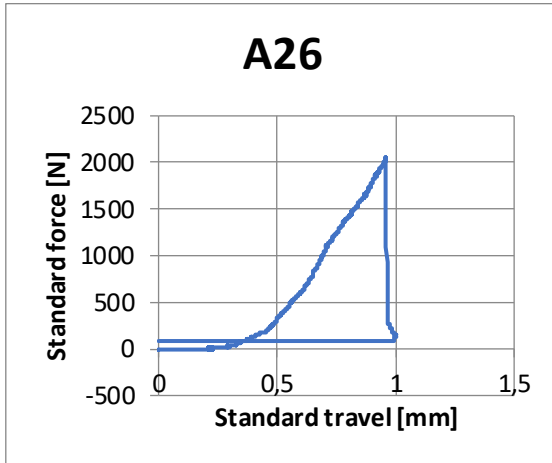
Compression test



Pmax [kN]	σ flex [MPa]	F1 [kN]	F2 [kN]	σ 1 [MPa]	σ 2 [MPa]
2,06	4,69	46,13	47,59	28,83	29,74

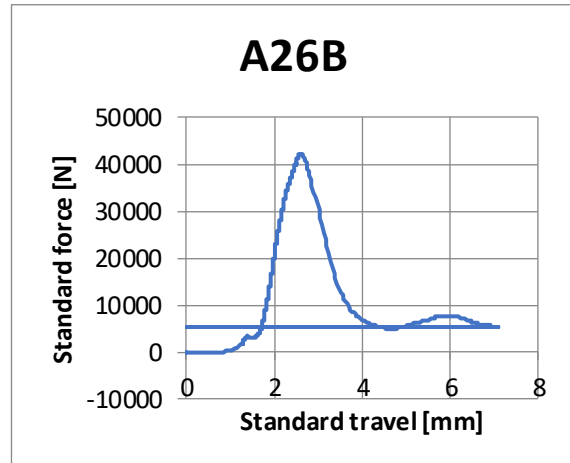
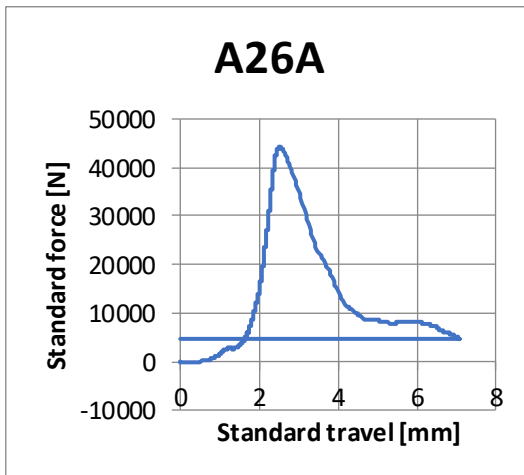
A26

Bending test



Specimen size [mm]		Weight [g]	
160.2	39.74	40.44	532.21

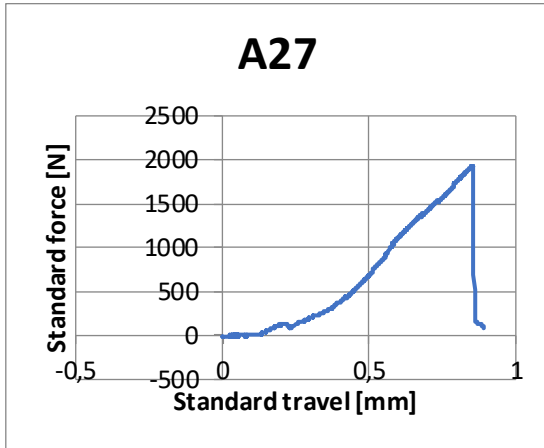
Compression test



Pmax [kN]	σ flex [MPa]	F1 [kN]	F2 [kN]	σ 1 [MPa]	σ 2 [MPa]
2,05	4,72	44,30	42,01	27,69	26,26

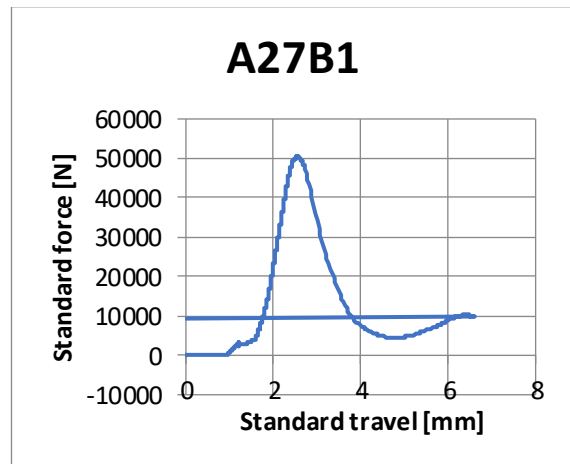
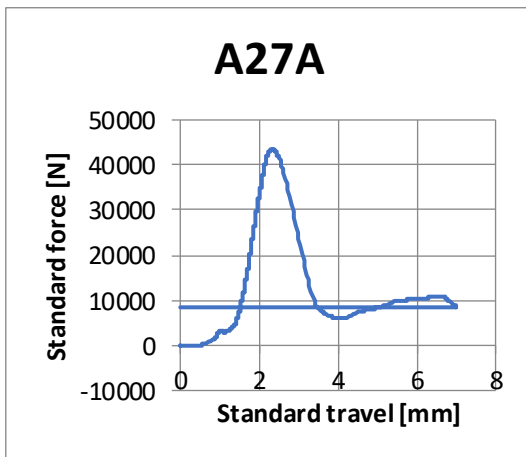
A27

Bending test



Specimen size [mm]		Weight [g]	
159.97	40.01	40.46	539.85

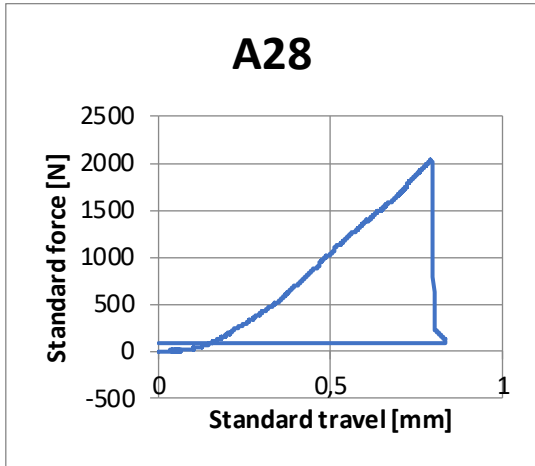
Compression test



Pmax [kN]	σ flex [MPa]	F1 [kN]	F2 [kN]	σ 1 [MPa]	σ 2 [MPa]
1,92	4,40	43,56	50,39	27,23	31,49

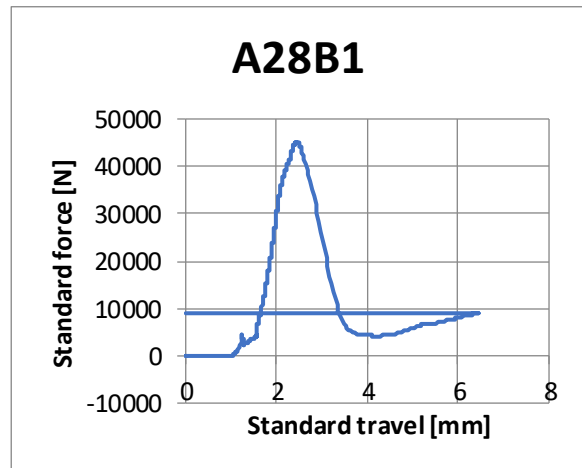
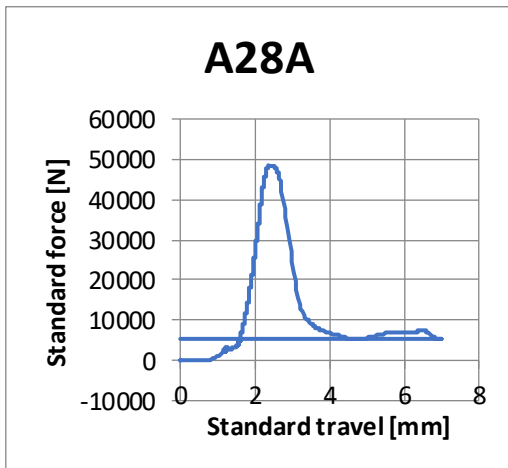
A28

Bending test



Specimen size [mm]		Weight [g]	
160.01	39.85	40.52	525.21

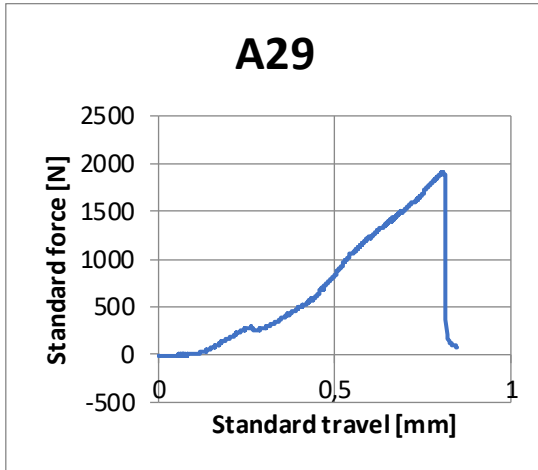
Compression test



Pmax [kN]	σ flex [MPa]	F1 [kN]	F2 [kN]	σ 1 [MPa]	σ 2 [MPa]
2,03	4,65	48,49	45,07	30,30	28,17

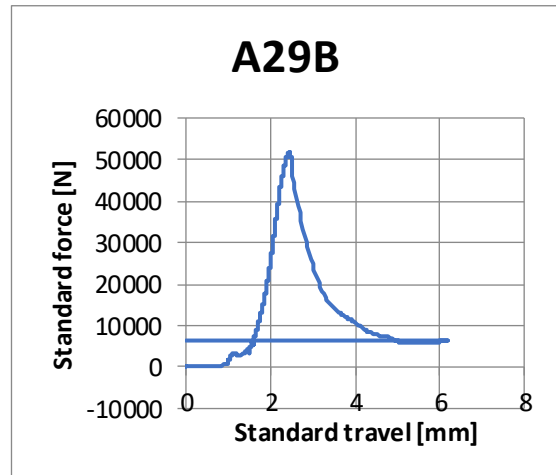
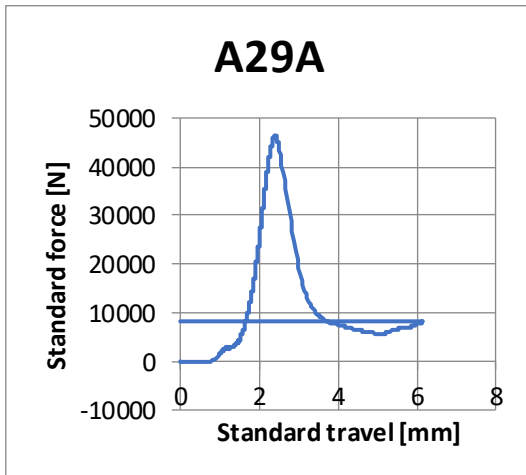
A29

Bending test



Specimen size [mm]		Weight [g]	
160.26	39.98	40.58	532.41

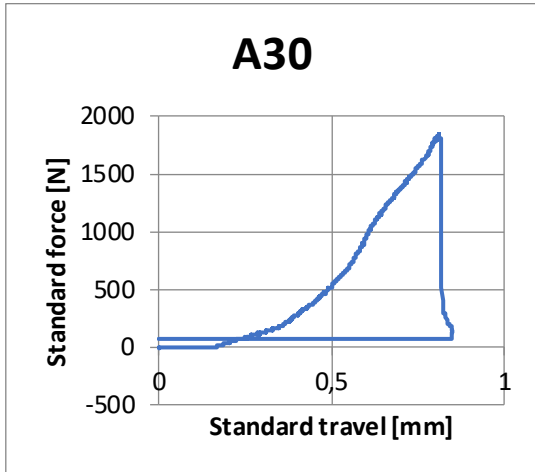
Compression test



Pmax [kN]	σ flex [MPa]	F1 [kN]	F2 [kN]	σ 1 [MPa]	σ 2 [MPa]
1,91	4,36	46,37	51,81	28,98	32,38

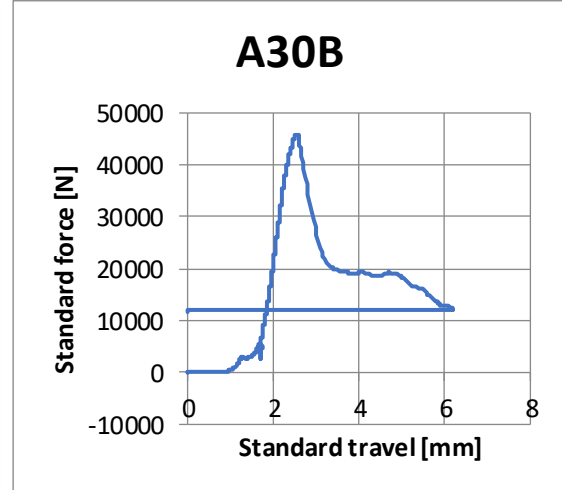
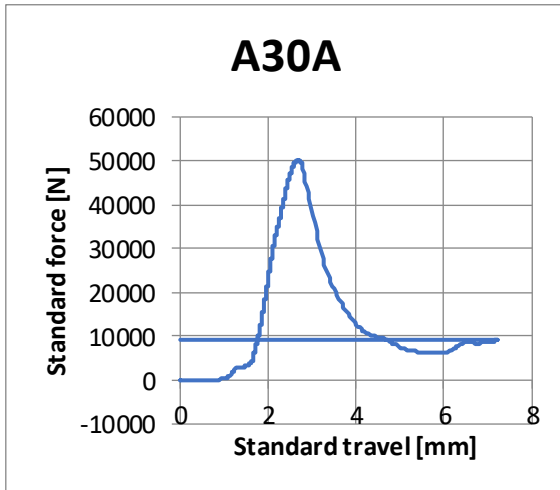
A30

Bending test



Specimen size [mm]		Weight [g]	
160.25	40.6	40.38	542.46

Compression test



Pmax [kN]	σ flex [MPa]	F1 [kN]	F2 [kN]	σ 1 [MPa]	σ 2 [MPa]
1,84	4,16	50,18	45,76	31,36	28,60

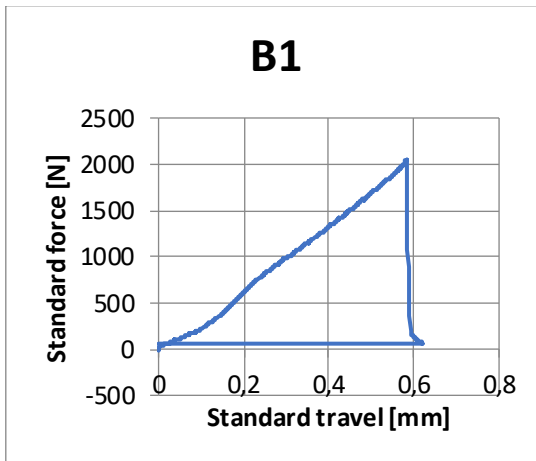
Campione B – Carbon

Qui sono riportate tutte le prove fatte durante il test #3

In alcuni casi ci sono provi che sono stati rifatti per problemi tecnici, questi sono nominati con il nome successivo al corrispettivo.

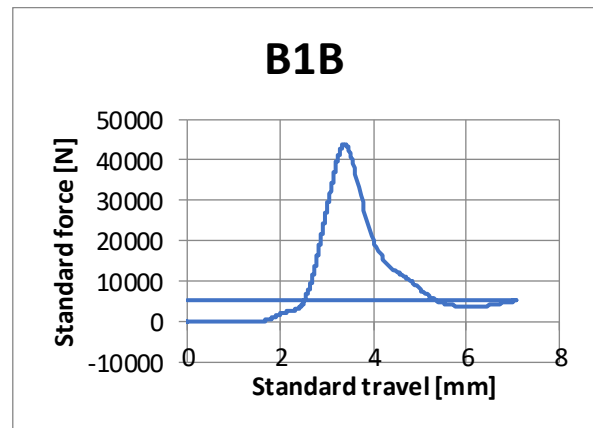
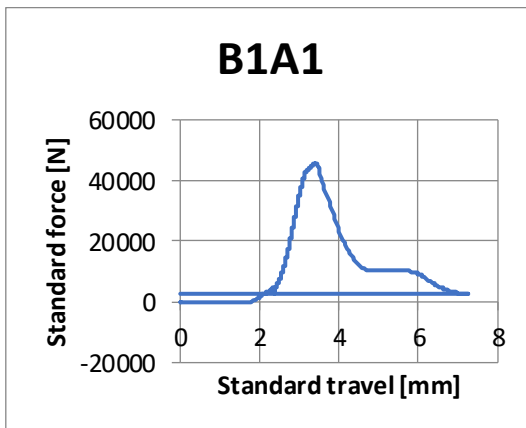
B1

Bending test



Specimen size [mm]		Weight [g]	
160.37	39.87	40.48	525.84

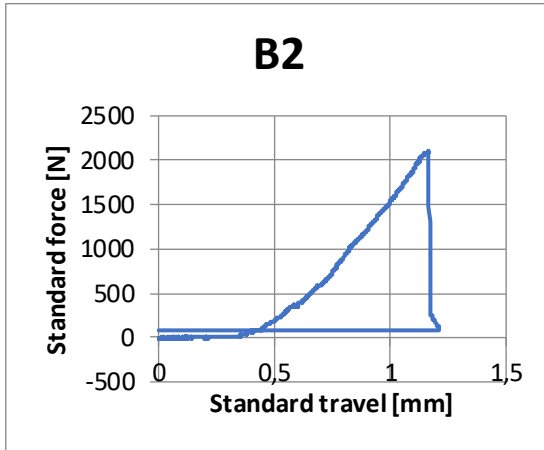
Compression test



Pmax [kN]	σ flex [MPa]	F1 [kN]	F2 [kN]	σ 1 [MPa]	σ 2 [MPa]
2,05	4,71	45,67	43,79	28,54	27,37

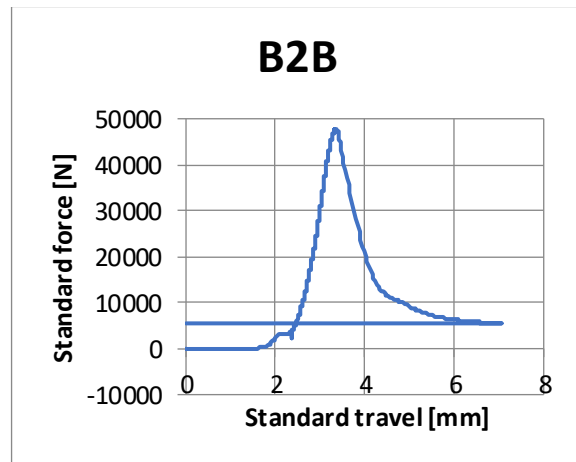
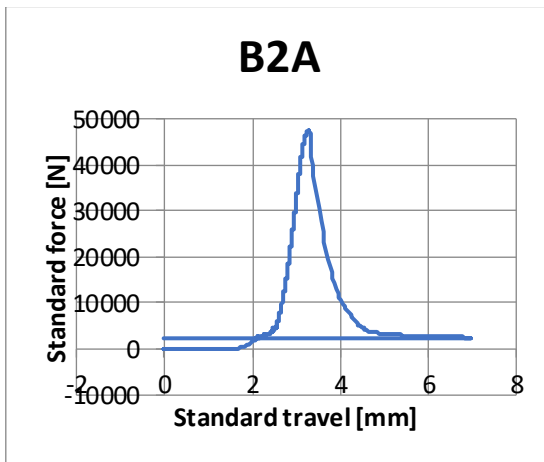
B2

Bending test



Specimen size [mm]		Weight [g]	
160.4	41.11	40.66	531.83

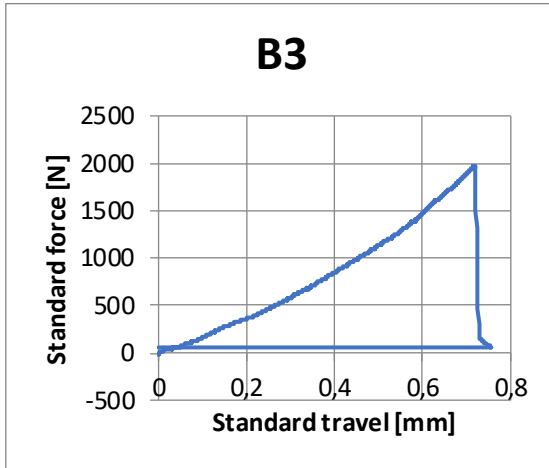
Compression test



Pmax [kN]	σ flex [MPa]	F1 [kN]	F2 [kN]	σ 1 [MPa]	σ 2 [MPa]
2,10	4,64	47,50	47,57	29,69	29,73

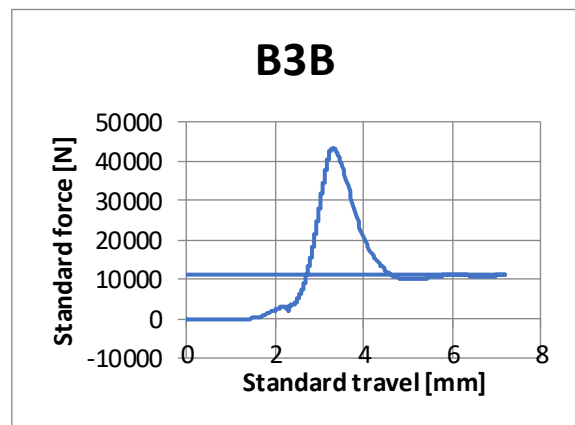
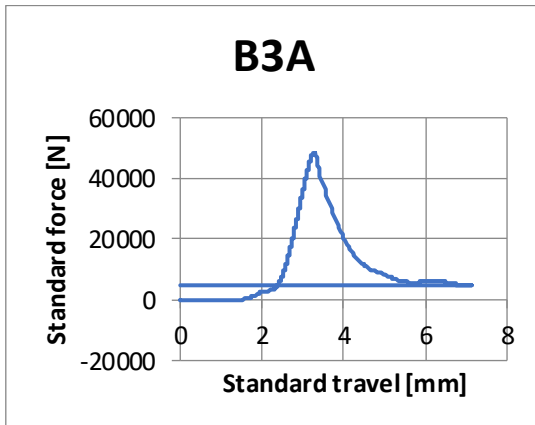
B3

Bending test



Specimen size [mm]		Weight [g]	
160.53	40.76	40.49	536.94

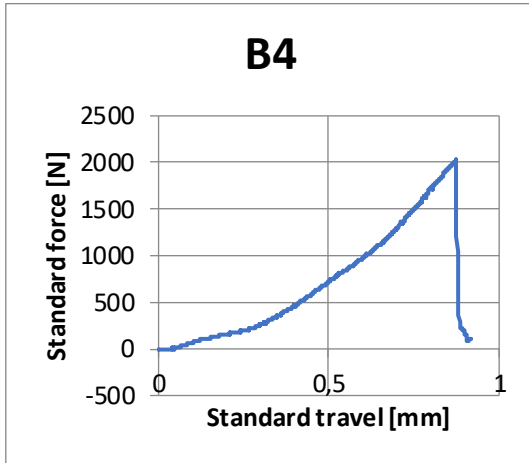
Compression test



Pmax [kN]	σ flex [MPa]	F1 [kN]	F2 [kN]	σ 1 [MPa]	σ 2 [MPa]
1,96	4,40	48,36	43,25	30,23	27,03

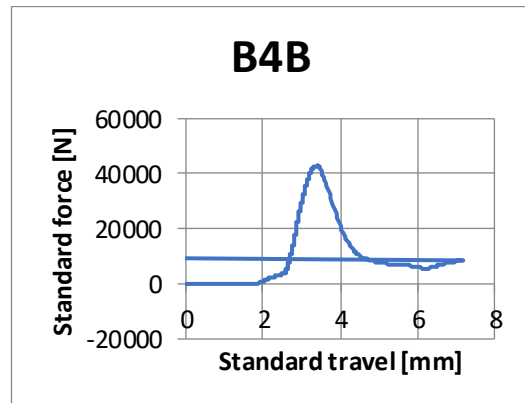
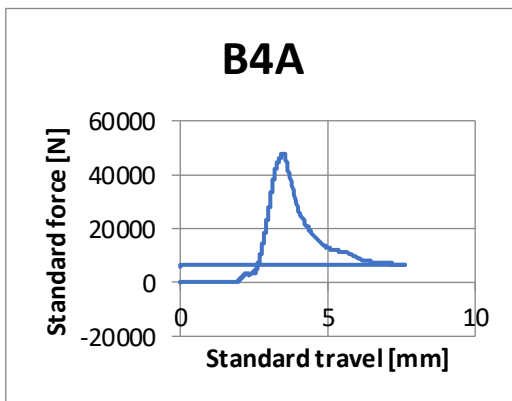
B4

Bending test



Specimen size [mm]			Weight [g]
160.55	41.02	40.32	543.67

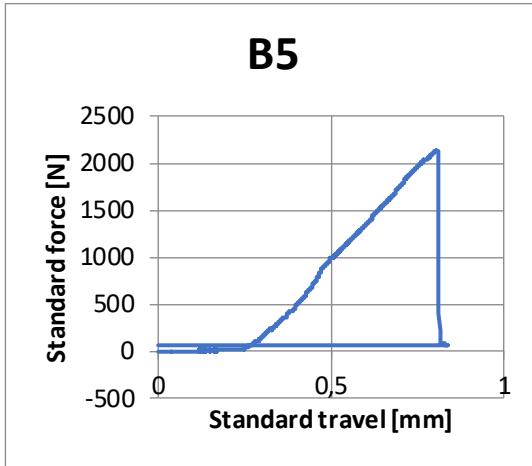
Compression test



Pmax [kN]	σ flex [MPa]	F1 [kN]	F2 [kN]	σ 1 [MPa]	σ 2 [MPa]
2,02	4,55	47,68	43,03	29,80	26,90

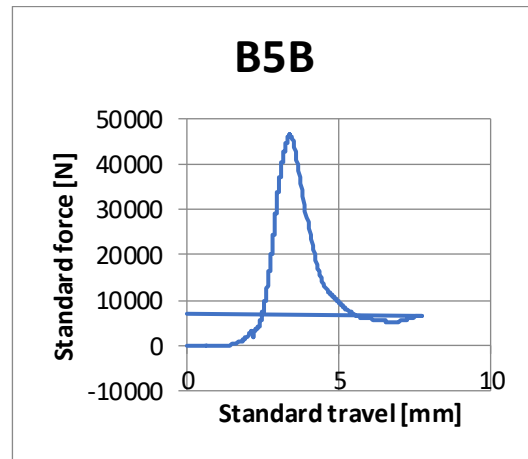
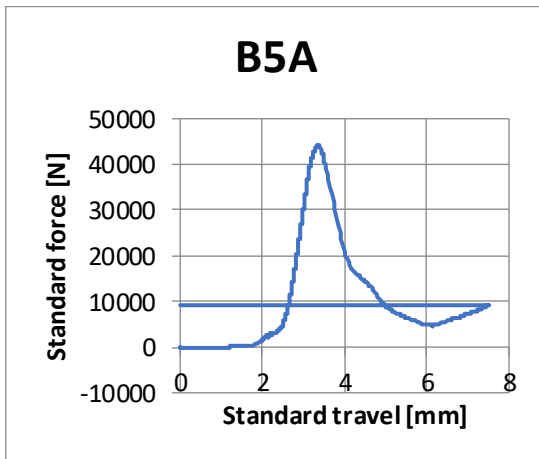
B5

Bending test



Specimen size [mm]		Weight [g]	
160.77	39.66	40.84	525.37

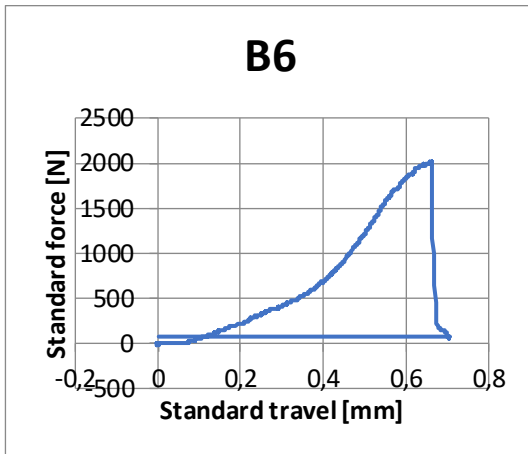
Compression test



Pmax [kN]	σ flex [MPa]	F1 [kN]	F2 [kN]	σ 1 [MPa]	σ 2 [MPa]
2,13	4,84	44,11	46,33	27,57	28,95

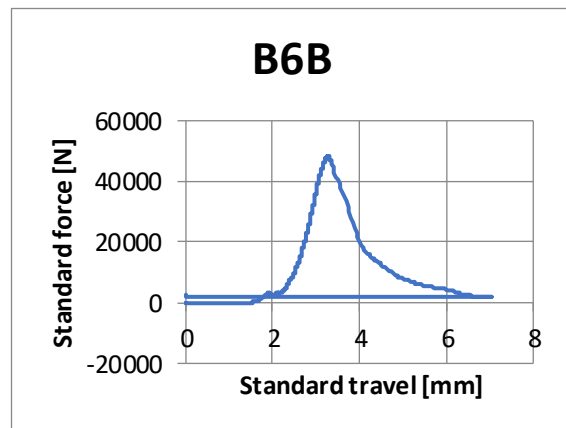
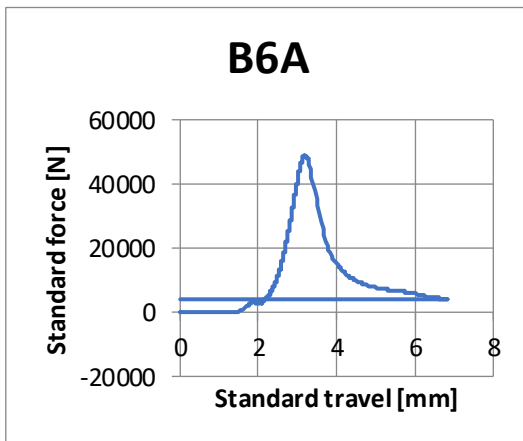
B6

Bending test



Specimen size [mm]		Weight [g]	
160.9	39.99	40.84	535.17

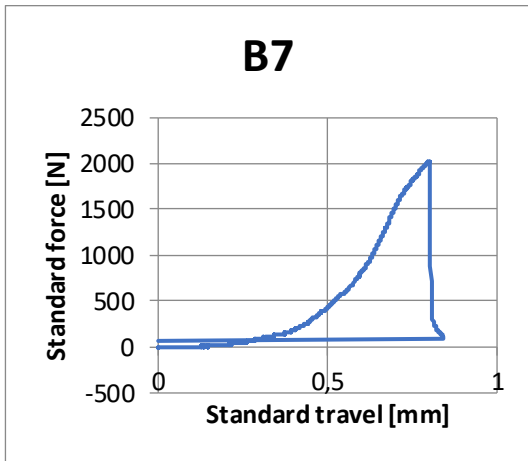
Compression test



Pmax [kN]	σ flex [MPa]	F1 [kN]	F2 [kN]	σ 1 [MPa]	σ 2 [MPa]
2,01	4,51	48,90	48,13	30,56	30,08

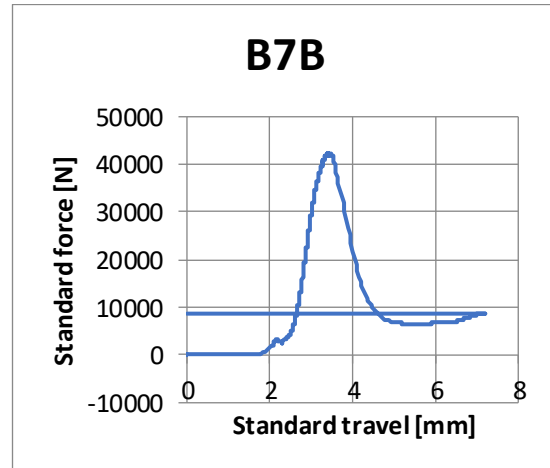
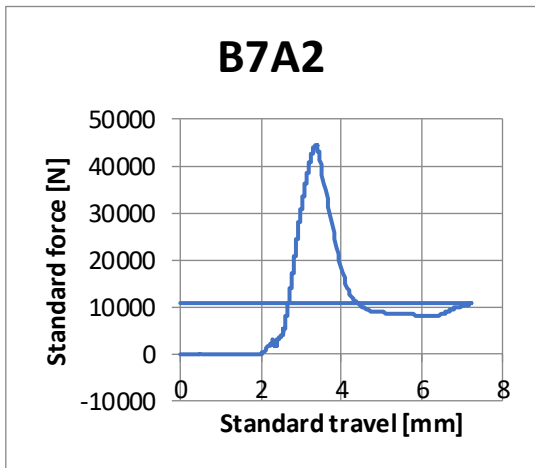
B7

Bending test



Specimen size [mm]		Weight [g]	
160.48	40.15	40.66	527.48

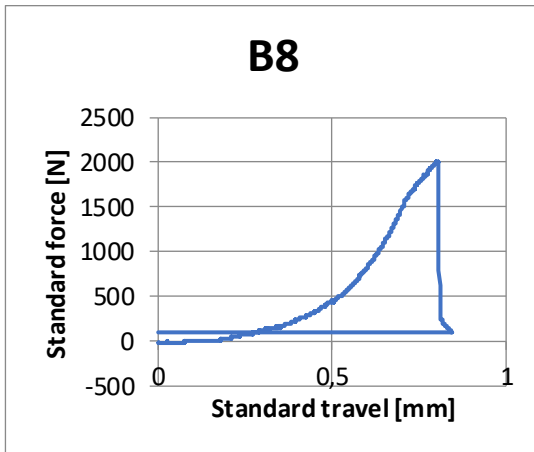
Compression test



Pmax [kN]	σ flex [MPa]	F1 [kN]	F2 [kN]	σ 1 [MPa]	σ 2 [MPa]
2,02	4,57	44,33	42,19	27,71	26,37

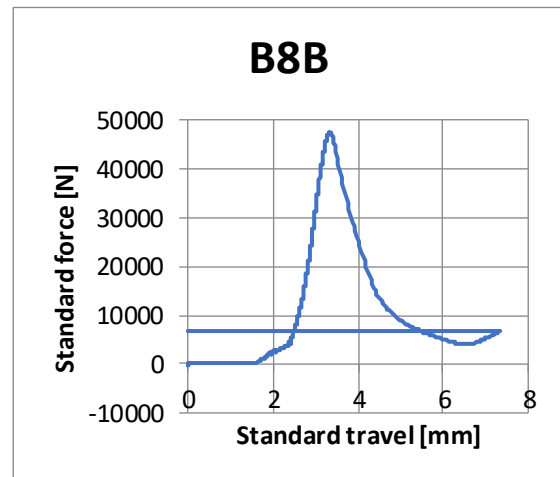
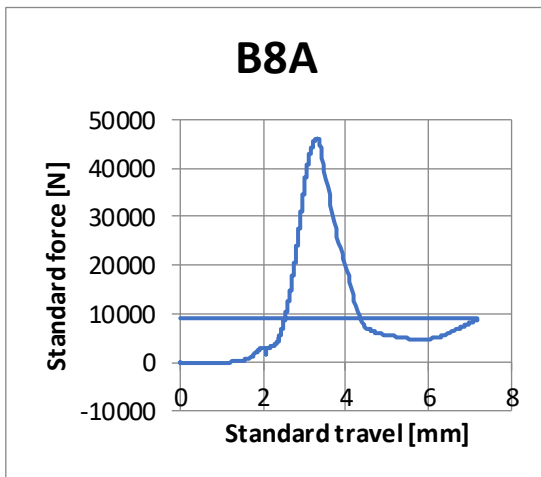
B8

Bending test



Specimen size [mm]		Weight [g]	
160.32	39.55	40.44	523.3

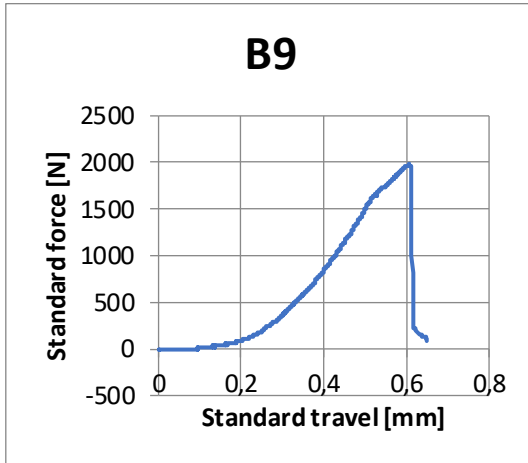
Compression test



Pmax [kN]	σ flex [MPa]	F1 [kN]	F2 [kN]	σ 1 [MPa]	σ 2 [MPa]
2,00	4,65	46,10	47,41	28,81	29,63

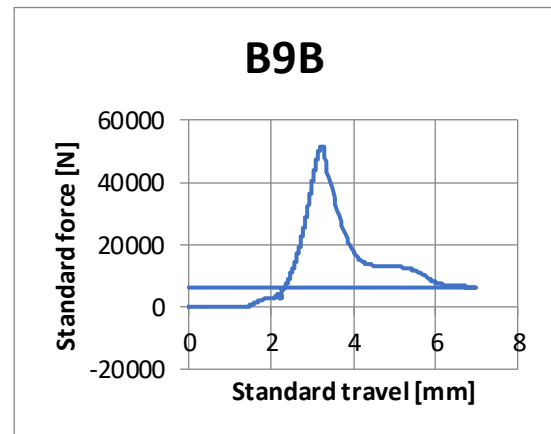
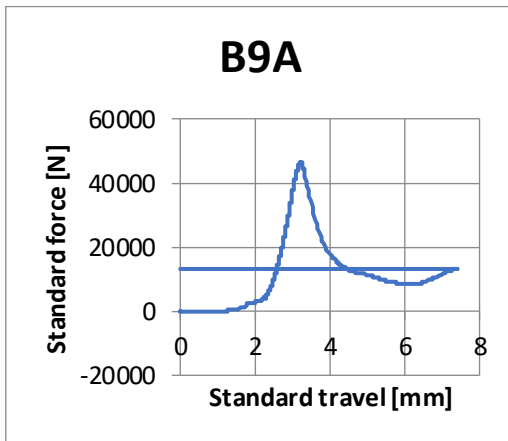
B9

Bending test



Specimen size [mm]		Weight [g]	
160.26	40.01	40.66	536.72

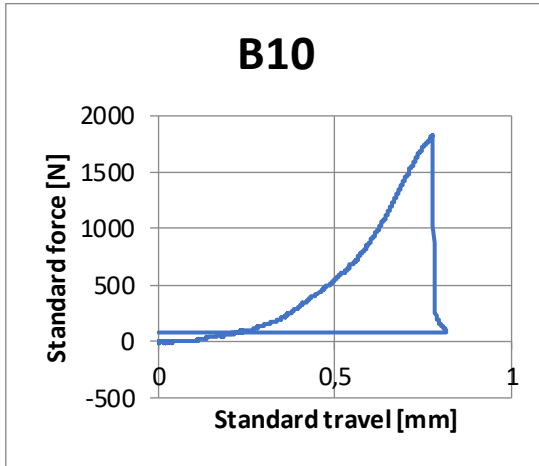
Compression test



Pmax [kN]	σ flex [MPa]	F1 [kN]	F2 [kN]	σ 1 [MPa]	σ 2 [MPa]
1,97	4,48	46,19	51,28	28,87	32,05

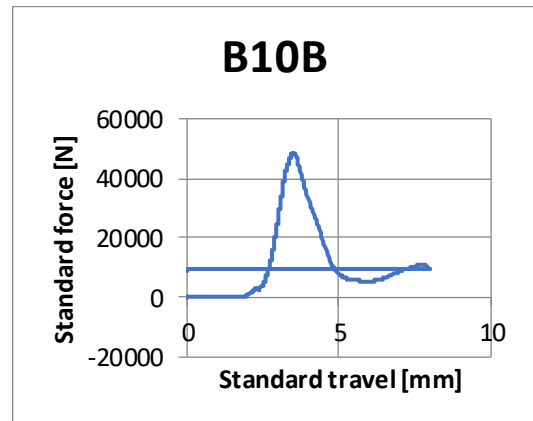
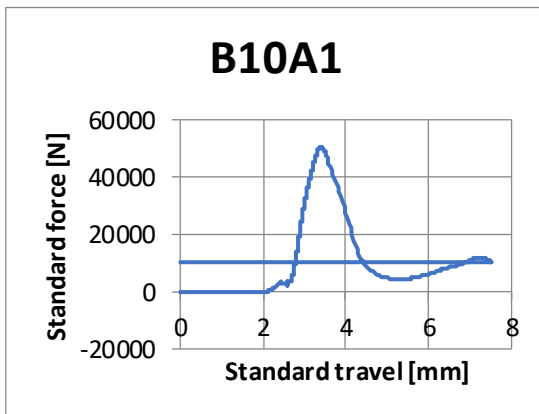
B10

Bending test



Specimen size [mm]		Weight [g]	
160.15	40.14	40.64	535.08

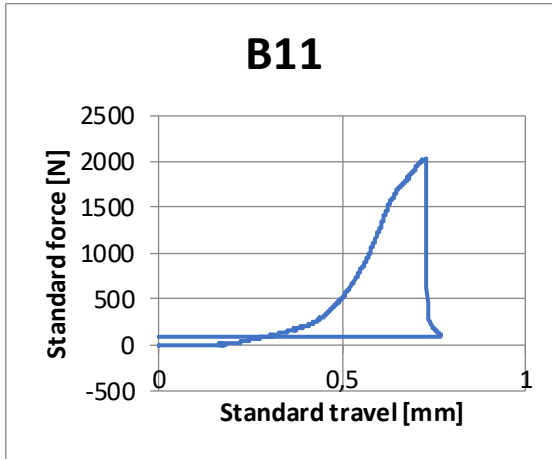
Compression test



Pmax [kN]	σ flex [MPa]	F1 [kN]	F2 [kN]	σ 1 [MPa]	σ 2 [MPa]
1,83	4,14	50,34	48,48	31,46	30,30

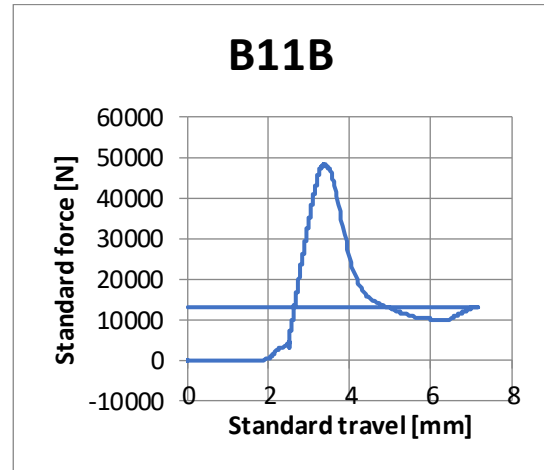
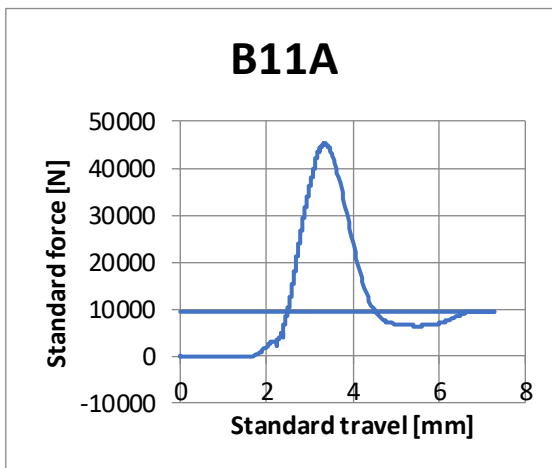
B11

Bending test



Specimen size [mm]		Weight [g]	
160.06	39.69	40.62	528.56

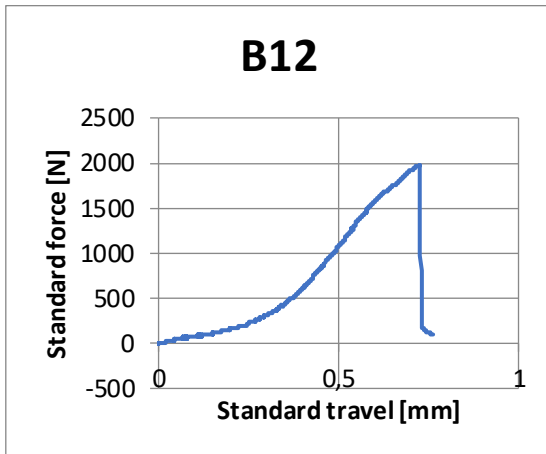
Compression test



Pmax [kN]	σ flex [MPa]	F1 [kN]	F2 [kN]	σ 1 [MPa]	σ 2 [MPa]
2,03	4,66	45,12	48,12	28,20	30,08

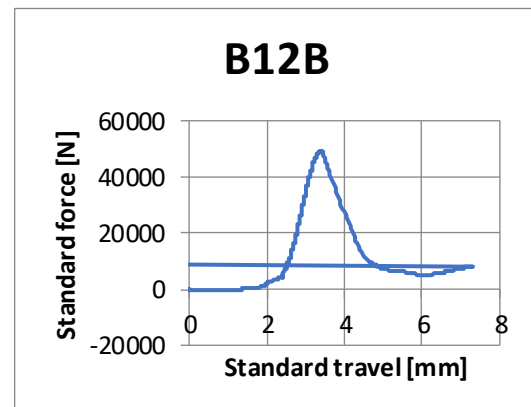
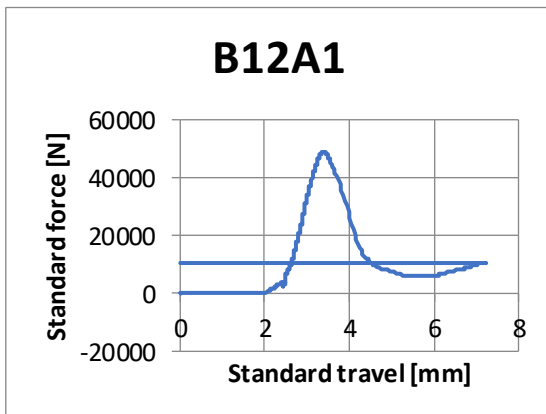
B12

Bending test



Specimen size [mm]		Weight [g]	
160.12	40.1	40.55	531.91

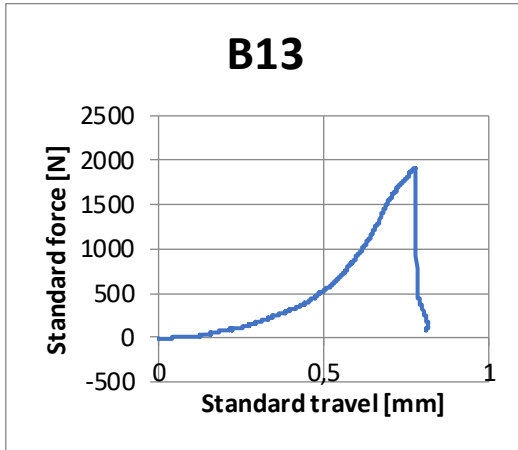
Compression test



Pmax [kN]	σ flex [MPa]	F1 [kN]	F2 [kN]	σ 1 [MPa]	σ 2 [MPa]
1,98	4,50	48,85	49,27	30,53	30,79

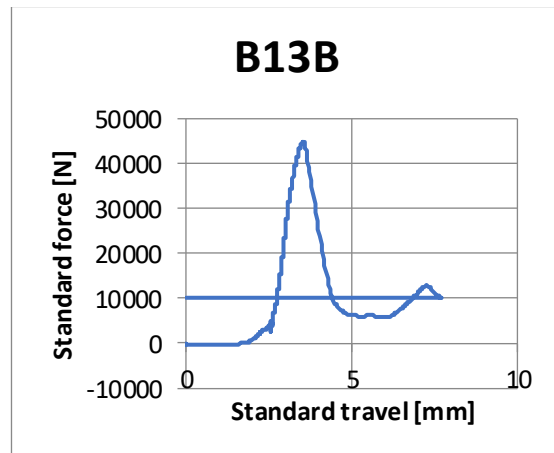
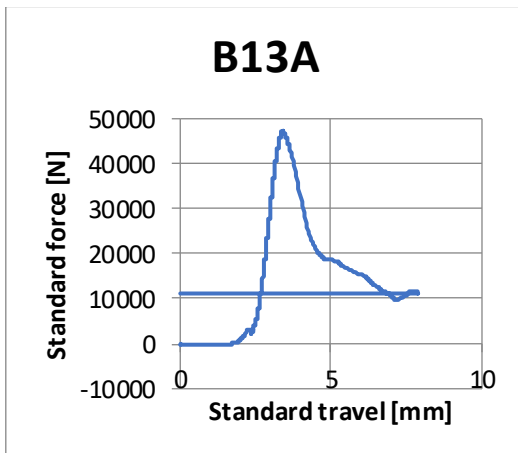
B13

Bending test



Specimen size [mm]		Weight [g]	
160.46	39.9	40.93	535.81

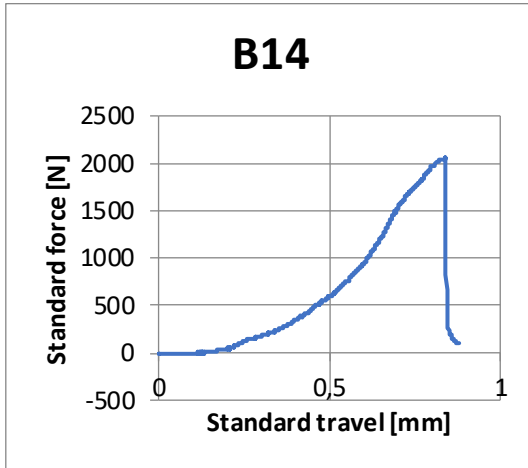
Compression test



Pmax [kN]	σ flex [MPa]	F1 [kN]	F2 [kN]	σ 1 [MPa]	σ 2 [MPa]
1,91	4,28	47,33	44,87	29,58	28,04

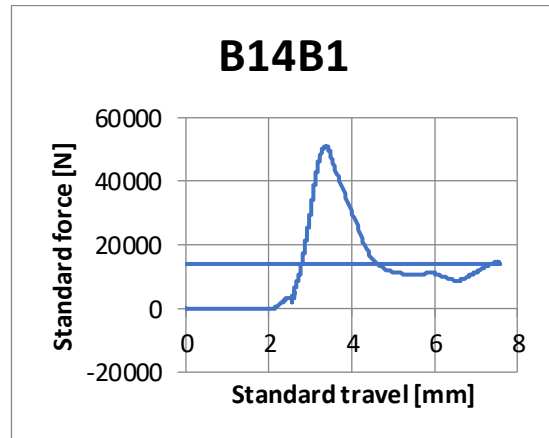
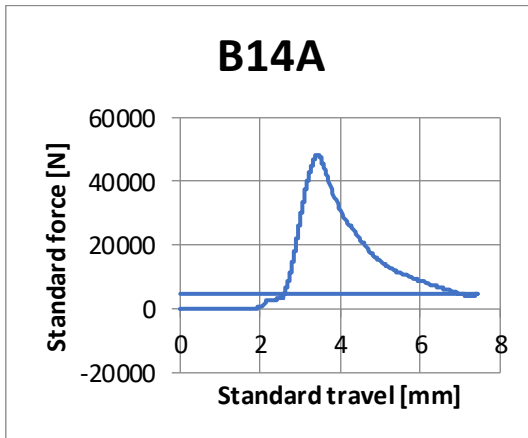
B14

Bending test



Specimen size [mm]		Weight [g]	
160.48	40.7	40.6	546.44

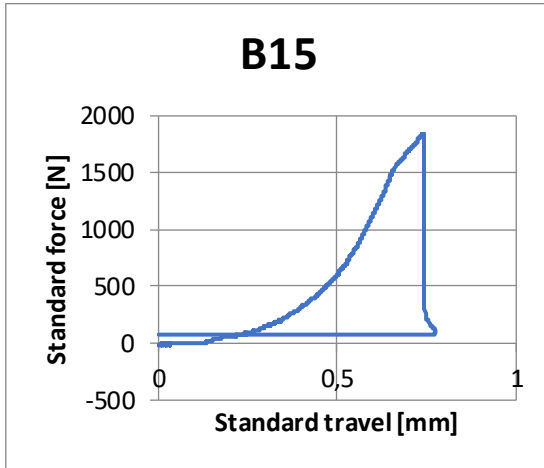
Compression test



Pmax [kN]	σ flex [MPa]	F1 [kN]	F2 [kN]	σ 1 [MPa]	σ 2 [MPa]
2,05	4,59	48,28	51,01	30,18	31,88

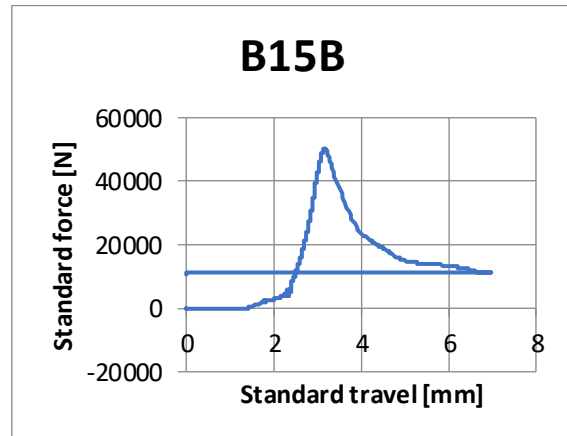
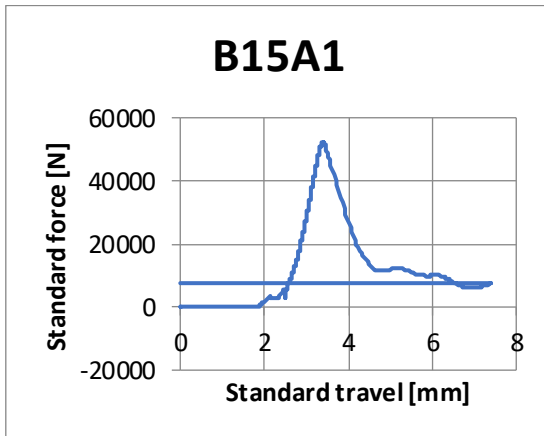
B15

Bending test



Specimen size [mm]			Weight [g]
160.34	41.26	40.66	552.6

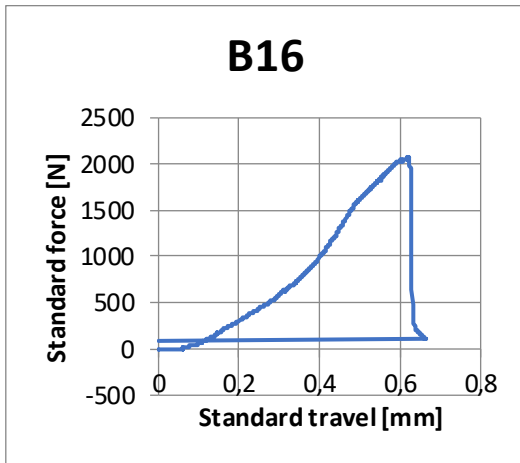
Compression test



Pmax [kN]	σ flex [MPa]	F1 [kN]	F2 [kN]	σ 1 [MPa]	σ 2 [MPa]
1,84	4,04	52,13	50,25	32,58	31,41

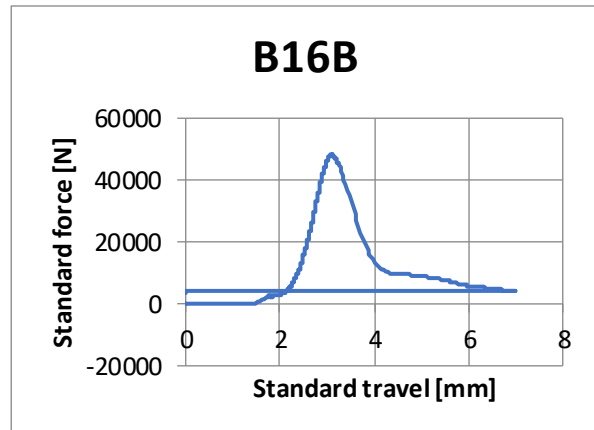
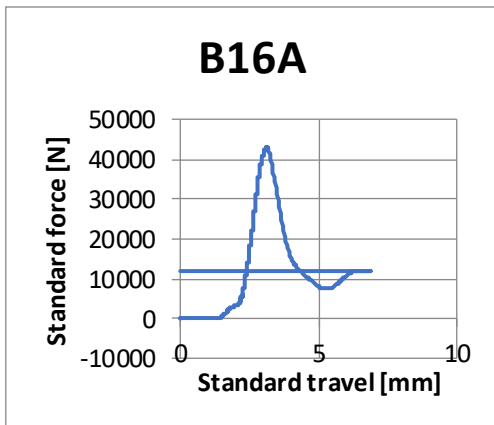
B16

Bending test



Specimen size [mm]		Weight [g]	
160.43	39.65	41.05	527.26

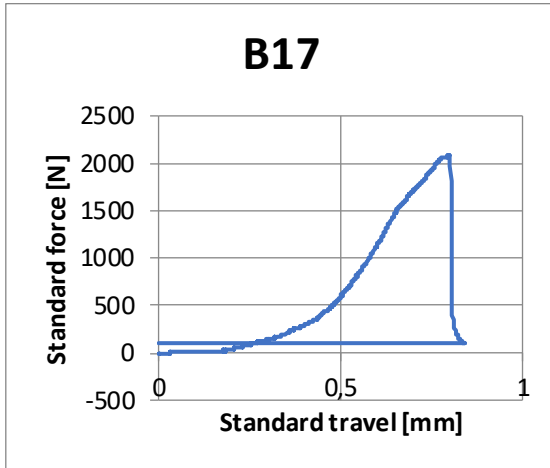
Compression test



Pmax [kN]	σ flex [MPa]	F1 [kN]	F2 [kN]	σ 1 [MPa]	σ 2 [MPa]
2,07	4,65	42,79	48,07	26,74	30,05

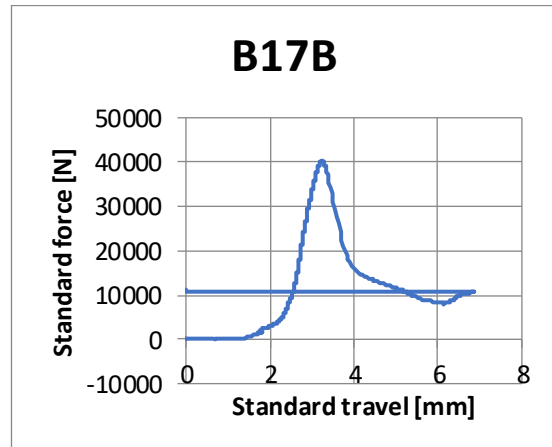
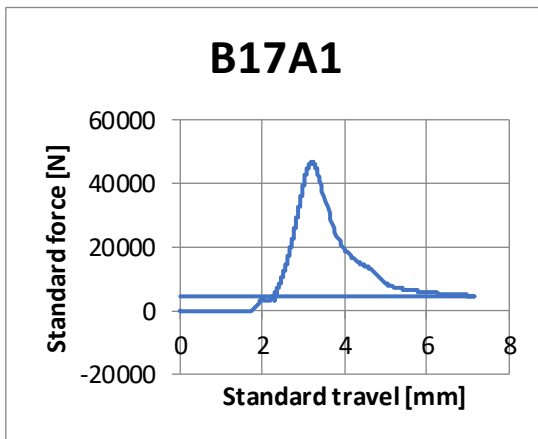
B17

Bending test



Specimen size [mm]		Weight [g]	
160.66	40.08	40.68	529.84

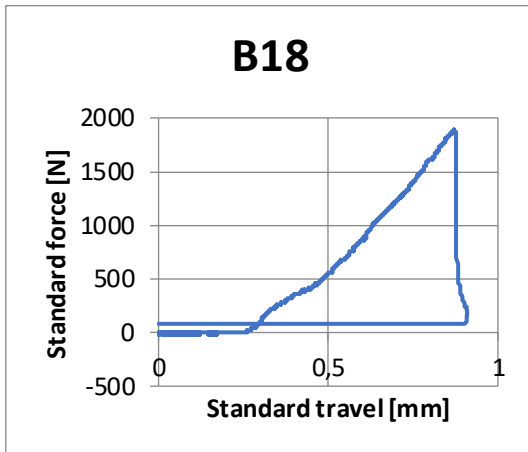
Compression test



Pmax [kN]	σ flex [MPa]	F1 [kN]	F2 [kN]	σ 1 [MPa]	σ 2 [MPa]
2,08	4,71	46,44	40,29	29,02	25,18

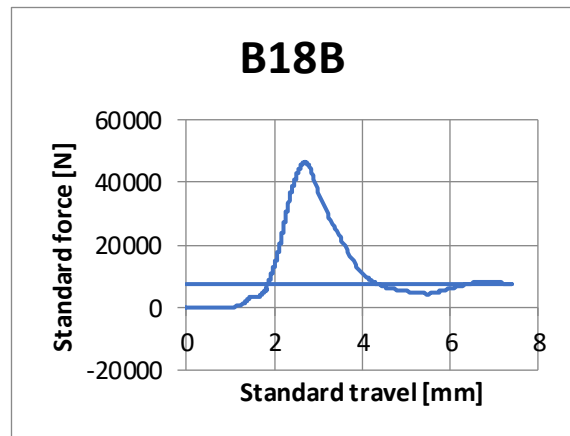
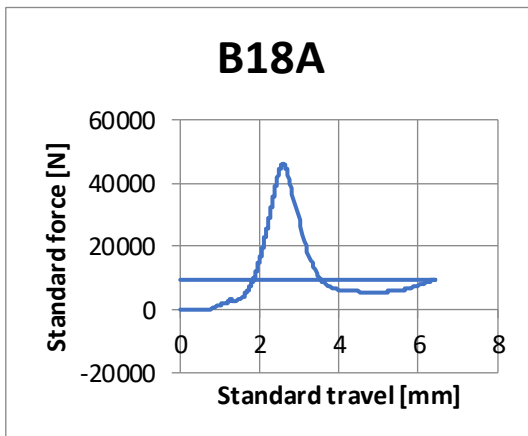
B18

Bending test



Specimen size [mm]		Weight [g]	
160.36	40.04	40.89	533.69

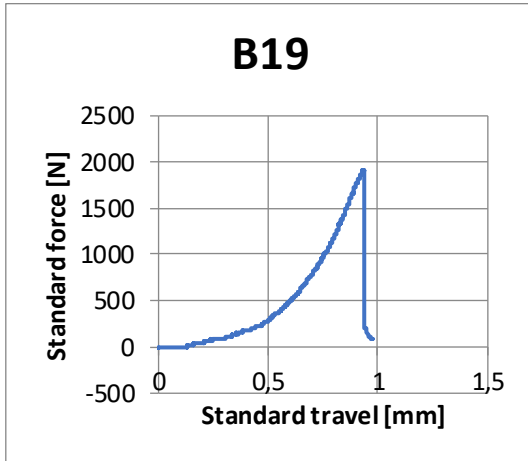
Compression test



Pmax [kN]	σ flex [MPa]	F1 [kN]	F2 [kN]	σ 1 [MPa]	σ 2 [MPa]
1,89	4,22	46,07	46,56	28,79	29,10

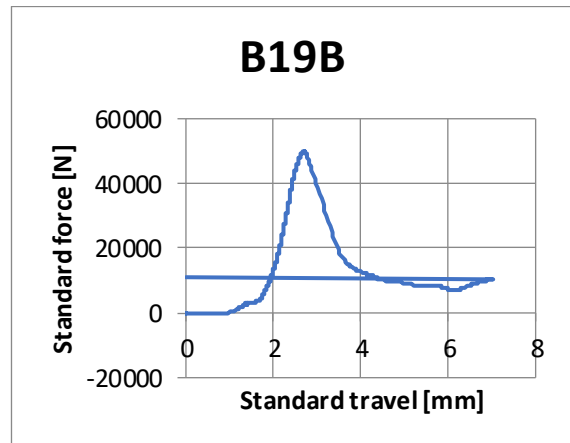
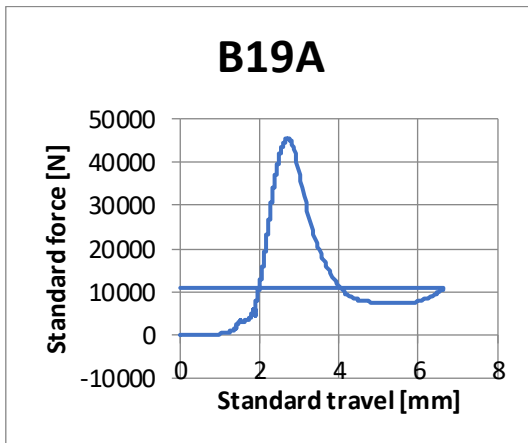
B19

Bending test



Specimen size [mm]		Weight [g]	
160.3	40.72	40.8	541.59

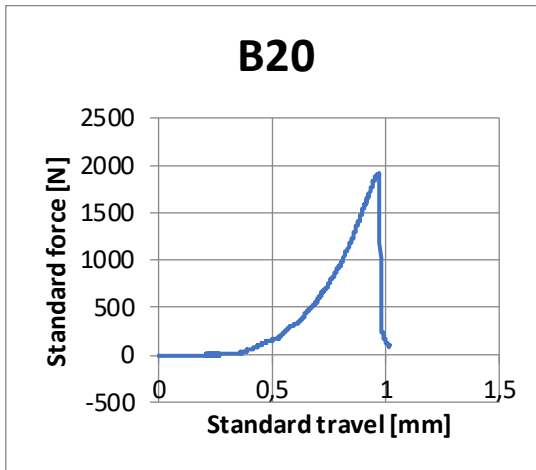
Compression test



Pmax [kN]	σ flex [MPa]	F1 [kN]	F2 [kN]	σ 1 [MPa]	σ 2 [MPa]
1,91	4,22	45,42	49,72	28,39	31,08

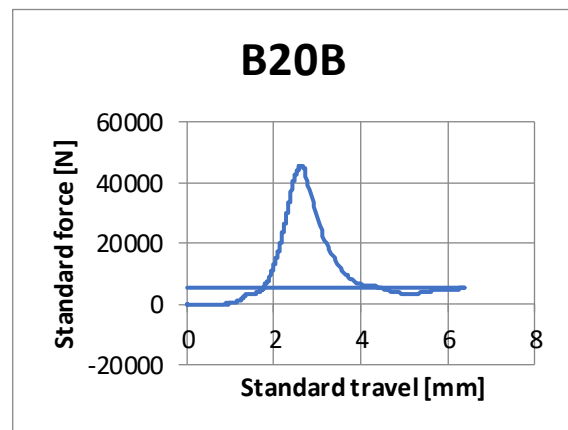
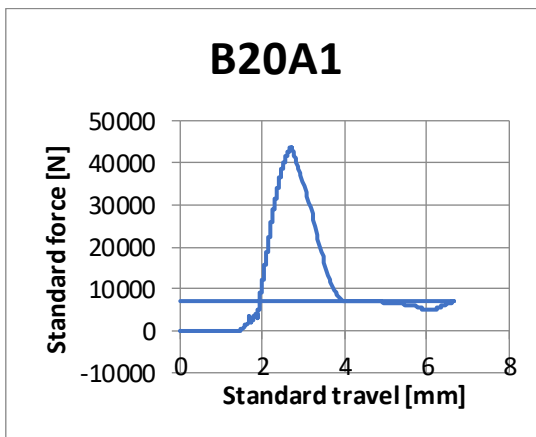
B20

Bending test



Specimen size [mm]		Weight [g]	
160.49	39.65	40.68	521.55

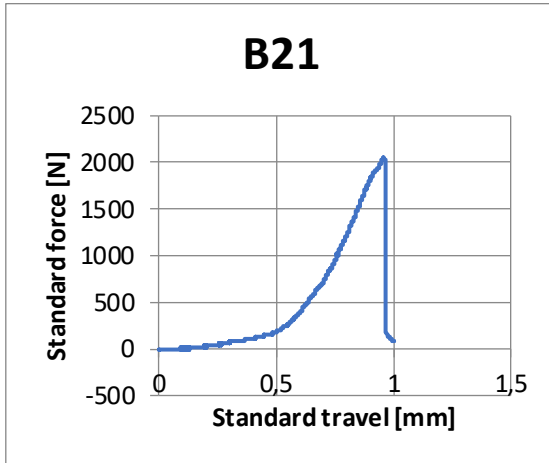
Compression test



Pmax [kN]	σ flex [MPa]	F1 [kN]	F2 [kN]	σ 1 [MPa]	σ 2 [MPa]
1,91	4,38	43,56	45,45	27,23	28,41

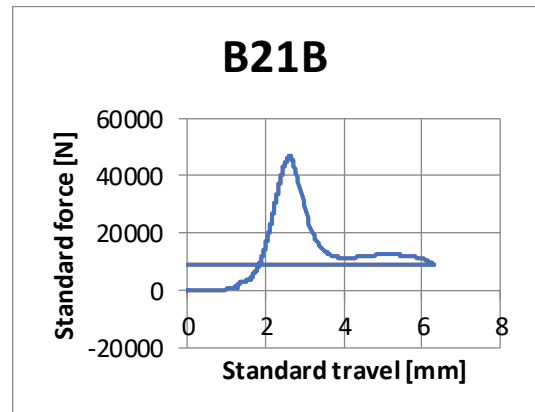
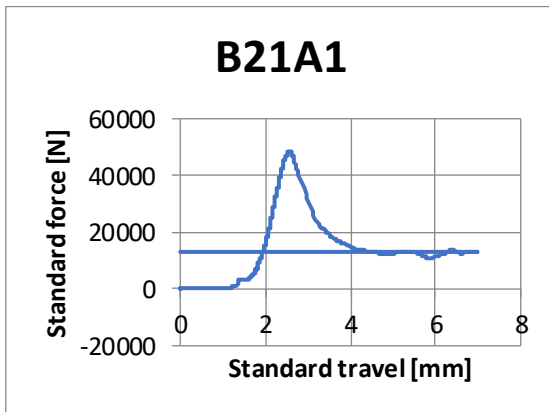
B21

Bending test



Specimen size [mm]		Weight [g]	
160.95	40.06	40.77	529.99

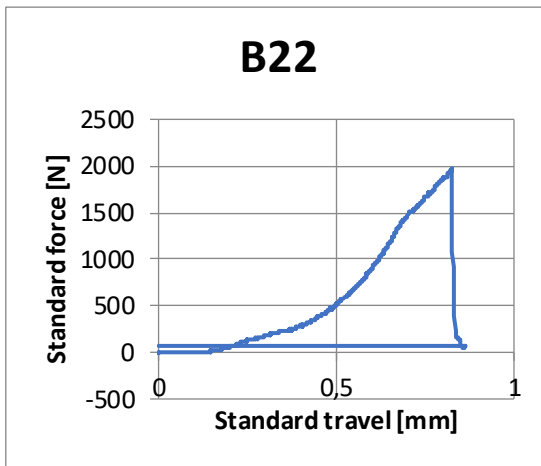
Compression test



Pmax [kN]	σ flex [MPa]	F1 [kN]	F2 [kN]	σ 1 [MPa]	σ 2 [MPa]
2,04	4,61	48,28	46,84	30,18	29,28

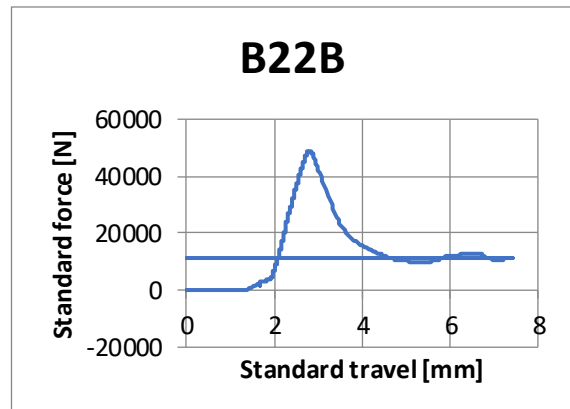
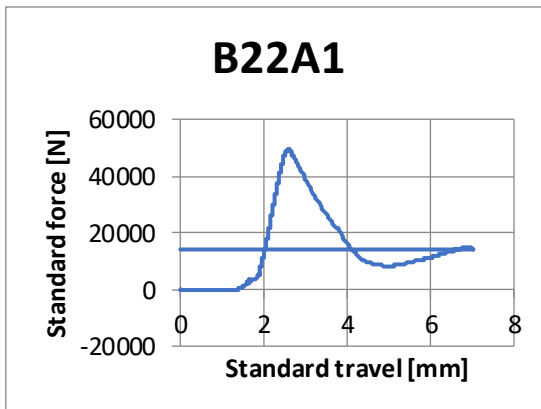
B22

Bending test



Specimen size [mm]		Weight [g]	
160.18	39.86	40.43	530.65

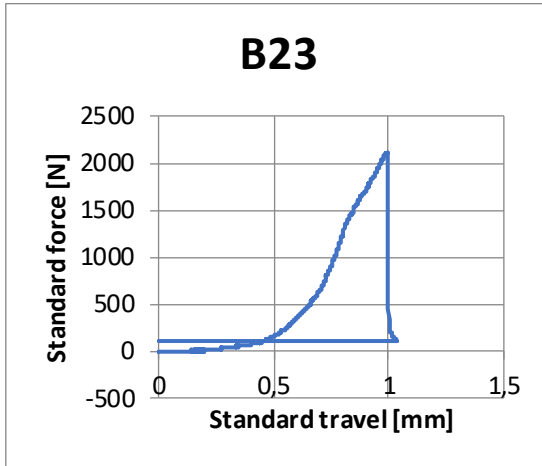
Compression test



Pmax [kN]	σ flex [MPa]	F1 [kN]	F2 [kN]	σ 1 [MPa]	σ 2 [MPa]
1,97	4,53	49,52	48,75	30,95	30,47

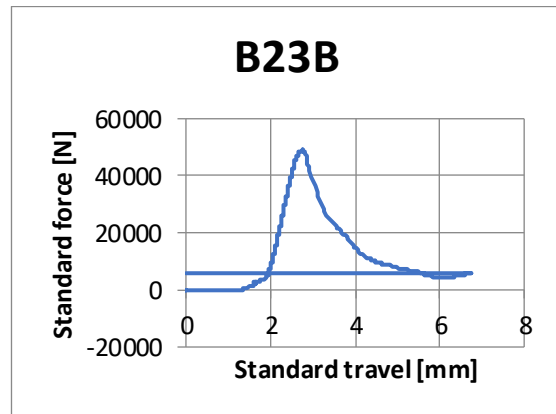
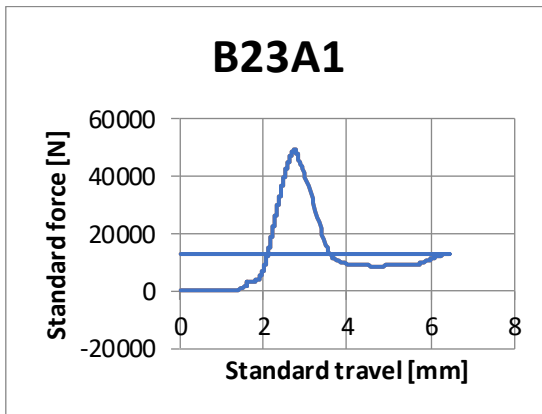
B23

Bending test



Specimen size [mm]		Weight [g]	
160.33	39.85	40.57	528.75

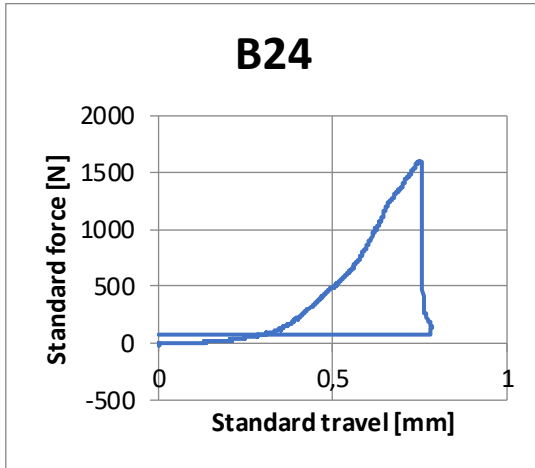
Compression test



Pmax [kN]	σ flex [MPa]	F1 [kN]	F2 [kN]	σ 1 [MPa]	σ 2 [MPa]
2,11	4,83	49,17	48,87	30,73	30,54

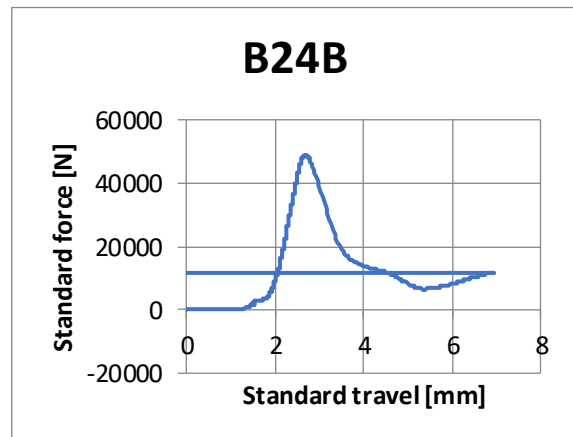
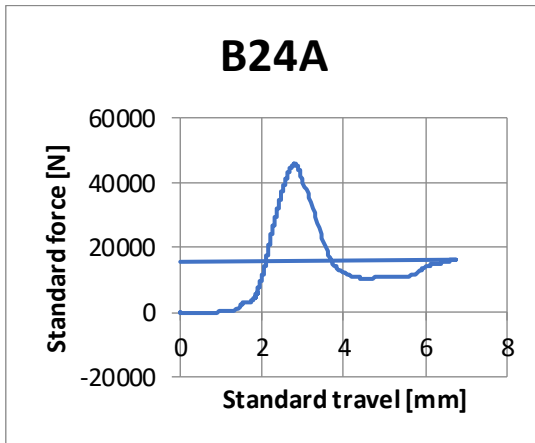
B24

Bending test



Specimen size [mm]		Weight [g]	
160.23	39.89	40.67	531.99

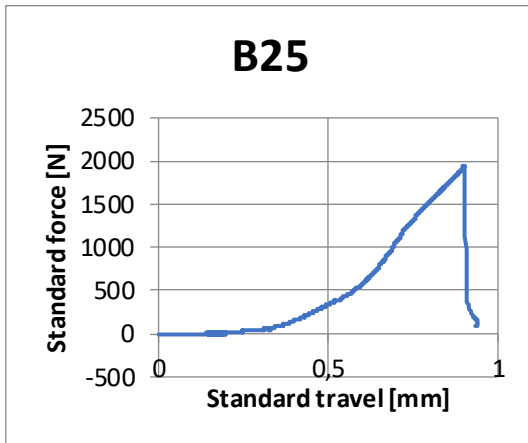
Compression test



Pmax [kN]	σ flex [MPa]	F1 [kN]	F2 [kN]	σ 1 [MPa]	σ 2 [MPa]
1,60	3,63	45,62	48,85	28,51	30,53

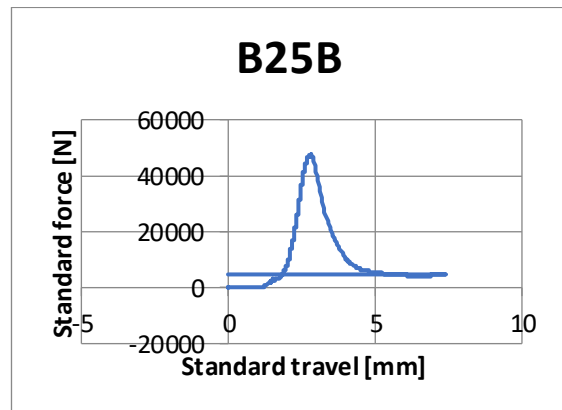
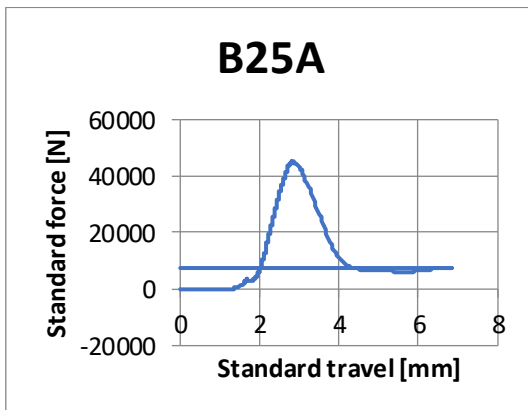
B25

Bending test



Specimen size [mm]		Weight [g]	
160.98	39.99	40.57	531.58

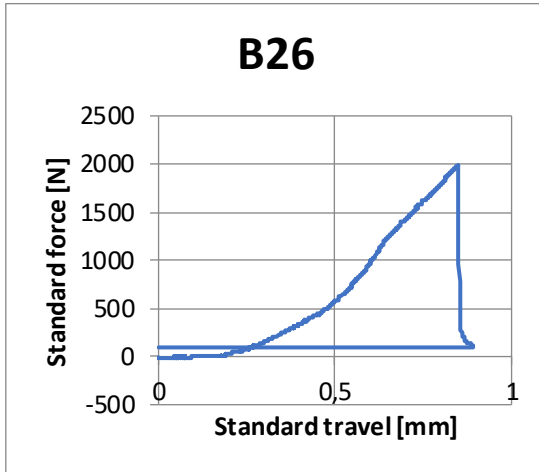
Compression test



Pmax [kN]	σ flex [MPa]	F1 [kN]	F2 [kN]	σ 1 [MPa]	σ 2 [MPa]
1,94	4,42	44,99	47,67	28,12	29,79

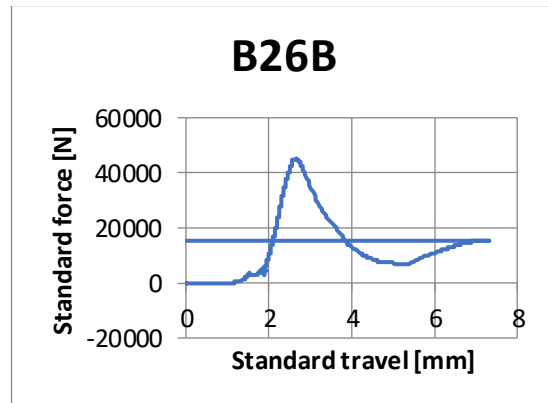
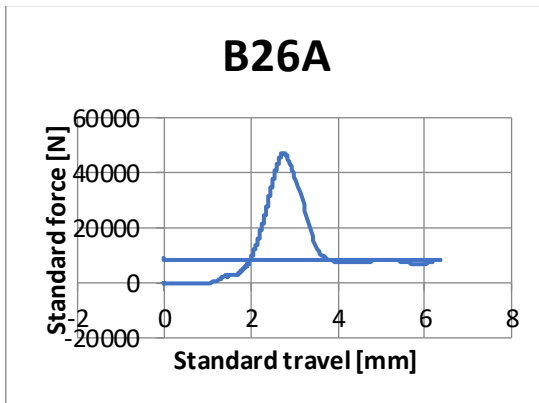
B26

Bending test



Specimen size [mm]		Weight [g]	
160.36	40.15	40.8	533.79

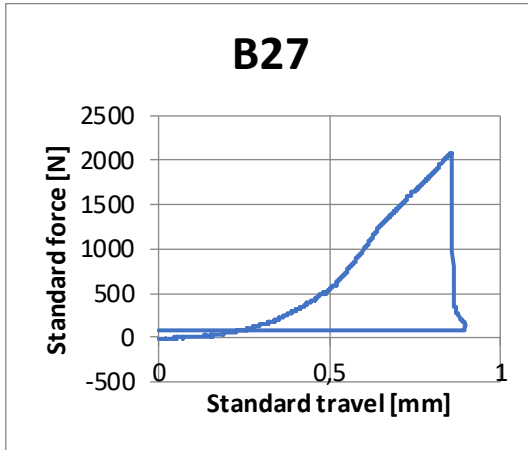
Compression test



Pmax [kN]	σ flex [MPa]	F1 [kN]	F2 [kN]	σ 1 [MPa]	σ 2 [MPa]
1,99	4,46	47,09	45,17	29,43	28,23

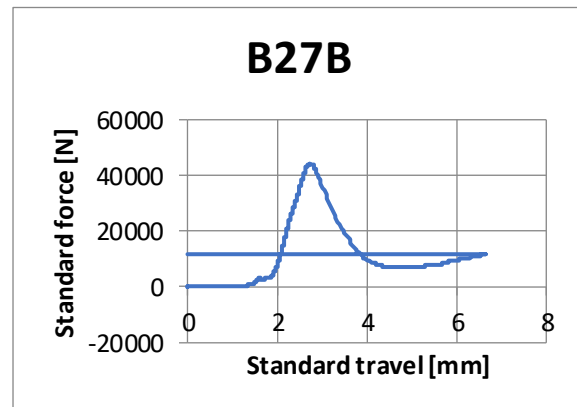
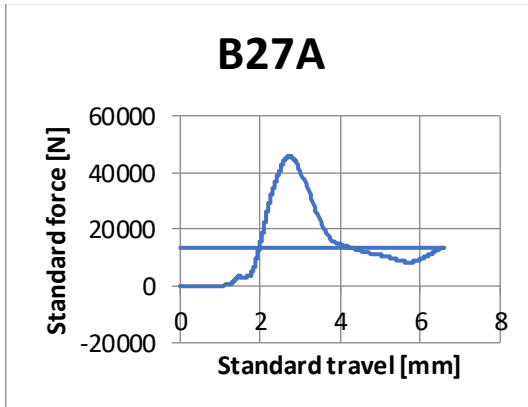
B27

Bending test



Specimen size [mm]		Weight [g]	
160.66	39.88	40.74	527.14

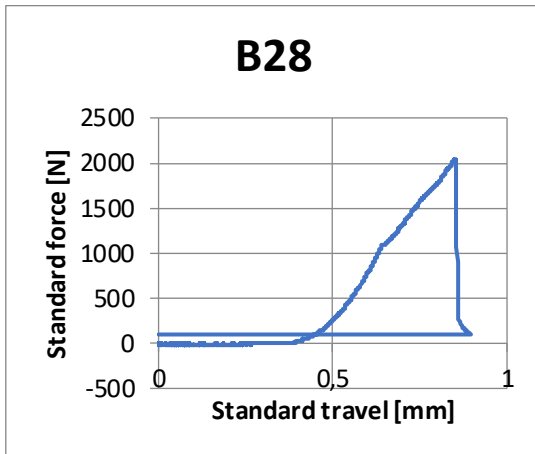
Compression test



Pmax [kN]	σ flex [MPa]	F1 [kN]	F2 [kN]	σ_1 [MPa]	σ_2 [MPa]
2,07	4,70	45,49	44,23	28,43	27,64

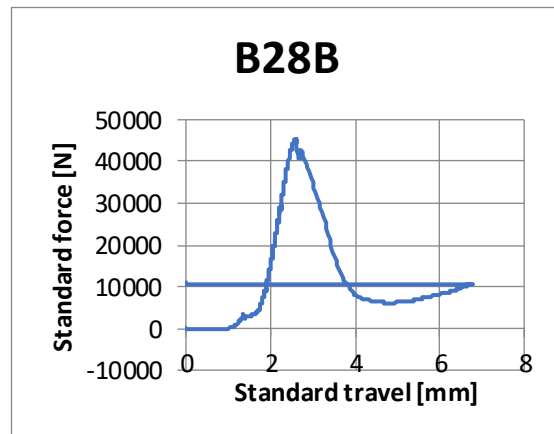
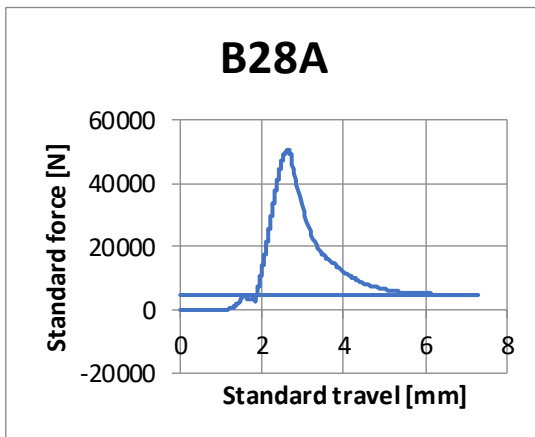
B28

Bending test



Specimen size [mm]		Weight [g]	
160.19	40.04	40.41	532.5

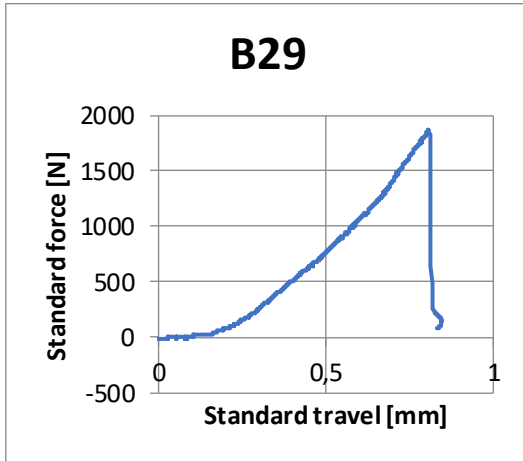
Compression test



Pmax [kN]	σ flex [MPa]	F1 [kN]	F2 [kN]	σ 1 [MPa]	σ 2 [MPa]
2,03	4,66	50,32	45,29	31,45	28,31

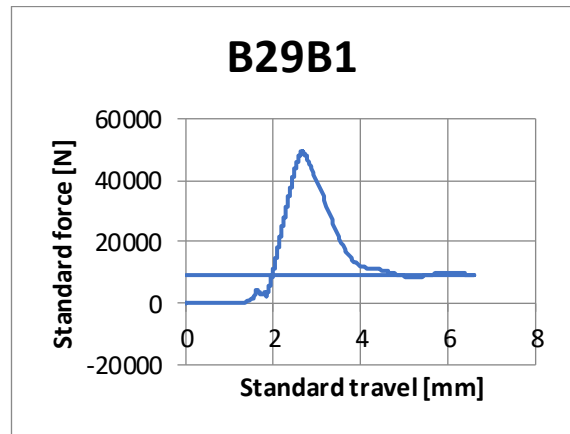
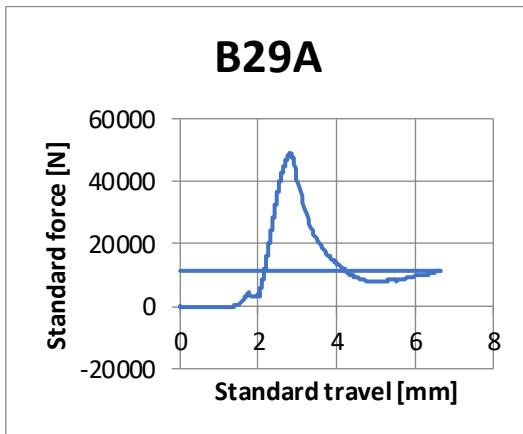
B29

Bending test



Specimen size [mm]		Weight [g]	
160.5	39.5	40.22	529.23

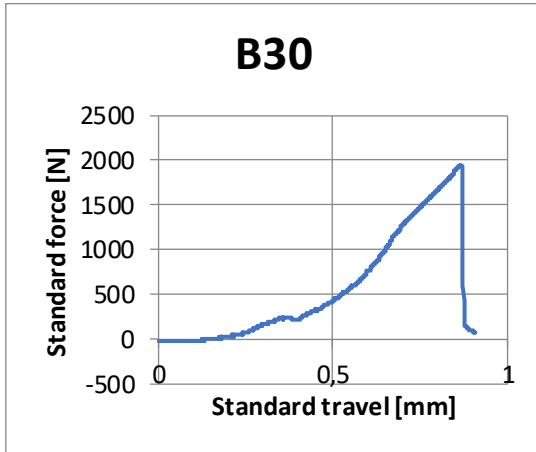
Compression test



Pmax [kN]	σ flex [MPa]	F1 [kN]	F2 [kN]	σ 1 [MPa]	σ 2 [MPa]
1,87	4,39	48,72	49,23	30,45	30,77

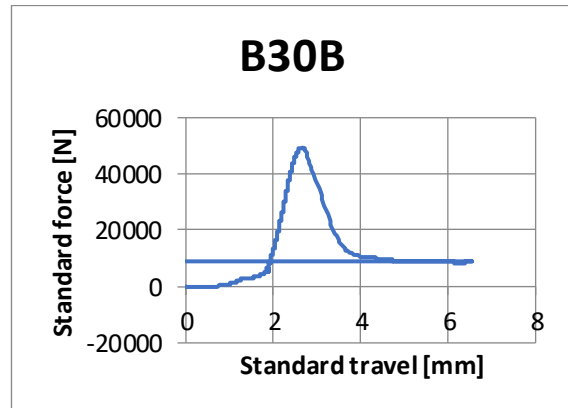
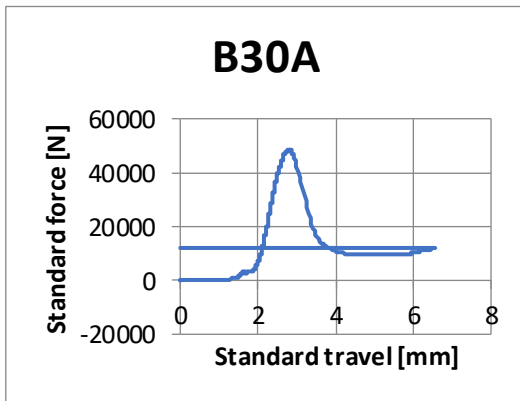
B30

Bending test



Specimen size [mm]		Weight [g]	
160	40	40.35	535.69

Compression test



Pmax [kN]	σ flex [MPa]	F1 [kN]	F2 [kN]	σ 1 [MPa]	σ 2 [MPa]
1,95	4,49	48,26	49,34	30,16	30,84

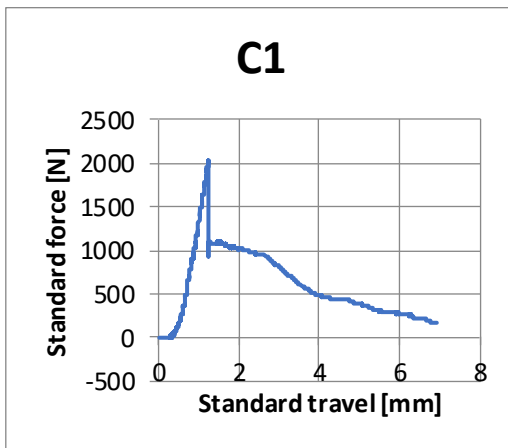
Campione C - Fiber

Qui sono riportate tutte le prove fatte durante il test #3

In alcuni casi ci sono provi che sono stati rifatti per problemi tecnici, questi sono nominati con il nome successivo al corrispettivo.

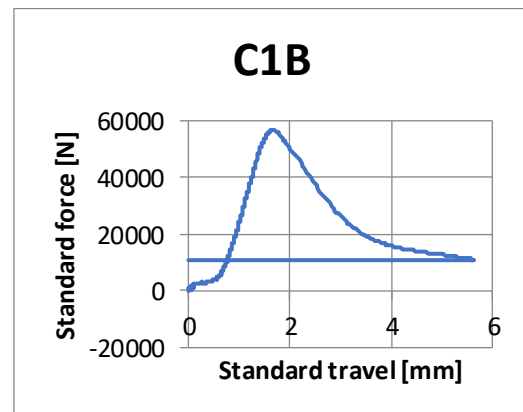
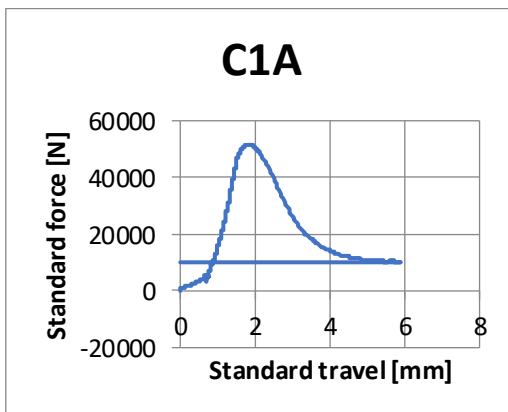
C1

Bending test



Specimen size [mm]		Weight [g]	
159.9	41.18	40.54	557.65

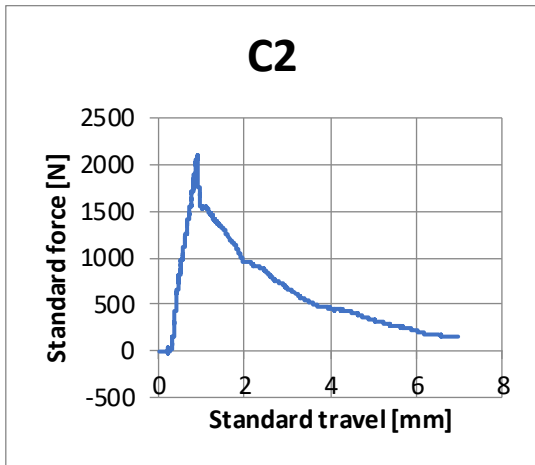
Compression test



Pmax [kN]	σ flex [MPa]	F1 [kN]	F2 [kN]	σ 1 [MPa]	σ 2 [MPa]
2,02	4,49	51,54	56,70	32,21	35,44

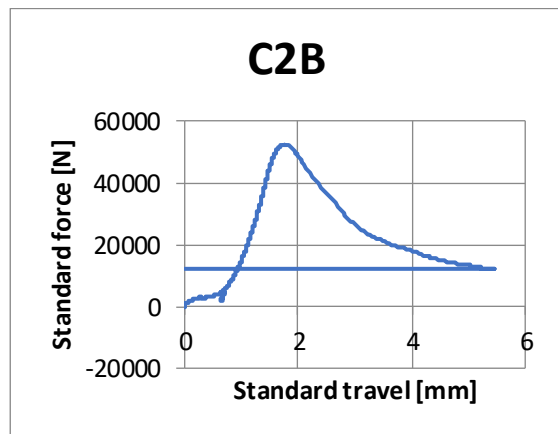
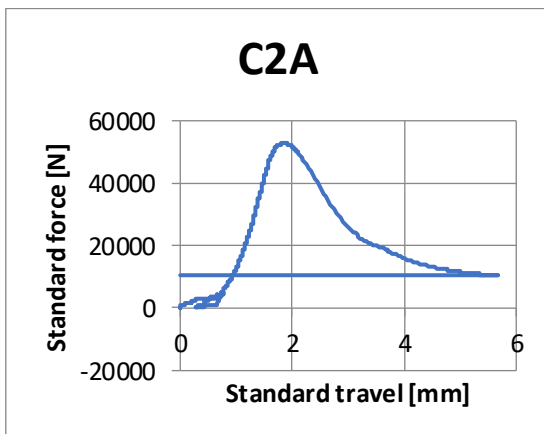
C2

Bending test



Specimen size [mm]		Weight [g]	
160.28	40.92	40.91	548.78

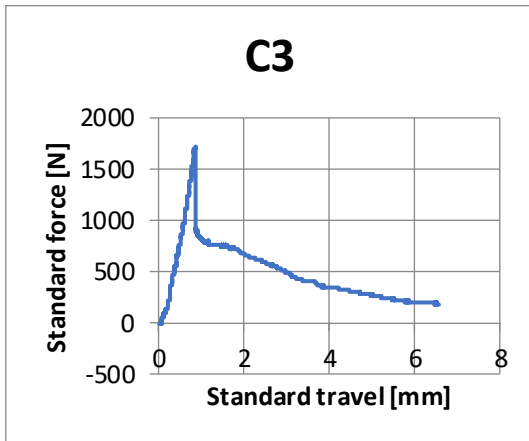
Compression test



Pmax [kN]	σ flex [MPa]	F1 [kN]	F2 [kN]	σ 1 [MPa]	σ 2 [MPa]
2,11	4,62	52,81	52,24	33,00	32,65

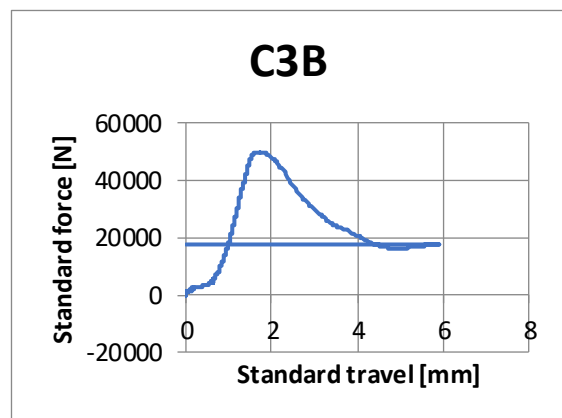
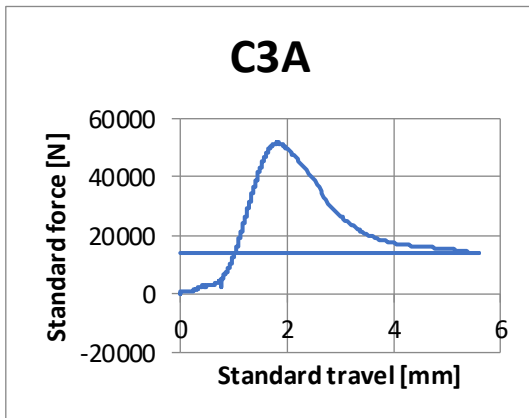
C3

Bending test



Specimen size [mm]		Weight [g]	
160.15	41.49	40.84	551.27

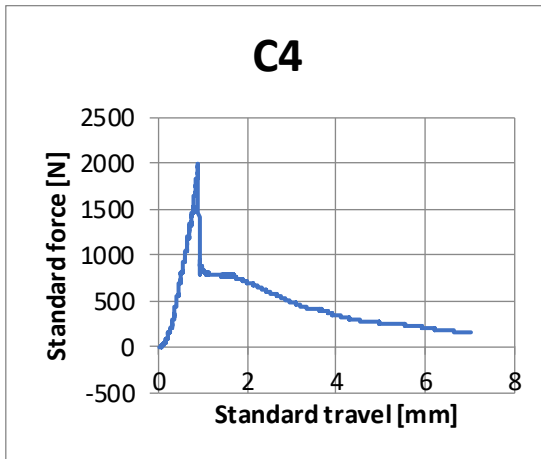
Compression test



Pmax [kN]	σ flex [MPa]	F1 [kN]	F2 [kN]	σ 1 [MPa]	σ 2 [MPa]
1,72	3,72	51,71	49,64	32,32	31,02

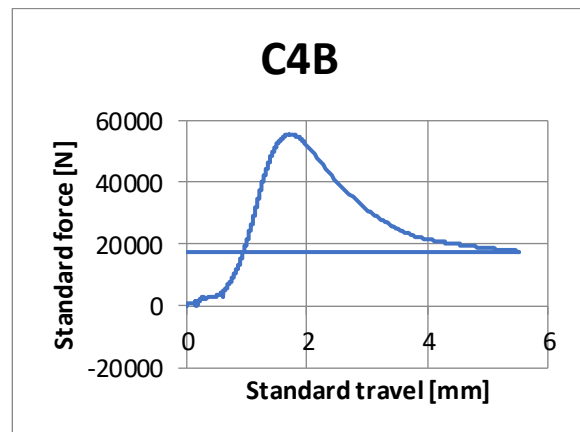
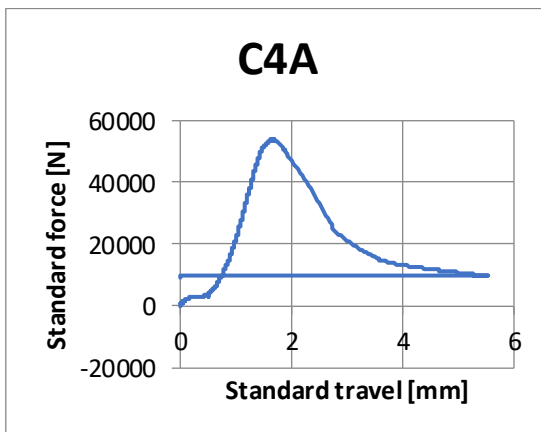
C4

Bending test



Specimen size [mm]		Weight [g]	
160.28	40.28	40.34	548.4

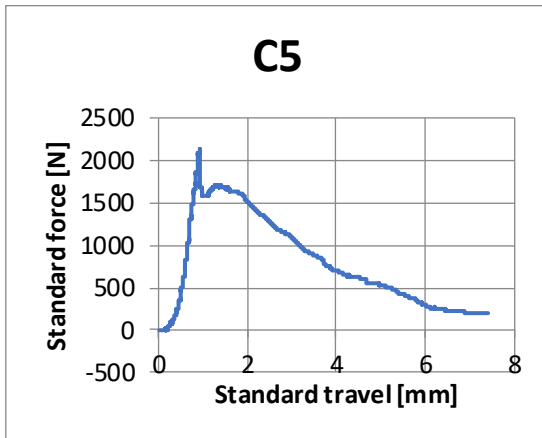
Compression test



Pmax [kN]	σ flex [MPa]	F1 [kN]	F2 [kN]	σ 1 [MPa]	σ 2 [MPa]
2,01	4,59	53,82	55,54	33,64	34,71

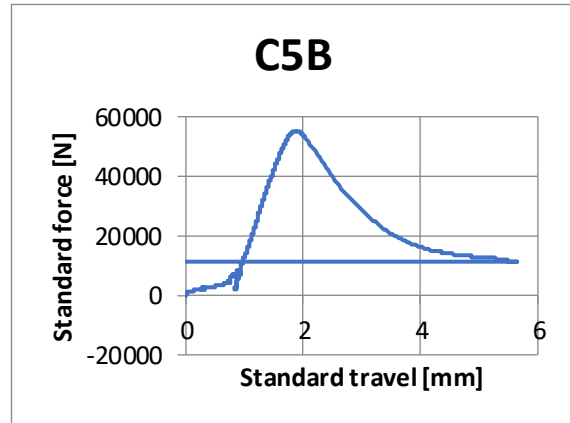
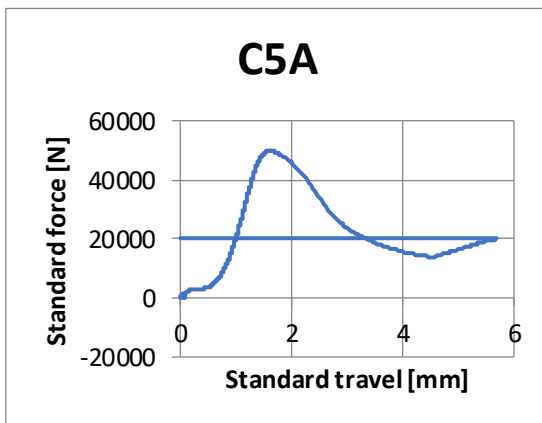
C5

Bending test



Specimen size [mm]		Weight [g]	
160.5	40.33	40.81	549.92

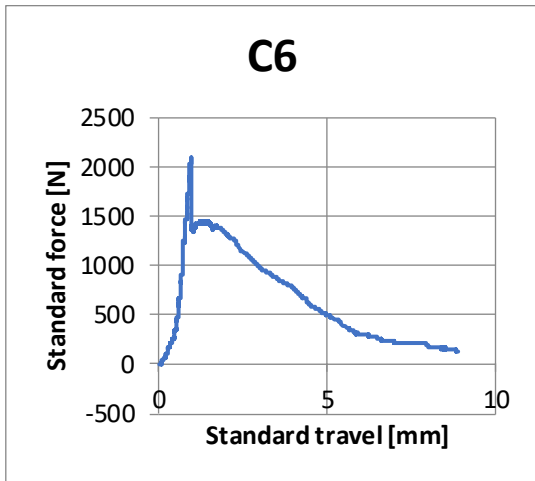
Compression test



Pmax [kN]	σ flex [MPa]	F1 [kN]	F2 [kN]	σ 1 [MPa]	σ 2 [MPa]
2,14	4,78	49,85	55,19	31,16	34,49

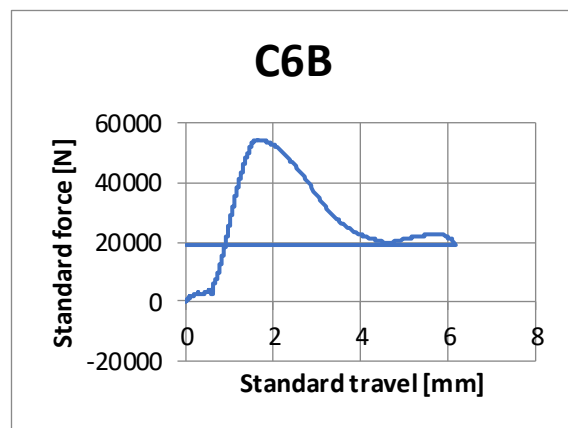
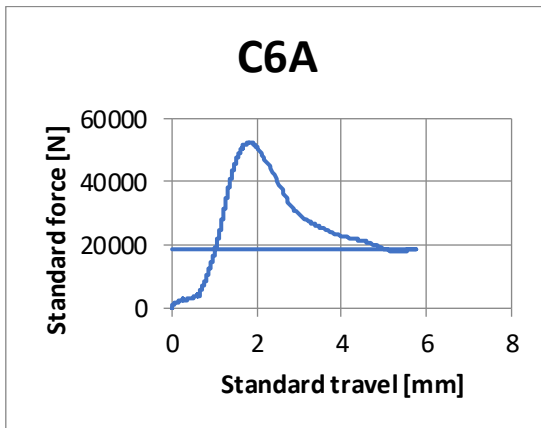
C6

Bending test



Specimen size [mm]		Weight [g]	
160.88	40.3	40.82	549.98

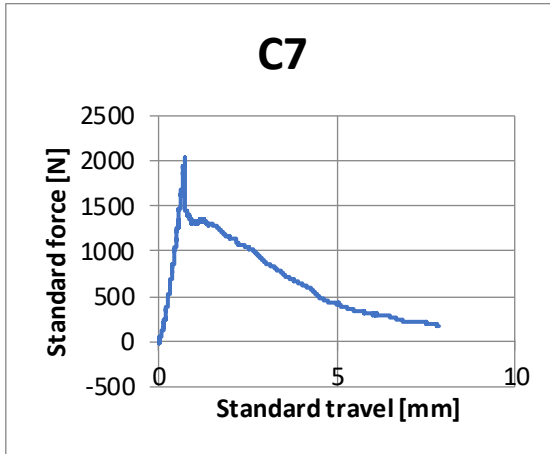
Compression test



Pmax [kN]	σ flex [MPa]	F1 [kN]	F2 [kN]	σ 1 [MPa]	σ 2 [MPa]
2,10	4,69	52,41	54,22	32,75	33,89

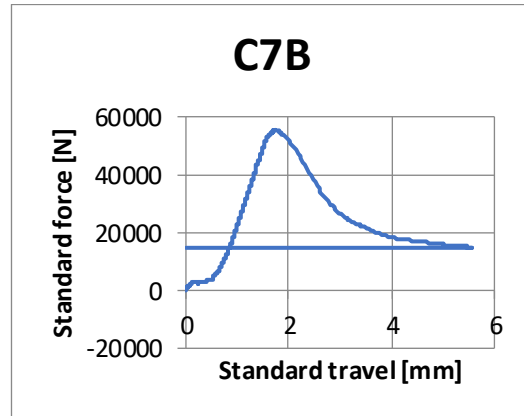
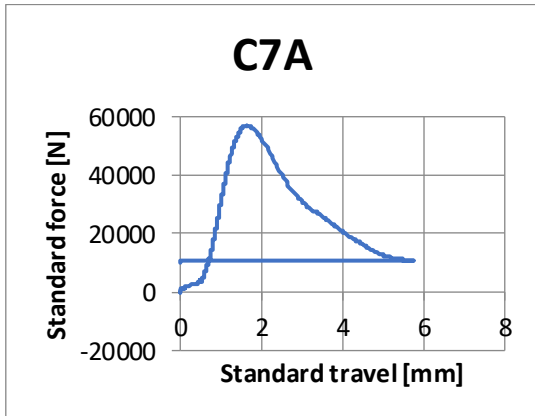
C7

Bending test



Specimen size [mm]		Weight [g]	
159.75	39.44	40.44	543.62

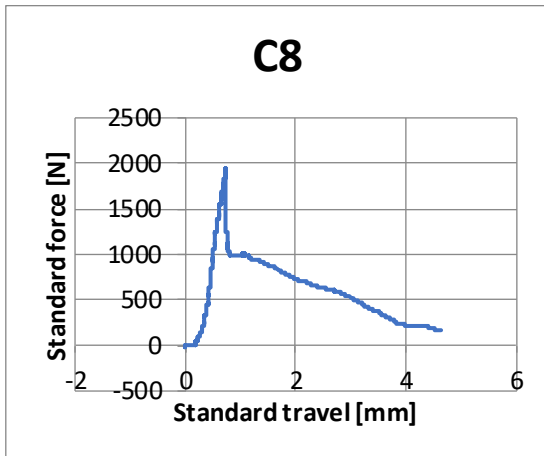
Compression test



Pmax [kN]	σ flex [MPa]	F1 [kN]	F2 [kN]	σ 1 [MPa]	σ 2 [MPa]
2,04	4,75	56,97	55,46	35,61	34,66

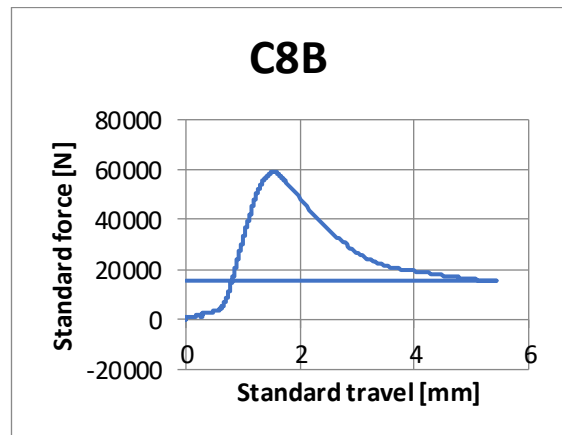
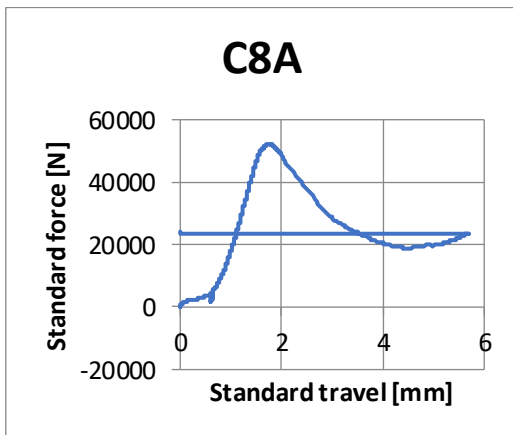
C8

Bending test



Specimen size [mm]		Weight [g]	
160.37	39.67	40.31	548.35

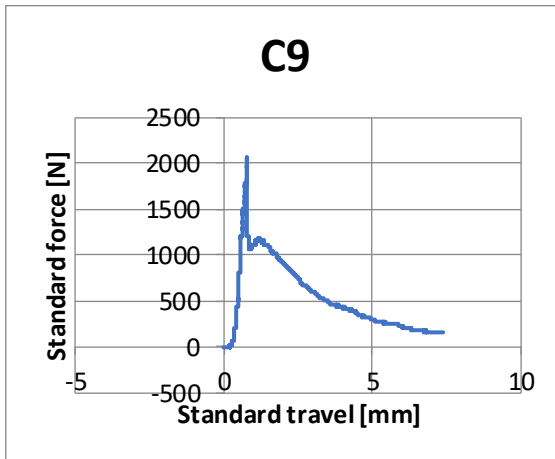
Compression test



Pmax [kN]	σ flex [MPa]	F1 [kN]	F2 [kN]	σ 1 [MPa]	σ 2 [MPa]
1,95	4,53	51,93	59,02	32,46	36,89

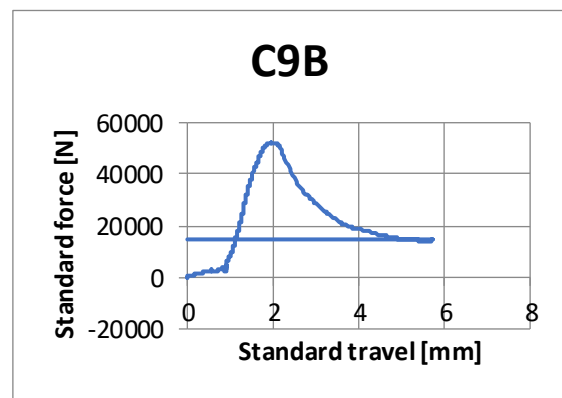
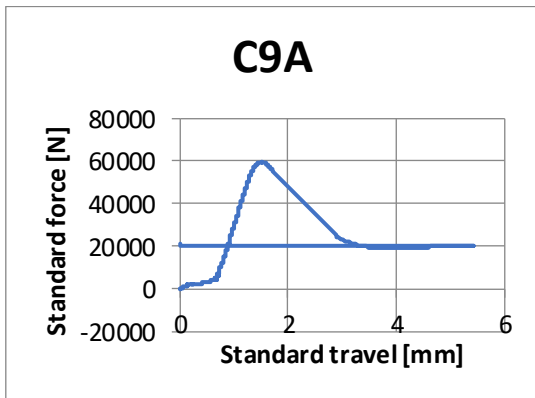
C9

Bending test



Specimen size [mm]		Weight [g]	
159.61	40.55	40.16	553.55

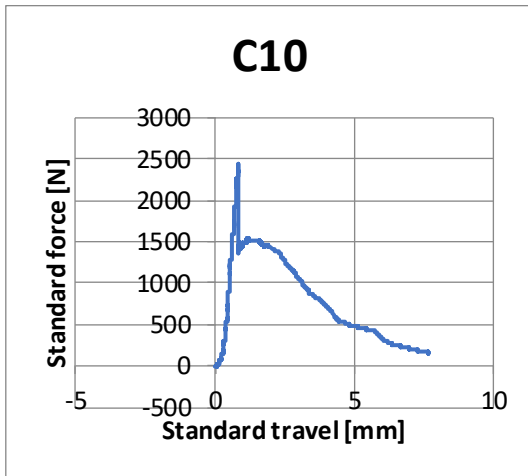
Compression test



Pmax [kN]	σ flex [MPa]	F1 [kN]	F2 [kN]	σ 1 [MPa]	σ 2 [MPa]
2,07	4,75	59,80	52,39	37,38	32,74

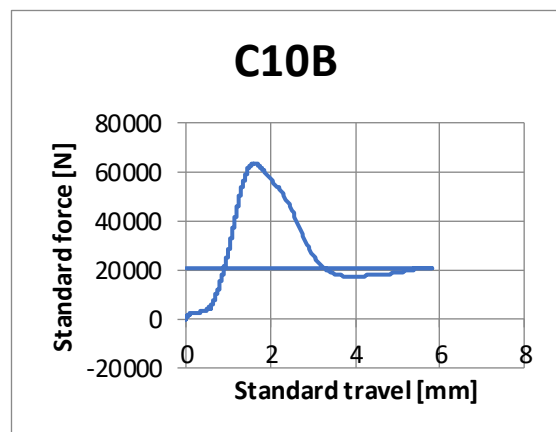
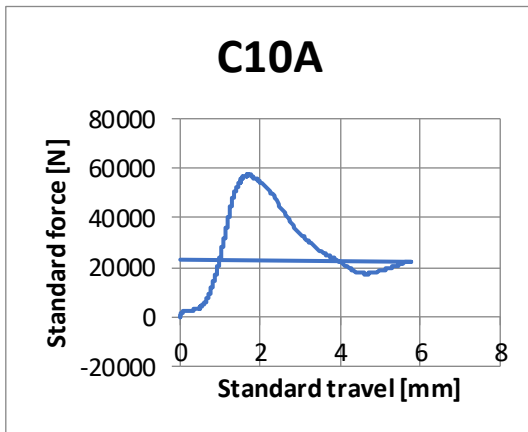
C10

Bending test



Specimen size [mm]		Weight [g]	
159.65	40.18	40.38	557.55

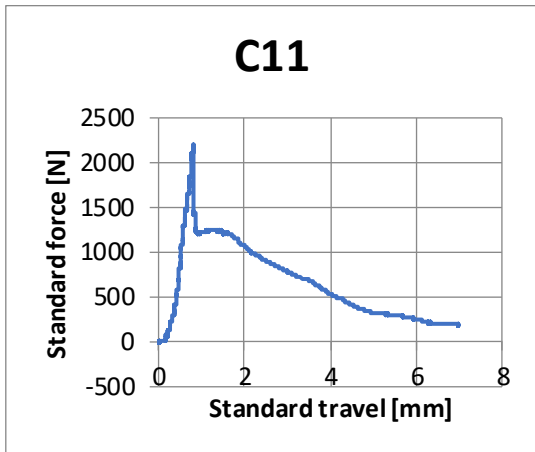
Compression test



Pmax [kN]	σ flex [MPa]	F1 [kN]	F2 [kN]	σ_1 [MPa]	σ_2 [MPa]
2,46	5,62	57,20	63,27	35,75	39,54

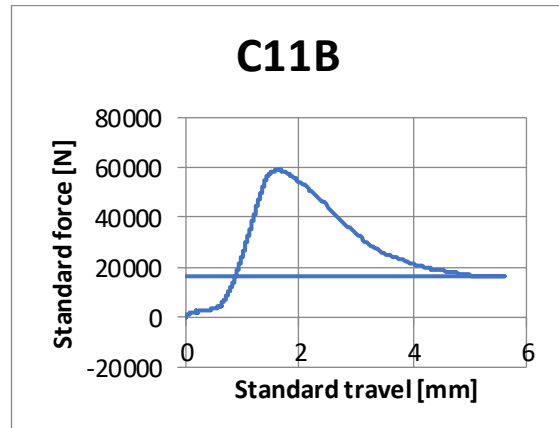
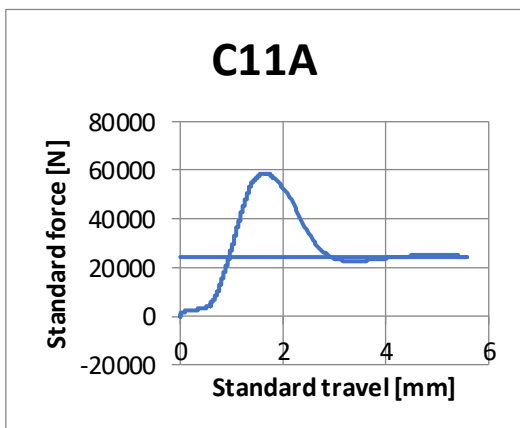
C11

Bending test



Specimen size [mm]		Weight [g]	
160.28	40.58	40.24	562.39

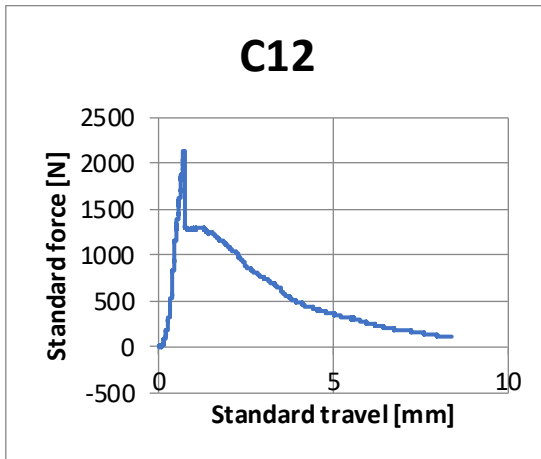
Compression test



Pmax [kN]	σ flex [MPa]	F1 [kN]	F2 [kN]	σ 1 [MPa]	σ 2 [MPa]
2,20	5,02	58,56	59,05	36,60	36,90

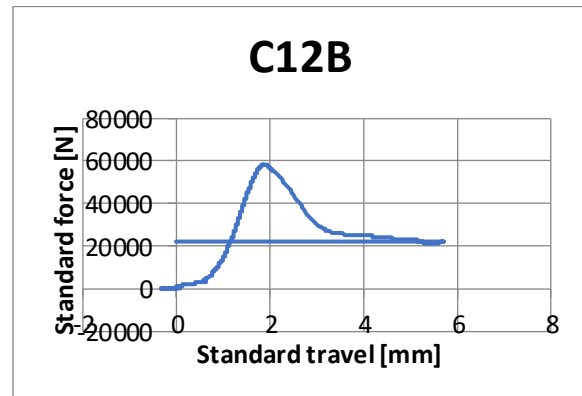
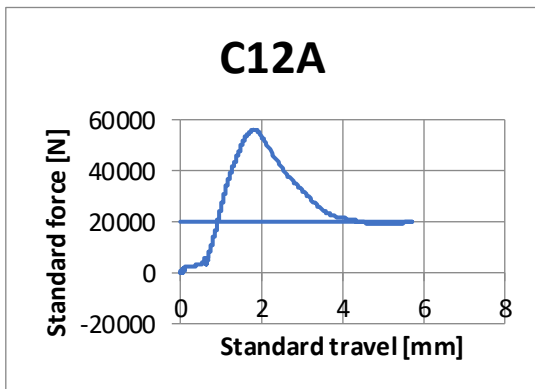
C12

Bending test



Specimen size [mm]		Weight [g]	
159.94	40.63	40.55	562.1

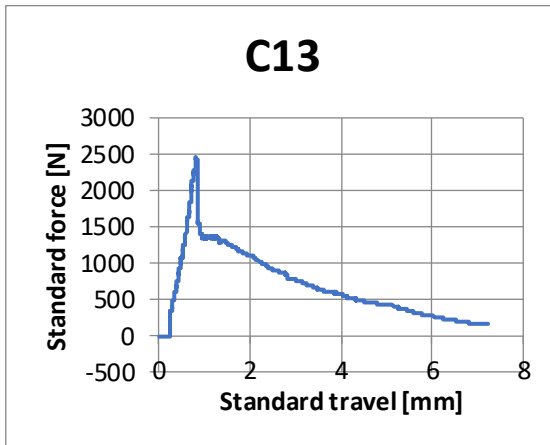
Compression test



Pmax [kN]	σ flex [MPa]	F1 [kN]	F2 [kN]	σ_1 [MPa]	σ_2 [MPa]
2,15	4,83	56,06	58,47	35,04	36,54

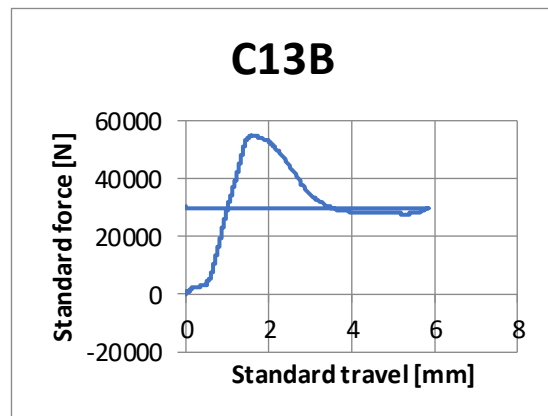
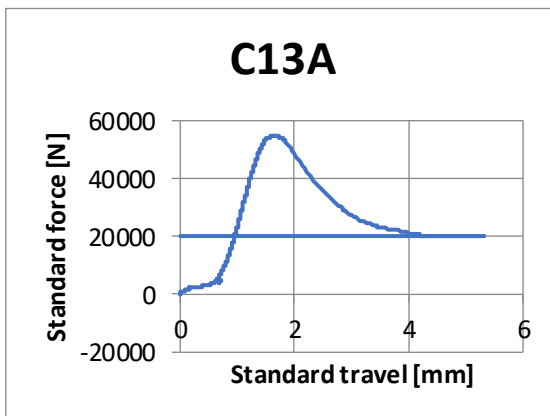
C13

Bending test



Specimen size [mm]		Weight [g]	
160.08	40.82	40.04	558.96

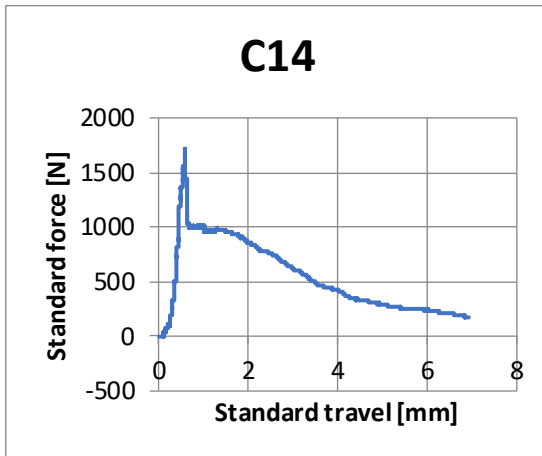
Compression test



Pmax [kN]	σ flex [MPa]	F1 [kN]	F2 [kN]	σ 1 [MPa]	σ 2 [MPa]
2,45	5,62	54,82	54,89	34,26	34,30

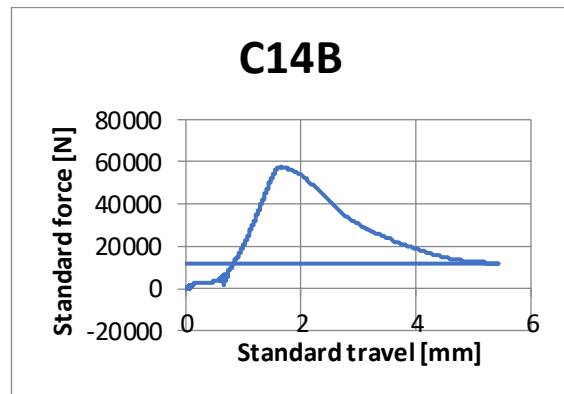
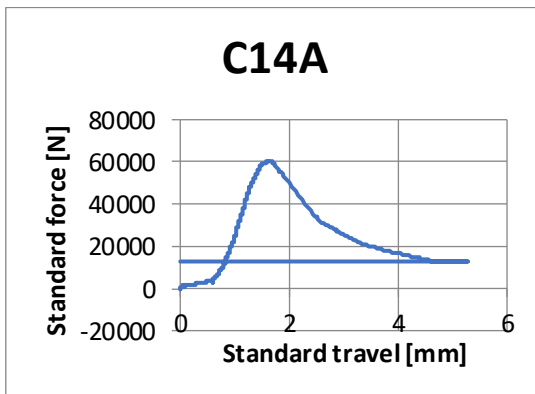
C14

Bending test



Specimen size [mm]		Weight [g]	
159.93	41.25	40.25	563.55

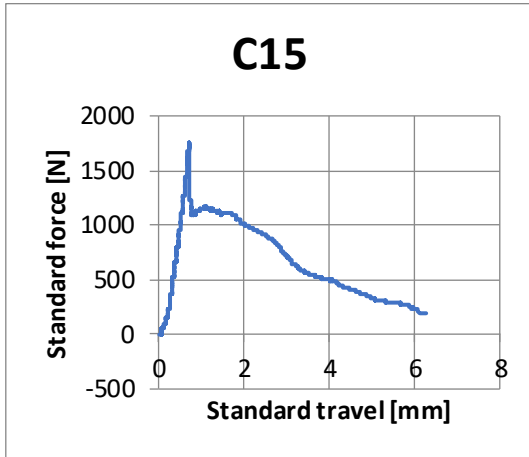
Compression test



Pmax [kN]	σ flex [MPa]	F1 [kN]	F2 [kN]	σ 1 [MPa]	σ 2 [MPa]
1,71	3,84	60,22	57,72	37,64	36,07

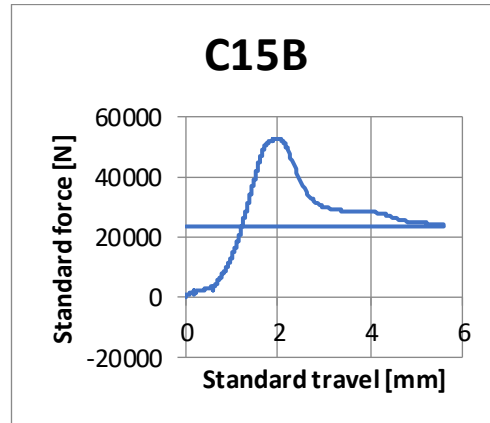
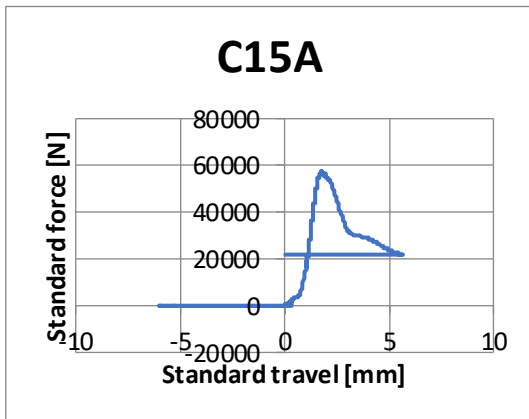
C15

Bending test



Specimen size [mm]		Weight [g]	
160.08	41.2	40.07	560.75

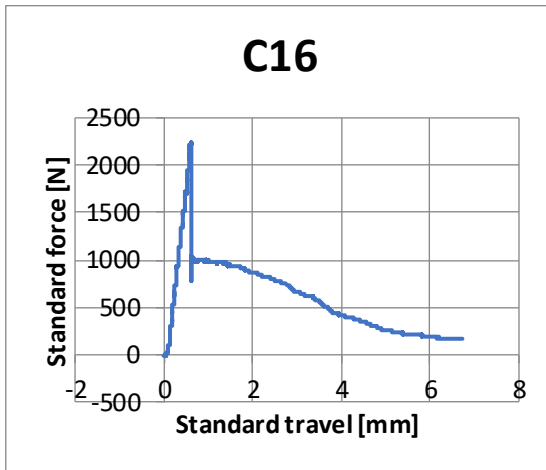
Compression test



Pmax [kN]	σ flex [MPa]	F1 [kN]	F2 [kN]	σ 1 [MPa]	σ 2 [MPa]
1,76	3,99	57,50	52,54	35,94	32,84

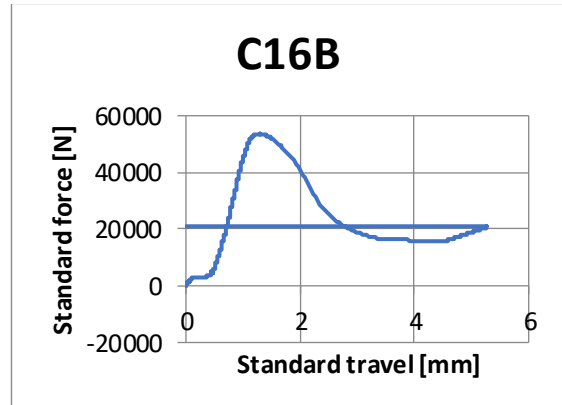
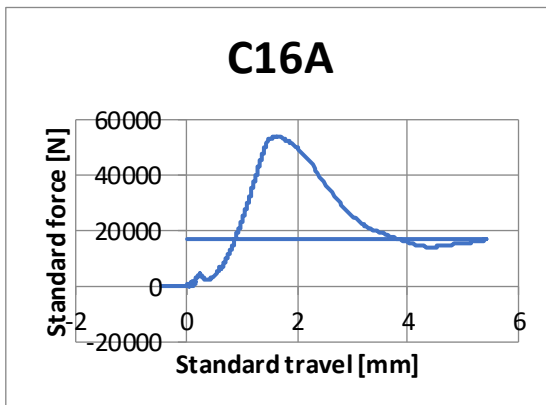
C16

Bending test



Specimen size [mm]		Weight [g]	
159.89	39.94	40.41	547.38

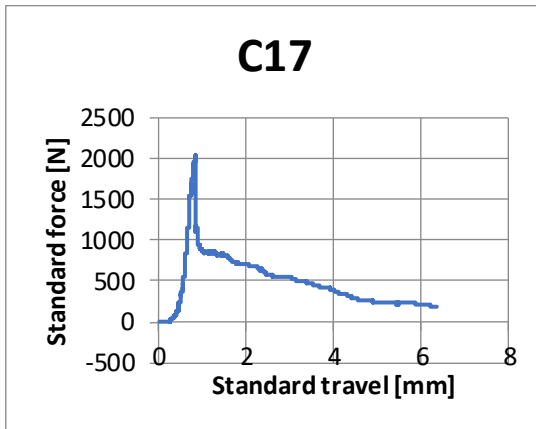
Compression test



Pmax [kN]	σ flex [MPa]	F1 [kN]	F2 [kN]	σ 1 [MPa]	σ 2 [MPa]
2,25	5,17	53,85	53,71	33,66	33,57

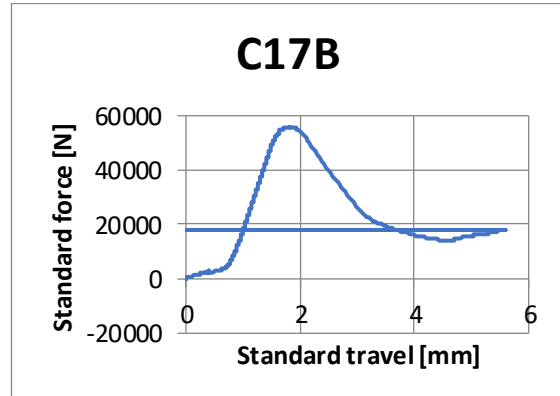
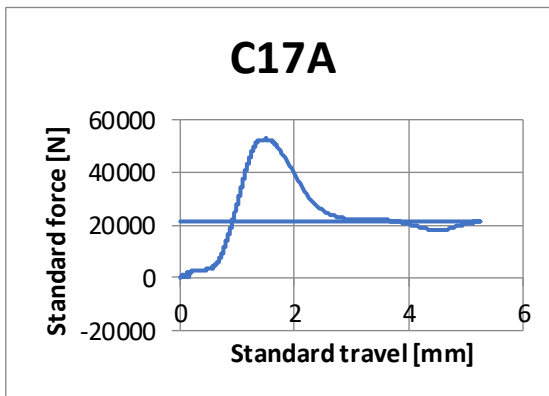
C17

Bending test



Specimen size [mm]		Weight [g]	
159.62	40.18	40.12	543.21

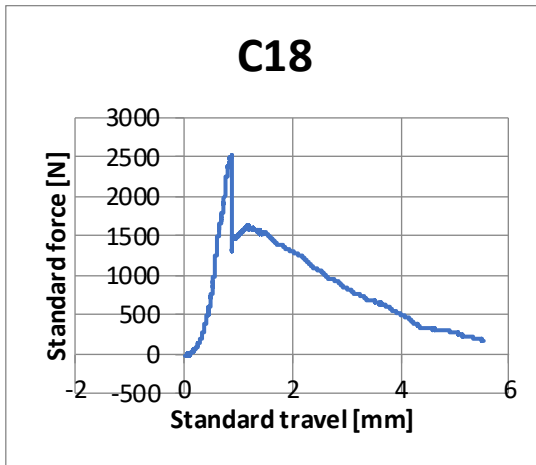
Compression test



Pmax [kN]	σ flex [MPa]	F1 [kN]	F2 [kN]	σ 1 [MPa]	σ 2 [MPa]
2,04	4,72	52,58	55,89	32,86	34,93

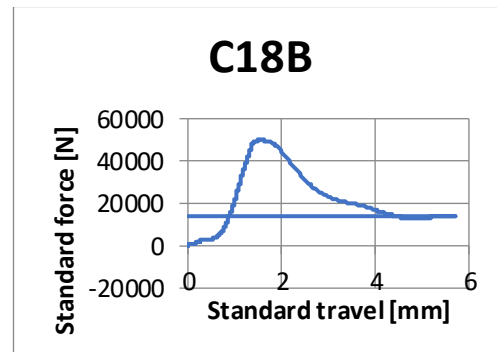
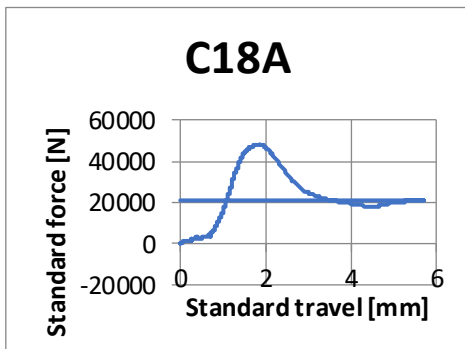
C18

Bending test



Specimen size [mm]		Weight [g]	
159.62	40.69	40.24	550.87

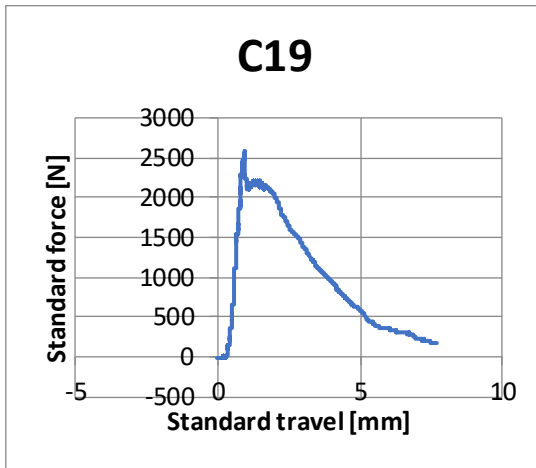
Compression test



Pmax [kN]	σ flex [MPa]	F1 [kN]	F2 [kN]	σ 1 [MPa]	σ 2 [MPa]
2,54	5,77	47,96	49,84	29,97	31,15

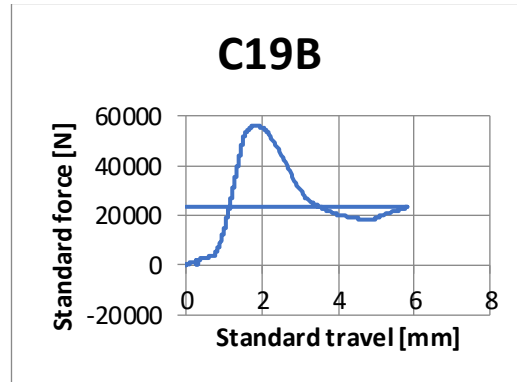
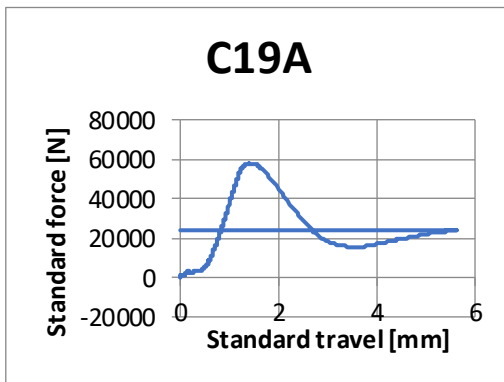
C19

Bending test



Specimen size [mm]		Weight [g]	
160.31	39.71	40.16	539.47

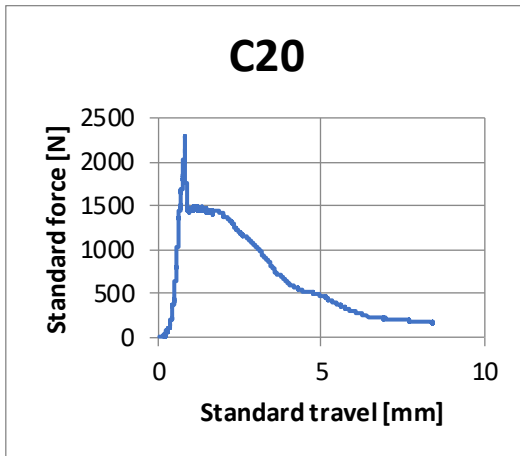
Compression test



Pmax [kN]	σ flex [MPa]	F1 [kN]	F2 [kN]	σ 1 [MPa]	σ 2 [MPa]
2,57	6,02	57,94	55,99	36,21	34,99

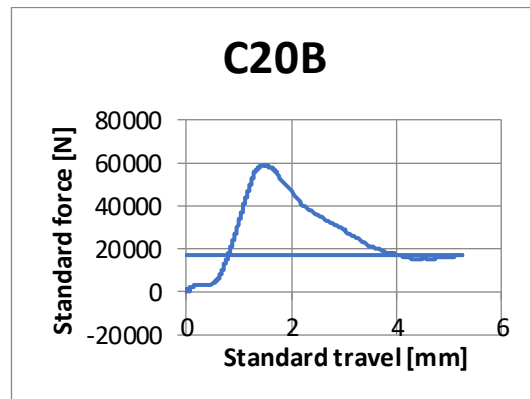
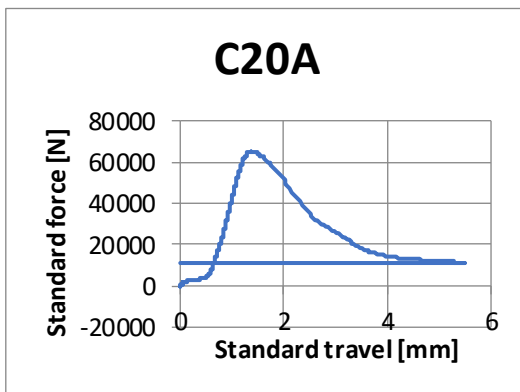
C20

Bending test



Specimen size [mm]		Weight [g]	
159.8	40.64	40.18	554.48

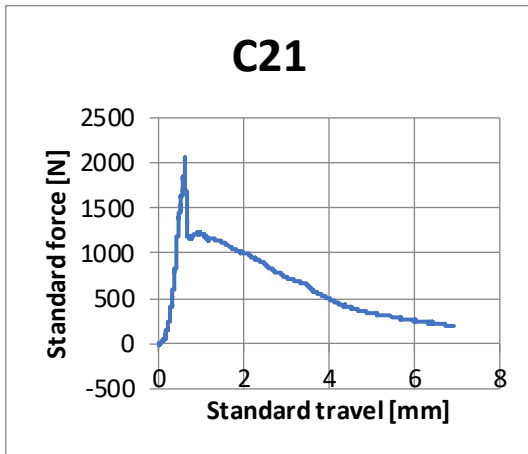
Compression test



Pmax [kN]	σ flex [MPa]	F1 [kN]	F2 [kN]	σ 1 [MPa]	σ 2 [MPa]
2,28	5,22	65,11	58,54	40,69	36,58

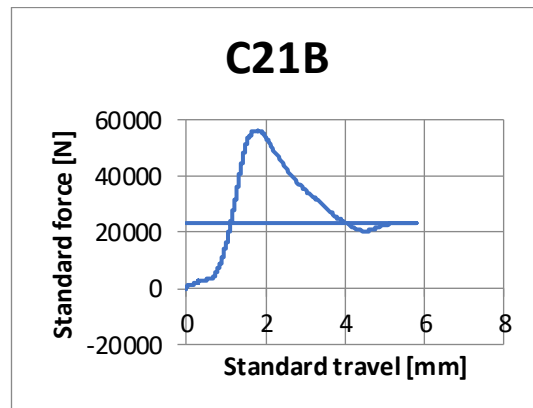
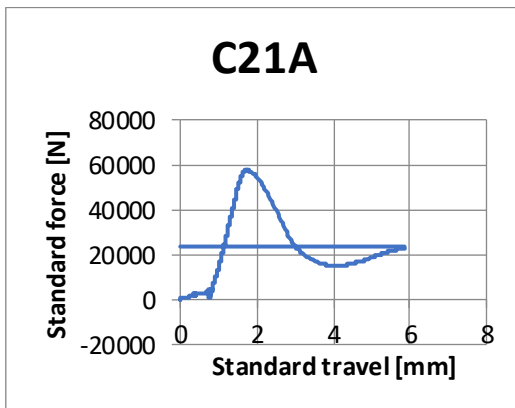
C21

Bending test



Specimen size [mm]		Weight [g]	
159.79	40.85	40.39	560.03

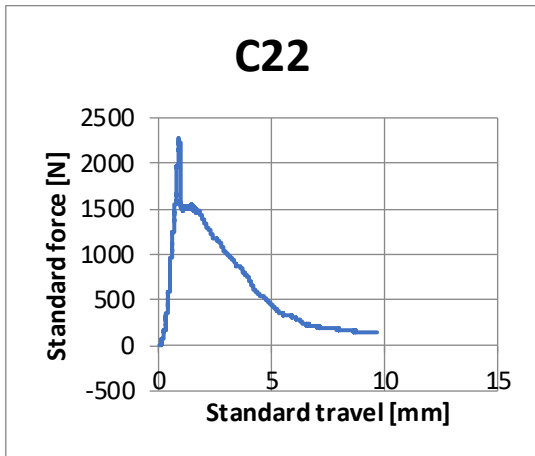
Compression test



Pmax [kN]	σ flex [MPa]	F1 [kN]	F2 [kN]	σ 1 [MPa]	σ 2 [MPa]
2,07	4,65	57,38	56,14	35,86	35,09

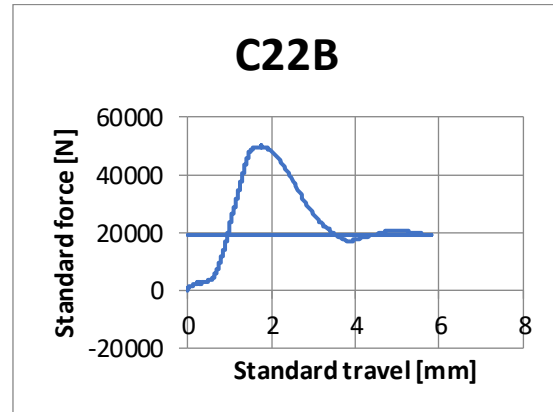
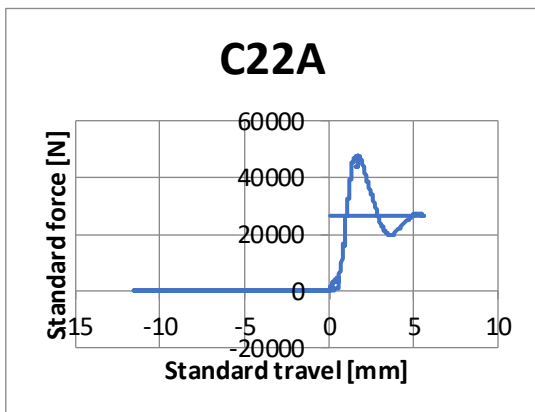
C22

Bending test



Specimen size [mm]		Weight [g]	
159.86	39.94	40.37	547.95

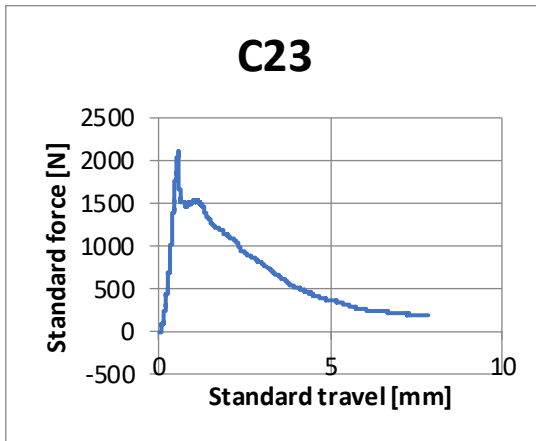
Compression test



Pmax [kN]	σ flex [MPa]	F1 [kN]	F2 [kN]	σ 1 [MPa]	σ 2 [MPa]
2,27	5,22	47,73	49,73	29,83	31,08

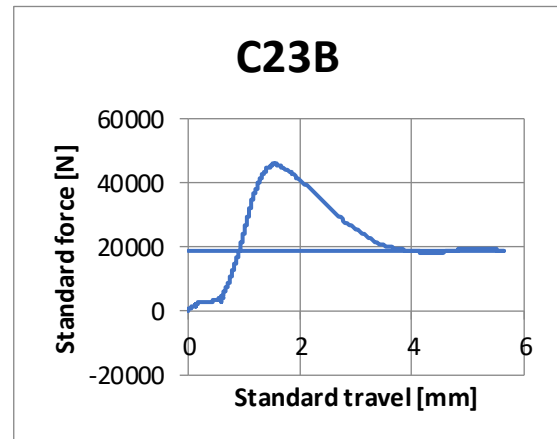
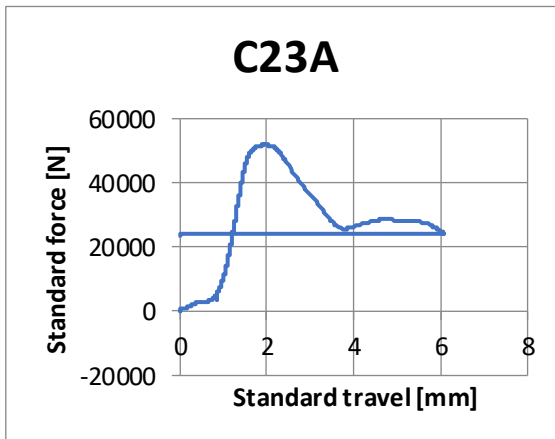
C23

Bending test



Specimen size [mm]		Weight [g]	
160.2	40.23	40.36	548.15

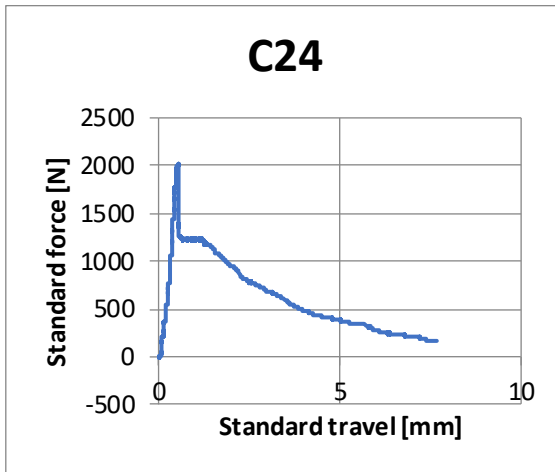
Compression test



Pmax [kN]	σ flex [MPa]	F1 [kN]	F2 [kN]	σ 1 [MPa]	σ 2 [MPa]
2,11	4,83	51,87	45,93	32,42	28,70

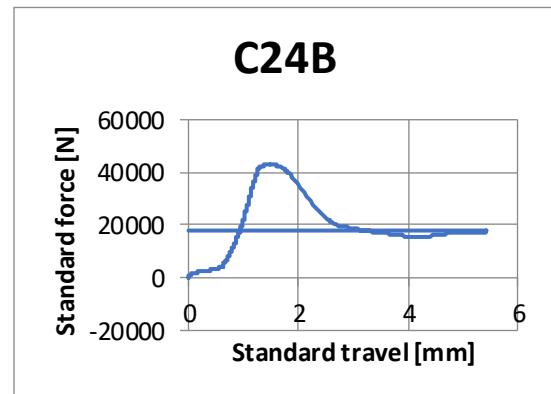
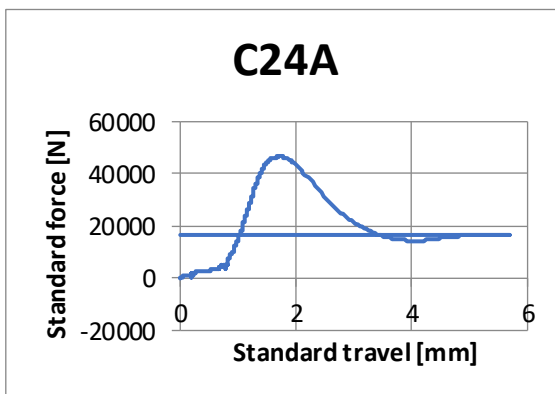
C24

Bending test



Specimen size [mm]		Weight [g]	
159.82	39.81	40.58	538.05

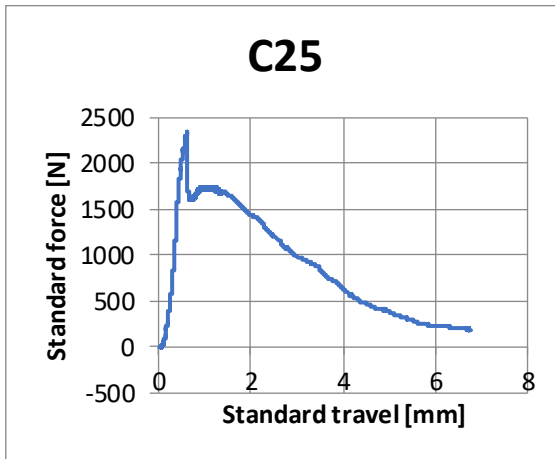
Compression test



Pmax [kN]	σ flex [MPa]	F1 [kN]	F2 [kN]	σ 1 [MPa]	σ 2 [MPa]
2,02	4,63	46,63	43,03	29,15	26,89

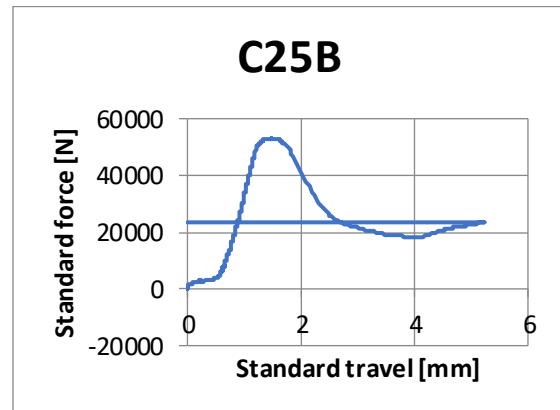
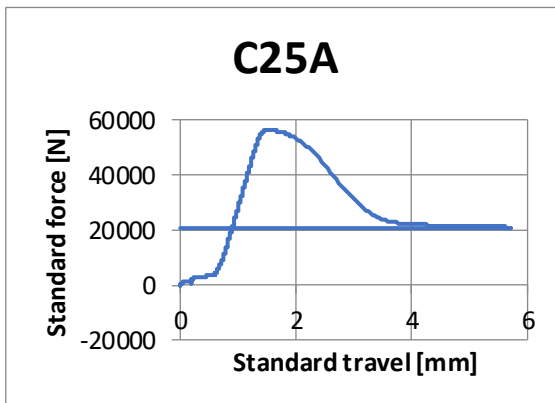
C25

Bending test



Specimen size [mm]		Weight [g]	
160.07	39.63	40.4	543.34

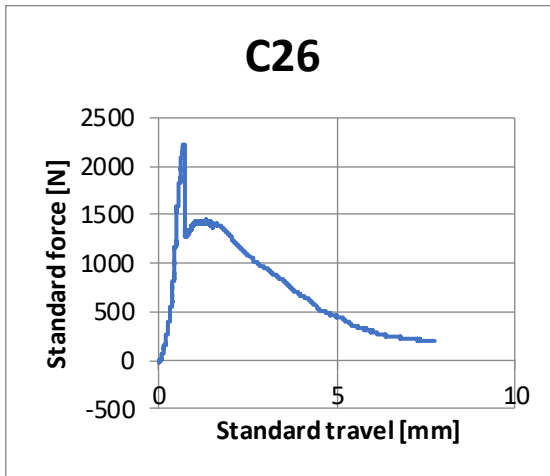
Compression test



Pmax [kN]	σ flex [MPa]	F1 [kN]	F2 [kN]	σ 1 [MPa]	σ 2 [MPa]
2,34	5,44	56,22	53,15	35,14	33,22

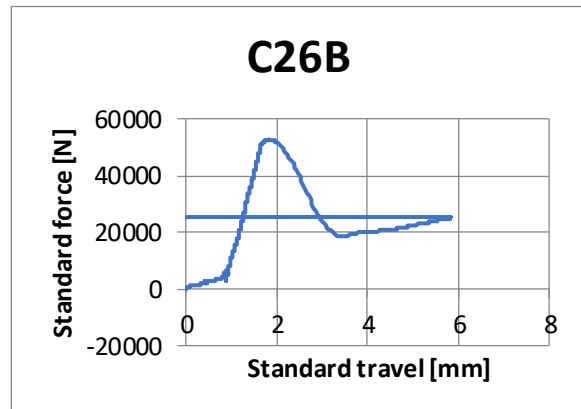
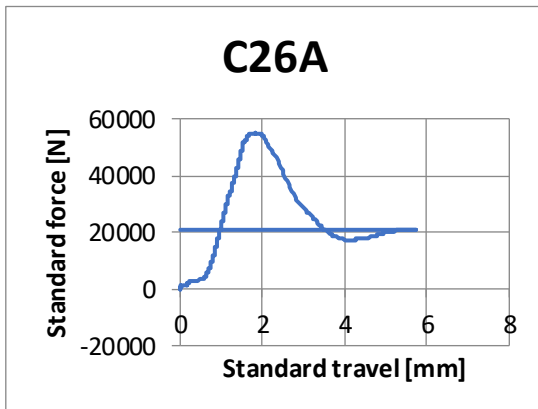
C26

Bending test



Specimen size [mm]		Weight [g]	
160.17	40.45	40.51	556.38

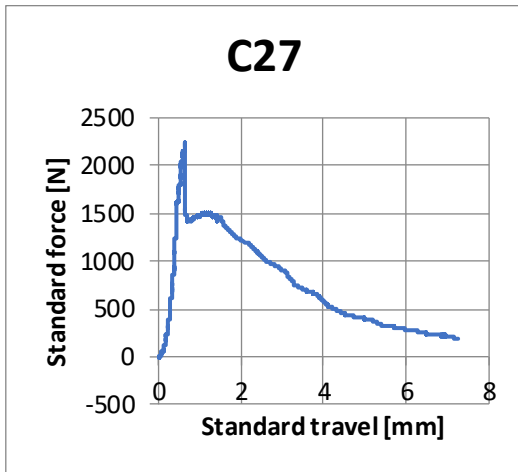
Compression test



Pmax [kN]	σ flex [MPa]	F1 [kN]	F2 [kN]	σ 1 [MPa]	σ 2 [MPa]
2,23	5,05	55,06	52,64	34,41	32,90

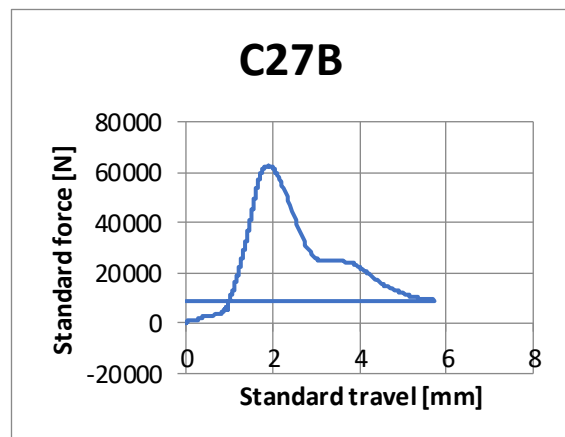
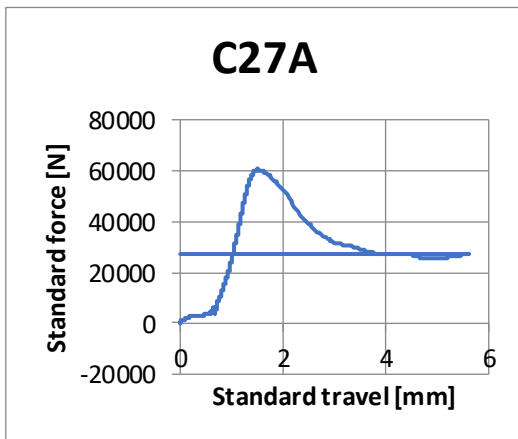
C27

Bending test



Specimen size [mm]		Weight [g]	
160.09	40.03	40.42	553.09

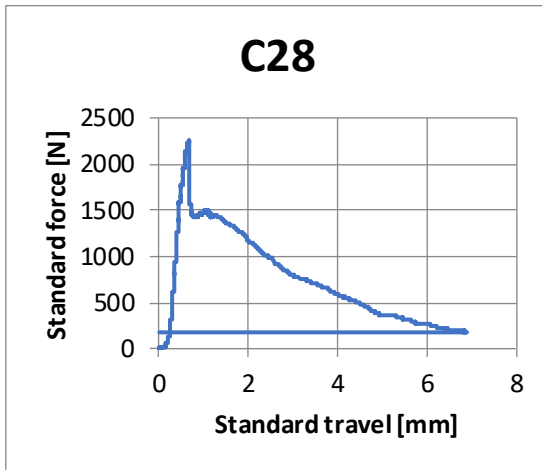
Compression test



Pmax [kN]	σ flex [MPa]	F1 [kN]	F2 [kN]	σ 1 [MPa]	σ 2 [MPa]
2,23	5,12	60,38	62,58	37,74	39,11

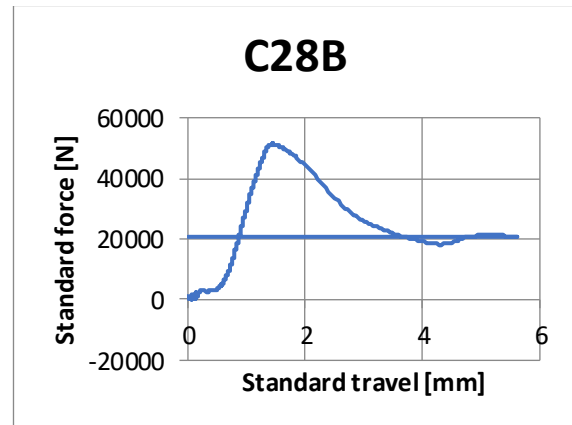
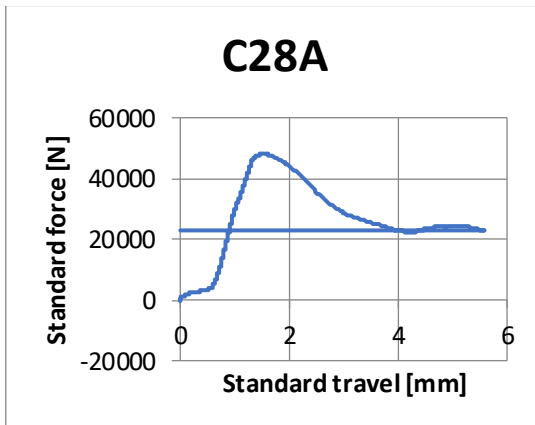
C28

Bending test



Specimen size [mm]		Weight [g]	
159.38	40.82	40.44	554.7

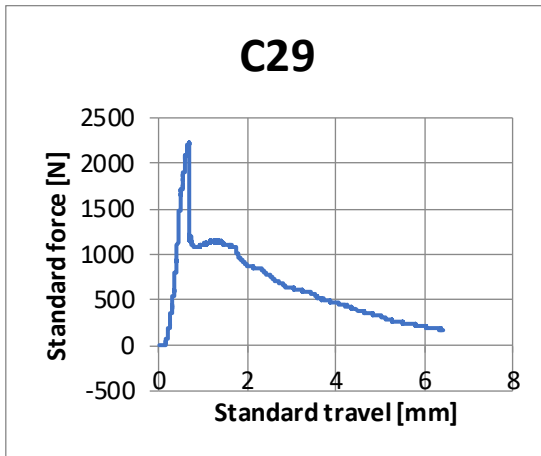
Compression test



Pmax [kN]	σ flex [MPa]	F1 [kN]	F2 [kN]	σ 1 [MPa]	σ 2 [MPa]
2,25	5,05	47,99	51,34	29,99	32,09

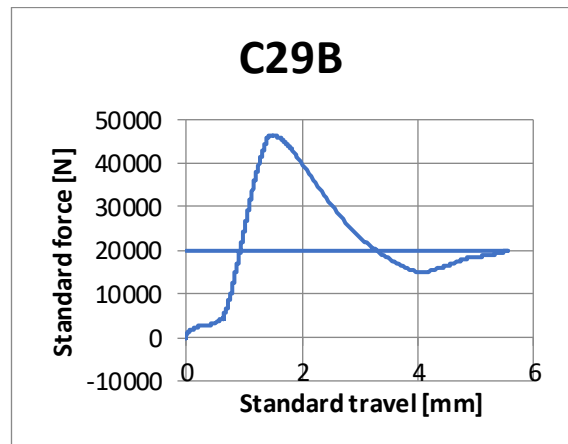
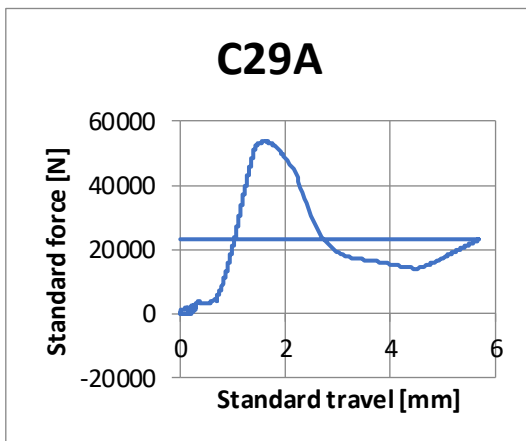
C29

Bending test



Specimen size [mm]		Weight [g]	
160.02	40.22	40.21	547.4

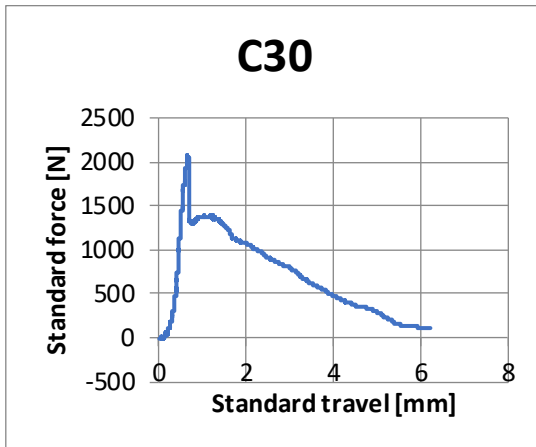
Compression test



Pmax [kN]	σ flex [MPa]	F1 [kN]	F2 [kN]	σ 1 [MPa]	σ 2 [MPa]
2,24	5,16	53,53	46,33	33,46	28,96

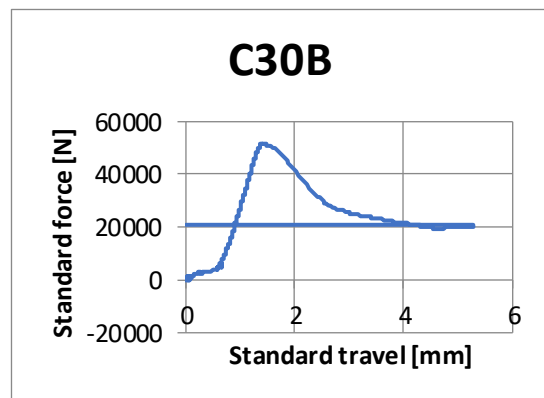
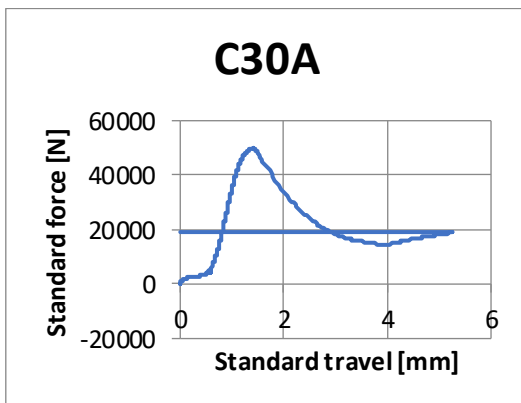
C30

Bending test



Specimen size [mm]		Weight [g]	
159.63	39.94	40.21	544.59

Compression test



Pmax [kN]	σ flex [MPa]	F1 [kN]	F2 [kN]	σ 1 [MPa]	σ 2 [MPa]
2,07	4,81	50,04	51,53	31,28	32,20

ACKNOWLEDGEMENT

Un sincero ringraziamento a chi, in questo percorso, ha saputo trasmettermi il proprio sapere, dedicarmi il proprio tempo e il proprio entusiasmo con professionalità e passione.

Ringrazio il Professore Alessandro Pasquale Fantilli per la sua estrema disponibilità e per la sua competenza e professionalità nel coordinare il mio lavoro di tesi. La ringrazio per i suoi indispensabili consigli e per il tempo prezioso a me dedicato.

Il più grande ringraziamento va ai miei genitori, Raffaele e Francesca, che mi hanno permesso di studiare e mi hanno sempre sostenuto in tutte le scelte fatte. Vi ringrazio per l'affetto infinito che dimostrate ogni giorno e per essere la mia guida, fonte di educazione e ispirazione. Ringrazio mia sorella Carla che mi spinge ad essere un esempio anche quando non credo di esserne capace.

Un ringraziamento speciale va a Emma, Antonio, Marialaura e al piccolo Alessandro che grazia alla loro compagnia mia hanno fatto sentire a casa anche se a più di mille km di distanza.

Ringrazio tutti i miei amici a cui devo il mio successo perché con un piccolo gesto mi hanno sempre aiutato e hanno condiviso con me questa esperienza di vita. Amici di una vita e i compagni fedeli di università a cui devo molto e grazie ai quali ho raggiunto questo traguardo.

Ringrazio le mie due fantastiche coinquiline Alessia e Blerta. Ho avuto la fortuna e il privilegio di aver passato un anno fantastico con persone estremamente migliori di me e da cui ho potuto imparare molto.

Il periodo dell'università mi ha insegnato che ogni grande desiderio e obiettivo richiede grandi azioni per soddisfarlo, ma che l'importante è non arrendersi mai, anche se questo implica grandi sacrifici.

